

# For Reference

---

NOT TO BE TAKEN FROM THIS ROOM

# For Reference

NOT TO BE TAKEN FROM THIS ROOM

Ex libris  
UNIVERSITATIS  
ALBERTAENSIS



## Regulations Regarding Theses and Dissertations

[illegible]



THE UNIVERSITY OF ALBERTA  
RAPID TEMPERATURE PROGRAMMING AND PYROLYSIS  
GAS CHROMATOGRAPHY

by

RONALD R. GOFORTH, B.S., M.S.



A THESIS  
SUBMITTED TO THE FACULTY OF GRADUATE STUDIES  
IN PARTIAL FULFILLMENT OF THE REQUIREMENTS FOR THE DEGREE  
OF DOCTOR OF PHILOSOPHY

DEPARTMENT OF CHEMISTRY

EDMONTON, ALBERTA

AUGUST, 1967



THE UNIVERSITY OF ALBERTA  
FACULTY OF GRADUATE STUDIES

The undersigned hereby certify that they have read, and recommend to the Faculty of Graduate Studies for acceptance, a thesis entitled

RAPID TEMPERATURE PROGRAMMING AND PYROLYSIS

GAS CHROMATOGRAPHY

submitted by Ronald R. Goforth, B.S., M.S., in partial fulfillment of the requirements for the degree of Doctor of Philosophy.



Digitized by the Internet Archive  
in 2019 with funding from  
University of Alberta Libraries

<https://archive.org/details/Goforth1967>

## ABSTRACT

A system has been developed whereby a pyrogram may be obtained for each separated component in a gas chromatographic effluent. These pyrograms may be used for "fingerprint" identifications of the peaks on a chromatogram. During the development of this system the characteristics of a low-pressure-drop packed column were examined as well as gas phase pyrolysis and rapid temperature programming.

Linear temperature programming with program rates up to 400°C per minute was developed and used with a wide range of carrier gas flow rates. Retention temperatures predicted from isothermal data were verified. The importance of correctly specifying the flow rate during rapid temperature programming became apparent during the investigation when predicted retention temperatures were otherwise less than the experimentally observed values.

Pyrolyzer design for gas phase pyrolysis was considered. The temperature profile for a tubular pyrolyzer was examined experimentally. The effects of temperature and residence time on gas phase pyrolysis were studied using several hydrocarbons.



## ACKNOWLEDGEMENTS

I wish to acknowledge the guidance and encouragement of my research advisor, Professor W. E. Harris. Any professional polish of the presentation in this thesis is primarily a result of his efforts, but the errors undoubtedly present I claim for myself.

Special thanks go to Dr. H. W. Habgood, particularly for his help in the interpretation of experimental results given in Chapter 3.

I should also like to acknowledge R. Kadlec and J. Love who detailed the electronic design and constructed a number of devices which made a large part of the research possible.

Financial assistance was provided by the National Research Council and the University of Alberta, and is gratefully acknowledged.



# C O N T E N T S

	Page
Abstract	i
Acknowledgements	ii
List of Tables	v
List of Figures	vi
Principal Symbols	xiii

## CHAPTER 1

INTRODUCTORY STATEMENT OF THE PROBLEM	2
1.01 Introduction	2
1.02 The Problem	2
1.03 Terms and Definitions	6

## CHAPTER 2

AN EXAMINATION OF A LOW-PRESSURE-DROP PACKED COLUMN	11
2.01 Preparation and Handling of the Low-Pressure-Drop Packing	12
2.02 Determination of Flow Rate, Temperature, and Sample Size for Use in the Study of the Effect of Packing Openness and the Proportion of Stationary Phase	17
2.03 The Effects of the Proportion of Stationary Phase and Packing Openness on Column Performance	21
2.04 Discussion	34

## CHAPTER 3

RAPID TEMPERATURE PROGRAMMING IN GAS CHROMATOGRAPHY	37
3.01 Methods of Calculation of Predicted Retention Temperature, Resolution, and Intrinsic Resolution	37
3.02 Experimental Requirements and Design	44
3.03 Prediction and Verification of the Retention Temperature as a Proof of the Theory of PTGC	52
3.04 Effect of Rapid Temperature Programming on Resolution	57
3.05 Discussion	63



## CHAPTER 4

GAS PHASE PYROLYSIS	69
4.01 Brief Survey of Pyrolysis in the Literature	69
4.02 Pyrolyzer Design	70
4.03 Systems for Pyrolysis Gas Chromatography	83
4.04 Results and Discussion	88

## CHAPTER 5

SYSTEM FOR THE IDENTIFICATION OF GAS CHROM- ATOGRAPHIC EFFLUENTS BY PYROLYSIS GAS CHROMATOGRAPHY	93
5.01 Experimental Design	94
5.02 Typical Results	104
5.03 Alternate System Arrangements	110
5.04 Final Comments	118

## CHAPTER 6

SUMMARY	122
BIBLIOGRAPHY	125
APPENDIX I	131
APPENDIX II	147
APPENDIX III	162



# LIST OF TABLES

Table	Title	
1.01	Gas Chromatography References	7
2.01	Weight of Stationary Phase Deposited in Low-Pressure-Drop Packed Columns.	15
2.02	Plate Height and Resolution as Functions of Packing Openness on the Proportion of Stationary Phase.	33
2.03	Effect of Loading Technique on Plate Height and Resolution for a Low-Pressure-Drop Packed Column.	35
2.04	Comparison of Best Results: Conventional and Low-Pressure-Drop Packed Columns.	36
3.01	Errors in Predicted Retention Temperatures.	56
4.01	Transition Times for Pyrolyzers of Different Geometries and Flow Rates.	79



## LIST OF FIGURES

### Figure

1.01	Representation of Dhont's application of P.G.C. to the identification of gas chromatographic peaks.	3
1.02	Sample collection and pyrolysis apparatus of Dhont.	3
1.03	Schematic representation of the system for the identification of gas chromatographic peaks by P.G.C.	4
1.04	Idealized chromatogram.	5
1.05	The relationship of temperature and time in linear temperature programming.	10
2.01	Low-pressure-drop packing.	12
2.02	Injection tee for direct on-column injection using a low-pressure-drop packed column.	17
2.03	Plate height as a function of flow rate for a low-pressure-drop packed column.	18
2.04	Effect of temperature on plate height.	19
2.05	Change in resolution with column temperature.	19
2.06	Plate height as a function of sample size.	20
2.07	Plate height as a function of sample size for a low-pressure-drop packed column and an open tube column.	21
2.08	Plate height and resolution as functions of the proportion of stationary phase.	22
2.09	Plate height as a function of flow rate for different proportions of stationary phase.	23
2.10	Specific retention volume as a function of the proportion of stationary phase for conventional packings.	26
2.11	Specific retention volume as a function of the proportion of stationary phase for low-pressure-drop packing.	26
2.12	Specific retention volume as a function of the packing openness with the proportion of stationary phase as a parameter.	27



2.13	Net retention volume as a function of the proportion of stationary phase with column openness as a parameter.	28
2.14	Plate height as a function of the proportion of stationary phase, the effect of sample capacity.	29
2.15	Plate height as a function of column openness.	30
2.16	Resolution as a function of packing openness.	31
2.17	Plate height and resolution as functions of column openness.	31
2.18	Plate height as a function of flow rate with packing openness as a parameter.	32
3.01	Procedure for the calculation of retention temperature in PTGC from isothermal data.	38
3.02	Procedure for the calculation of intrinsic resolution in PTGC.	40
3.03	Column- and oven-temperature lags.	44
3.04	Schematic diagram of direct electrical heating device of Bowen and Marks and its heating capabilities.	45
3.05	Apparatus for linear temperature programming using direct electrical heating of column tube.	46
3.06	Arrangement of flow control and measurement with a flame ionization and a thermal conductivity detector.	47
3.07	Maximum allowable time for complete elution of the second component of a resolved pair as a function of program rate.	48
3.08	Experimentally determined time required for the elution of an unretained component as a function of flow rate.	49
3.09	Flow rate required for elution of an unretained component in the time allowed by the duration of the program as a function of the program rate.	50
3.11	Experimentally accessible ranges of $r/\bar{F}_T$ .	51
3.12	The net retention volumes of pentane and heptane as functions of the reciprocal of the absolute temperatures for two columns.	52



3.13	The reciprocal of the retention volumes of pentane and heptane as a function of the absolute temperature for two columns.	53
3.14	The dependency of retention temperature of pentane and heptane on the ratio $r/F$ predicted from isothermal data for two columns.	54
3.15	Comparison experimentally determined and predicted retention temperatures.	54
3.16	Error in predicted retention temperature as a function of the $r/F$ ratio with individual heating rates indicated.	55
3.17	Absolute error in retention temperature as a function of the predicted retention temperature.	56
3.18	Peak separation required for the precise measurement of resolution.	58
3.19	Experimental coverage of $r/\bar{F}_{T_o}$ .	59
3.20	Resolution as a function of $r/\bar{F}_{T_o}$ for a conventional column and an open-tube column.	61
3.21	Intrinsic resolution as a function of $r/\bar{F}_{T_o}$ for a conventional and open-tube column.	62
3.22	Effect of dead space volume on intrinsic resolution.	65
3.23	The flow rate-plate height relationship for the conventional column and for the open-tube column.	66
3.24	The flow rate - plate height relationship as a function of temperature.	66
3.25	The $r/\bar{F}$ ratio at which $R$ or $R_i$ is at a maximum as a function of program rate.	67
4.01	Pyrolyzer of Dhont.	71
4.02	Expected temperature profile for a tubular pyrolyzer.	71
4.03	Idealized temperature profiles.	72
4.04	Apparatus for obtaining temperature profile of pyrolyzer.	74
4.05	Effect of linear flow velocity on the temperature profile of a tubular pyrolyzer.	75



4.06	Expected temperature profile for a tubular pyrolyzer showing the effect of the tube radius.	75
4.07	Graphical definition of transition zone.	76
4.08	Effect of linear flow velocity on transition zone length and transition time.	78
4.09	Effect of flow rate and linear flow velocity on the transition time.	80
4.10	Pyrolysis tube and furnace cavity dimension.	82
4.11	Schematic systems for independent control and optimization of pyrolysis parameters and subsequent gas chromatographic separation of pyrolysate.	85
4.12	n-Hexane pyrolysis as a function of temperature.	89
4.13	2,3-Dimethylbutane pyrolysis as a function of temperature.	89
4.14	2,3-Dimethylbutane pyrolysis as a function of residence time.	89
4.15	Comparison of the extent of pyrolysis as a function of temperature for 2,3-dimethylbutane, n-hexane, and benzene.	90
4.16	Idealized temperature profile of gradient temperature pyrolyzer.	92
4.17	Construction of gradient temperature pyrolyzer.	92
5.01	Schematic diagram of a system for the identification of gas chromatographic peaks by pyrolysis gas chromatography.	94
5.02	The effect of additive flow rates on retention time and peak shape.	95
5.03	Details of the construction of the trapping column.	96
5.04	Positioning of thermocouple for the determination of the heating-cooling characteristics of the trapping column.	97
5.05	Heating-cooling characteristics for the trapping column.	98
5.06	Effectiveness of trapping column.	98



5.07	Effectiveness of trapping column in retaining a $C_1 - C_4$ mixture of hydrocarbons.	99
5.08	Heating-cooling characteristics for column II.	101
5.09	Required differences in retention times, $\Delta t_R$ , and resolution $R$ , required in the initial chromatographic separation for the subsequent application of pyrolysis gas chromatography.	102
5.10	Resolution required in the initial chromatographic separation as a function of the difference in retention times, $\Delta t_R$ , of adjacent peaks.	104
5.11	Application of pyrolysis gas chromatography to the identification of gas chromatographic peaks.	105
5.12	Reduction of analysis time possible with temperature programming and the consequent improvement in system performance.	106
5.13	Chromatograms of $C_5$ to $C_{12}$ mixture of normal hydrocarbons.	108
5.14	Chromatogram for $C_5$ to $C_{12}$ mixture of normal hydrocarbons with sequential pyrogram for each component.	109
5.15	Temperature-time relationship for a 1 m 0.10" i.d. steel tube using direct electrical heating.	110
5.16	Effect of the duration of carrier flow stoppage on the peak broadening in stopped-flow chromatography.	111
5.17	Effect of band position in column on the peak broadening stopped-flow chromatography.	112
5.18	Pyrogram of 2,3-dimethylbutane and a pyrogram of 2,3-dimethylbutane + 10% n-hexane impurity.	114
5.19	Selective trapping of effluent from initial chromatographic separation.	115
5.20	Schematic of time requirements for system with two columns in the second chromatographic step employing selective trapping.	116
5.21	Isothermal and programmed temperature pyrograms for 2,3-dimethylbutane.	117



5.22	Schematic diagram of the analysis system of Merritt and Robertson.	118
5.23	Apparatus for gas phase photolysis.	119
5.24	Mass spectrogram, pyrogram, and chromatogram of the photolytic degradation products of 2,3-dimethylbutane.	120
A 1.01	Schematic of Aerograph Linear Temperature Programmer Model 326 with modifications for switch selection of internal or external control and for use with direct electrical heating.	133
A 1.02	Low voltage power supply for use with direct electrical column heating.	134
A 1.03	Temperature-time relationship for direct electrical heating.	134
A 1.04	Schematic diagram of high current capacity silicon controlled rectifier bank.	135
A 1.05	Linearity of program rate and temperature uniformity during temperature programming using direct electrical heating.	136
A 1.06	Rate determining resistance system and program rate as a function of the controlling resistance.	137
A 1.07	External switch arrangement on injection tee for program initiation and event marking.	138
A 1.08	Schematic of Aerograph Linear Temperature Programmer Model 326 with modifications for external program initiation.	139
A 1.09	Gas tight electrically insulating connections for use with direct electrical heating.	140
A 1.10	Noise in F.I.D. detection using direct electrical heating.	141
A 1.11	Calibration for initial temperature control and internal pyrometer correction.	141
A 1.12	Air bath for coiled columns.	145
A 1.13	Calibration of recorder for an iron-constantin thermocouple.	146
A 1.14	Power supply for rapid heating of trapping column.	145



A 1.15	Trapping U-tubes for gas chromatographic effluents.	146
A 1.16	Rotometer calibration for helium.	146
A 2.01	Idealized chromatogram from IUPAC recommendations.	149
A 2.02	Idealized chromatogram illustrating resolution as defined by Kaiser.	150
A 2.03	Effect of column on relative peak separation, hypothetical chromatograms.	151
A 2.04	Effect of relative peak sharpness of resolution.	152
A 2.05	Relative peak sharpness, $Q$ , relative peak separation, $S$ , plate height, $H$ , and resolution, $R$ , as functions of the carrier gas flow rate.	155
A 2.06	Spread per unit length and plate height as functions of the carrier gas flow rate.	156
A 2.07	Intrinsic resolution as a function of the ratio $r/F$ for a conventional and a capillary column.	157
A 2.08	The variation in plate height and the number of theoretical plates and resolution with the proportion of stationary phase.	159



## PRINCIPAL SYMBOLS

$A$	Cross-sectional area, $\text{cm}^2$
$F$	Flow rate, ml per minute
$F_{T_o}$	Flow rate corrected for pressure gradient measured at a column temperature $T_o$ and corrected to $25^\circ\text{C}$
$F_o$	Flow rate at column outlet
$F_p$	Flow rate in pyrolysis zone
$\bar{F}, \bar{F}_{T_o}$	Flow rates per gram of stationary phase
$H(\text{HETP})$	Plate height, height equivalent to a theoretical plate
$j$	Pressure-gradient correction factor
$k$	Partition ratio, ratio of moles of solute in the stationary phase to moles of solute in the mobile phase
$K$	Partition coefficient
$L$	Column or tube length
$n$	Number of theoretical plates
$p_i, p_o$	Pressure at inlet and outlet of column
$\underline{p}$	Ratio $p_i/p_o$
$r$	Program rate, degrees per minute
$r/F$	Ratio of program rate to flow rate in PTGC
$R$	Resolution, pyrolyzer tube radius, or gas constant
$R_i$	Intrinsic resolution
$T$	Temperature
$T_a$	Ambient temperature
$T_o$	Initial temperature of a program
$T_p$	Pyrolysis temperature
$T_R$	Retention temperature
$t$	Time
$t_{ds}$	Retention time for a nonretained material
$t_r$	Pyrolyzer residence time
$t_z$	Transition time, Equation (4.04)
$u$	Linear flow velocity, cm per second
$V$	Isothermal retention volume



$V_{ds}$	Dead space volume
$V_P$	Retention volume in PTGC
$V_{T_R}$	Retention volume at the retention temperature
$\bar{V}, V_{ds}$	Volumes per gram of stationary phase
$v$	Pyrolyzer tube volume
$W$	peak base width
$w$	weight of stationary phase in grams
$Z$	Length of transition zone, Figure 4.07
$\alpha$	relative volatility
$\sigma$	Standard deviation
$\rho$	Relative velocity difference



# RAPID TEMPERATURE PROGRAMMING AND PYROLYSIS GAS CHROMATOGRAPHY

## 1. INTRODUCTORY STATEMENT OF THE PROBLEM

### 1.01 INTRODUCTION

The analysis of materials, particularly solids such as high molecular weight polymers, using pyrolysis gas chromatography (PGC) is a well established practice (15,18,29,30,35,83). The pyrolysis technique has been shown to be of considerable practical value for the identification of complex organic molecules (64). Structural information has also been obtained by the examination of the nature and distribution of pyrolysis products (30,48,92).

The application of mass spectrometry to the examination of individual components in gas chromatographic effluents is finding increasing use. If PGC can be adequately developed it may find use as a substitute for, or an accessory to, the mass spectrograph in such an application. By decreasing the cost and complexity of such a system the technique would become available for more applications and its full potential more nearly realized.

Dhont (19,20) applied PGC to the identification of gas chromatographic peaks by pyrolysis of the material condensed in a cold trap at the outlet of the gas chromatograph as illustrated in Figure 1.01.

The system described by Dhont entails the pyrolysis of materials in the gas phase. The pyrolysis system shown in Figures 1.01 and 1.02 required appropriate valving and transfer of the sample.

### 1.02 THE PROBLEM

An investigation of the possibilities of the application of rapid gas chromatographic analysis of the products of a



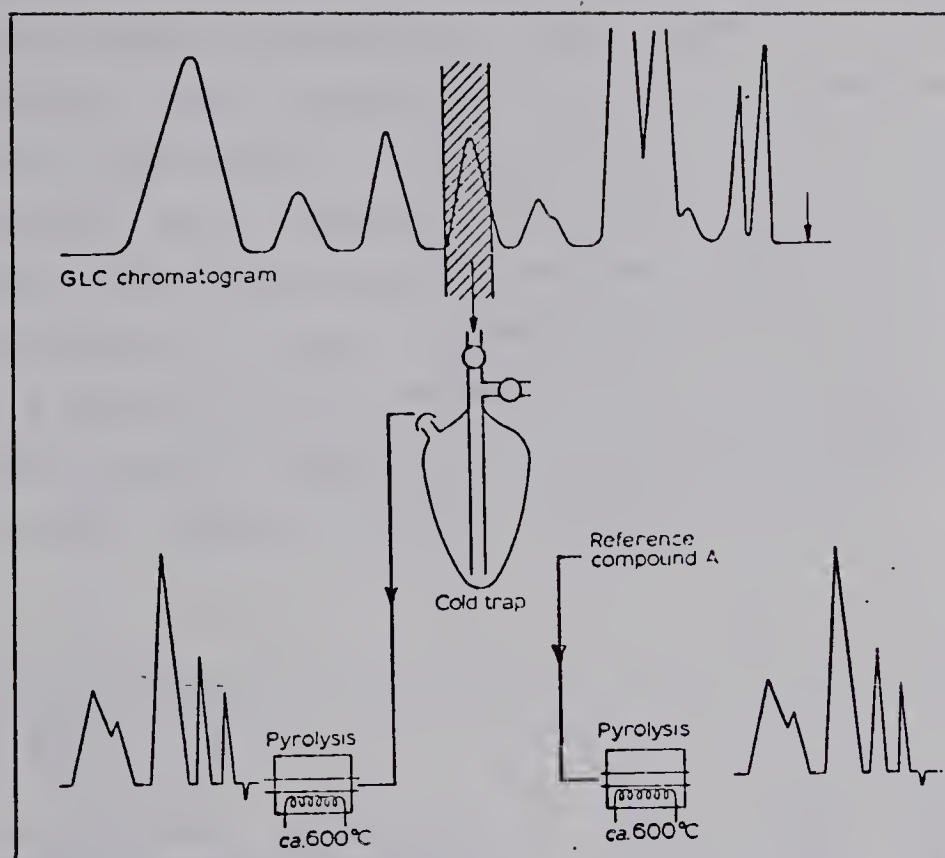


Figure 1.01 Representation of Dhont's application of P.G.C. to the identification of gas chromatographic peaks (101).

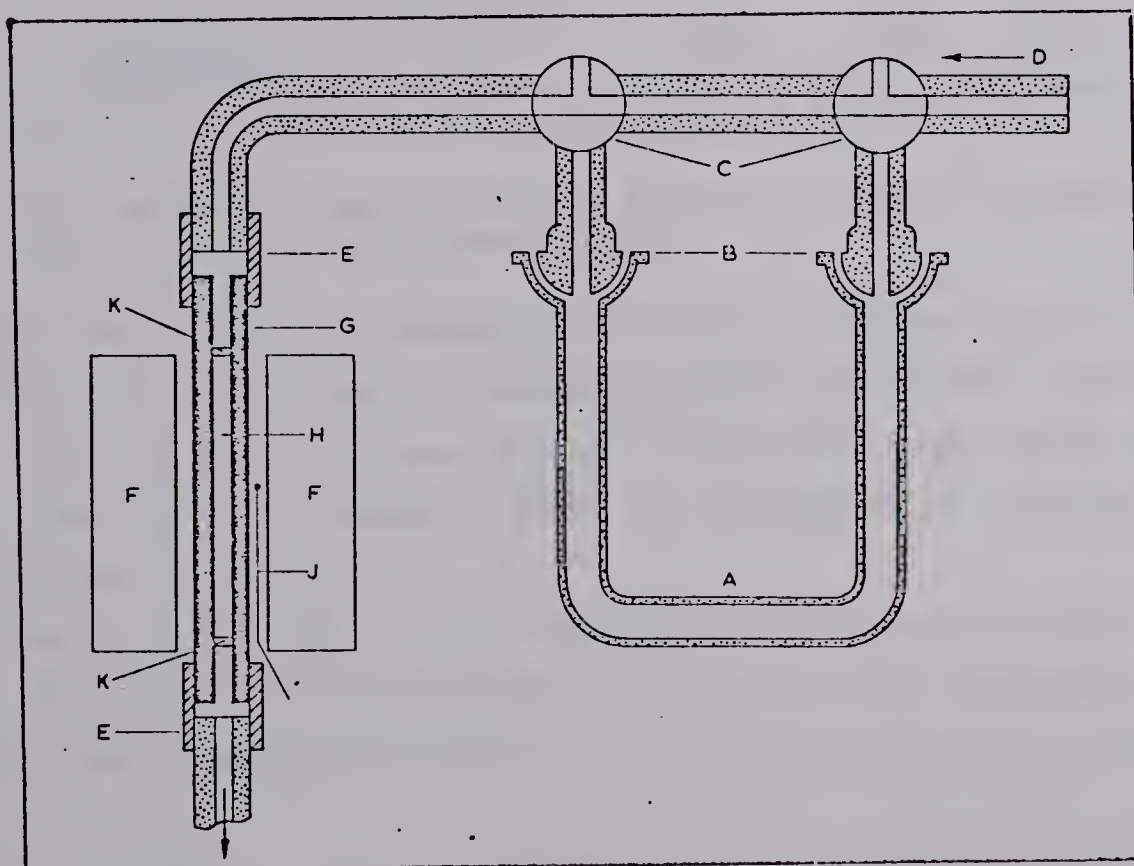


Figure 1.02 Sample collection and pyrolysis apparatus of Dhont (19).



gas phase pyrolysis to the identification of gas chromatographic peaks was the basis for the research to be covered in this thesis. This technique was to be based on the pyrolysis of components in the effluent stream from a gas chromatograph. As an identifying technique the products from the pyrolysis were subsequently to be analyzed in a second gas chromatographic step. A system will be described with which this process may be carried out on a continuous basis without intermediate handling or transfer of samples. The system is shown schematically in Figure 1.03.

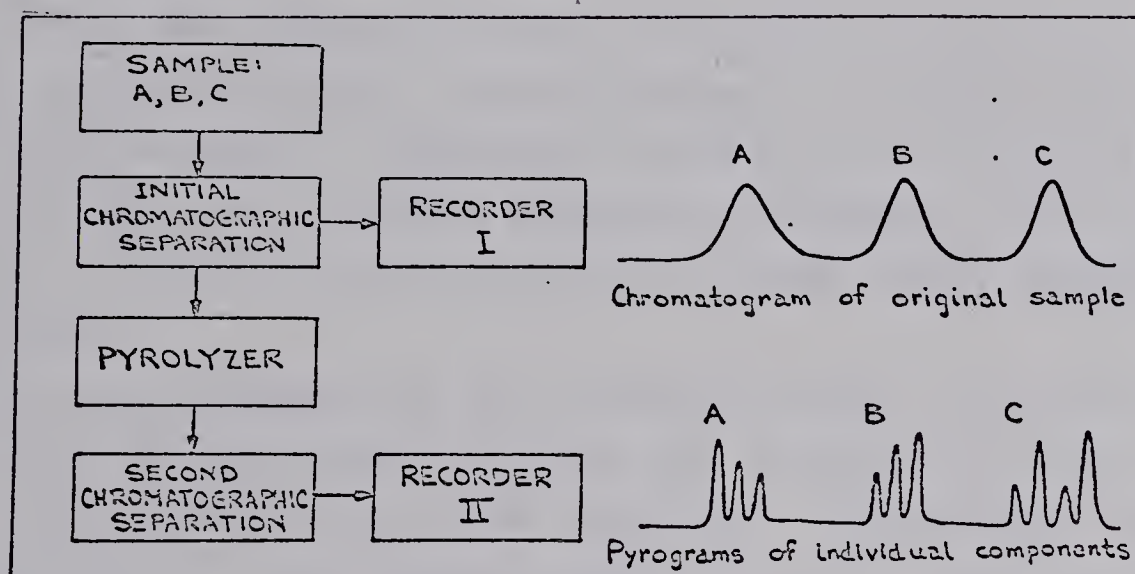


Figure 1.03 Schematic representation of the system for the identification of gas chromatographic peaks by PGC.

The general requirements of such a system are a pyrolysis technique, a rapid gas chromatographic technique, and a system design having some automation to allow uninterrupted operation. These several requirements will be examined in separate sections of this thesis.

The initial gas chromatographic separation is conventional and will be considered only by way of example in describing the completed system as was illustrated in Figure 1.03.

In pyrolysis it is necessary to have clearly defined and reproducible experimental conditions. A particularly difficult problem in the pyrolysis of liquids or solids is the defi-



nition of the pyrolysis temperature since the sample may be subjected to a range of temperatures even during a supposedly constant temperature pyrolysis. Poor temperature control, catalytic effects, uncontrolled sample size and concentration, and variations in the amount of oxygen present all cause erratic results. Although gas phase pyrolysis (79) has found relatively infrequent application it can minimize the problems arising from erratic results. Details of pyrolyzer design and operation to accomplish this for a gas phase pyrolysis, the logical choice for the system being developed, will be examined.

Little has appeared in the literature concerning quantitative reproducibility using pyrolysis in combination with gas chromatography. Keulemans and Perry (62) studied repetitive pyrolysis of a single compound and Andrew, Phillip, and Semlyen (5) made an interlaboratory study using different pyrolyzers.

The requirements of the chromatographic separation subsequent to pyrolysis dictated the general direction of a large part of the work to be described. Programmed temperature techniques were deemed essential as it was anticipated that the boiling point range of the pyrolysis products would be greater than 50°C (41). Requirements of resolution and analysis time, which will be examined in detail, made it necessary to develop a system for rapid programming. The use of PTGC influenced the type of columns examined with particular regard to the desirability of a wide latitude in flow rate.

Parallel to the practical approach thus far indicated was an extension of the theory of PTGC to rapid programming. This was made possible by the development of a new technique allowing linear programming at rates previously inaccessible.



### 1.03 TERMS AND DEFINITIONS

The definitions and methods of calculation for some important chromatographic parameters used in the subsequent sections of this thesis are given here. This material may be found in detail in any of several books on gas chromatography such as those given in Table 1.01. A discussion of significant parameters is included in Appendix II.

The nomenclature and symbolism is consistent with that used in Programmed Temperature Gas Chromatography by Harris and Habgood (40). A list of symbols is given on page xiii.

#### Peak Characterization

A peak on a chromatogram is conventionally characterized by its position and shape. This characterization is accomplished using the factors shown on the idealized chromatogram in Figure 1.04.

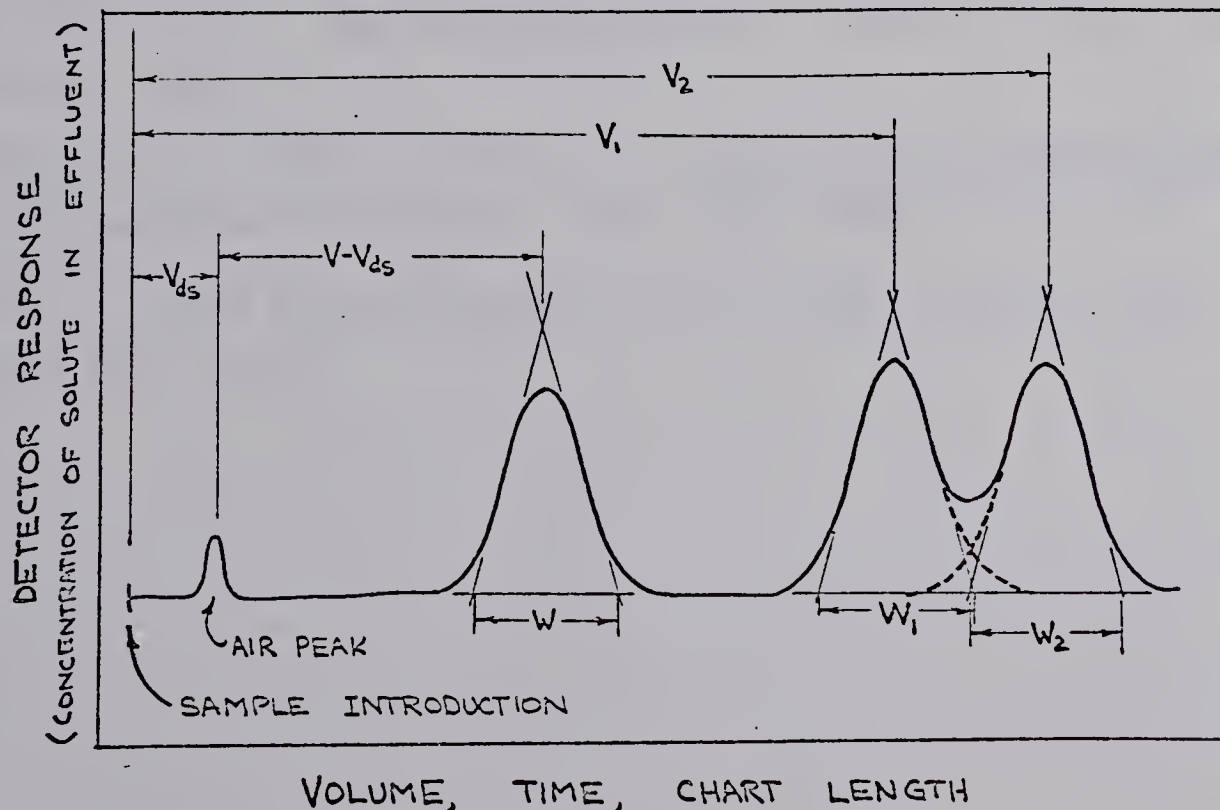


Figure 1.04 Idealized chromatogram.



TABLE 1.01 GAS CHROMATOGRAPHY REFERENCES

- Ambrose, D., Ambrose, B. A., Gas Chromatography, Newnes Ltd., London, 1961.
- Ettre, L. S., Open Tubular Columns in Gas Chromatography, Plenum Press, New York, 1965.
- Giddings, J. C., Dynamics of Chromatography, Marcel Dekker, Inc., New York, 1965.
- Harris, W. E., Habgood, H. W., Programmed Temperature Gas Chromatography, John Wiley & Sons, Inc., New York, 1966.
- Kaiser, R., Gas Phase Chromatography, Vols. 1, 2, and 3, Butterworths, London, 1963.
- Keulemans, A. I. M., Gas Chromatography, Reinhold Publishing Corporation, New York, 1959.
- Knox, J. H., Gas Chromatography, Academic Press, New York, 1962.
- Littlewood, A. B., Gas Chromatography, Academic Press, New York, 1962.
- Dal Nogare, S., Juvet, R. S., Jr., Gas-Liquid Chromatography, Interscience Publishers, New York, 1962.
- Purnell, H., Gas Chromatography, John Wiley & Sons, Inc., New York, 1962.



The peak position is referred to by the time on the chromatogram from the point of sample introduction to the maximum of the peak of the eluted component and is called the uncorrected retention time,  $t_R$ . A knowledge of the flow rate,  $F$ , allows calculation of the retention volume,  $V$ .

$$V = F \cdot t_R \quad (1.01)$$

The area between the extrapolated base line and the peak is the peak area. The peak area is proportional to the amount of the component in the sample and is a function of detector response (21) and such mechanical details as recorder chart speed and attenuation.

The peak itself is generally characterized by its width. The width,  $W$ , is measured at the base line intercepts of tangents to the inflection points on either side of the peak. Assuming a Gaussian peak (33) this base width corresponds to four standard deviations,  $\sigma$ .

#### Flow Rate

In gas chromatography the mobile phase is compressible and subject to large volumetric temperature effects. The flow rate,  $F$ , which is the volume of gas per unit time, must be corrected for pressure gradient and expressed at a standard temperature. With wet flowmeters such as the soap-film flowmeter, a correction should be made for the vapor pressure of water in calculating the volume of gas.

As a necessary condition for carrier gas flow the pressure at the column inlet,  $p_i$ , must be greater than at its outlet,  $p_o$ . The ratio of  $p_i$  to  $p_o$  is denoted by the symbol  $\underline{P}$ . James and Martin (50) developed a pressure-gradient correction factor,  $j$ , in terms of this ratio.

$$j = \frac{3}{2} \frac{(\underline{P}^2 - 1)}{(\underline{P}^3 - 1)} \quad (1.02)$$

Throughout this work the pressure-gradient-correction factor was applied to gas volumes and flow rates measured at the



column outlet to obtain values equivalent to those that would be produced by a noncompressible fluid.

#### Calculation of Plate Height and Resolution

Plate height or the height equivalent to a theoretical plate,  $H$  or HETP, is the length of the column divided by the number of theoretical plates,  $n$ .

$$H = \frac{L}{n} \quad (1.03)$$

In isothermal gas chromatography  $n$  is defined by the equation

$$n = 16 \left( \frac{V}{W} \right)^2 \quad (1.04)$$

$V$  and  $W$  must be in the same units, commonly distances on the chromatogram, and are illustrated in Figure 1.04.

Resolution is defined as the ratio of the peak separation to the average peak width.

$$R = \frac{(V_2 - V_1)}{0.5(W_2 + W_1)} \quad (1.05)$$

where  $V_2, V_1, W_2$  and  $W_1$  are as illustrated in Figure 1.04.

Karger (57) recently reviewed and evaluated this expression for resolution. While resolution, as defined by Equation (1.05) is not an expression in fundamental chromatographic terms it is nevertheless useful in evaluating a chromatogram. Karger derived from the internationally accepted Equation (1.05) a new expression for resolution.

$$R = \frac{1}{2(1+W')} \left( \frac{\alpha-1}{\alpha} \right) \left( \frac{k_2}{1+k_2} \right) n^{\frac{1}{2}} \quad (1.06)$$

where  $W'$  is the peak ratio  $W_1/W_2$ . This equation relates resolution to the fundamental parameters of relative volatility,  $\alpha$ , and partition ratio,  $k$ , and introduces the new factor  $W'$ . The number of theoretical plates,  $n$ , is also used.



Appendix II includes a discussion of the historical development, theoretical significance, and alternative characterizing factors for H(or HETP), and the number of theoretical plates,  $n$ .

#### Linear Temperature Programming

During a linear temperature program the rate of temperature increase,  $r$ , is constant. The temperature,  $T$ , of the system at any time,  $t$ , may be calculated from a program rate and the initial temperature,  $T_0$ , by the equation

$$T = T_0 + rt \quad (1.07)$$

These relationships are shown in Figure 1.05.

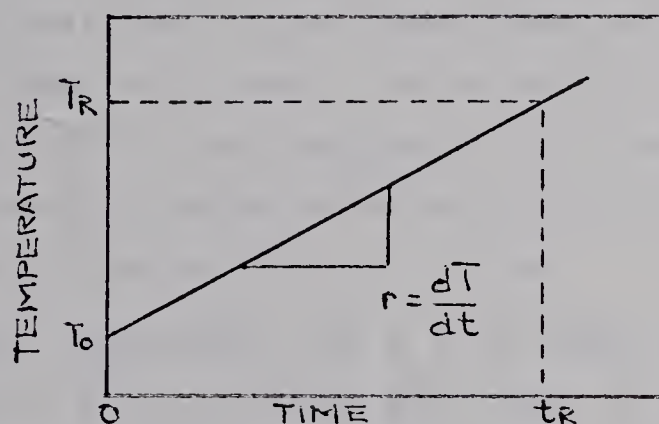


Figure 1.05 The relationship of temperature and time in linear temperature programming.

Throughout this thesis programming will refer exclusively to linear temperature programming. Non-linear programming (94) may be advantageous in some cases but was not examined in the work reported here.



## 2. AN EXAMINATION OF A LOW-PRESSURE-DROP PACKED COLUMN

Teranishi (97) described a low-pressure-drop column the packing for which was in the form of helices of small diameter wire. Column packing in this general form has also been reported by other workers (65,90). The use of open tubular columns of diameters larger than those of capillary columns has been described (26,74,81).

Teranishi reported a column efficiency of 100 plates per foot for the low-pressure-drop packed column. In the work described here column efficiencies of 100 plates per foot were also found but only under conditions of poor resolution, as will be discussed later. The initial publication of Teranishi gave no details concerning the method of preparing the packing with regard to spacing the turns of the helices. Neither was there justification for the particular tube or wire diameters used. In a later publication (96), which appeared after the completion of the experimental work on low-pressure-drop packing reported in this thesis, details of the packing preparation were given.

The column efficiency of a 0.10 inch i.d. unpacked tube was estimated to be 10 plates per foot by Teranishi (97). As determined here, this was shown to be low by a factor of ten, that is, an open 0.10 inch tube can be operated at conditions giving an efficiency of 100 plates per foot. Operation of the open tubular column under the condition required to give this efficiency resulted in a much lower sample capacity than that of the low-pressure-drop packed column with the same number of theoretical plates.

Such low-pressure-drop packed columns as prepared by Teranishi, when used with non-destructive detectors, allow isolation of tenths of a milligram quantities of pure materials per run. These quantities are desirable where mass spectrometry and other techniques need to be applied for identification.

As pointed out in the introduction, a wide latitude in flow rates is desirable in the study of programmed tempera-



ture gas chromatography (PTGC). The low-pressure-drop packed column would have permitted this wide latitude. Further, there were other considerations which would have made the column readily adaptable to rapid temperature programming. These properties include a low heat capacity, allowing high heating and cooling rates, and a high thermal conductivity ensuring a uniform temperature distribution even with high heating rates.

## 2.01 PREPARATION AND HANDLING OF THE LOW-PRESSURE-DROP PACKING

### Preparation of the Packing

The helices of the low-pressure-drop packing were formed from 33 gauge (0.007" diameter) Karma wire.\* As the packing consists of two concentric helices two winding mandrels were required. The larger was 0.062 inch in diameter and the smaller 0.022 inch. The mandrels were 35 cm long supported at each end by pin chucks. One chuck was freely rotating in a ball bearing race while the other was driven with a variable speed motor.

The helices were wound on the mandrels usually to a length of 33 cm. When the winding tension was removed there was some springing open of the coils that increased their inside diameter slightly. The relative sizes of the two helices and the tube are shown in Figure 2.01.

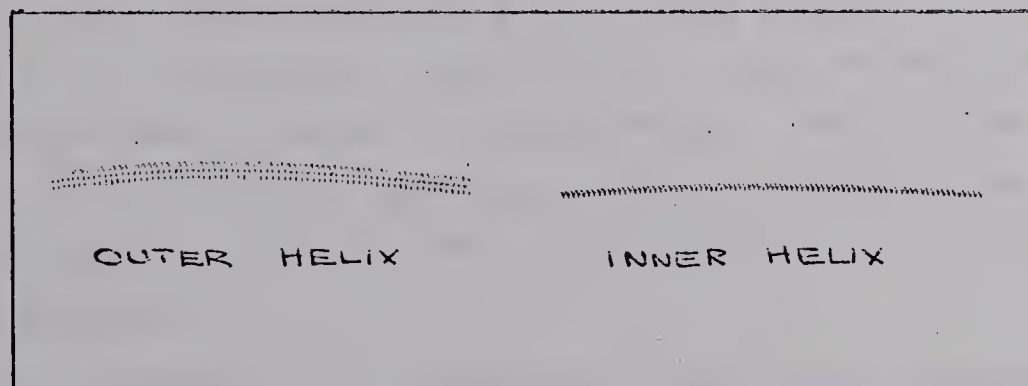


Figure 2.01 Low-pressure-drop packing. Scale 1:1 with helices expanded linearly approximately threefold for greater clarity.

\*Dryer-Harris Company, Harrison, New Jersey.



To obtain varying degrees of separation between adjacent turns (i.e., openness) two approaches could have been used. Teranishi (95) spaces the turns as they are wound on the mandrel. To do this would, besides being tedious, be less reproducible. In this work it was necessary to know as accurately as possible the openness of the helices.

With this in mind the packing of different degrees of openness was prepared by giving the closed helices a permanent stretch. For example a helix of unit length that was stretched to 1.3 units is described by an openness of 1.3. The ends of the stretched helix were not uniform and it was necessary to remove about 1 cm from each.

The packing was loaded into the tube by suction with the larger diameter helices all added before any of the smaller. No difficulty was encountered until the tube was packed with helices of 1.5 openness. In the cases of 1.4 or 1.5 openness there was some compression of the spring-like helices. The total length of the helices was measured before they were placed in the tube. The final length was known so the openness figure could be corrected for the compression which occurred.

Above an openness of 1.5 the helices were visually not uniform, some sections being less open than others. Although a net openness of 1.6 could be obtained this lack of uniformity would have introduced an additional unknown. Loading helices of 1.6 openness into the tube was so difficult that deformities were caused in the packing. For these reasons an openness of 1.5 is the maximum studied although Teranishi (95) estimates a 200% stretch, equivalent to an openness of 4, for his packing.

A comparison of the Teranishi-prepared low-pressure-drop packing and that prepared here is in order. The Teranishi packing was made in short 2 to 3 cm lengths which were dropped



one after another into the column tube. These short lengths allowed both the larger and smaller diameter helices to be formed from one continuous piece of wire. The inner helix was then held concentrically in the larger, at least at one end. This should limit longitudinal compression. Teranishi apparently has not been much concerned with the exact openness of the packing or at least has not reported its effect on performance or the effect of compression.

The packing prepared here does undergo compression but this can be corrected for and a net openness reported. That the inner helix is unsupported seems, on reflection, to be of minor importance. The geometry of the system is such that the number of points of contact would be small.

### Cleaning Sequence

The wire from which the packing was prepared had a thin oil film on it probably as a result of the fabrication process. To remove this oil and to prepare the metal surface for coating with the stationary phase the following sequence of solvents was used. Chloroform, acetone, methanol, water, 1% aqueous phosphoric acid, water, methanol, acetone, and finally chloroform again. Two 10 ml portions of each solvent were passed through the packed tube under suction at 25°C. This regimen is that used by Teranishi (95). The mechanics of the process are also recommended by Ettre (25) and the sequence of solvents is similar to that suggested by Hollis (45). The complete cleaning process as carried out took from 10 to 20 minutes.

To remove a coating of the stationary phase, in preparation for recoating, four 15 ml portions of chloroform were found to be sufficient.

### Stationary Phase Deposition

The amount of stationary phase deposited on the helical packing was found to be critically dependent on the loading



technique. The following technique was carefully followed for the preparation of each column. Ten milliliters of the liquid phase in a solvent were added at the inlet end of the column. With the temperature at 25°C, carrier gas was used to blow the excess solution from the tube. This was done at a rate of 20 ml per minute for 15 minutes. After this time vacuum was applied to the exit end of the column to remove the remaining solvent and solvent vapors. Fifteen minutes were adequate for this step.

The amount of stationary phase deposited was controlled by using solutions of different concentrations. These concentrations varied from 0.2 to 5.0% and are used as an indication of the proportion of stationary phase in the following sections.

The absolute amount of stationary phase deposited in the column was estimated experimentally by recovery and subtraction of the excess solution from the known amount added. Values for a column with 1.2 openness packing and an open tube column are given in Table 2.01. The data in Table 2.01 indicate that the addition of the packing approximately doubles the amount of stationary phase retained in the column.

TABLE 2.01 WEIGHT OF STATIONARY PHASE (SF-96) DEPOSITED IN LOW PRESSURE PACKED COLUMNS\*

Column	% Stationary Phase	gms Stationary Phase/3 m	gms/m
1.2 openness	5	0.19	0.06
	2	0.076	0.025
	1	0.038	0.013
	0.5	0.019	0.006
	0.2	0.0076	0.0025
open tube	5	0.085	0.029

\*Values for 2,1,0.5 and 0.2% stationary phase were estimated assuming retention of a constant volume of the coating solution and from the experimental data for the 5% solution.



## Apparatus

The sources of the chemicals used and descriptions of the apparatus finding common use throughout the research reported in this thesis are given in Appendix I. The following comments on apparatus are of specific importance to this portion of the research.

### Constant Temperature Apparatus

Temperature control was made possible through the use of oil bath arrangement essentially as described by Habgood and Harris (36). A six inch diameter Dewar Flask permitted the use of larger coils and the 3 m columns were coiled to a 5 1/2 inch diameter. Heating was by means of a 150 watt knife heater and cooling was accomplished by using a 3 inch diameter water coil of 1/4 inch copper tubing. For work at 25°C the apparatus was adequate. Using a 610 mm, -1 to 101°C thermometer the measured temperature was always within  $\pm 0.1^\circ\text{C}$  at 25°C. For work at elevated temperatures, 50°C and above, the temperature control was more difficult and demanded frequent attention.

### Sample Injection

All sample injections were made with a No. 701-N Hamilton 10  $\mu\text{l}$  syringe. A No. 7001-N 1.0  $\mu\text{l}$  syringe was tried but the reproducibility of sample injection using it was poor.

The injection port was a silicone rubber disc in a 1/4" brass all-tube Swagelok tee. The injection port was used at room temperature and no effect was noted on raising the temperature to about 65°C even for the samples of highest boiling point injected. The design of the column and injection port was such as to allow the sample to be placed directly on the head of the column and is shown in Figure 2.02. This probably accounts for the lack of a temperature effect on injection as the sample is placed directly on the top of the column and need not be vaporized or transported in the body of the injection port.



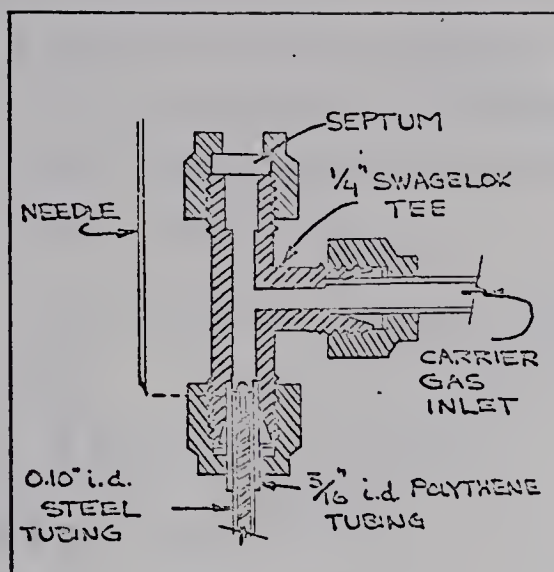


Figure 2.02 Injection tee for direct on-column injection using a low-pressure-drop packed column.

## 2.02 DETERMINATION OF FLOW RATE, TEMPERATURE, AND SAMPLE SIZE FOR USE IN THE STUDY OF THE EFFECTS OF PACKING OPENNESS AND THE PROPORTION OF STATIONARY PHASE.

The comprehensive examination of the numerous variables of gas chromatographic column operation and their complex interrelationships demands simplifying initial assumptions. The starting point for this work was an investigation of the operational parameters of flow rate (F), temperature (T) and sample size with a column of fixed dimensions and constant stationary phase loading. It was recognized that each of these parameters could be separately optimized for each column in the latter work. To do so would have vastly multiplied the work required and would have been of marginal value for the comparative relationships.

From the graphs that appear in the following sections the effects of flow rate, temperature, and sample size on plate height (H) and resolution (R) may be noted. Pertinent experimental data are included on each graph.

### Flow Rate

The dependence of plate height on flow rate for the



low -pressure-drop column follows that of more conventially packed columns. A plot of plate height as a function of the flow rate, Figure 2.03, reveals a minimum in plate height. The flow rate at which this minimum occurs will be referred to as the optimum flow rate,  $F_{opt}$ .

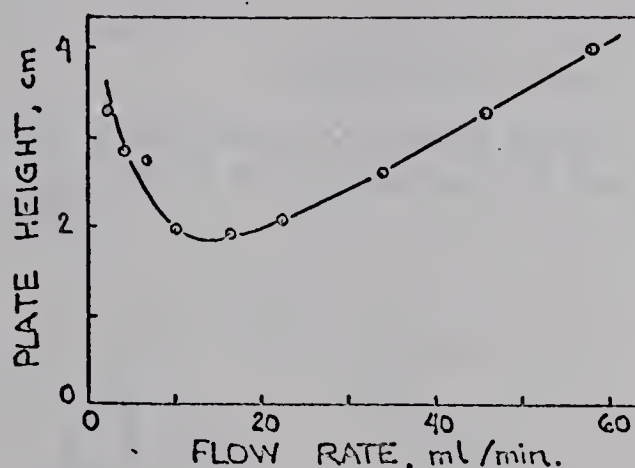


Figure 2.03 Plate height as a function of flow rate for a low-pressure-drop packed column. The column was 3m with 5% SF-96 on 1.3 openness packing at 25°C. Sample was 0.2  $\mu$ l n-pentane.

A flow rate, 20 ml per minute, for the examination of the other column parameters was chosen primarily on the basis of convenience. The optimum flow rate,  $F_{opt}$ , depends on the construction at the column and other factors and is examined in more detail in a section that follows.

#### Temperature

Harris and Habgood (39) have carefully examined temperature effects in gas chromatography. The effect of temperature on column efficiency is complex and requires the examination of many factors for its interpretation.

It is recognized that, for a given solute-solvent system plate height usually decreases with increasing temperature. For example, Figure 2.04, taken from Duffield and Rogers (22) illustrates this phenomenon.

Resolution similarly decreases with increasing temperature as shown in Figure 2.05 for two pairs of normal hydrocarbons in a low-pressure-drop packed column.



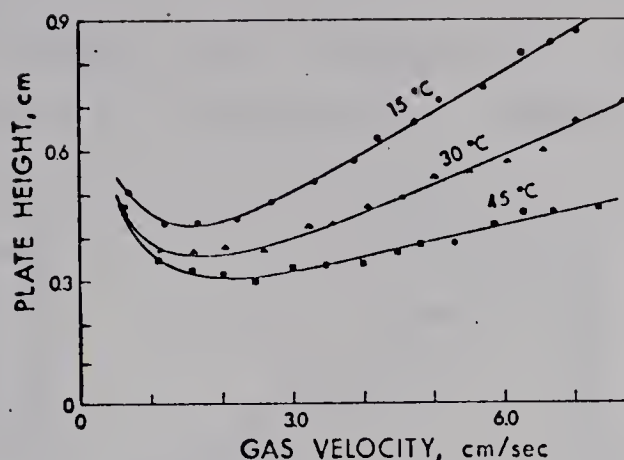


Figure 2.04 Effect of temperature on plate height. Samples were 2,3-dimethylbutane. Column, 1 m containing 39% carbowax 400. From Duffield and Rogers (22).

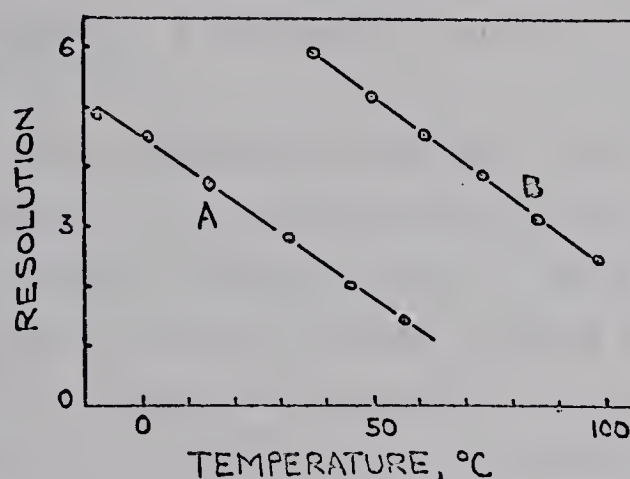


Figure 2.05 Change in resolution with column temperature for the pair n-pentane-n hexane (A) and n-hexane-n octane (B) column as described in Figure 2.03. Flow rate of 20 ml per minute.

An operating temperature of 25°C was chosen primarily on the basis of convenience. A lower temperature would have given improved resolution but would have, at the same time, increased retention times. The rate of change of resolution with temperature was found to be essentially constant over a wide range of temperatures, Figure 2.05, necessitating the same careful attention to temperature control regardless of the specific temperature chosen.

#### Sample Size

The choice of a fixed sample size eliminates some difficulties in the interpretation of column performance. It is generally recognized that the larger the sample the poorer



the performance. Boheman and Purnell (9) demonstrated the effect of sample size for isopropanol, Figure 2.06.

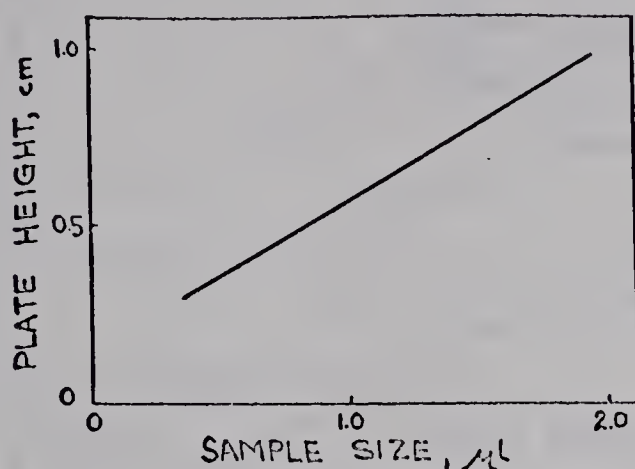


Figure 2.06 Plate height as a function of sample size for isopropanol. From Boheman and Purnell (9).

A decrease in the proportion of the stationary phase necessitates the use of a smaller sample size to prevent overload broadening. In one sense, then, it would seem best to use small samples with those columns having a low proportion of stationary phase. There are practical reasons why this is not always possible. It should be recognized in what follows that the sample size was fixed and that overload broadening can at least partially account for the deteriorating performance of the columns having the lower proportions of stationary phase.

A reduction in temperature would have given improved resolution and it would have also increased sample capacity. The temperature was not examined extensively as a variable because its effects have been examined in detail elsewhere (39, 40) and are not unique to the type of column being considered here.

The choice of 0.2  $\mu\text{l}$  was made as the best compromise suiting injection reproducibility, detector sensitivity and convenience. From Figure 2.07 it can be seen that 0.2  $\mu\text{l}$  is in the region where plate height is changing only slowly with increasing sample size, particularly for the compounds of lower molecular weight and for columns containing a high or moderate proportion of stationary phase.



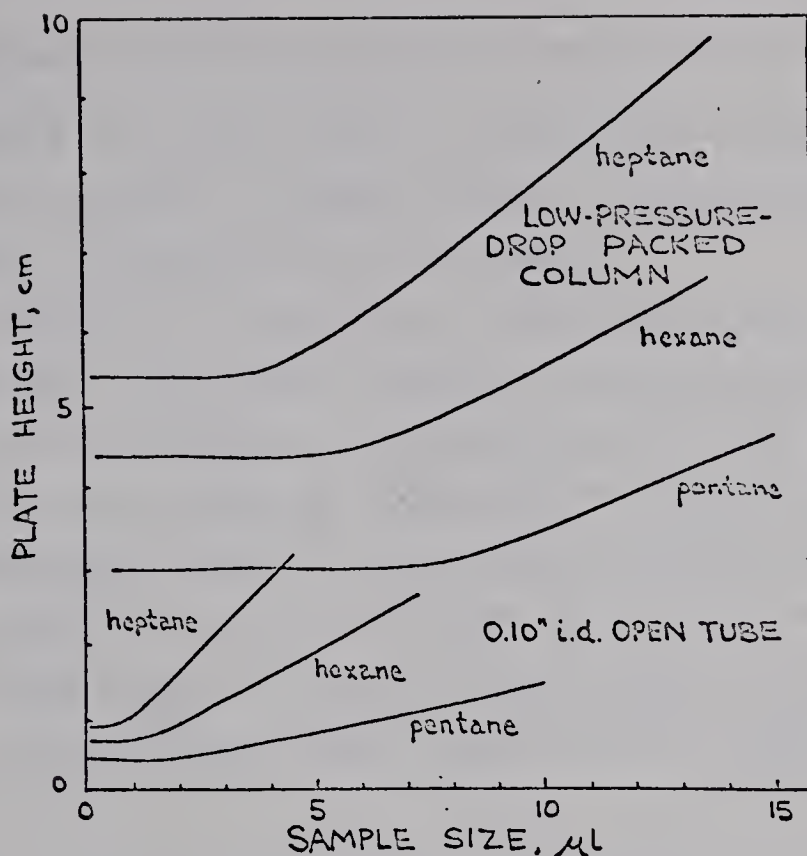


Figure 2.07 Plate height as a function of sample size for a low-pressure-drop packed column and an open tube column. Packing of 1.4 openness was employed. Column temperature was 25°C and the flow rate was 20 ml per minute.

In all cases the sample size of 0.2  $\mu$ l is less than the "maximum permissible sample size" defined by Keulemans (60) as the "maximum amount which can be injected into a column without more than 10% loss in efficiency".

### 2.03 THE EFFECTS OF PROPORTION OF STATIONARY PHASE AND PACKING OPENNESS ON COLUMN PERFORMANCE

The unique feature of the low-pressure-drop column described by Teranishi is the nature of the support used for the liquid phase. The helices of small diameter wire may be formed in such a manner as to allow successive turns to touch or by expanding them to allow varying degrees of openness. The thickness of the deposited stationary phase may also be controlled. These two parameters may be independently studied for this type of packing. The methods for the preparation of columns of different degrees of openness and stationary phase loading have already been described.



## Effects of Proportion of Stationary Phase

The effect of proportion of stationary phase on the conventionally packed columns and the low-pressure-drop packed column is essentially the same.

As the amount of stationary phase per unit length of column decreases the plate height also decreases. This decrease in plate height is accompanied by an increase in resolution up to a certain point, after which resolution also begins to decrease with the decreasing proportion of stationary phase, as may be seen in Figure 2.08. As can be seen in Figure 2.08 and also as will be discussed in Appendix II, resolution may increase even though plate height is also increasing.

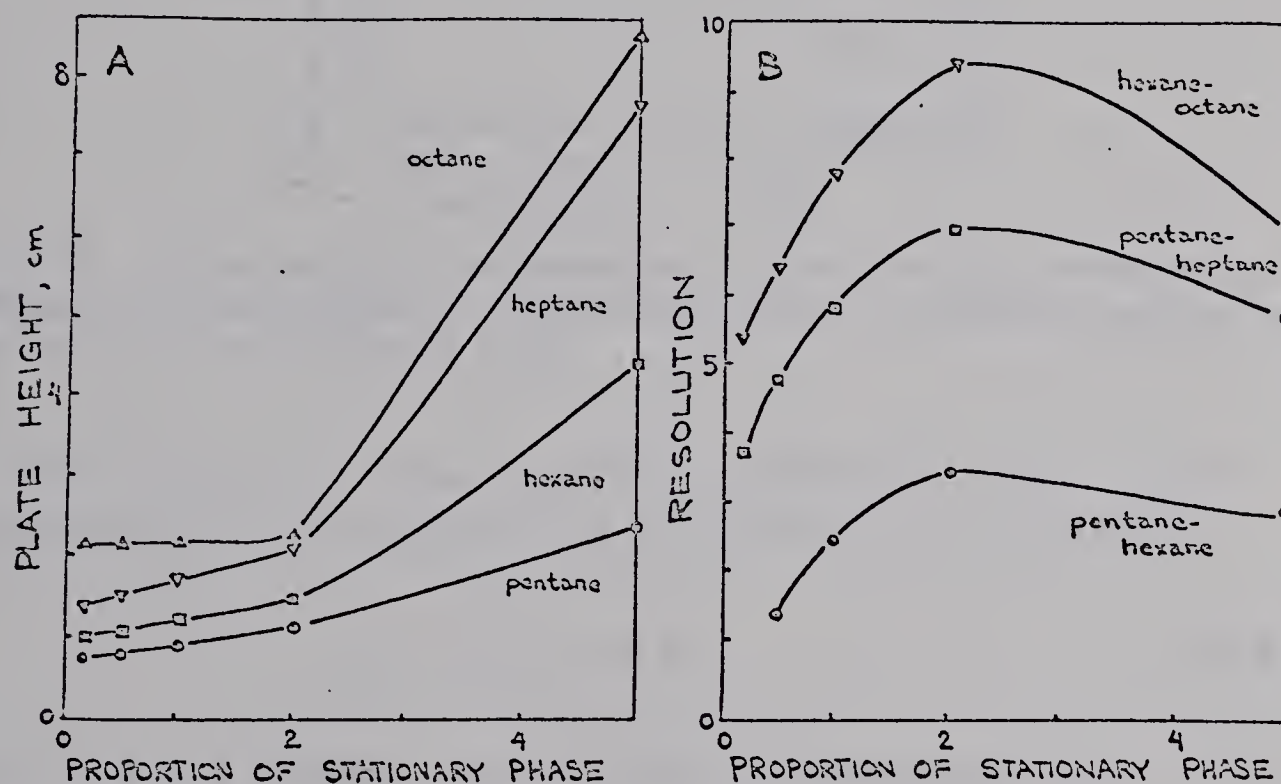


Figure 2.08 Plate height (A) and resolution (B) as functions of the proportion of stationary phase for a 3m column of 1.5 openness at 25°C. The sample size was 0.2  $\mu$ l and the carrier flow rate was 20 ml per minute.

The relationship of plate height to flow rate is changed when the relative proportions of stationary phase is altered. A reduction in the proportion of stationary phase not only reduces the plate height but reduces the rate of change in plate height with increasing flow rate. This behavior may be seen in Figure 2.09 and illustrates that the choice of



flow rate in low loaded columns is not critical. For example with low proportions of stationary phase it is possible to increase the flow rate without appreciably increasing the plate height. Such an increase in flow rate decreases analysis time requirements.

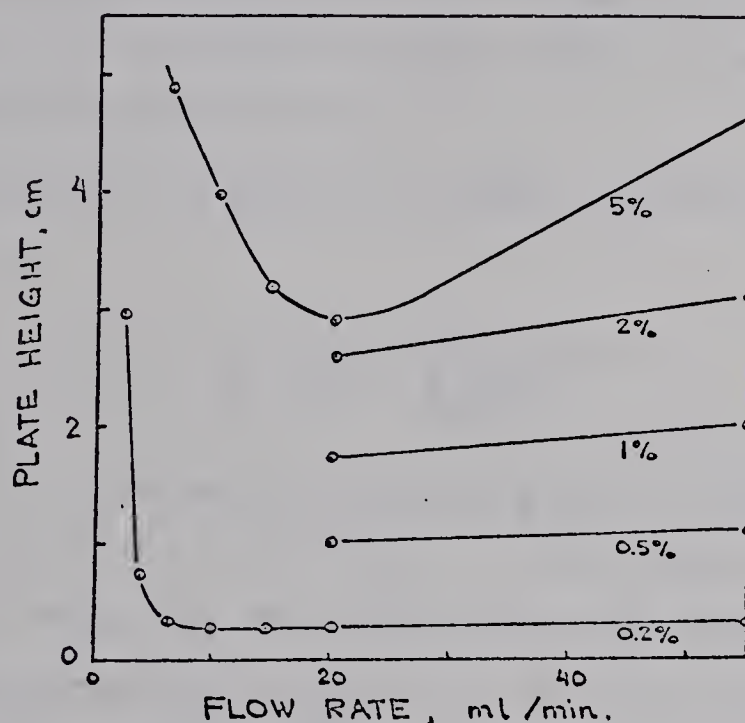


Figure 2.09 Plate height as a function of flow rate for different proportions of stationary phase. A 3m column with 1.4 openness packing was used with 0.2  $\mu$ l n-pentane at 25°C.

The retention time,  $t_R$ , for a component under normal chromatographic conditions may be given by the equation

$$t_R = \frac{L}{u} (1 + k) \quad (2.01)$$

where  $L$  is the column length,  $u$  the compressibility corrected flow velocity, and  $k$  is the partition ratio. Substitution for  $k$  yields the equivalent equation

$$t_R = \frac{L}{u} \left( 1 + \frac{V_s}{V_{ds}} K \right) \quad (2.02)$$

where  $V_s$  is the volume of the stationary liquid phase,  $V_{ds}$  is the dead space volume, and  $K$  the partition coefficient. The development of this equation is given in most of the general reference books given in Table 1.01.



Reduction of the proportion of stationary phase, hence  $V_s$ , or an increase in the flow rate, hence  $u$ , reduces retention time. The desirability of columns with a low proportion of stationary phase is primarily a result of the reduced retention times made available. This in turn allows the chromatographic examination of compounds well below their boiling points in reasonable times; this is an advantage for thermally unstable materials.

The resolution of peaks of equal widths is given by the equation

$$R = \frac{1}{4} \left( \frac{\alpha-1}{\alpha} \right) \left( \frac{k_2}{k_2+1} \right) n^{1/2} \quad (2.03)$$

where  $\alpha$  is the relative volatility and  $n$  is the number of theoretical plates in the column. This equation is from Purnell (82A); also see the references in Table 1.01.

A reduction in the proportion of stationary phase reduces the plate height as shown in Figure 2.08A, therefore increases the number of theoretical plates,  $n$ , and consequently tends to increase the resolution. At the same time the partition ratio,  $k$ , is reduced since the volume of stationary phase,  $V_s$ , becomes smaller and because the partition ratio is related to the partition coefficient,  $K$ , by the equation

$$k = \frac{V_s}{V_{ds}} K \quad (2.04)$$

As the partition ratio,  $k$ , becomes smaller the ratio  $(k/k+1)$  in Equation 2.03 also becomes smaller, tending to reduce the resolution. These two opposing trends, both functioning as the proportion of stationary phase is decreased, are the basis for a partial explanation of the appearance of a maximum in the resolution vs proportion of stationary phase curves in Figure 2.08B.



Karger and Cooke (58) exhaustively studied lightly loaded columns using time normalization and discuss the above concepts at length.

The principal limitation of columns with a low stationary phase loading has been the lack of inertness of the solid support. A number of treatments for conventional supports have been introduced including deactivation with hexamethyl disilazane (HMDS) and more recently a radiation-induced copolymerization technique (RIC) (98). Palframan and Walker (78) recently reviewed the available solid supports and noted their deactivators.

The metal helices of the low-pressure-drop packed columns can be expected to be inert compared to conventional columns, as will be shown in the following figures and discussion.

In Figure 2.10 the specific retention volume, that is the net retention volume,  $(V - V_{ds})$ , per gram of stationary phase, may be seen to increase with a decreasing proportion of stationary phase. This may be attributed to the increasing availability of the solid support surface, either through incomplete coverage by the stationary phase or diffusion of the solute through the stationary phase layer to interact with the support as described by Keller and Stewart (59).

Urone and Parcher (98) do not explain the decreasing retention volume for the larger percentages of stationary phase but nevertheless this manner of presenting data is useful in revealing support surface activity.

For the non-polar normal hydrocarbons used in the research reported in this thesis there was no evidence to indicate that the low-pressure-drop packing was not inert. For example, a plot of the specific retention volume for several hydrocarbons against the proportion of stationary phase for the low-pressure-drop packing is given in Figure 2.11.



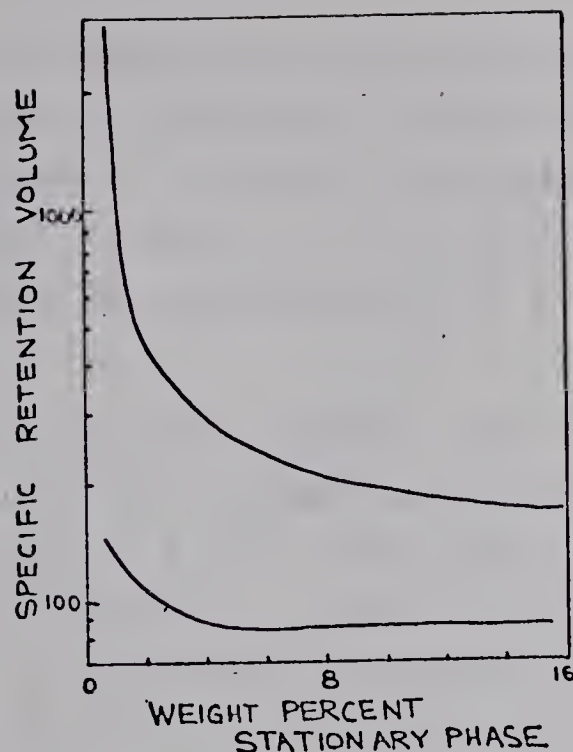


Figure 2.10 Specific retention volume as a function of the proportion of stationary phase for conventional packings. Data from Urone and Parcher (98). The stationary phase was tri-*o*-tolyl-phosphate at a temperature of 25°C with 0.3  $\mu$ l methanol. A non-deactivated acid washed fire brick gives line A whereas a deactivated (RIC) acid washed fire brick gives the results shown by line B.

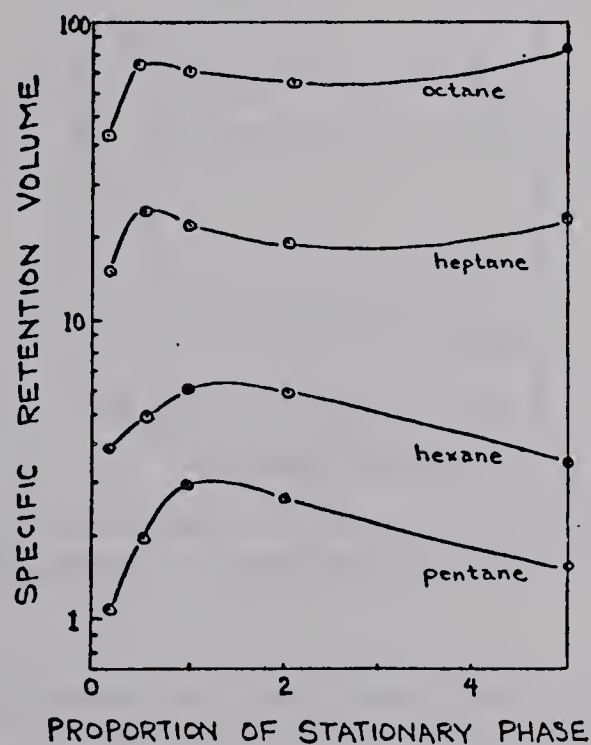


Figure 2.11 Specific retention volume as a function of the proportion of stationary phase for low-pressure-drop packing. Samples 0.2  $\mu$ l, 0 : n-pentane;  $\Delta$  : n-hexane;  $\circ$  : n-heptane;  $\nabla$  : n-octane. A 3m column of 1.8 openness packing was used at 25°C with carrier gas flow rate of 20 ml/min.  $V_{ds} = 18.4$  ml.



There is no evidence of an increase in the specific retention volume with a decreasing proportion of stationary phase. The decrease in specific retention volume at the lowest loadings may be due to a proportionally greater part of the liquid phase being deposited in less geometrically accessible areas.

The specific retention volume may be plotted against column openness with the proportion of stationary phase as a parameter as in Figure 2.12. This shows a maximum at an openness of about 1.2 for the more heavily coated columns. The maximum must be the result of geometrical factors in the packing and the accumulation of the liquid in films of non-uniform thickness. Non-uniformities in the stationary phase thickness would seem more likely at heavier liquid loading.

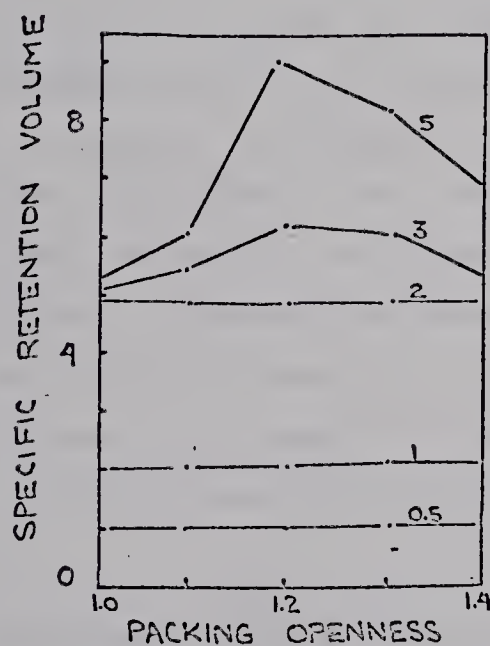


Figure 2.12 Specific retention volume as a function of the packing openness with the proportion of stationary phase as a parameter.

As final evidence to indicate that the packing was inert, consider the examination of the net retention volume,  $V - V_{ds}$ . The net retention volume should be a function of the proportion of stationary phase and independent of the packing openness even for low stationary phase loading, if the packing is inert. Figure 2.13 indicates that this was the case for this system.



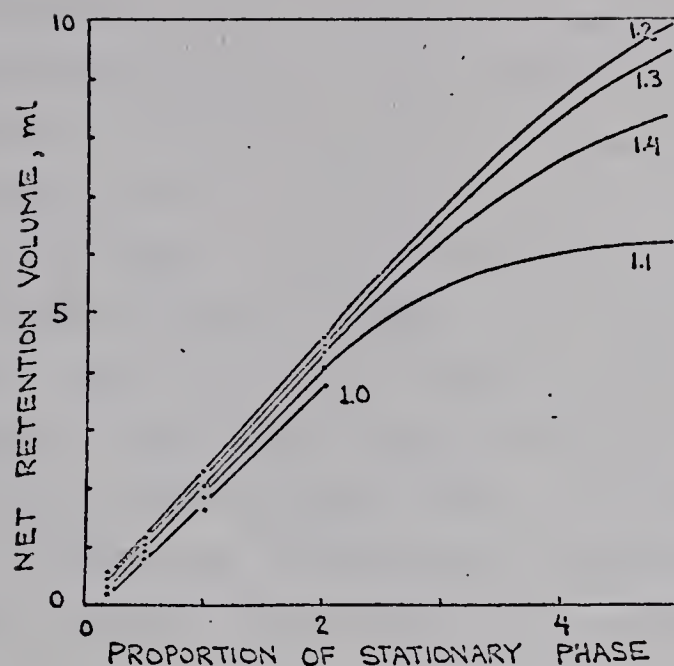


Figure 2.13 Net retention volume as a function of the proportion of stationary phase with column openness as a parameter. The column temperature was 25°C and the flow rate was 20 ml per minute. The sample was 0.2  $\mu$ l n-pentane.

A careful examination of the air peak (representative of a non-retained material) showed a uniform peak broadening with any fixed degree of openness independent of liquid loading. This indicates that there are minimal changes in linear flow velocity or path tortuosity with increasing liquid loading. Therefore observed changes in the effectiveness of the liquid phase in retaining a component such as shown in Figures 2.12 and 2.13 must be the result of solute-solvent interactions and not the result of flow effects.

All of the foregoing study of the effects of the proportion of stationary phase was done using a constant 0.2 $\mu$ l sample size, some additional consideration of sample size is required to complete the study.

The necessity for using a fixed sample size has been explained and it was noted that smaller proportions of stationary phase required the use of smaller sample sizes to prevent peak broadening caused by column overloading. This overload broadening would be most pronounced for the higher molecular weight members of the hydrocarbon series (Figures 2.07 and 2.08A).



Figure 2.14 illustrates overload broadening at low proportions of stationary phase for n-octane. n-Pentane is shown for comparison. In the absence of overload broadening the plate height decreases as the proportion of stationary phase decreases as it does for pentane in the figure. The sample capacity of the column is less for octane than for pentane and at low liquid loadings with a constant sample size the plate height increases rather than continuing to decrease. Reduction of the sample size, as shown by the use of vapor samples, reduces or eliminates the overload broadening and the plate height curve shows a continuing decrease as expected.

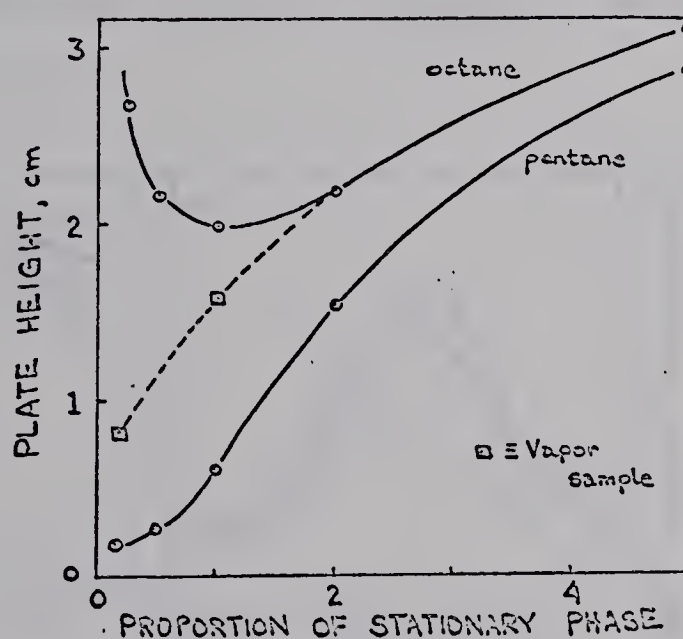


Figure 2.14 Plate height as a function of the proportion of stationary phase. The effect of sample capacity column 1.1 openness packing at 25°C. The sample size was 0.2  $\mu$ l except as noted. The vapor sample was 10  $\mu$ l helium saturated with n-octane.

The plate height vs proportion of stationary phase curve, and to a lesser extent resolution vs proportion of stationary phase curve, Figures 2.08A and B respectively, should be examined with the now demonstrated effect of overload broadening in mind. The leveling-off of the plate height, rather than a continued decrease, for n-octane is probably due to overload broadening.



## Effect of the Packing Openness

The effect of packing openness on plate height is shown in Figure 2.15 for  $C_5$  through  $C_8$  normal hydrocarbons with changing proportions of stationary phase.

Plate height increases with an increasing proportion of stationary phase as was shown in Figure 2.09. This trend is again evident when plate height is examined as a function of packing openness for different liquid loadings. In Figure 2.15A the 0.2% stationary phase has the lowest plate height and it is nearly independent of packing openness. As the proportion of stationary phase increases, Figures 2.15 B and C, the plate height increases and becomes highly influenced by packing openness passing through at maximum at an openness of 1.2 to 1.3.

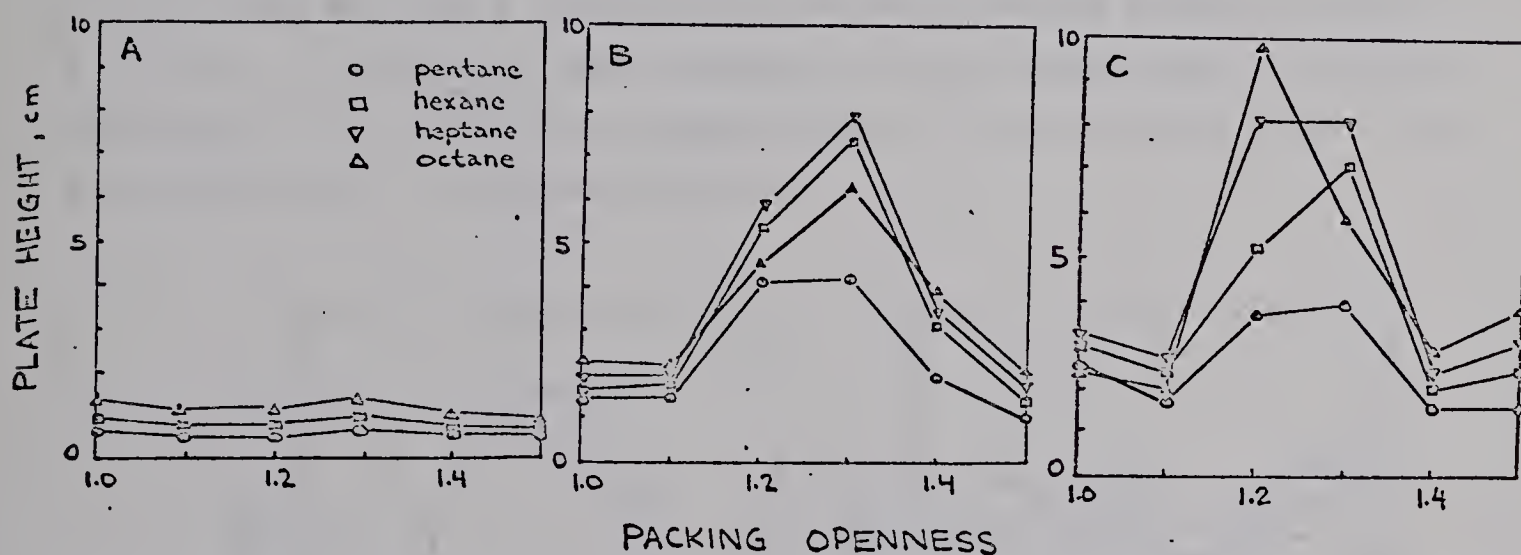


Figure 2.15 Plate height as a function of column openness for stationary phases of 0.2% (A), 2% (B), and 5% (C).

The resolution of pairs of normal hydrocarbon homologs is shown as a function of packing openness in Figure 2.16. Where the proportion of stationary phase was small, Figure 2.16 A, the pair pentane-hexane was not resolved because the retention time difference was too small.



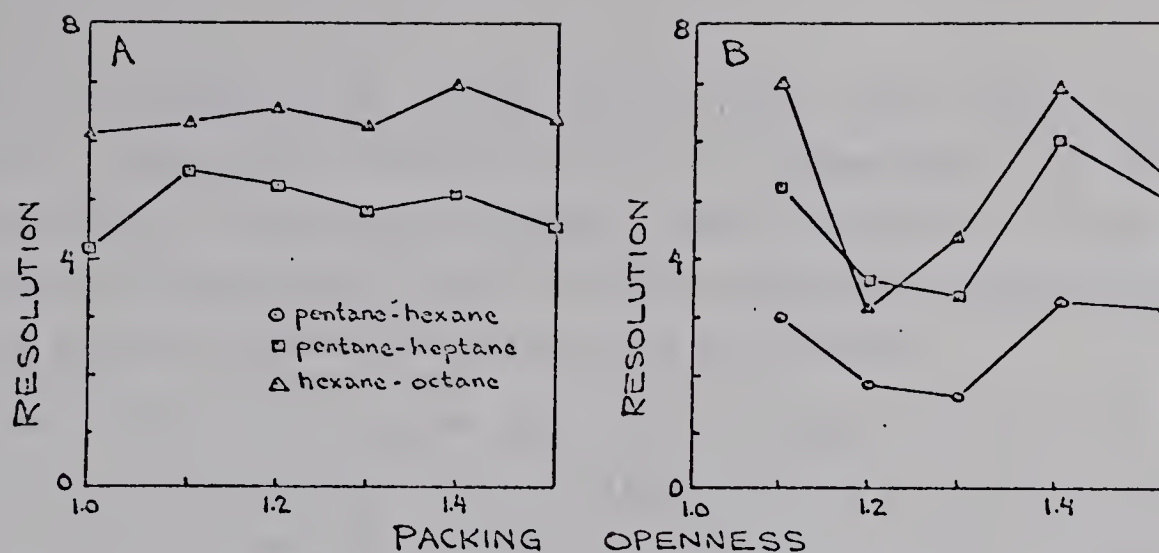


Figure 2.16 Resolution as a function of packing openness for 0.2% (A) and 5% (B) stationary phase. Pairs of hydrocarbons examined as noted in the figure.

Resolution is nearly independent of packing openness when the proportion of stationary phase is small (Figure 2.16 A), but passes through a minimum at an openness of 1.2 to 1.3 for a larger proportion of stationary phase (Figure 2.16 B). A detailed examination of this phenomena is shown in Figure 2.17 for five proportions of stationary phase and a single pair of hydrocarbons.

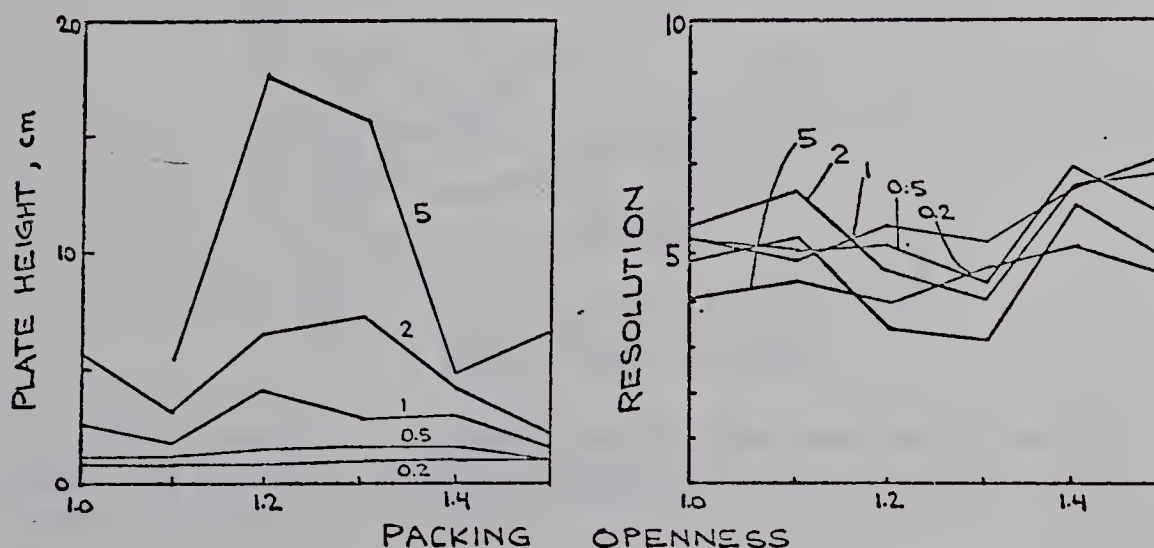


Figure 2.17 Plate height (A) and resolution (B) as functions of column openness for heptane and pentane-heptane respectively. Proportion of stationary phase is shown as a parameter.

The correspondence of the maximum in plate height with a minimum in resolution at a packing openness of 1.2 to 1.3 may be seen in Figure 2.17 A and B. The plate



height, as previously noted, diminishes with liquid loading, however, resolution remains at  $5 \pm 1$  independent of the proportion of stationary phase. The influence of the proportion of stationary phase on the number of theoretical plates and on resolution has been discussed.

Note that the maxima for plate height, Figures 2.15, 2.17 A, and minima for resolution, Figure 2.16 B correspond to the maxima in specific retention volume, Figure 2.12. The reason for this is not obvious at this time.

### Flow Rate

The dependence of the plate height flow rate relationship on the packing openness is shown in Figure 2.18. It can be seen that both the minimum plate height and the optimum flow rate shift with changing packing openness.

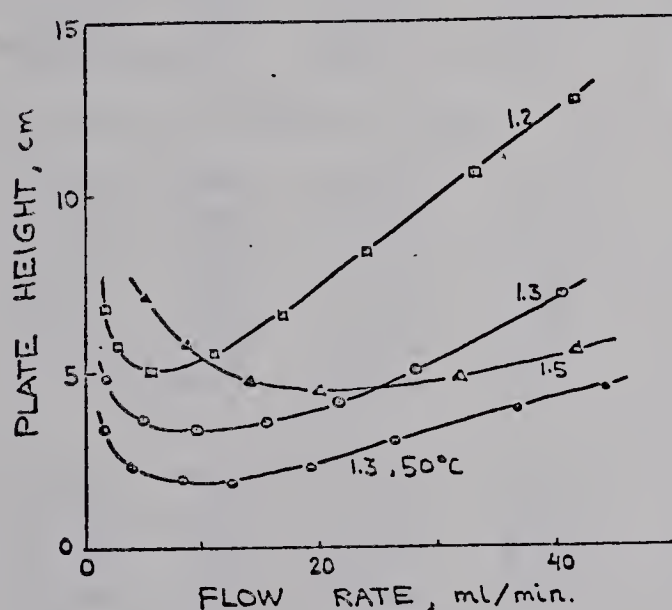


Figure 2.18 Plate height as a function of flow rate with packing openness as a parameter. A 0.2  $\mu$ l n-heptane sample was used at 25°C except as noted. 5% SF-96 liquid loading.

### Summary of Data

A summary of the data on plate heights and resolution for columns of varying degrees of openness and proportions of stationary phase is given in Table 2.02. Much of these data were used in the graphs in the preceding sections.



TABLE 2.02 PLATE HEIGHT AND RESOLUTION AS FUNCTIONS OF PACKING OPENNESS AND THE PROPORTION OF STATIONARY PHASE

Openness	% SF-96	Plate Height, H (cm)				Resolution, R		
		C <sub>5</sub>	C <sub>6</sub>	C <sub>7</sub>	C <sub>8</sub>	C <sub>5,6</sub>	C <sub>5,7</sub>	C <sub>6,8</sub>
1.0	0.2	0.65	0.80	1.14	2.48	--	4.19	6.37
	0.5	0.82	0.98	1.42	2.57	--	5.27	7.28
	1.	1.77	2.18	2.93	3.14	1.69	5.45	7.34
	2	4.56	6.22	6.32	4.17	1.52	4.74	6.37
1.1	0.2	0.50	0.53	1.04	2.55	--	4.74	6.38
	0.5	0.57	0.59	1.26	2.18	--	5.45	6.48
	1	0.81	1.12	1.58	2.18	3.17	5.18	9.05
	2	1.73	2.41	2.72	2.74	3.45	6.47	8.24
	5	3.24	4.37	4.75	3.53	3.05	5.71	7.06
1.2	0.2	0.53	0.54	0.93	2.47	--	4.00	6.07
	0.5	0.72	0.91	1.34	2.40	--	5.20	6.90
	1	1.24	1.81	3.69	2.53	2.33	5.46	7.16
	2	4.53	5.94	6.19	4.90	1.89	4.60	5.94
	5	6.68	10.9	17.3	19.6	1.80	3.50	3.20
1.3	0	0.43	0.42	0.58	1.76	--	--	1.84
	0.2	0.69	0.86	1.35	2.65	--	4.72	6.60
	0.5	0.84	1.04	1.77	2.73	--	4.63	6.04
	1	1.97	1.68	2.78	3.30	2.01	5.14	6.64
	2	4.63	7.35	8.17	6.55	2.01	4.34	5.26
	5	8.00	14.1	16.2	11.5	1.66	3.35	4.28
1.4	0.2	0.50	0.50	0.88	2.12	--	5.22	7.18
	0.5	0.63	0.91	1.77	2.18	2.80	6.81	5.98
	1	1.23	1.99	2.86	3.77	3.17	6.28	7.17
	2	2.09	3.27	3.60	3.59	3.52	6.35	7.47
	5	2.87	3.64	4.83	5.30	3.43	6.03	6.63
1.5	0.2	0.40	0.48	0.88	1.95	--	4.52	6.59
	0.5	0.46	0.62	0.84	2.20	2.28	5.98	7.72
	1	0.61	0.82	1.34	2.10	3.22	7.23	9.18
	2	1.17	1.71	2.06	2.20	3.70	7.02	8.91
	5	3.03	5.26	8.09	7.14	3.22	4.89	5.52



## Loading Technique

If a column packing is to find use, its characteristics must be reproducible. Table 2.03 gives data from an investigation of the reproducibility of the low pressure drop packed column. Column (A) was prepared by removing the excess stationary phase from the column with a 100 ml per minute gas purge. Columns (B) and (C) were prepared in the same manner but with a 20 ml per minute gas purge. The relative percent differences in measured plate height and resolution was 6 percent or less between (B) and (C) but varied from 15 to 110 percent between (A) and (B).

This rather dramatically illustrates the importance of carefully controlling the loading technique (loading here referring to the deposition of the stationary phase on the solid support).

There is a certain variability in plate height determined for a single column and this should not be considered part of the variation due to the column preparation. It was found that this variation in plate height for five duplicate sample injections was from 3 to 7 percent depending on peak shape. Since the peak shape is only partially controllable, through recorder chart speed control and attenuation, this variability therefore cannot be taken at less than about 5 percent. The relative difference between the duplicate columns, B and C, is of this order. The reproducibility of column preparation is therefore good if care is taken in exactly duplicating the loading technique.

## 2.04 DISCUSSION

Had it not been for the poor resolution achieved with the Teranishi column relative to conventional packed columns of the same length and diameter (see Table 2.04), additional parameters would have been examined. Tube diameters down to 0.02 inch i.d. could conceivably be used as could wire diameters of 0.003 inch or less. The amount of work necessary



for even a cursory examination of these two additional parameters was not justified by the performance of the column investigated. It would have been necessary to obtain at least a five fold improvement in resolution to equal the performance of a simple conventionally packed column of equal length.

TABLE 2.03 EFFECT OF LOADING TECHNIQUE ON PLATE HEIGHT AND RESOLUTION FOR A LOW-PRESSURE-DROP PACKED COLUMN

Column Characteristics	Plate Height, H (cm)				Resolution, R		
	C <sub>5</sub>	C <sub>6</sub>	C <sub>7</sub>	C <sub>8</sub>	C <sub>5,6</sub>	C <sub>5,7</sub>	C <sub>6,8</sub>
(A) removed excess stationary phase with 100 ml/min gas purge	2.87	3.64	4.83	5.30	3.43	6.03	6.63
(B) 20 ml/min gas purge	3.64	7.40	16.2	14.1	4.02	3.61	3.02
(C) duplicate of (B) 20 ml/min gas purge	3.72	7.70	15.2	13.7	3.88	3.58	3.20
relative difference %							
A-B	24	68	110	80	16	50	75
B-C	2.2	4.0	6.0	2.6	3.5	0.8	5.8

The plate height is independent of the column length when the pressure drop across the column is small (80). The low pressure drop packed column, having the property implied in its name, should give plate heights independent of length and this parameter was not investigated. All columns used were 300 cm in length.

To use the low pressure drop packed column with the efficiencies found would necessitate a length greatly in excess of 3 meters. To increase the length would multiply the experimental problems in its application to temperature programming at high rates.



At flow rates up to 150 ml per minute the pressure drop through a 3 m low pressure drop packed column was negligible (less than 1 mm Hg). For applications demanding large numbers of theoretical plates the low pressure drop packed column could be increased in length and it is this type of application where the packing will probably find most use. The number of theoretical plates could be as great as in capillary columns and the low pressure drop column could operate at lower pressures and with a greater sample capacity.

TABLE 2.04 COMPARISON OF BEST RESULTS: CONVENTIONAL AND LOW PRESSURE DROP-PACKED-COLUMNS

Column	Plate Height, H (cm)				Resolution, R		
	C <sub>5</sub>	C <sub>6</sub>	C <sub>7</sub>	C <sub>8</sub>	C <sub>5,6</sub>	C <sub>5,7</sub>	C <sub>6,8</sub>
Conventional: SE-30 5%, 60-80 mesh Chromosorb P, 3 meters, 0.10" I.D.	0.31	0.33	0.36	0.39	15.5	23.2	23.2
Low-pressure-drop: 1.2 openness, 2% SF-96*	0.53	0.54	0.93	2.47 <sup>#</sup>	--	4.00	6.07
Low-pressure-drop: 1.3 openness, no column liquid*	0.43	0.42	0.58	1.76	--	--	1.84
Low-pressure-drop: 1.5 openness, 1% SF-96**	0.61	0.82	1.34	2.0	3.22	7.23	9.18

Note: All columns at 25°C with carrier gas flow rate of 20.0 ml/min. Constant sample size of 0.2 ul

\* indicates column optimum in H  
 \*\* indicates column optimum in R  
 # indicates column overloaded



### 3. RAPID TEMPERATURE PROGRAMMING IN GAS CHROMATOGRAPHY

From theoretical considerations it has been possible to develop a method for the prediction of retention temperatures for a temperature programmed determinations from isothermal data alone (40). Experimental verification of the predicted retention temperatures constitutes a check on the theory of programmed temperature gas chromatography (PTGC). The effects of program rate, flow rate, and the ratio of the two on both plate heights and resolution may be examined with suitable experimentation. The development of a new apparatus allows an examination of the effects of rapid temperature programming in a range previously not experimentally accessible.

#### 3.01 METHODS OF CALCULATION OF PREDICTED RETENTION TEMPERATURE, RESOLUTION, AND INTRINSIC RESOLUTION

The procedure for calculating retention temperatures from isothermal data is outlined in Figure 3.01. The development of this procedure and its theoretical basis is thoroughly covered by Harris and Habgood (40).

The definition of resolution is given by the equation

$$R = \frac{2(V_2 - V_1)}{W_2 + W_1} \quad [1.04] (3.01)$$

In PTGC the equation for number of theoretical plates,  $n$ ,

$$n = 16 \left( \frac{V_{TR}}{W} \right)^2 \quad (3.02)$$

Fryer, Habgood, and Harris (28) have combined these equations in such a way as to develop an expression for resolution in which one part depends only on the solute-solvent interaction, and is called intrinsic resolution,  $R_i$ , and another depending on column efficiency. Following their treatment and rearranging equation (3.02)

$$W = \frac{4\sqrt{V_{TR}}}{n} \quad (3.03)$$



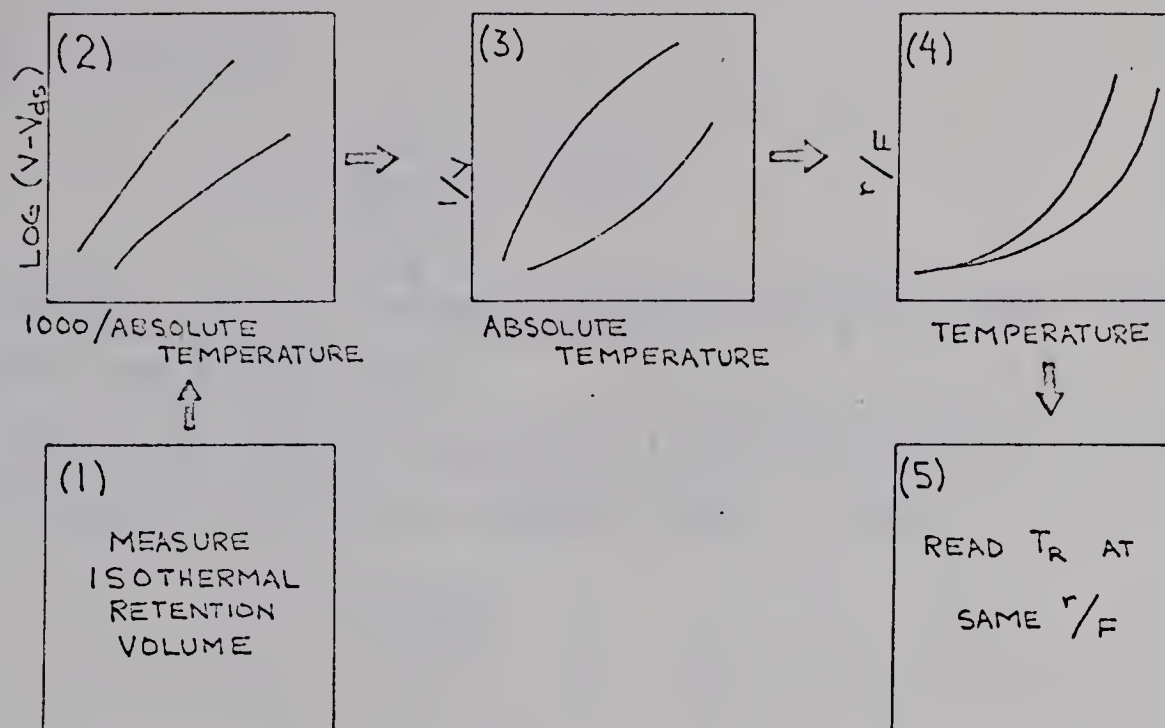


Figure 3.01 Procedure for the calculation of retention temperature in PTGC from isothermal data (from Harris and Habgood (40))

Step (1) Measure the isothermal retention volume at 3 or 4 temperatures. Correct for dead space and pressure gradient.

Step (2) Plot  $\text{Log } (V-V_{ds})$  against  $1000/T, ^\circ\text{K}$

Step (3) Read net retention volume from graph, add dead space and plot sum against the absolute temperature.

Step (4) Numerically integrate area under curves from an initial temperature,  $T_o$ , to a series of higher temperatures. Plot areas against upper temperature limit.

These areas =  $\int_{T_o}^{T_R}$  which =  $r/F$ . This plot therefore yields  $r/F$  vs  $T$ .

Step (5) Read retention temperature for compound at  $r/F$  chosen.

Substituting for  $W$  in equation (3.01) yields

$$R = \frac{2(V_2 - V_1)}{(4 V_{T_R} / \sqrt{n})_2 + (4 V_{T_R} / \sqrt{n})_1} \quad (3.04)$$

With the assumption that for neighboring peaks the values of  $n_1$  and  $n_2$  will not differ much, it is possible to factor



out  $\sqrt{n}$  av\* giving

$$R = \frac{V_2 - V_1}{(V_{T_R})_{av}} \frac{\sqrt{n}_{av}}{4} \quad (3.05)$$

The validity of the assumption that  $n_1 = n_2$  has been examined in detail by Karger (57).

The first term of equation (3.05) is intrinsic resolution as defined by Harris and Habgood (40) so that

$$R = R_i \frac{\sqrt{n}_{av}}{4} \quad (3.06)$$

where

$$R_i = \frac{(V_2 - V_1)}{(V_{T_R})_{av}} = \frac{\Delta V}{(V_{T_R})_{av}} \quad (3.07)$$

The values of  $V$  and  $V_{T_R}$  are obtained from chromatograms as shown in Figure 3.02.

Retention volume may be given by the equation

$$V_{T_R} = \frac{(T_R - T_0)}{r} \cdot F \quad (3.08)$$

where  $r$  is the heating rate in degrees per minute and  $F$  is the flow rate in ml per minute.

Substituting for  $V_{T_R}$  in equation (3.07) gives

$$R_i = \frac{F}{r} \frac{(T_{R2} - T_{R1})}{0.5(V_{T_{R2}} + V_{T_{R1}})} = \frac{F}{r} \cdot \frac{\Delta T_R}{(V_{T_R})_{av}} \quad (3.09)$$

It is the ratio of  $F/r$  or  $r/F$  that is important in determining the value of  $R_i$  or  $R$  and not  $F$  or  $r$  alone.

---

\*Note here that  $\sqrt{n}_{av} = (\sqrt{n_1} + \sqrt{n_2})/2$  but that

$\sqrt{n}_{av} = [(n_1 + n_2)/2]^{1/2}$  and that  $\sqrt{n}_{av} = \sqrt{n_{av}}$  only if  $n_1 = n_2$ .

This is the simplifying assumption implicit in Equation (3.05). Harris and Habgood (40-A) use  $\sqrt{n}_{av}$  where  $\sqrt{n}_{av}$  is mathematically correct (28).



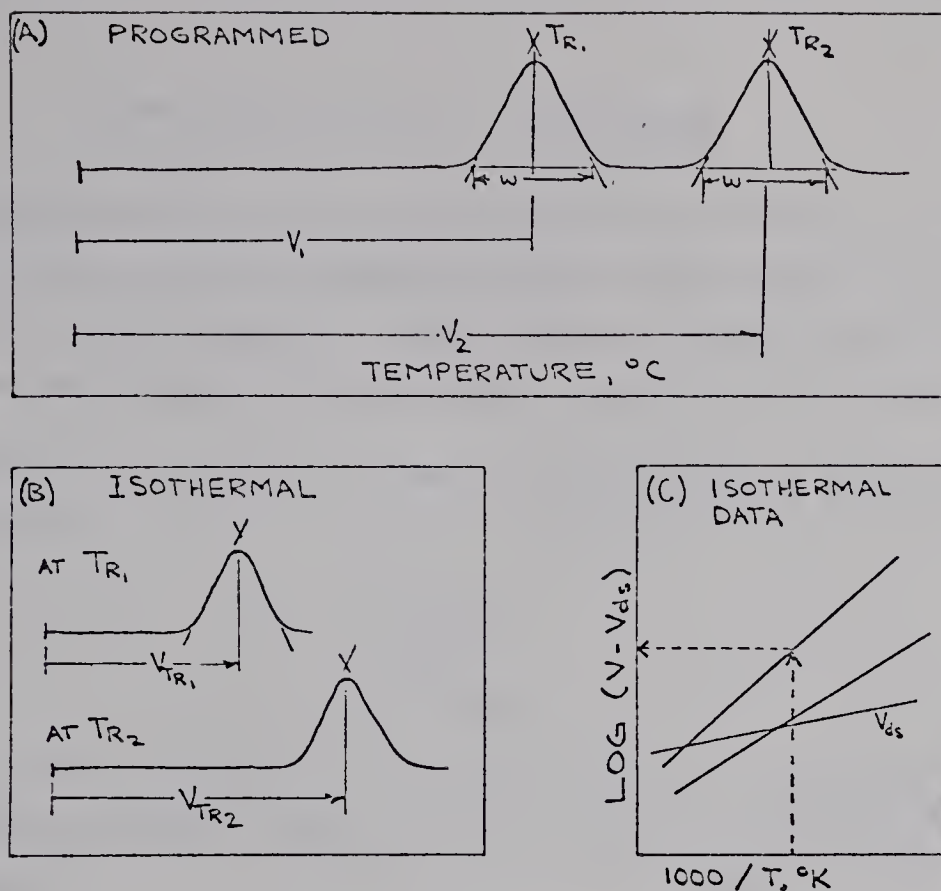


Figure 3.02 Procedure for the calculation of intrinsic resolution in PTGC.

Step (1) Calculate R according to the equation

$$R = \frac{2(V_2 - V_1)}{W_2 + W_1}$$

for the programmed determination.

Step (2) From isothermal determinations at  $T_R$  (B) or from graphical data (C) obtain values for  $V_{TR}$ . Calculate the average number of theoretical plates.

$$\sqrt{n}_{av} = 0.5 \left[ 4 \left( \frac{V_{TR1}}{W_1} \right) + 4 \left( \frac{V_{TR2}}{W_2} \right) \right]$$

Step (3) Determine intrinsic resolution from the equation

$$R = R_i \frac{\sqrt{n}_{av}}{4}$$



## Consideration of Flow Rates

An ambiguity in the meaning of flow rate in temperature programmed gas chromatography makes otherwise straightforward calculations difficult. This may be illustrated by considering the calculation of intrinsic resolution in PTGC.

Intrinsic resolution may be calculated using the following equation:

$$R_1 = \frac{V_2 - V_1}{\left( V_{T_R} \right)_{av}} \quad (3.07)$$

$V$  and  $V_{T_R}$  were defined in Figure 3.02. Intrinsic resolution is a dimensionless number hence  $V$  and  $V_{T_R}$  must be in the same units.

The retention volume at the retention temperature,  $V_{T_R}$ , may be obtained from an isothermal determination at the retention temperature,  $T_R$ , or, more conveniently, from a plot of the log of the net retention volume,  $(V - V_{ds})$ , against the reciprocal of the absolute temperature.

In the isothermal cases the conversion of  $V_{T_R}$  from chart centimeters, as measured on the chromatogram, to ml is simple as the flow rate is unambiguous.

$$V_{T_R} \text{ (cm)} \times \frac{F \text{ (ml)}}{S \text{ (cm)}} = V_{T_R} \text{ (ml)} \quad (3.14)$$

where  $F$  is the flow rate and  $S$  is the chart speed in cm per minute.

The conversion of  $V(\text{cm})$  to  $V(\text{ml})$  in PTGC is complicated by the potential ambiguity of flow under programmed temperature conditions.

The changes in viscosity and volume of the carrier gas with temperature were considered by Harris and Habgood in developing characteristic equations for expressing the relationship between isothermal retention volumes and the



program and retention temperature in PTGC. For operation at constant outlet pressure and constant outlet flow rate with allowance for changing pressure drop with changing temperature the equation

$$l = \frac{\bar{F}_O}{r} \int_{T_O}^{T_R} \frac{dt}{(Ae^{\Delta h/RT} + 273 \bar{V}_{ds}^T/T) [1 + (T/T_O)^{1.7} (P_{T_O}^2 - 1) (1 - 2/L)]}$$

was developed. Evaluation of this equation is complex. The important consideration here is that the effective flow rate changes during the program as a result of the changing pressure drop.

The flow rate measured at the initial temperature (25°C) and corrected for pressure drop at that temperature,  $F_{T_O}$ , will be used in the following sections. The assumption implicit in this use is that the change in effective flow rate with changing temperature will be negligible. In the case of the calculation of characteristic curves for the prediction of retention temperatures (as in Figure 3.01) the use of pressure-corrected flow rates for the column at 25°C is valid provided that both isothermal and programmed measurements are made with the same column at the same flow rate (85A). If a higher but constant flow rate is used for the isothermal measurements necessary to calculate the characteristic curves they will be slightly displaced towards higher temperatures.

Two types of columns have been used on a conventionally packed and an open tubular column. The amount of stationary phase in the conventionally packed column may be accurately determined but its relatively high pressure drop will make the assumption of constant effective carrier gas flow rate with changing temperature somewhat in error. The effective flow rate will tend to decrease as the temperature increases



because the  $j$  factor will decrease. The open tubular column, having a large diameter and a negligibly small pressure drop at all temperatures, should indeed have a constant effective carrier gas flow rate but it becomes much more difficult to determine accurately the amount of stationary phase which it contains. A knowledge of the amount of stationary phase is important when comparison of different columns is undertaken.

This discussion has emphasized the importance of flow rate and the effect that temperature programming has on it. A complete theoretical treatment has been published by Harris and Habgood (44).



### 3.02 EXPERIMENTAL REQUIREMENTS AND DESIGN

Crucial to the acquisition of valid data in PTGC is a knowledge of the temperature-time history of the chromatographic column. Previous research has clearly demonstrated that the heated air bath, the most commonly used device in temperature programming, may be subject to gross errors (73).

In the case shown in Figure 3.03 the equipment failed to give the desired column temperature-time relationship. Had uncritical use been made of the indicated temperature this failure could have gone unnoticed.

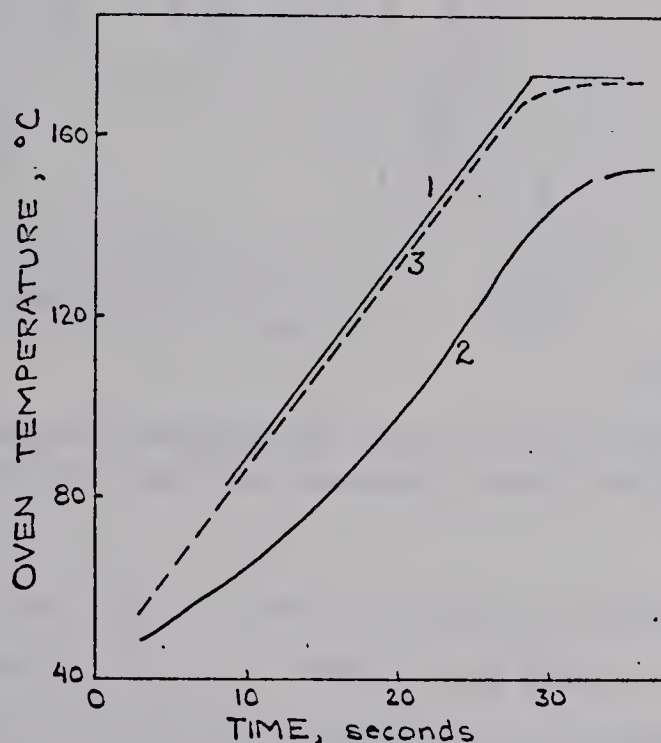


Figure 3.03 Column- and oven-temperature lags. Curve 1 represents the indicated thermocouple temperature. Curve 2 represents the temperature recorded from a thermometer near the column and curve 3 the temperature as read from a thermometer whose bulb was placed in the heater support. From McEwen (73).

For work described in the following section, careful design and control of experimental conditions were established.

Program rates of 40°C per minute are possible using commercially available equipment. To obtain a rates an order of magnitude greater than this it was necessary to develop a new heating system.



Bowen and Marks (12) developed a technique for programming based on direct heating of the column tube wall by a variable low-voltage current. Their apparatus is shown schematically in Figure 3.04.

The temperature-time relationship shown in the figure clearly indicates that the program is not linear.

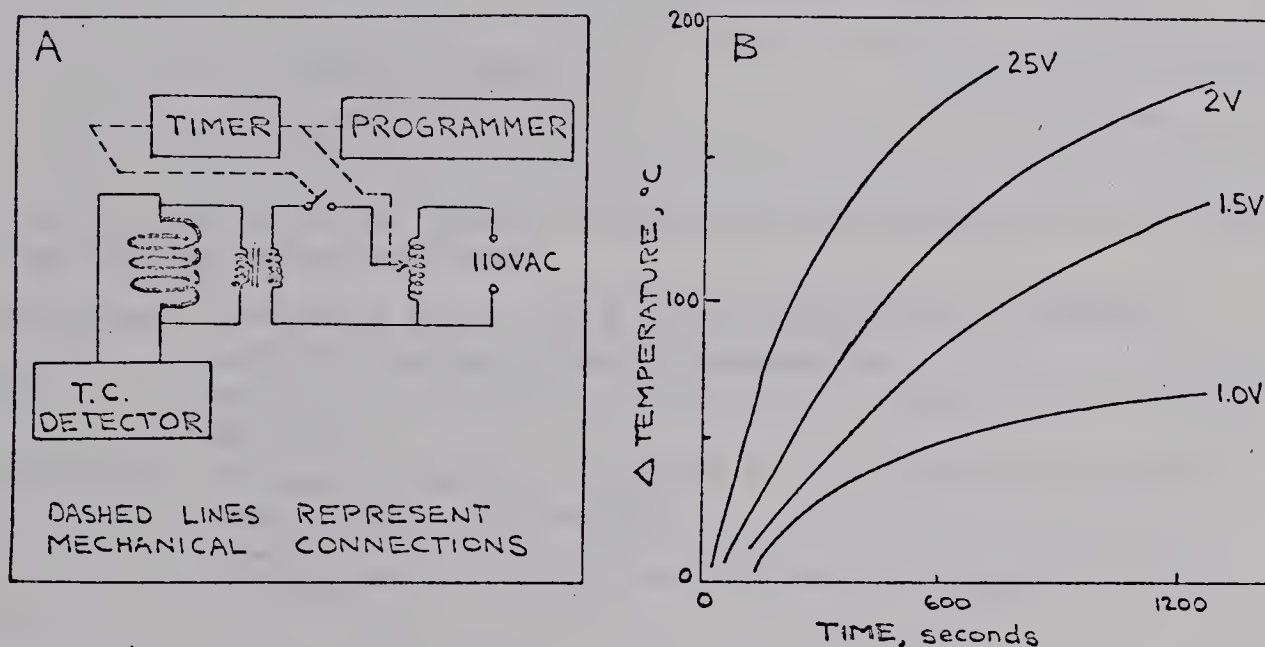


Figure 3.04 Schematic diagram of direct electrical heating device (A) of Bowen and Marks (12) and its heating capabilities (B).

Substitution of a true controlling programmer for the mechanical arrangement of Bowen and Marks allows linear programming using direct electrical heating. This new arrangement is shown in Figure 3.05. Full details of the construction, operation, testing, and performance of this apparatus are given in Appendix I.

The principal advantages of direct electrical heating are the high rates attainable and the good temperature control possible. The low thermal inertia of a thin wall metal tube allows rapid heating. This is important since a normal requirement for programmers is a heating rate of at least 1.5 times the program rate desired. Thus, to program at  $400^{\circ}\text{C}$  per minute the heating system must be capable of  $600^{\circ}\text{C}$  per minute. Rates such as these are attainable with the apparatus



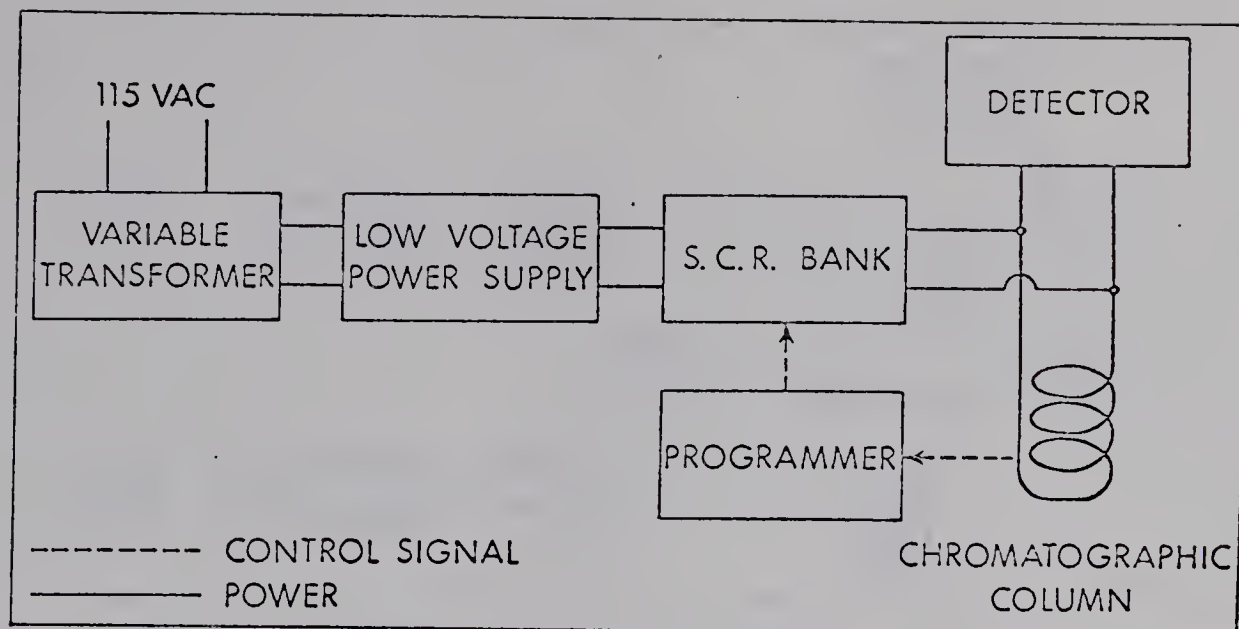


Figure 3.05 Apparatus for linear temperature programming using direct electrical heating of column tube.

Programmer: Aerograph Model 326 Linear Temperature Programmer modified as described in Appendix I.

SCR Silicon controlled rectifier bank capable of switching 30 amps.

Operation Voltage to column adjusted to accommodate different resistances with variac.

Programmer sees only the SCR control signal as load.

developed for this research. The high thermal conductivity of the metal tube tends to reduce any localized differences in temperature along the length of the tube such as could result from local differences in electrical resistance. (See Appendix I).

Beyond the precise determination and control of the column temperature are requirements of another experimental variable. The carrier gas flow rate must be determined and precisely controlled. The arrangement of the controlling and measuring devices depends on the type of detector being used and is shown in Figure 3.06.

Flow control for all PTGC determinations was with a Moore Products Co. Model 63BU-L, constant differential type flow controller. For isothermal determinations using the thermal conductivity arrangement (Figure 3.06 B), a short-range thermometer capillary, as described by Habgood and Harris (36) was used for flow control.



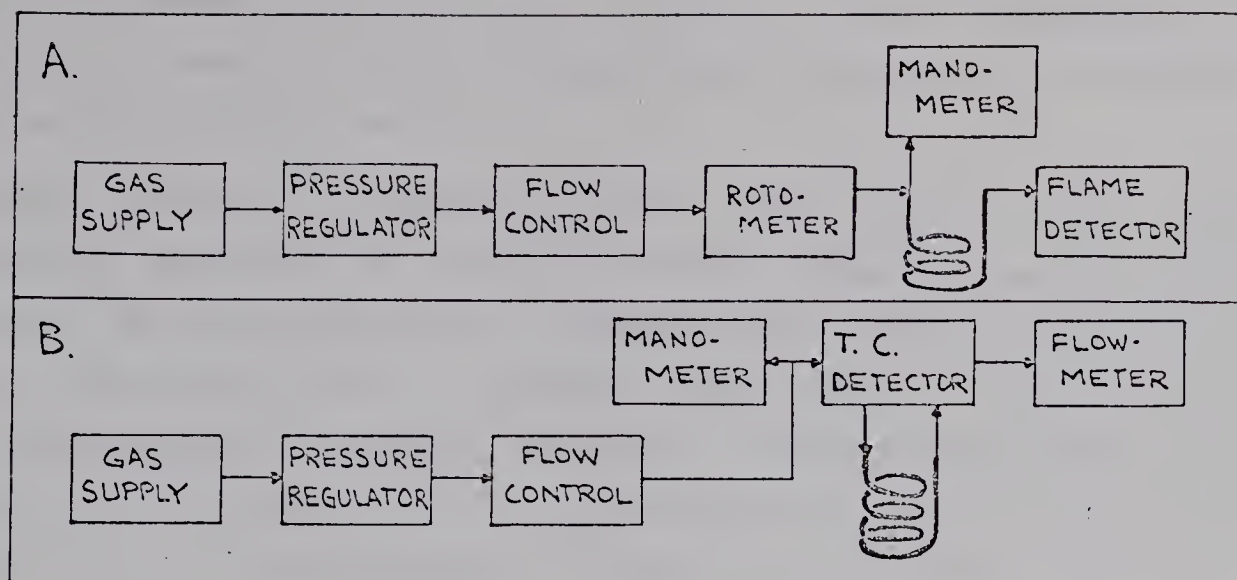


Figure 3.06 Arrangement of flow control and measurement with a flame ionization detector (FID), A, and a thermal conductivity (TIC) detector, B.

The simple soap-film flow meter is conventionally used with thermal conductivity (TC) detectors as shown in Figure 3.06 A. With the flame ionization detector (FID) the soap-film flow meter necessitates extinguishing the flame, cooling the burner tip, and removing the protective housing and electrodes for each required flow measurement. This awkward procedure is made time consuming by the slow thermal re-equilibration of the restored flame head. With the many changes of flow rate that were required in this research, an alternative method had to be used. Shown in Figure 3.06 A is a rotometer, Matheson Model 642B Flowmeter with No. 600 tubes, in this case, used in conjunction with the FID. The rotometer calibration was made prior to the chromatographic determinations. The flow rate at the column outlet was obtained for a series of rotometer readings. The rotometer is sensitive to changes in gas density or pressure and therefore a separate calibration was required for each column having a different pressure drop. Typical calibration curves, pressure-gradient and temperature corrected flow rate as a function of rotometer reading, are given in Appendix I.

This research was designed to give as great a range of experimental parameters as possible consistent with good



return in information for time invested. The following is a discussion of some of the considerations necessary in developing the scope of this work.

In the study of resolution the second peak of the resolved pair must be recorded by the end of the temperature program. This is not a requirement in conventional chromatographic practice but necessary here to prevent unnecessary complications in the interpretation of the results. This requirement fixes a maximum value allowable for the residence time of the second component,  $t_{R_2}$ . The maximum allowable  $t_{R_2}$  is determined by the program rate,  $r$ , and the temperature interval,  $T-T_0$ , over which it operates.

$$t_R = \frac{T-T_0}{r} \quad (3.10)$$

Figure 3.07 shows the maximum  $t_{R_2}$  as a function of program rate. This figure was constructed assuming a fixed temperature interval,  $T-T_0$ , of  $200^\circ\text{C}$ .

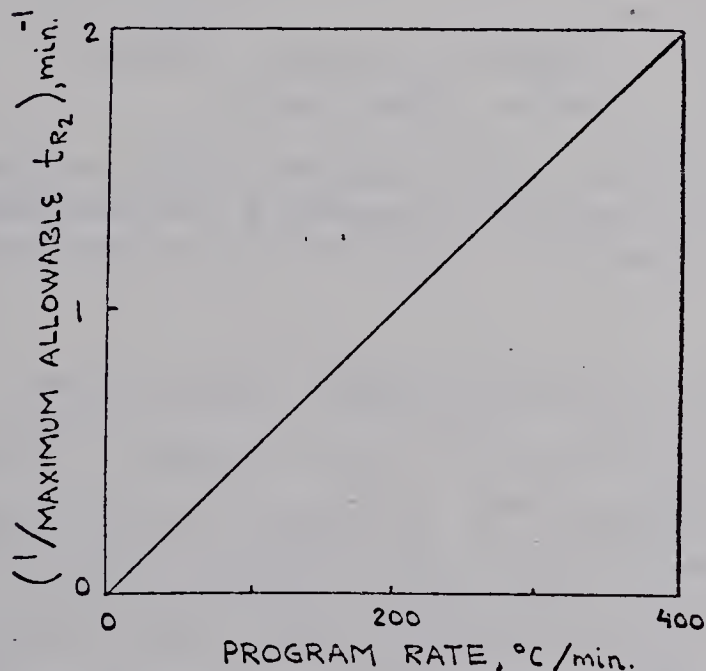


Figure 3.07 Maximum allowable time for complete elution of the second component of a resolved pair as a function of program rate. Fixed temperature interval of  $200^\circ\text{C}$  corresponding to initial and final temperatures of  $25^\circ$  and  $225^\circ\text{C}$ .



The residence time,  $t_R$ , is critically dependent upon the carrier gas flow rate,  $F$ . For any fixed value of the flow rate the minimum residence time is that of an unretained component. This minimum residence time must be determined experimentally using the air peak or other non-retained material. For each column it depends on column length, dead space volume, and other equipment variables. Figure 3.08 shows the minimum time required for the elution of an unretained material as a function of flow rate for a 1 meter 0.10" i.d. conventionally packed column.

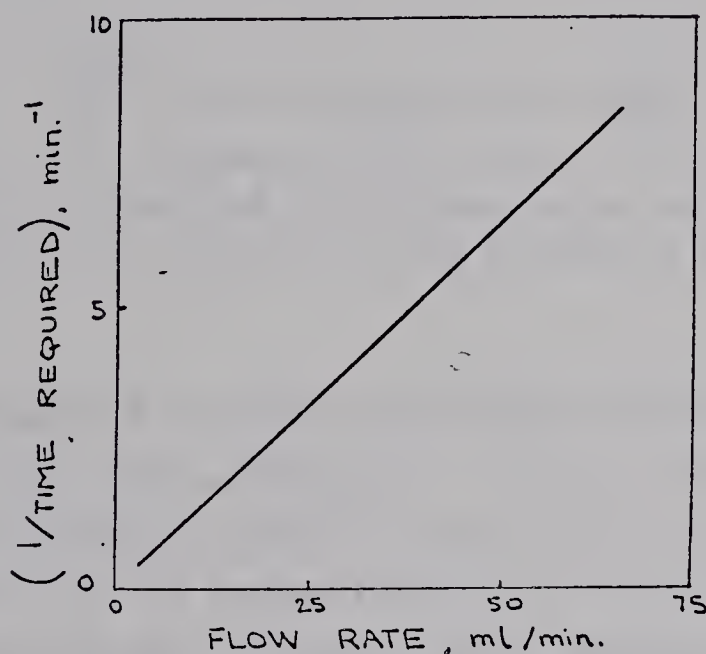


Figure 3.08 Experimentally determined time required for the elution of an unretained component as a function of flow rate. Column was 5% SF-96 on 60-80 mesh Chromosorb P in a 1m 0.10" i.d. tube.

If, as a limiting but experimentally unrealizable situation, the second component of a resolved pair were represented by an unretained material, the minimum flow rate required for a chosen program rate may be determined. It is a necessary condition that the minimum possible  $t_{R_2}$  as established by the flow rate be less than maximum  $t_{R_2}$  allowed by the chosen program rate. That is, as a limit, a non-retained material must be eluted before the temperature program is completed. These considerations allow the determination of the minimum flow rate required for any particular heating rate. This relationship is shown in Figure 3.09. For each



heating rate the maximum value of the ratio  $r/F$  is also established by these considerations.

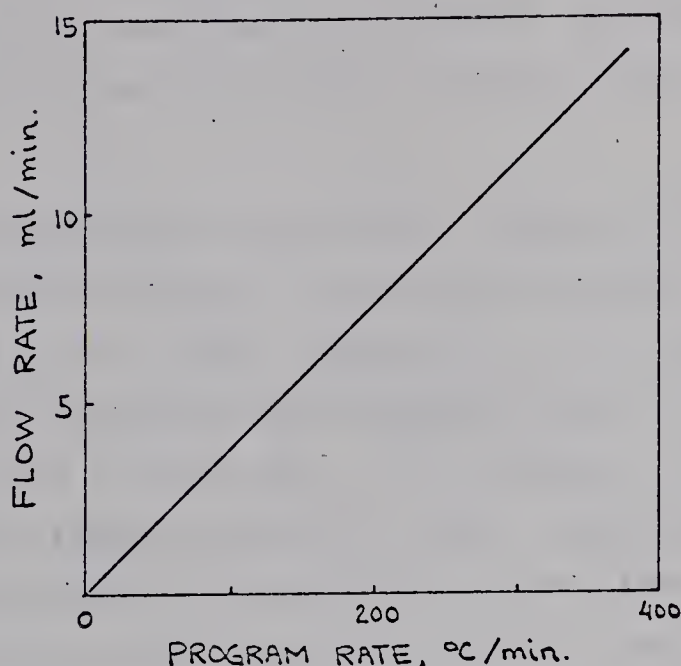


Figure 3.09 Flow rate required for elution of an unretained component in the time allowed by the duration of the program as a function of the program rate.

The relationships in PTGC have been generalized so that columns of the same type, that is columns differing only in the amount of stationary phase present, may be compared. This is done by referring to retention volumes and flow rates reduced to a common amount of stationary phase of one gram. These quantities are symbolized  $\bar{V}$  and  $\bar{F}$  and related to  $V$  and  $F$  by the weight of stationary phase,  $w$ , by the equation

$$V = w\bar{V} \quad (3.11)$$

$$F = w\bar{F} \quad (3.12)$$

A knowledge of the weight of stationary phase in a column allows the calculation of  $\bar{F}$  from  $F$ .

The minimum ratio  $r/\bar{F}$ , for any heating rate,  $r$ , is determined by the maximum flow rate per gram of stationary phase,  $\bar{F}$ , obtainable. The maximum flow rate,  $F$ , with the thermal conductivity (TC) detector used in this research was 50 ml per minute. Beyond this flow rate deleterious flow effects appear. The flame ionization detector (FID) used was capable of functioning with a flow rate of up to 170 ml per



minute beyond which a stable flame could not be maintained. The detector limited flow rates are used in the following calculations as the maximum obtainable although it is recognized that stream-splitting would allow even greater rates.

The experimentally accessible ranges  $r/\bar{F}$  for values of  $r$  from 0.4 to 400°C/minute for three different columns are shown in Figure 3.11. The values for  $r/\bar{F}$  used to construct this figure were based on the required and attainable values of  $r$  and  $\bar{F}$  as just discussed. In Section 3.04 to follow, Figure 3.16, the ranges of  $r/\bar{F}$  values experimentally attained and used in the study of resolution are shown. Figure 3.16 will also show in a qualitative manner, the factors establishing the experimental boundaries.

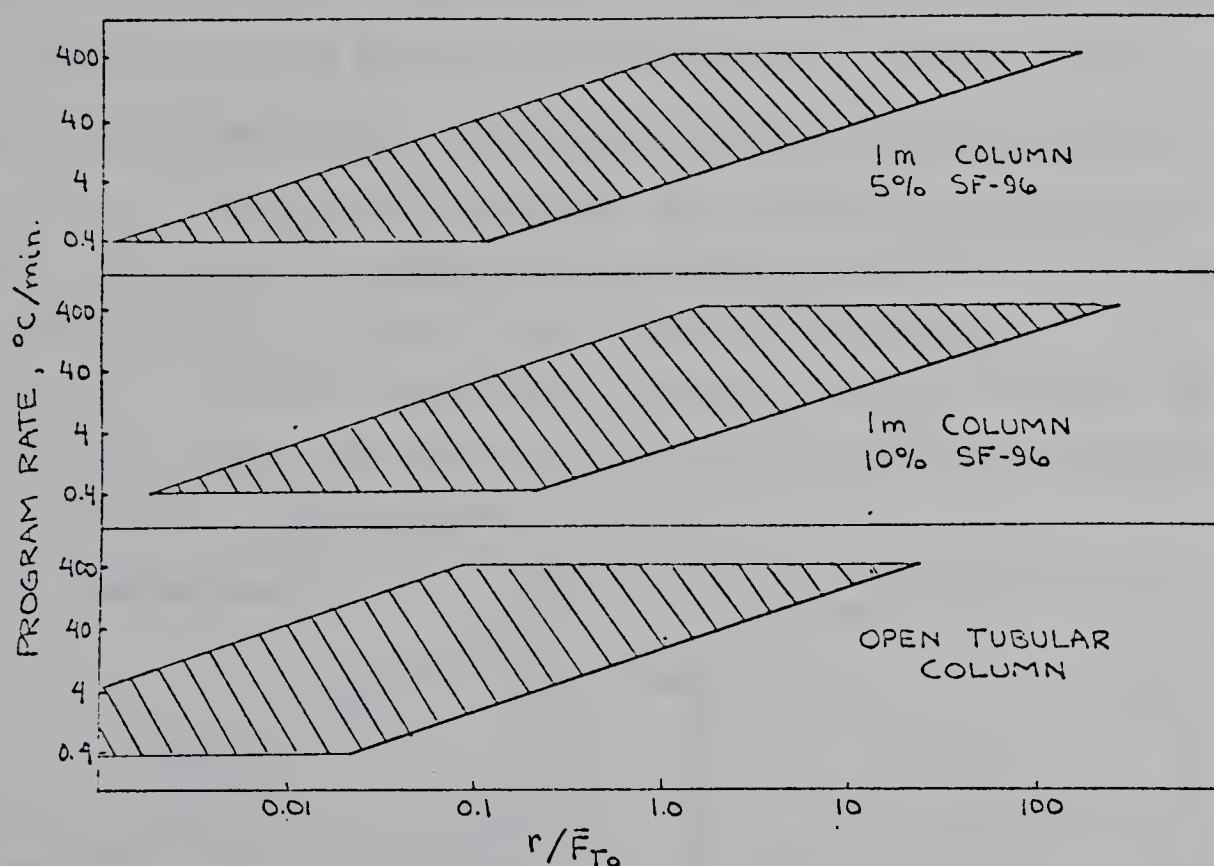


Figure 3.11 Experimentally accessible ranges of  $r/\bar{F}_{T_0}$  was calculated using experimental values for weight of stationary phase for each column and assuming a maximum and a minimum flow rate of 150 and 1 ml per minute respectively. The accessible ranges are shown by shaded areas. The subscript to the flow rate,  $\bar{F}$ , indicates that the flow rate was determined at the initial temperature,  $T_0$ .



### 3.03 PREDICTION AND VERIFICATION OF THE RETENTION TEMPERATURE, $T_R$ , AS PROOF OF THE THEORY OF PTGC EXTENDED TO HIGH PROGRAM RATES

The procedure for predicting the retention temperature of a material in PTGC from isothermal data was given in Figure 3.01. The retention temperature is a function of the ratio  $r/F$ .

Using the programming apparatus developed for this research the  $r/F$  ratio dependence of the retention temperature was examined with program rates to 400°C per minute. Two columns were used in this study: a conventional 1 m 0.10" i.d. column packed with 10 V wt% SF-96 on 60-80 mesh Chromsorb-P and an open tubular column of the same dimensions also using SF-96 as the stationary phase. Figures 3.12 through 3.15 show the results of these experiments and follow the procedure outlined in Figure 3.01.

The isothermal data required for the development of Figure 3.12 was obtained using the constant temperature oil bath described by Habgood and Harris (37), or, at temperatures above 150°C, the air bath shown in Appendix I. In Figure 3.12 the net retention volume ( $V - V_{ds}$ ) and the dead space volume ( $V_{ds}$ ) are shown as a function of the reciprocal of the absolute temperature.

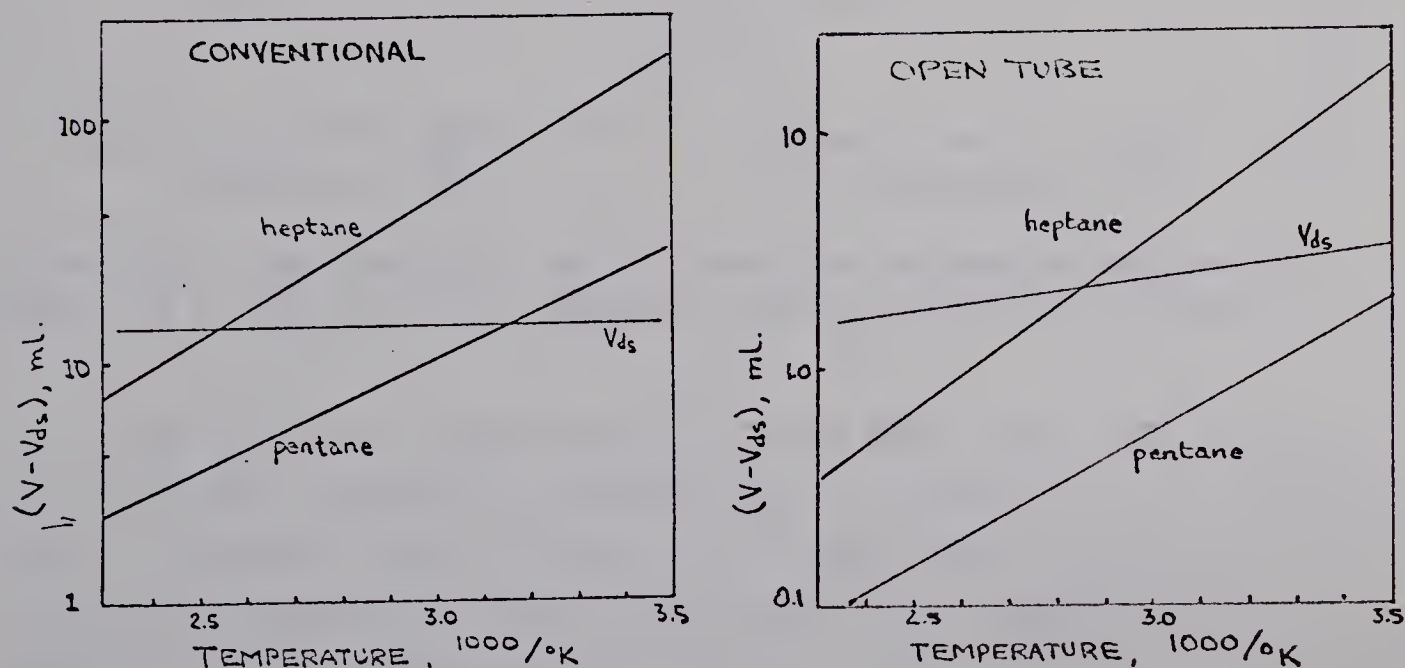


Figure 3.12 The net retention volumes of pentane and heptane as functions of the reciprocal of the absolute temperature.



In Figure 3.12 the volumes shown were calculated using the elution time and a flow rate determined at 25°C and corrected for pressure drop at that temperature. The outlet flow rate was constant due to the presence of a flow controller in the system. At higher temperatures the pressure drop in the conventional column would increase so that the effective flow rate would be somewhat less than that used to calculate the volumes indicated. The effect of neglecting this factor seems small since the conventional column gives essentially the same results as the open tubular column.

Figure 3.13 was developed from Figure 3.12. For experimental convenience the initial temperature  $T_0$ , was 25°C. The final temperature,  $T$ , was limited to 225°C by the volatility of the liquid phase (SF-96). Thus the program range was 200°C.

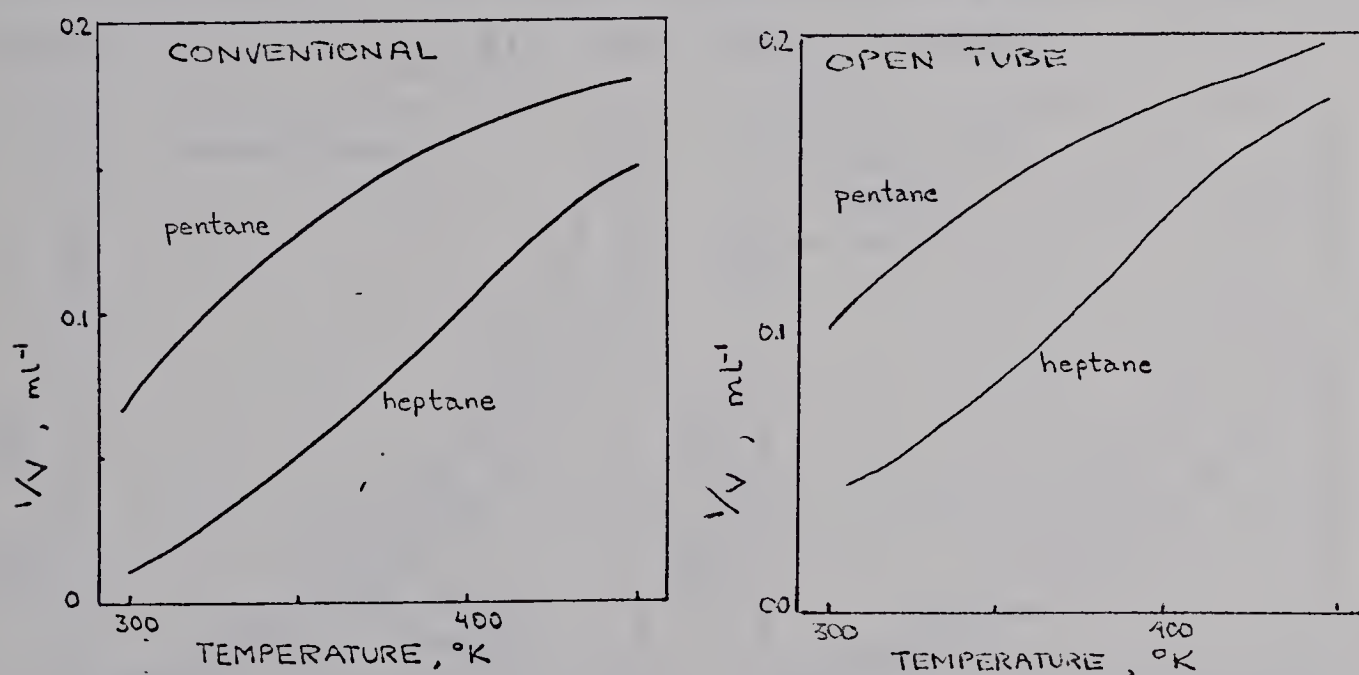


Figure 3.13 The reciprocal of the retention volumes of pentane and heptane as a function of the absolute temperature for two columns.

The initial temperature of 25°C was used with Figure 3.13 for the graphical integration of areas for the preparation of Figure 3.14. Figure 3.14 shows the predicted retention temperature for n-pentane and n-heptane as a function of the ratio  $r/F$ .



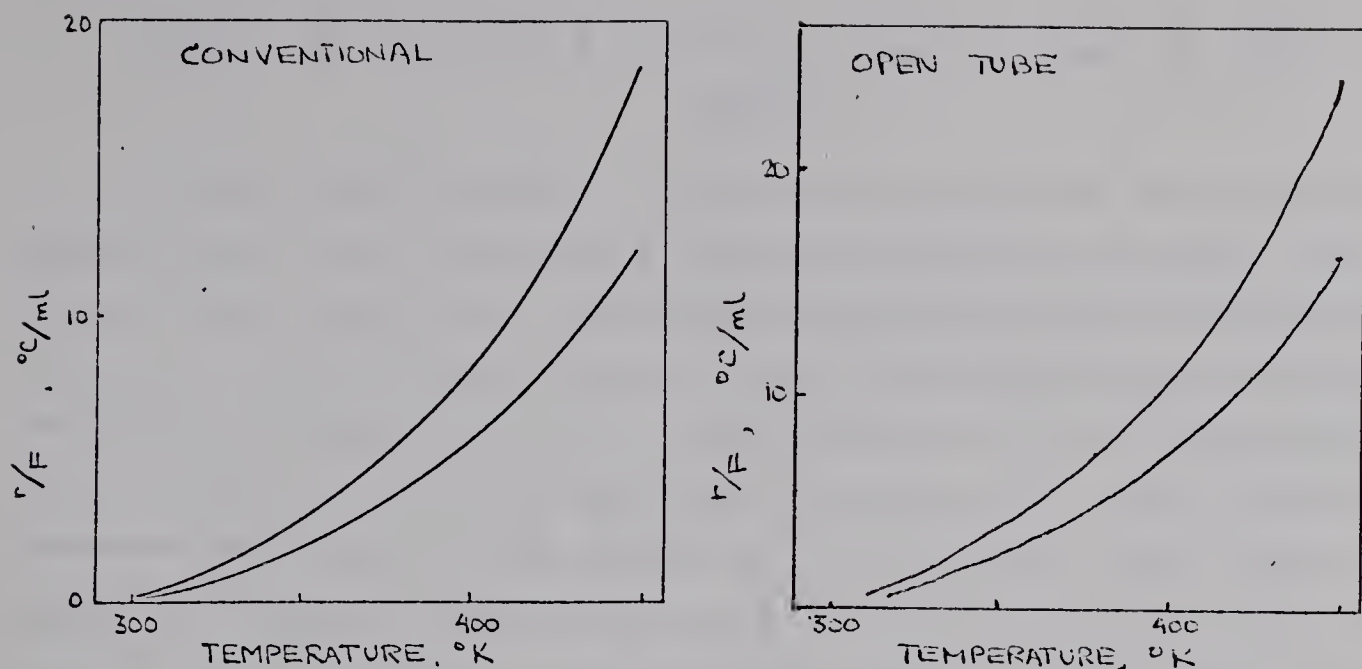


Figure 3.14 The dependency of the retention temperatures of pentane and heptane on the ratio  $r/F$  predicted from isothermal data for two columns.

Experimental data, represented by points, is plotted in Figure 3.15 for comparison with the values predicted from isothermal data. The experimental values generally fall at higher values of the  $r/F$  ratio than predicted.

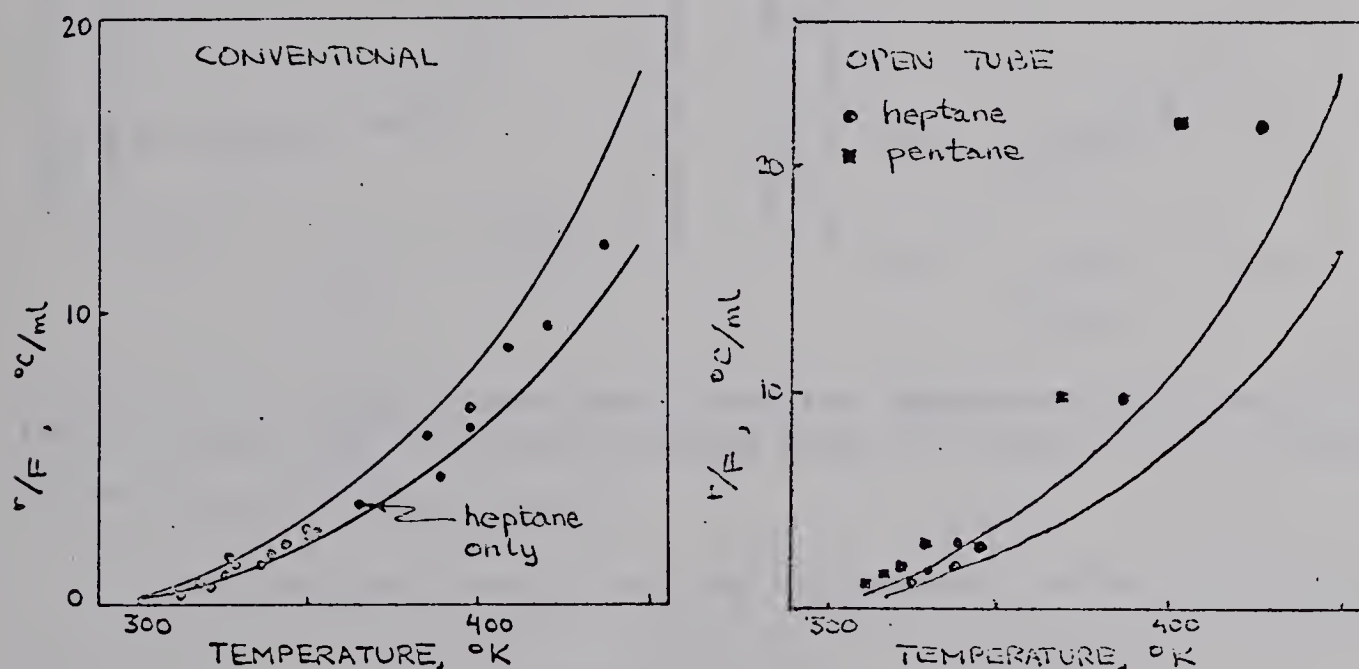


Figure 3.15 Comparison of experimentally determined and predicted retention temperatures.

The calculation of  $r/F$  in Figures 3.14 and 3.15 incorporated the flow rate as measured at  $25^{\circ}\text{C}$  and corrected for the pressure drop at that temperature for the series of isothermal runs (Figure 3.14) and for the programmed determination (experimental points in Figure 3.15).



## Errors in Predicted Retention Temperatures at High $r/F$ Ratios

If the theory which allows the prediction of retention temperature from isothermal data is correct any error in temperature should be independent of experimental parameters. In fact, the difference between the predicted and experimental retention temperatures, the absolute error, is independent of the program rate but correlates with the  $r/F$  ratio and increases abruptly in the range of 2 to 10 for that ratio. As shown in Figure 3.16A, the errors for all program rates fall on, or near a single line relating error to the ratio  $r/F$ .

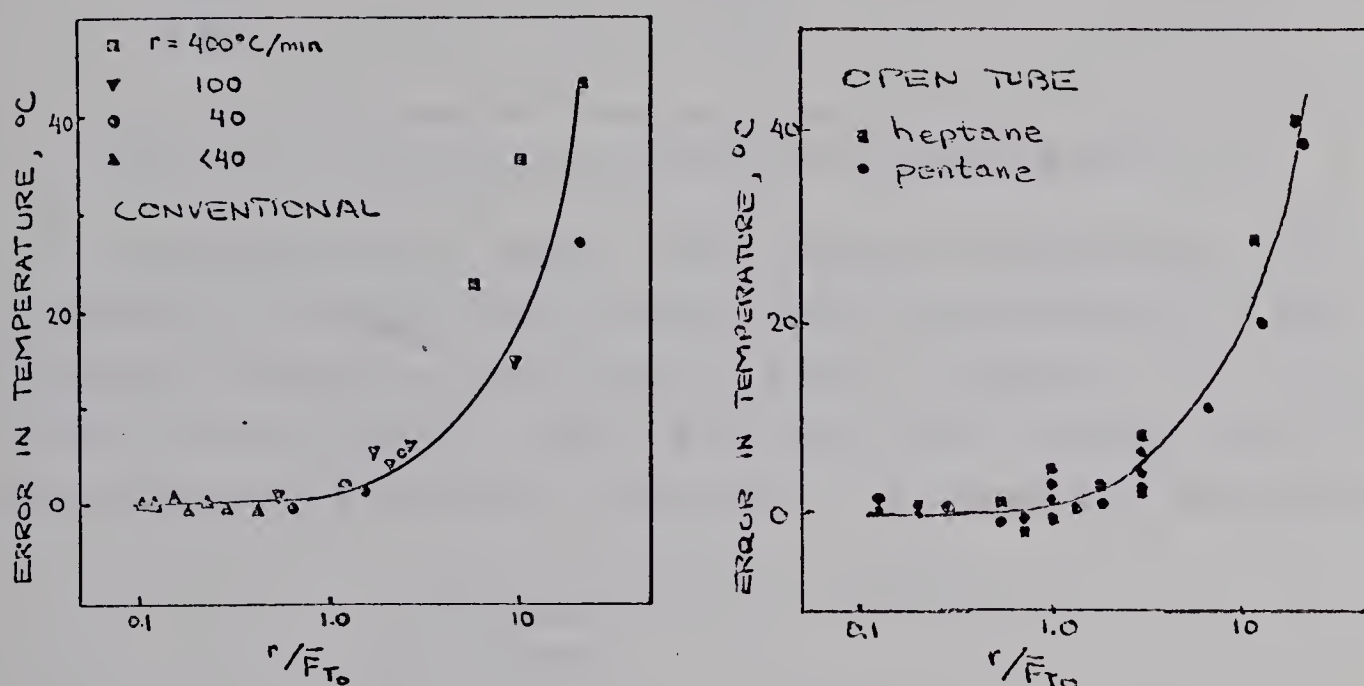


Figure 3.16 Error in predicted retention temperature as a function of the  $r/F$  ratio with individual heating rates indicated. Error defined as  $T_R(\text{predicted}) - T_R(\text{experimental})$ .

A normalized error may be calculated using the equation

$$\text{Error} = \frac{T_R(\text{experimental}) - T_R(\text{predicted})}{T_O - T_R(\text{predicted})} \quad (3.13)$$

which is equivalent to

$$\text{Error} = \frac{\text{absolute error}}{\text{predicted temperature increase}} \quad (3.14)$$

The normalized error, as defined in this manner, is also independent of program rate as may be seen in Table 3.01.



TABLE 3.01 ERRORS IN PREDICTED RETENTION TEMPERATURES \*

Program rate r (°C/min)	N Number of determinations all at different r/F ratios	Average of normalized error
0.4	4	0.21
1.0	6	0.36
4.0	13	0.25
40	12	0.21
100	10	0.15
400	6	0.25

\*These data represent the conventionally packed column only.

At high program rates the retention temperature will generally be high. The absolute error increases with the retention temperature as may be seen in Figure 3.17. It follows that absolute error increases with program rate to the extent that the rate increases the retention temperature.

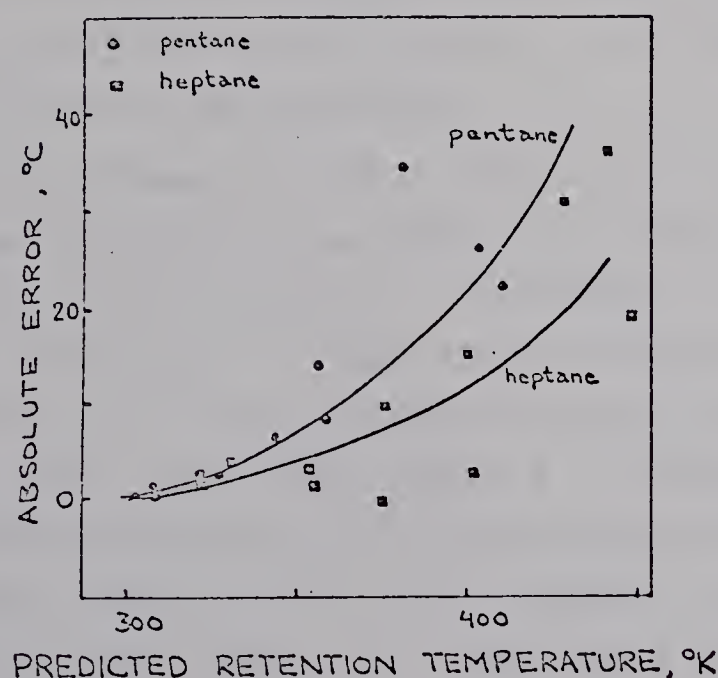


Figure 3.17 Absolute error in the retention temperature as a function of the predicted retention temperature. Data taken from determinations using only the conventionally packed column.



### 3.04 EFFECT OF RAPID TEMPERATURE PROGRAMMING ON RESOLUTION

Fryer, Habgood, and Harris (28) noted that at high values of the ratio of program rate to carrier flow rate,  $r/F$ , intrinsic resolution,  $R_i$ , approached zero. When the flow rate is expressed in ml/mn per gram of the stationary phase,  $\bar{F}$ , the range of 0.05 to 0.5 for  $r/\bar{F}$  appeared best. To keep the ratio  $r/\bar{F}$  at or below 0.5 when large values of  $r$  are expected it is necessary to use high flow rates. Either large absolute volumetric flow rates or low proportions of stationary phase would suffice. Both of these factors reduce retention time, the effect functioning with the high program rate to reduce analysis time.

The examination of high program rates, 40-400°C per minute, necessitates the use of flow rates far removed from the optimum value if the  $r/\bar{F}$  ratio is to be maintained in the 0.05 to 0.5 range. On the other hand, if a constant proportion of stationary phase is assumed, and if the flow rate is set at the optimum value, the  $r/\bar{F}$  ratio may be outside the desired range and the intrinsic resolution may be reduced.

The experiment to be described in the following sections were designed to allow examination of the influence of program rate on resolution and intrinsic resolution for as large a range of  $r/\bar{F}$  ratios as possible.

In these experiments it was necessary to calculate resolution, the procedure for which was described in Figure 3.02. The inflection points on a Gaussian curve occur at 0.607 of the peak height. When the inflection points are not clearly defined it is not possible to draw the tangent required to determine the base width,  $W$ . As shown in Figure 3.18 peaks with resolution of 0.5 or greater may be accurately measured in this respect. In this report, in any case where resolution fell lower than 0.5 the peaks were considered unresolved.



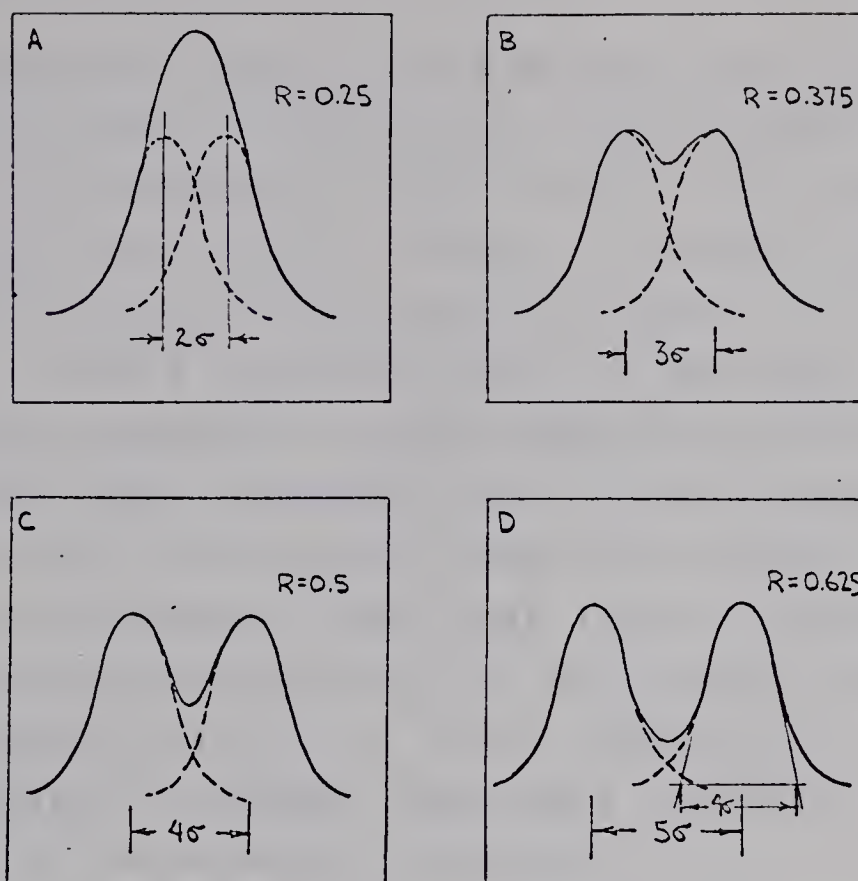


Figure 3.18 Peak separation required for the precise measurement of resolution.

For a normal error curve the base width, as drawn by extending the sides from the inflection point to the base line, is  $4\sigma$ , as shown in D.

Resolution is calculated according to the equation

$$R = \frac{2(\Delta V)}{W_1 + W_2}.$$

The separation between peaks above is given in terms of  $\sigma$ . The values for resolution accompanying each pair of peaks above are for two Gaussian peaks of identical size.

#### Program Rate and $r/F$ Ratio

As shown in Figure 3.11 the extreme ranges of the  $r/\bar{F}$  ratios predicted to be experimentally available could be attained using only two of the columns. Both columns were 1 meter long and 0.10" in inside diameter. One column was conventionally packed with 10% SF-96 coated on 60-80 mesh Chromosorb-P, and as in the preceding section referred to as the conventional column, and the second was the open tube column coated with SF-96, the open-tube column. The use of two such different columns allows the universality of the results to be examined.



The experimental coverage of  $r/\bar{F}$  ratios for program rates from 0.4 to 400°C per minute for both columns is shown in Figure 3.19. The boundaries of the area are shown in a qualitative way in the figure. Below a program rate of 0.4°C per minute the resolution was essentially that of isothermal chromatography. For a given program rate the upper limit of the  $r/\bar{F}$  ratio was determined by the ability to maintain and measure low flow rates precisely or, with the higher program rates, the failure of the second peak to be completely eluted during the program. The lower limits of the  $r/\bar{F}$  ratios is a function of the onset of disturbing flow effects in a thermal conductivity or of flame instability in the flame ionization detector. Program rates were limited to 400°C per minute or less by the equipment design.

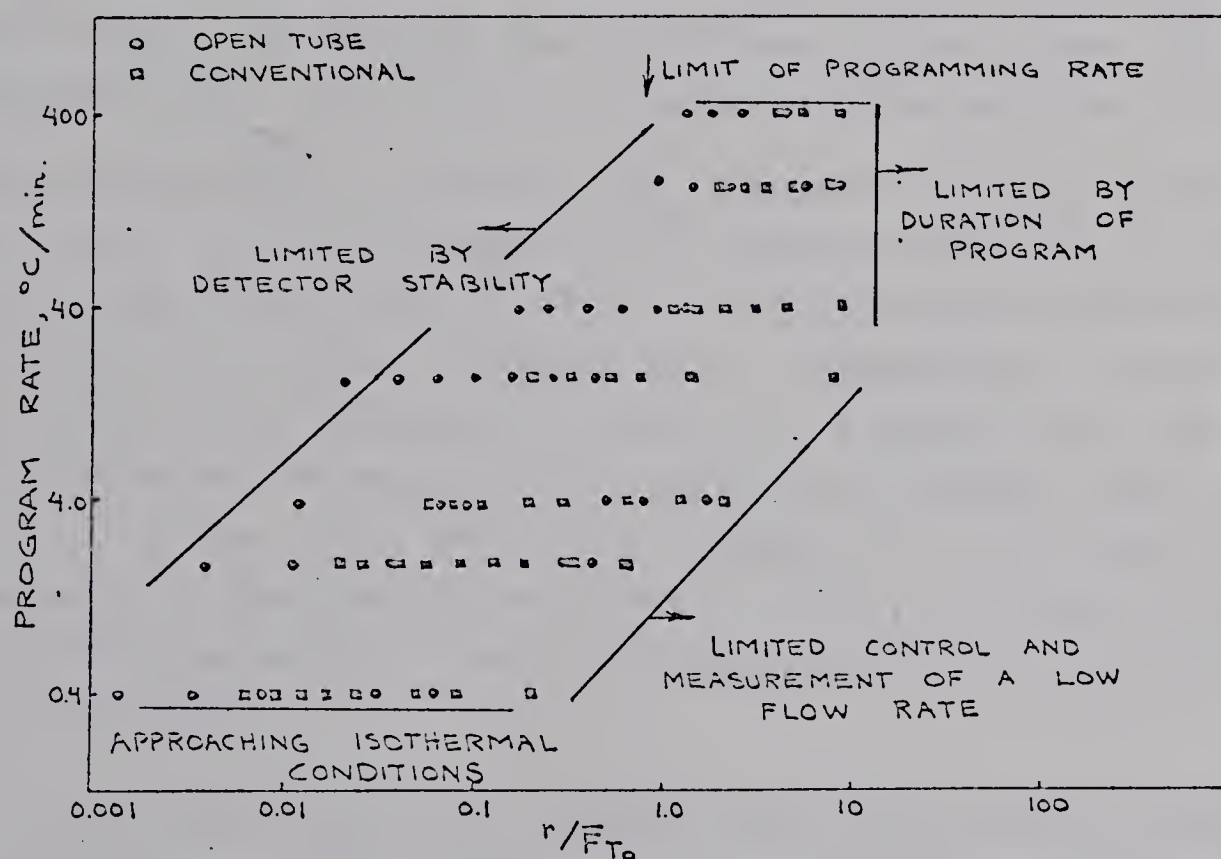


Figure 3.19 Experimental coverage of  $r/\bar{F}_{T_0}$ . The problem of determining the effective flow rate for a programmed  $T_0$  temperature determination, where pressure drop, gas viscosity, and volume are changing, will be considered later.

The flow rate used for the calculation of the program rate - flow rate ratio  $\frac{r}{\bar{F}_{T_0}}$  in Figure 3.16 was the flow rate



per gram of stationary phase at the initial temperature of the program corrected for pressure drop,  $\bar{F}_{T_0}$ .

Resolution and intrinsic resolution as functions of  $r/\bar{F}_{T_0}$  with  $r$  as a parameter are given for the conventional column and the open tubular column in Figures 3.20 and 3.21 respectively. The following discussion refers to these figures.

Each line in Figures 3.20 and 3.21 represents a single program rate with the  $r/\bar{F}_{T_0}$  determined by the flow rate. It can be seen that resolution passes through a maximum for each program rate except for the conventional column at 100 and 400°C per minute and for the open-tubular column at 400°C per minute. It appears that in these latter cases the smallest  $r/\bar{F}_{T_0}$  ratio was too large for the maximum to be seen. The maxima shift to higher  $r/\bar{F}_{T_0}$  ratios with increasing program rate up to 10°C per minute. At 0 program rates of 10°C per minute and above the  $r/\bar{F}$  for maximum resolution does not increase but remains at about 0.5. The maxima in resolution are essentially constant in value for program rates up to 10°C per minute and decrease with increasing program rate thereafter. If the  $r/\bar{F}_{T_0}$  ratio for maximum  $R$  does indeed remain constant as program rates increase above 10°C per minute the 400°C per minute time is displaced towards high values for resolution.

Intrinsic resolution follows the same general pattern as resolution. The displacement towards higher intrinsic resolution at high program rates is more pronounced; for the conventional column at 100 and 400°C per minute and for the open-tube column at 400°C per minute the line values are out of order.



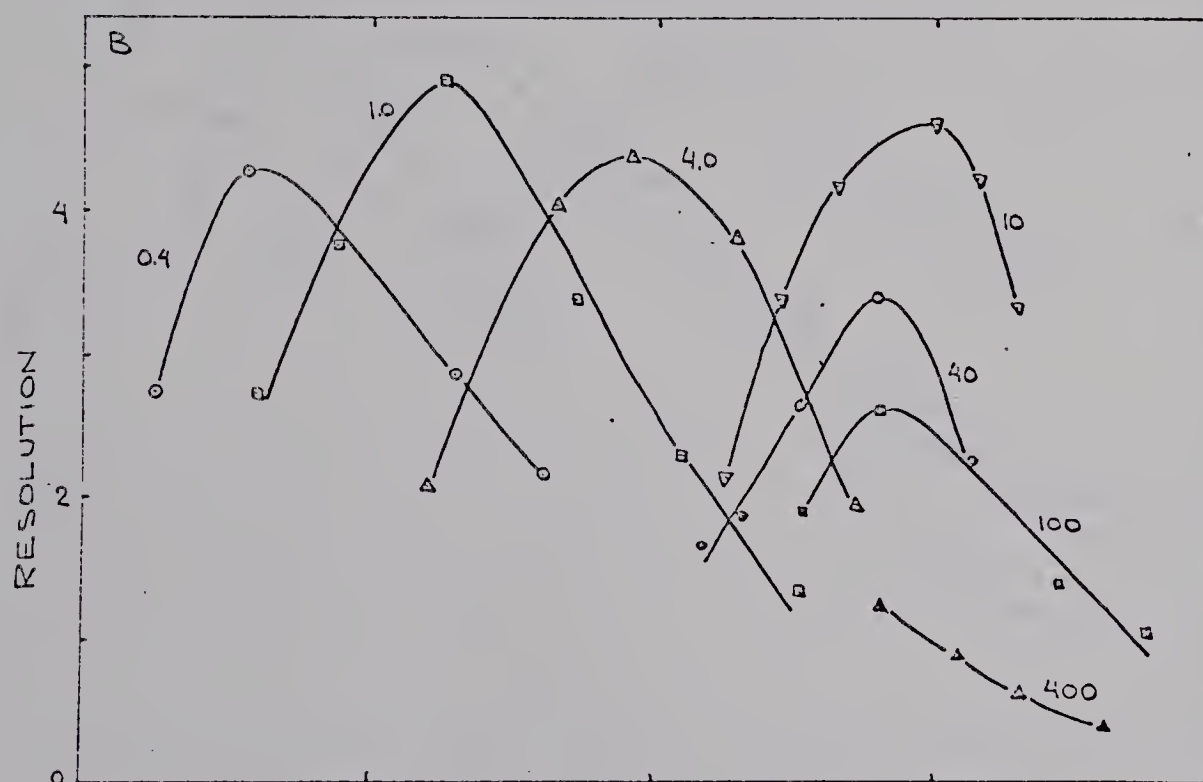
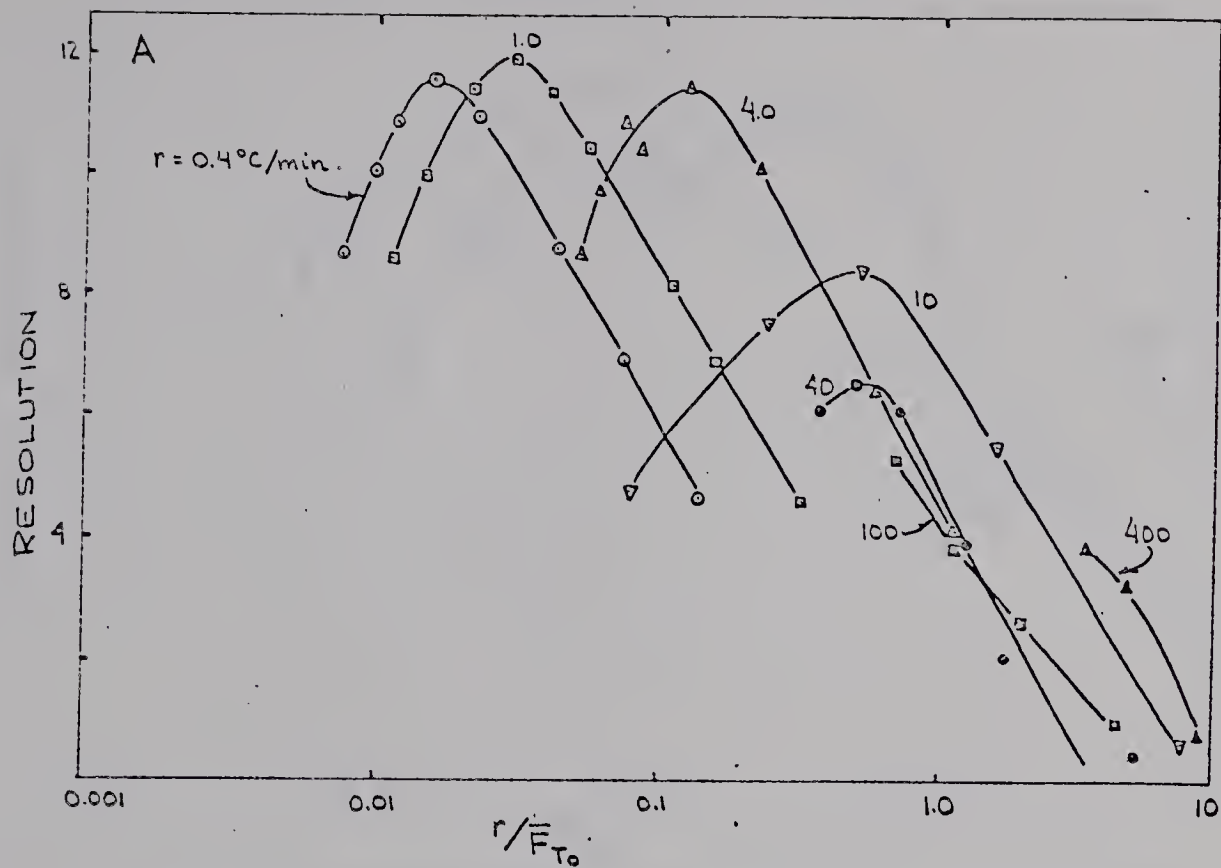


Figure 3.20 Resolution as a function of  $r/\bar{F}_{T_0}$  for a conventional column (A) and an open-tube column (B). Program rate in  $^{\circ}\text{C}$  per minute is shown as a parameter.



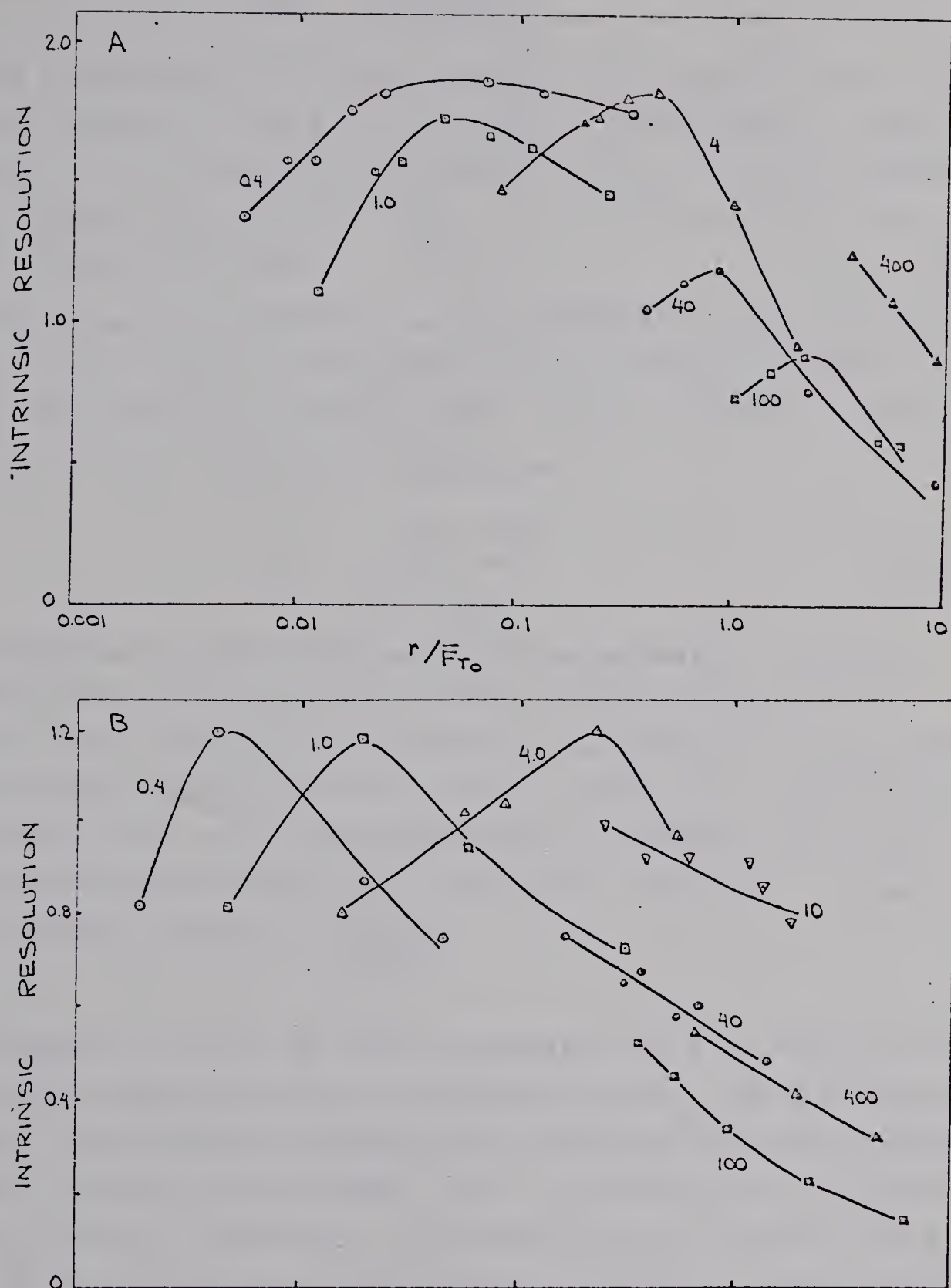


Figure 3.21 Intrinsic resolution as a function of  $r/\bar{F}_{T0}$  for a conventional (A) and an open-tube column (B). Program rate in °C per minute is shown as a parameter.



The essential difference between the conventional and the open tubular columns is the ratio of dead-space volume to amount of stationary phase present,  $\bar{V}_{ds}$ . For the conventional column the value of  $\bar{V}_{ds}$  is 2.1 ml/g and for the open tubular column 220 ml/g.

Dead space contributes to the retention volume of a component but does not contribute significantly to the difference between the retentions for two solutes. Thus in the equation for intrinsic resolution

$$R_i = \frac{V_2 - V_1}{\left( V_{T_R} \right)_{av}} \quad (3.07)$$

increasing dead space increases the denominator without increasing the numerator and intrinsic resolution is reduced. This decrease in intrinsic resolution is greatest at high values of the  $r/\bar{F}$  ratio where retention temperatures are highest. As retention temperature increases the dead space contributes more to the individual retention volumes, hence to their average,  $\left( V_{T_R} \right)_{av}$ .

Equation (3.07) is also the basis for a calculation of intrinsic resolution from isothermal data. The differences between the retention volumes are obtained from the characteristic curves as in Figure 3.14. A value of  $r/F$  is chosen and  $T_{R_1}$  and  $T_{R_2}$  recorded.  $T_R$  divided by  $r/F$  yields the  $V$ . Hence  $V_2 - V_1$  is equal to  $(T_{R_2}/r/F) - (T_{R_1}/r/F)$ . The average of the retention volumes for the corresponding retention temperatures,  $\left( V_{T_R} \right)_{av}$ , are obtained from a plot of the log of the net retention volume as a function of the reciprocal of the absolute temperature as in Figure 3.12.

Figure 3.22 is a duplicate of Figure 3.21 with the theoretical intrinsic resolution (that is  $R_i$  calculated from isothermal data) also included. For the open tubular



column the agreement is excellent over the range in which the theoretical values could be calculated. For the packed column the theoretical intrinsic resolution is generally smaller than that determined experimentally and calculated using the assumption of a constant effective carrier flow equal to that at the initial temperature. In reality the effective flow rate at higher temperatures will be slightly lower because the pressure gradient correction factor continually decreases as the inlet pressure rises with increasing temperature.

### Plate Height

It has been shown in the previous section that both resolution and intrinsic resolution pass through maxima when examined using a single program rate and increasing the value of the  $r/\bar{F}_T$  ratio. The position of these maxima may depend in part on how plate height changes with flow rate.

If the plate height largely determines the value of the  $r/\bar{F}$  ratio, for a given program rate, at which  $R$  and  $R_i$  are at a maximum, then this maximum should occur at  $r/\bar{F}_{opt}$ .  $\bar{F}_{opt}$  is defined by Van Deemter plots, as shown in Figure 3.23 for the two columns, and corresponds to the flow rate where plate height is at a minimum. The flow rate per gram of stationary phase at the plate height minimum,  $\bar{F}_{opt}$ , is calculated from  $F_{opt}$  knowing the amount of stationary phase in each column.



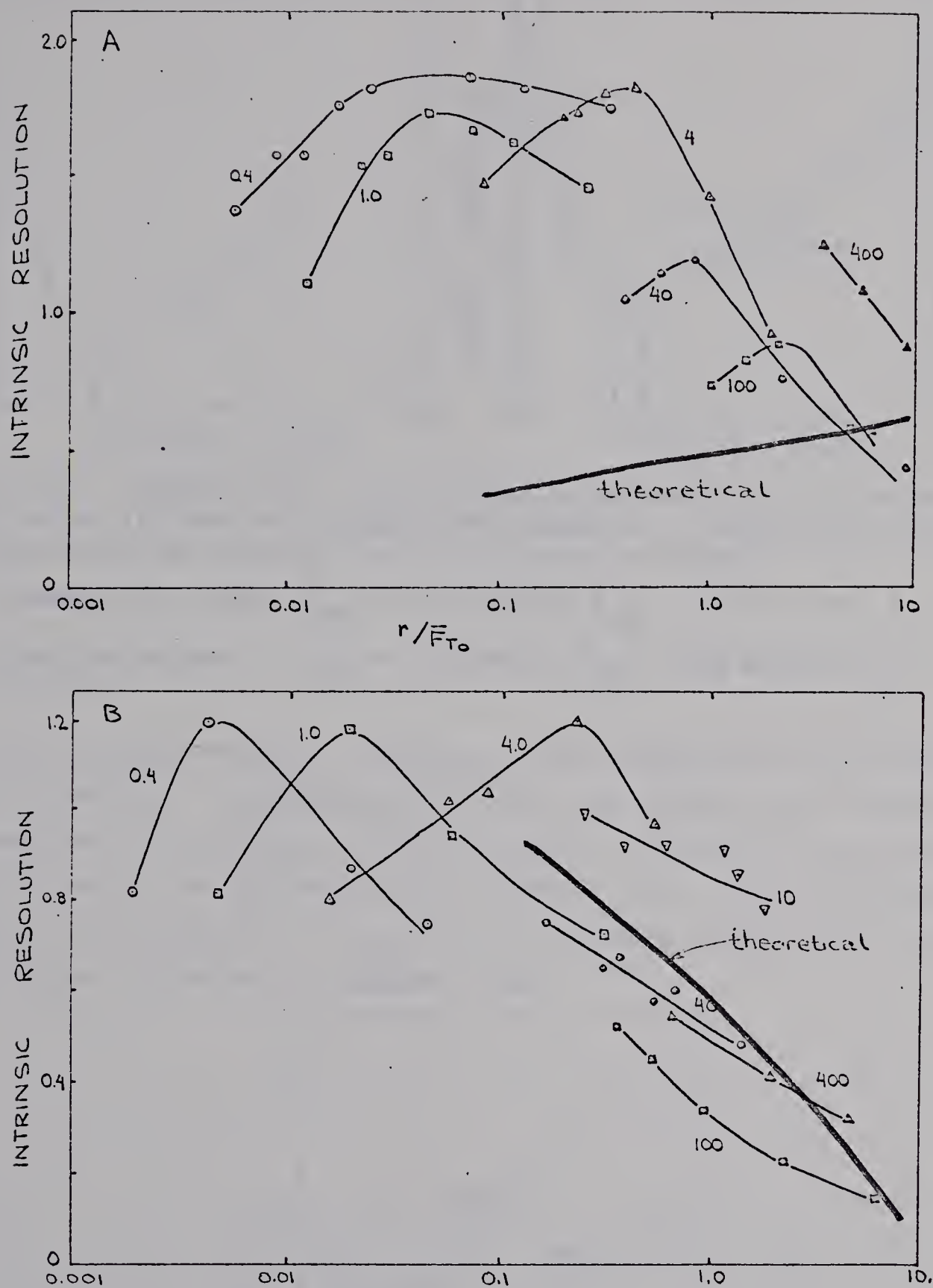


Figure 3.22 The effect of column dead space on intrinsic resolution; theoretical and experimental values. Experimental data for the conventional column (2 ml/g dead space) and for the open tube column (200 ml/g dead space) taken from Figure 3.21.



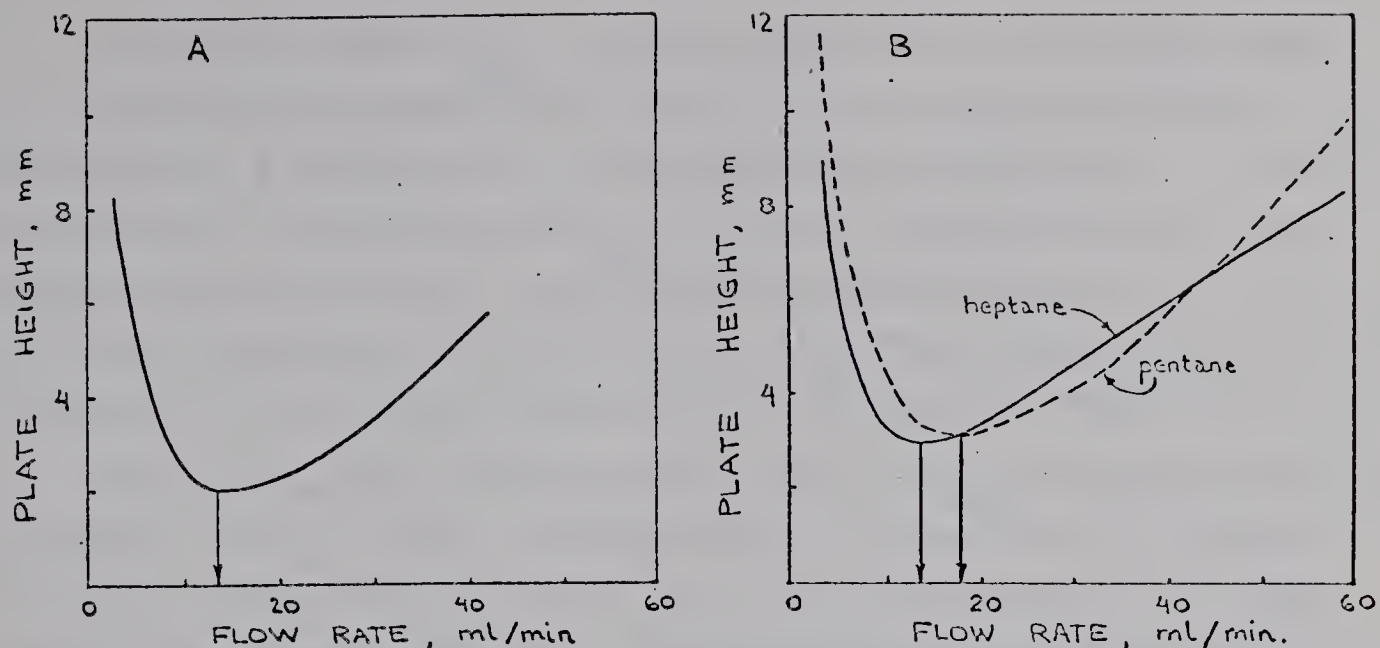


Figure 3.23 The flow rate - plate height relationship for the conventional column (A) and for the open-tube column (B). Isothermal at 25°C with n-heptane, the homologs used in the resolution study.

Conventional column:  $F_{opt} = 12.5$  ml/min;  $\bar{F}_{opt} = 3.20$  ml/min. g.

Open-tube column:  $F_{opt} = 14$  ml/min.;  $\bar{F}_{opt} = 495$  ml/min. g.

The change in  $F_{opt}$ , or  $\bar{F}_{opt}$ , with temperature is difficult to predict. Generally, for any one solute, an increase in temperature requires a corresponding increase in gas velocity to obtain an optimum plate height (39). Some solutes display little shift in  $F_{opt}$  with increasing temperature such as n-hexane as shown in Figure 3.24.

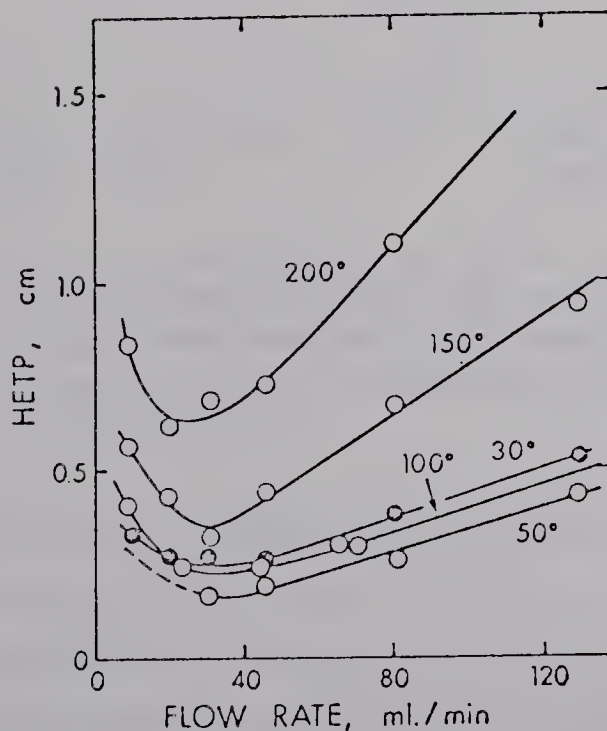


Figure 3.24 The flow rate - plate height relationship for n-hexane as a function of temperature, from Harris and Habgood (39).



Assuming that  $\bar{F}_{opt}$ , as obtained from isothermal data at the initial temperature used for the program, holds throughout a temperature programmed determination, it is possible to calculate  $r/\bar{F}_{opt}$  for each program rate. This approximation allows a qualitative investigation of the relative importance of flow rate in determining the  $r/\bar{F}$  ratio required for maximum resolution or intrinsic resolution.

For the series of program rates  $r/\bar{F}_{opt}$  ratios can be calculated. This ratio is plotted as a function of program rate in Figure 3.25 A and B for the conventional and open tube column respectively. The experimental  $r/\bar{F}$  ratios at which resolution, represented by circles, and intrinsic resolution, triangles, were at a maximum for each program rate were taken from Figures 3.20 and 3.21.

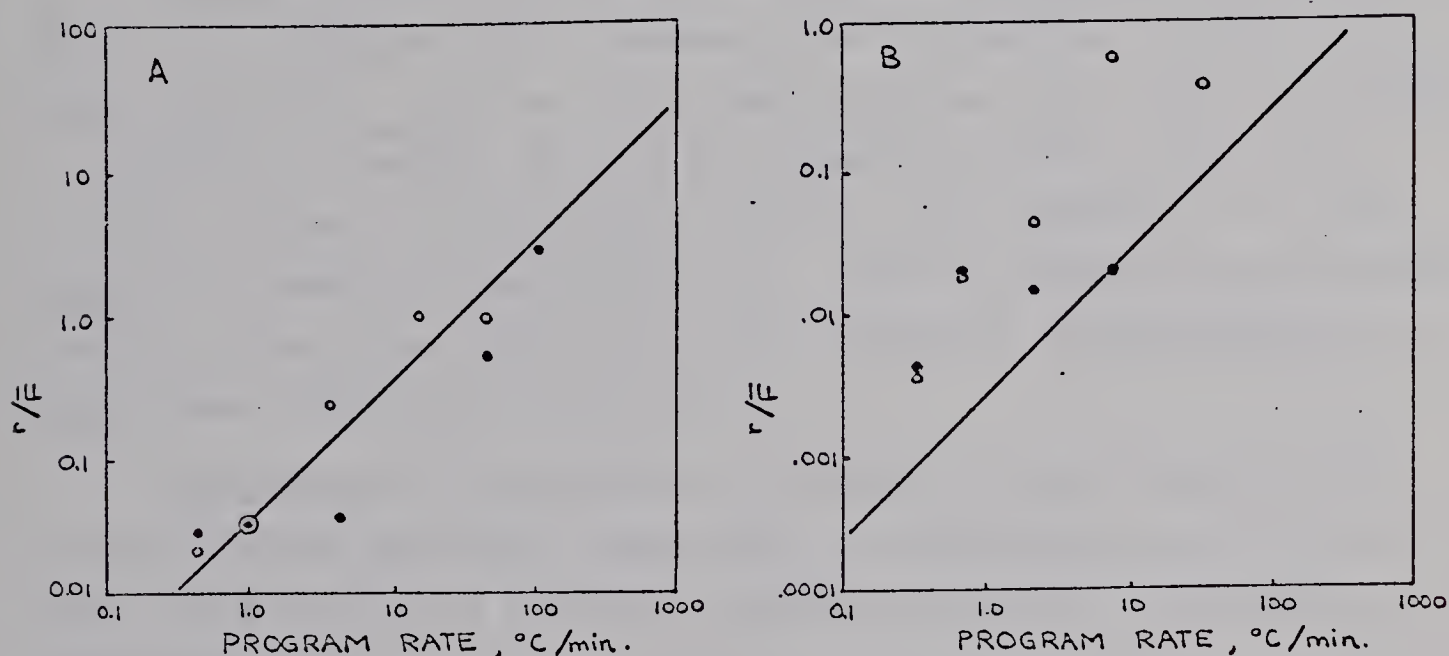


Figure 3.25 The  $r/\bar{F}$  ratio at which  $R$  or  $R_i$  is at a maximum as a function of program rate for the conventional column<sup>i</sup> (A) and the open-tube column (B). Lines represent values predicted on the basis of optimum flow rate. Open circles represent resolution, and solid points, intrinsic resolution as taken from Figures 3.20 and 3.21.

For the conventional column the agreement is good. From this it may be inferred that plate height considerations are of fundamental importance in establishing an optimum  $r/\bar{F}$  ratio to obtain a maximum in resolution for any specified program rate.



For the open tubular column the maxima in resolution and intrinsic resolution occur at  $r/\bar{F}$  ratios higher than predicted on the basis of the isothermal optimum flow rate. This may be a result of the influence of relatively large dead space volume on the linear flow velocity.

It is surprising, however, that intrinsic resolution displays any dependency on flow rate as this effect should be removed when the  $\sqrt{n}$  term is factored out of the resolution.

The utility of rapid linear temperature programming in investigating chromatographic phenomena has been demonstrated.

#### Comment

Deterioration of column performance with use was found. Harris and Habgood (40) stated that "repeated cycling of a column between low and high temperatures may cause particles of packing to settle during an expansion cycle and to be crushed during a contraction cycle, thus leading to a progressive change in permeability". Their calculations indicate, however, that the opportunity for particle rearrangement in the column should be negligible.

Degradation of performance caused by the fracture of the particles has been noted (93). The removal of fine particles has been found to give a marked increase in column efficiency (6).

A 1 m 0.10" i.d. column packed with 5% SF.96 on 60-80 mesh Chromosorb-P was found to have a plate height of 1.8 mm at its optimum flow rate. After 1500 heating and cooling cycles, 350°C to 225°C to 35°C in 180 seconds, the plate height increased to 2.2 mm at the same flow rate. This is a 22 percent increase.

Microscopic examination at 10x, 30x, and 100x of the particles subjected to the heating cycles revealed no marked change in their character. More fines were present in the bulk sample but it did not prove possible to photographically document this.



## 4. GAS PHASE PYROLYSIS

### 4.01 BRIEF SURVEY OF PYROLYSIS IN THE LITERATURE

Levy (67) has recently reviewed the methodology of pyrolysis gas chromatography (PGC) and lists more than 200 references from the literature through September, 1965. The development of the technique, both in its initial stages and more recently, is thoroughly covered.

The Gas Chromatography Abstracting Service, Preston Technical Abstract Co., Evanston, Illinois, abstracts the broad field of gas chromatography. Appearing among the abstracts issued between September, 1966, and March, 1967, are 28 in which pyrolysis has been involved. These papers, selected from the abstracts, are listed by author in Appendix III.

Pyrolysis gas chromatography is one aspect of a broader area which has been called reaction gas chromatography. Beroza and Coad (8) reviewed reaction gas chromatography and established the following classifications: subtractive processes, pyrolysis reactions, kinetic and catalytic studies, hydrogen reactions, and miscellaneous. An arbitrary classification system for pyrolysis according to the extent of degradation was given as follows: thermal degradation ( $100^{\circ} - 300^{\circ}\text{C}$ ), mild pyrolysis ( $300 - 500^{\circ}\text{C}$ ), normal pyrolysis ( $500 - 800^{\circ}\text{C}$ ), and vigorous pyrolysis ( $800 - 1100^{\circ}\text{C}$ ). These ranges may be extended according to operational conditions. This review (8), giving 447 references, includes classes of compounds which have been subjected to PGC, and with the review of Levy constitutes a general coverage of PGC.

Pyrolysis gas chromatography has been used for obtaining structural information concerning organic compounds (30). An examination of pyrolysis products does not always allow the determination of the general nature of the material being pyrolyzed. This is a result of compounds of similar products



configurations giving dissimilar distributions of pyrolysis products. Kirk (64) feels that this is a deficiency and is at least partially due to the poor state of basic information. He also feels this lack of basic information results from inadequate research interest and from the tendency of all complex compounds to break into a large number of small molecules, many of them simple hydrocarbons.

#### 4.02 PYROLYZER DESIGN

Pyrolysis apparatus (pyrolyzers) have been classified by heating mode by Levy (67). First, the pulse heating type (filament), generally used for microgram samples, and secondly the continuous heating type (reactor) used for milligram quantities. Further, each type was divided, according to the source of energy, into the following sub-groups: units using electrical resistive heating, electrical discharge, high frequency induction heating, radiation and arc. Such a classification scheme allows the inclusion of a broad range of techniques such as radiolysis, photolysis, and flash photolysis, which may find applications analogous to those of PGC.

Pyrolysis in the gas phase of microgram quantities of volatile materials, such as are found in gas chromatographic effluents, allows the use of continuously heated tubular pyrolyzers. Dhont (19), Figure 4.01, described such a unit using a chromosorb packed silica tube. Open tubes of pyrex and stainless steel for temperatures below and above 500°C respectively have also been described (70). Cramers and Keulemans (14), described a coiled metal tubular pyrolyzer of 1 mm inside diameter and 1 m length. Perry (79) also described a metal tubular pyrolyzer.

An open tubular pyrolyzer has a lower possibility of catalytic effects relative to packed tubes. For this reason and because of a greater latitude in design and a more easily calculable volume the open tube was chosen for this research.



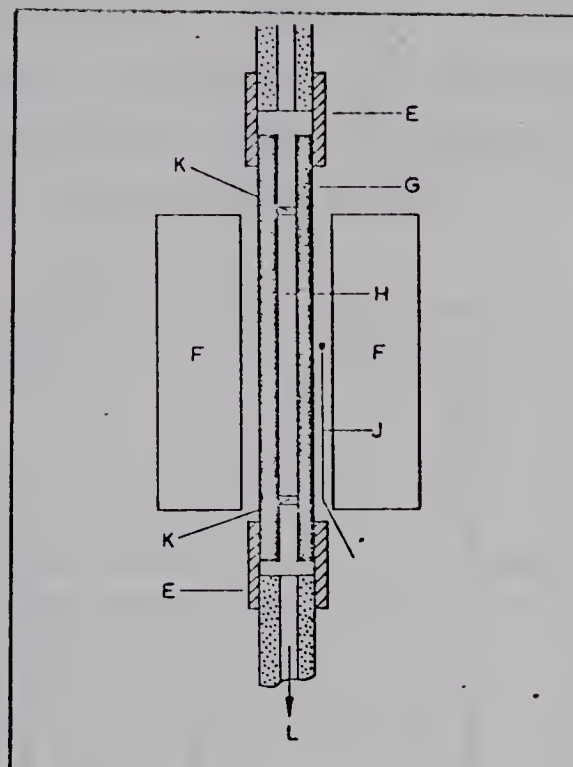


Figure 4.01 Pyrolyzer of Dhont(19).

E, silicon rubber tubing; F, tubular furnace; G, silica pyrolysis tube; H, Chromosorb; J, thermocouple; K, glass wool plug; L, flow to column.

### Temperature Profiles

Levy (67) qualitatively predicted the influence of linear flow velocity on the temperature profile of a tubular pyrolyzer as shown in Figure 4.02.

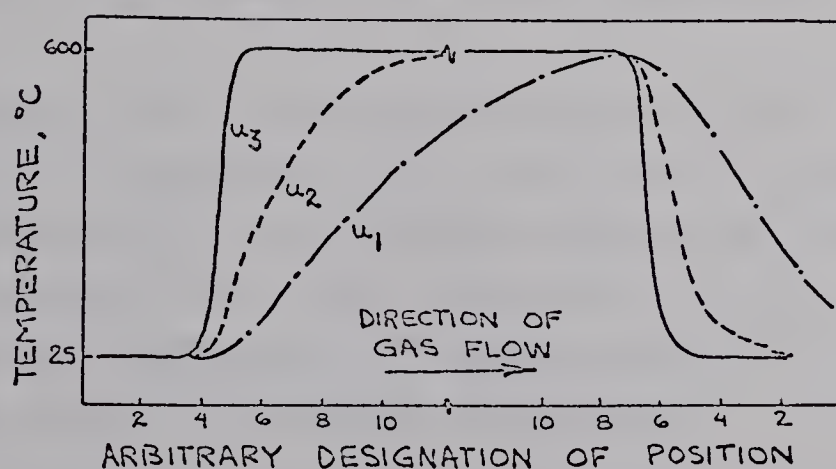


Figure 4.02 Expected temperature profile for a tubular pyrolyzer. From Levy (67). Linear flow velocities  $u_1 > u_2 > u_3$ .



The desirability of a "squared" temperature profile becomes apparent when attempting to compare programs obtained from pyrolyzers having different temperature profiles. Three different idealized temperature profiles are shown in Figure 4.03.

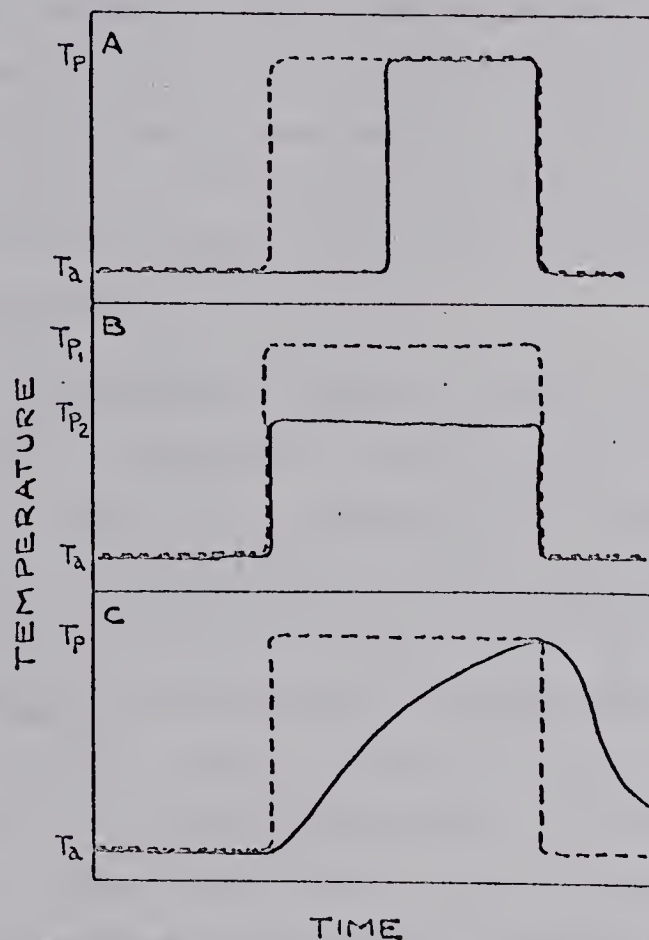


Figure 4.03 Idealized temperature profiles. Dashed line in each case represents a pyrolyzer with squared temperature profile at a pyrolysis temperature  $T_p$ .  $T_a$  represents the ambient temperature.

In Figure 4.03 A the temperature profile indicates that the pyrolysis temperature,  $T_p$ , for both pyrolyzers is the same and that only the residence time is different. It would be expected that only the extent of pyrolysis would be altered by the difference in residence time so that the pyrolyzers would be directly comparable.

The residence times for the two pyrolyses are the same in Figure 4.03 B but the pyrolysis temperature is different. Any differences in the distribution of pyrolysis products under these conditions may be directly correlated with the difference in pyrolysis temperature, a difference which can be precisely stated.



In Figure 4.03 C the situation is less clear. The pyrolysis temperature for the non-squared profile is not a constant, but changes during the pyrolysis. Pyrolysis can occur over a wide range of temperatures but the temperature specified as the pyrolysis temperature would probably be the same, fixed, value as for the squared profile. The residence time becomes more difficult to interpret. The comparison of pyrograms obtained under non-square temperature profile conditions is difficult because of the inexact manner in which both temperature and residence time would probably be specified.

To design a pyrolysis tube with flow characteristics giving the desired temperature profile with the required residence time it was necessary to determine, quantitatively, the influence of linear flow velocity. The apparatus arrangement for this determination is shown in Figure 4.04.

An experimentally determined temperature profile is shown in Figure 4.05. The coordinates are the same as in Figure 4.02, that is, the temperature is on the ordinate and the position along the tube is on the abscissa. The thermocouple was passed through the length of the pyrolyzer tube to measure temperatures at the inlet end. This is indicated in Figure 4.04 and was made necessary by the gas supply connections at the inlet. The thermal conductivity of the thermocouple wire may have caused the sensing portion to be hotter than the gas at the inlet end. This may have caused the measured temperature profile at the inlet to appear less square than it really was. Even so, the profile is more nearly square at the inlet than at the outlet where this type of problem was not encountered.

Levy (67) also predicted in a qualitative manner the influence of tube radius on the temperature profile of a tubular pyrolyzer, Figure 4.06. The tube radius will be a variable in the design considerations in the following section.



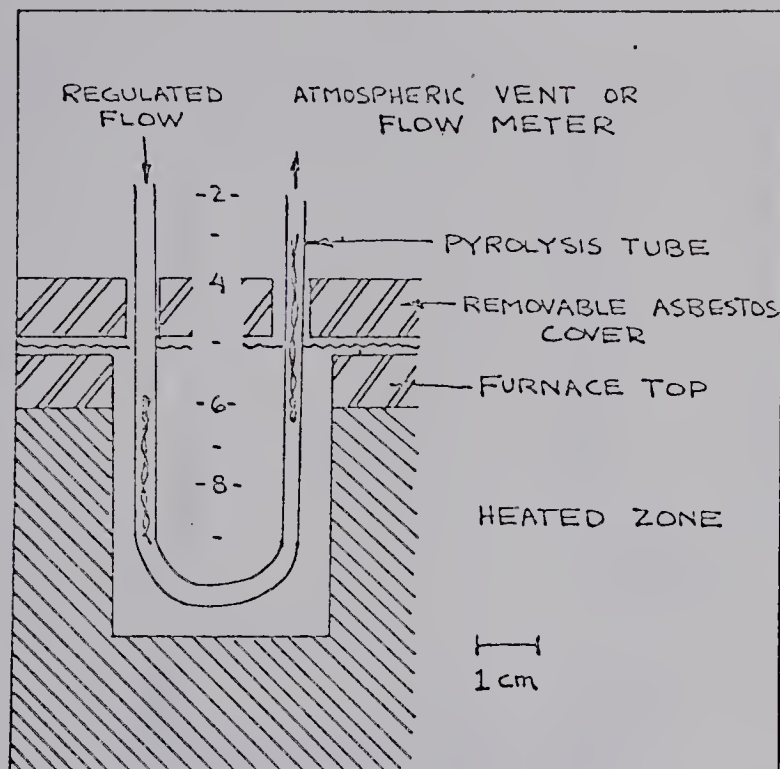


Figure 4.04 Apparatus for obtaining temperature profile of pyrolyzer. Thermocouple shown in position 6 in both inlet and exit legs.

The temperatures up to 250°C were measured with a calibrated pyrometer described in Appendix I, and temperatures above 250°C were measured with an iron-constantin thermocouple and calibrated recorder.

The flow rate was determined with a 50 or a 10 ml soap film flow meter at room temperature.

### Design Considerations

With a general knowledge of the effects of linear flow velocity and tube radius it is possible to design a tubular pyrolyzer with the desired temperature profile. Residence time requirements may be established after investigation of its effect on the distribution of product, and the degree of pyrolysis. Residence time,  $t_r$ , is given by Equation (4.01).

$$t_r = \frac{v}{F_p} \quad (4.01)$$

where  $v$  is the volume of the pyrolyzer tube and  $F_p$  is the volumetric flow rate in the pyrolyzer tube. The volume,  $v$ , is given by the equation

$$v = \pi R^2 \cdot L \quad (4.02)$$

where  $R$  is tube radius and  $L$  is its length.



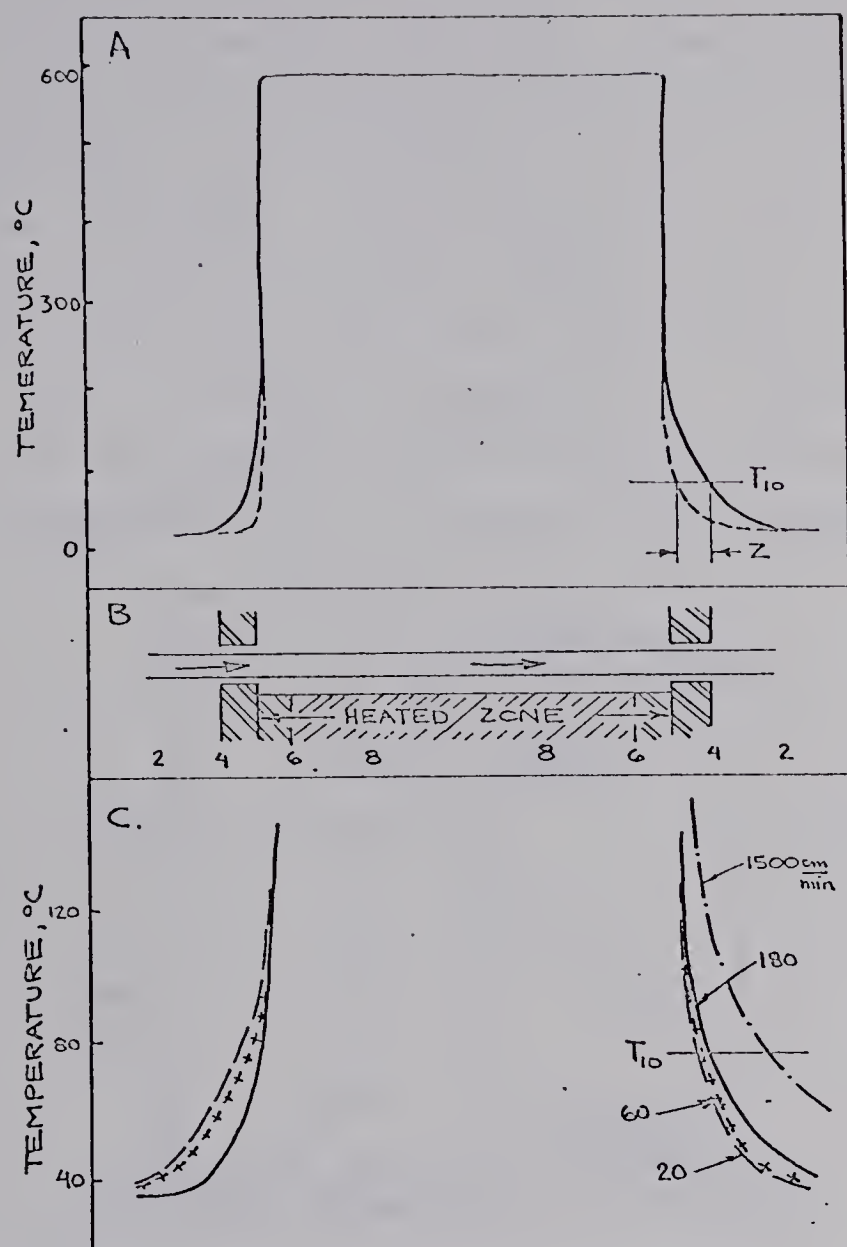


Figure 4.05 Effect of linear flow velocity on the temperature profile of a tubular pyrolyzer. Temperature profile A and with expanded temperature scale in B are shown against a schematic of the tubular pyrolyzer, B.  $T_{10}$  and Z are defined in the text. Complete details of pyrolyzer construction are given in Figure 4.10. Linear flow velocities calculated using tube cross sectional area and volumetric gas flow at the ambient temperature.

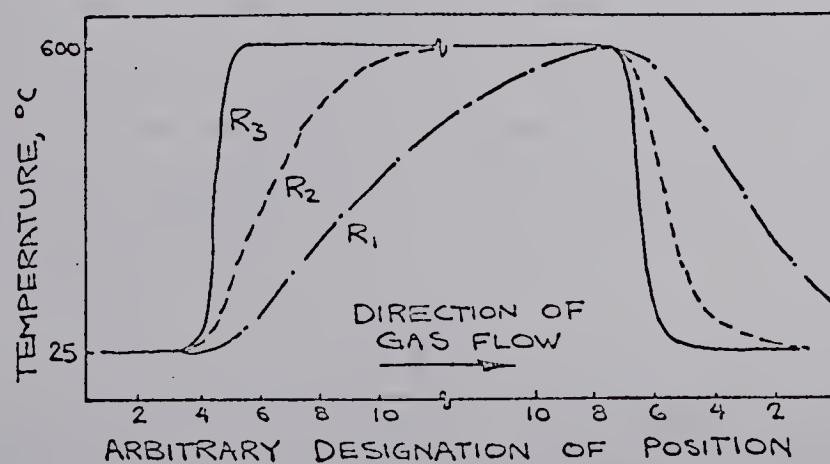


Figure 4.06 Expected temperature profile for a tubular pyrolyzer showing the effect of the tube radius,  $R$  where  $R_1 > R_2 > R_3$ . From Levy (67).



Because of the exponential return of the gas to the ambient temperature from the pyrolysis temperature it is not possible to state exactly the time required for the transition. A temperature,  $T_{10}$  is defined as that at which the temperature has decreased by 90 percent of the difference between the ambient and pyrolysis temperatures. It is possible to determine precisely the time required to reach this temperature. This is shown in Figure 4.07. The distance from the exit of the heated zone to the point where the temperature has returned to  $T_{10}$  is called the transition zone,  $Z$ .

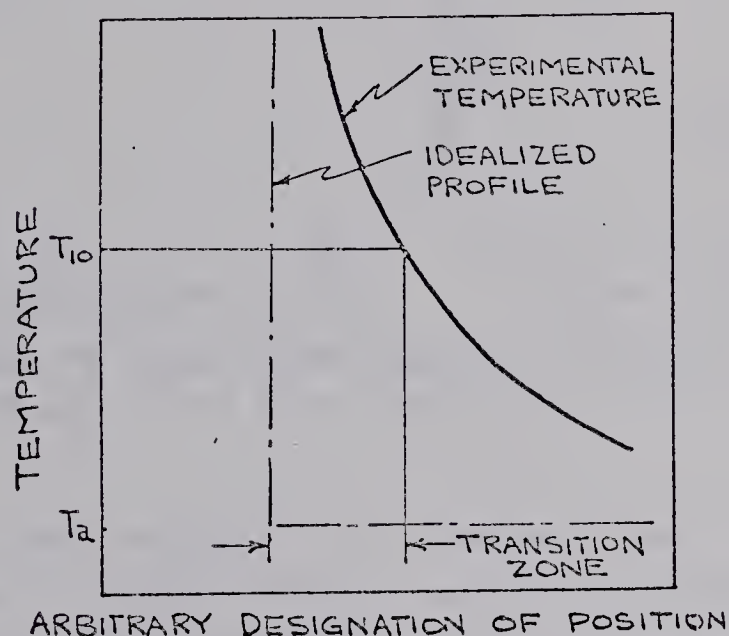


Figure 4.07 Graphical definition of transition zone.  $T_{10}$  defined by the equation

$$T_{10} = T_a + 0.1 (T_p - T_a)$$

where  $T_a$  and  $T_p$  are the ambient and pyrolysis temperatures respectively.

From Figure 4.05 C the transition zone, as just defined, may be determined as a function of linear flow velocity,  $u$ . This flow velocity, for all points outside of the heated zone, is calculated from the measured volumetric flow rate of the gas at the ambient temperature,  $F$ , and the cross sectional area of the pyrolysis tube,  $A$ .

$$u = \frac{F}{A} \quad (4.03)$$

Figure 4.08 A is a plot of the length of the transition zone as a function of the linear flow velocity. The length of the transition zone increases with increasing flow velo-



city. If the length of the transition zone were to be used as the criterion of the desirable square temperature profile the wrong conclusion would probably be reached as it would appear to favor low linear flow velocities.

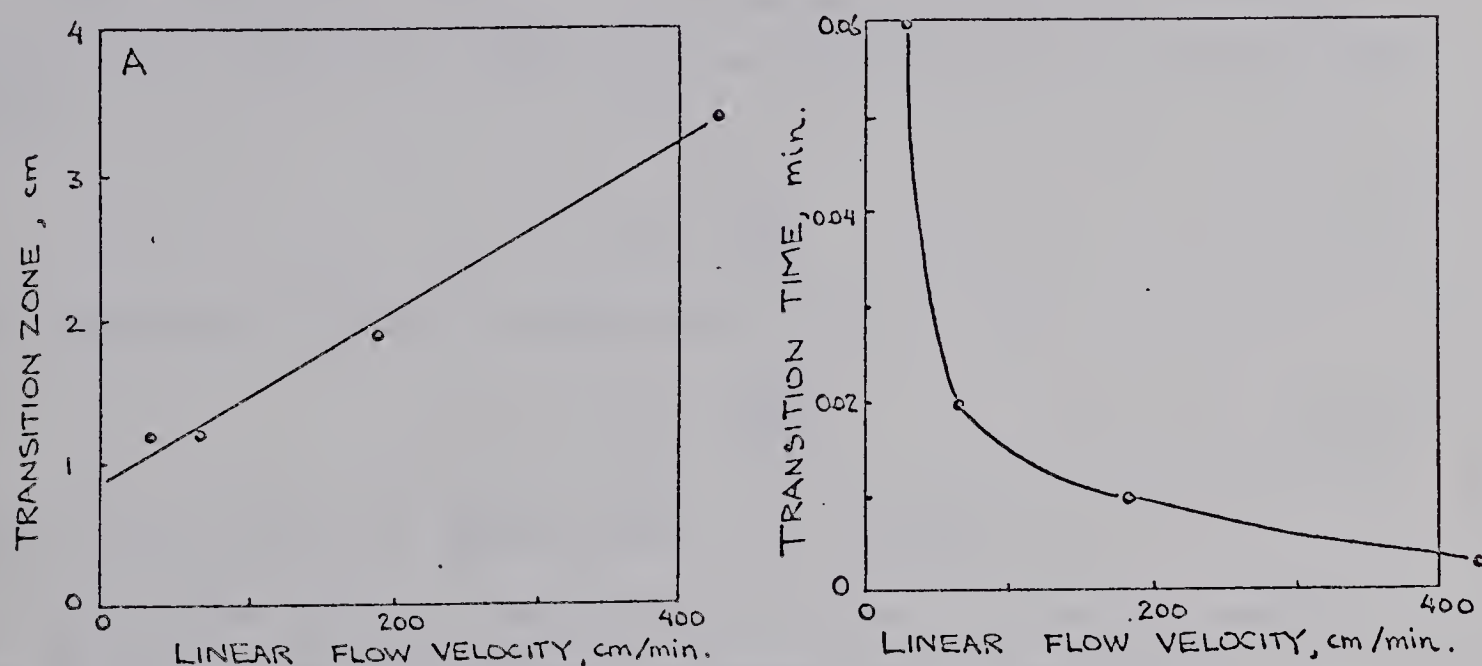


Figure 4.08 Effect of linear flow velocity on transition zone length (A) and transition time (B). Data from Figure 4.05 C.

It is the time required for the gas (and therefore the sample) to return to the ambient temperature that is of fundamental importance. This time should be as short as possible for reasons explained in conjunction with Figure 4.03. The effect of flow rate on the transition time may be determined as explained below.

The simple relationship of linear flow velocity,  $u$ , (cm/min) length of the transition zone,  $Z$  (cm), and the transition time  $t_z$  (min) is given in the equation

$$t_z = \frac{Z}{u} \quad (4.04)$$

Transition time as a function of linear flow velocity is shown in Figure 4.08 B. Transition time decreases with increasing flow velocities so that high flow velocities are better for obtaining the desired square temperature profile. The desirability of high linear flow velocities favors the use of small tube radii which were also indicated as best by Levy as shown in Figure 4.06.



In the heated zones the volumetric flow rate, hence the linear flow velocity, changes and must be considered when calculating pyrolysis residence time.

The residence time,  $t_r$ , may be calculated if the flow rate in the pyrolysis tube,  $F_p$ , and the volume of the tube are known.

$$t_r = \frac{V}{F_p} \quad (4.01)$$

This equation (4.01) is equivalent to

$$t_r = \frac{\pi R^2 L}{F_p} \quad (4.05)$$

where  $R$  is the tube radius and  $L$  its length.

The flow rate in the pyrolysis tube,  $F_p$ , is related to the flow rate at the ambient temperature,  $F$ , as in the equation

$$F_p = F \cdot \frac{T_p}{T_a} \quad (4.06)$$

where  $T_a$  is the ambient temperature and  $T_p$  is the pyrolysis temperature both in degrees Kelvin.

These simple equations used with experimental data of the type shown in Figure 4.08 B allow the calculation of the transition time as a percentage of the residence time for a wide range of pyrolyzer geometrics, flow rates, and temperatures. Table 4.01 shows the variation of the transition time as a percentage of the residence time for a range of pyrolyzer geometrics and flow rates and for a constant pyrolyzer residence time of 0.05 minutes. The ambient temperature was assumed to be 300°K and the pyrolysis temperature 600°K for the calculation of these data.

The transition time should be short. Furthermore, it should represent a small percentage of the residence time. These are the requirements for the desirable square temperature profile. In Table 4.01 the transition time as a per-



tage of the residence time for different volumetric flow rates with pyrolyzers of different cross sectional areas is shown. Figure 4.09 is a plot of these data. For fixed residence time the required cross-sectional area decreases with decreasing volumetric flow rate. The percent of the residence time represented by the transition time is constant for a given linear flow velocity and cannot be determined using volumetric flow rates alone.

The residence time required for pyrolysis is determined by the extent of degradation required and the rate of degra-

TABLE 4.01 TRANSITION TIMES FOR PYROLYZERS OF DIFFERENT GEOMETRIES AND FLOW RATES

$v$ $\text{cm}^3$	$F$ $\frac{\text{cm}^3}{\text{min}}$	$F_p$ $\frac{\text{cm}^3}{\text{min}}$	$A$ $\text{cm}^2$	$L$ $\text{cm}$	$u = \frac{F}{A}$ $\text{cm/min}$	$t_z$ (min)	$\frac{t_z}{t_r} \times 100 = \%$
0.1	1	2	0.001	100	1000	$\sim 0$	$\sim 0$
			0.01	10	100	0.016	32
			0.1	1	10	0.10	200
1	10	20	0.01	100	1000	$\sim 0$	$\sim 0$
			0.1	10	100	0.016	32
			1.0	1	10	0.10	200
10	100	200	0.01	1000	10,000	$\sim 0$	$\sim 0$
			0.1	100	1000	$\sim 0$	$\sim 0$
			1.0	10	100	0.016	32
100	1000	2000	0.01	10,000	100,000	$\sim 0$	$\sim 0$
			0.01	1000	10,000	$\sim 0$	$\sim 0$
			1.0	100	1000	$\sim 0$	$\sim 0$



dation for the particular material at the chosen pyrolysis temperature. The use of the pyrolyzer in conjunction with an inflexible chromatographic system may dictate the flow rate, and determine the pyrolyzer volume.

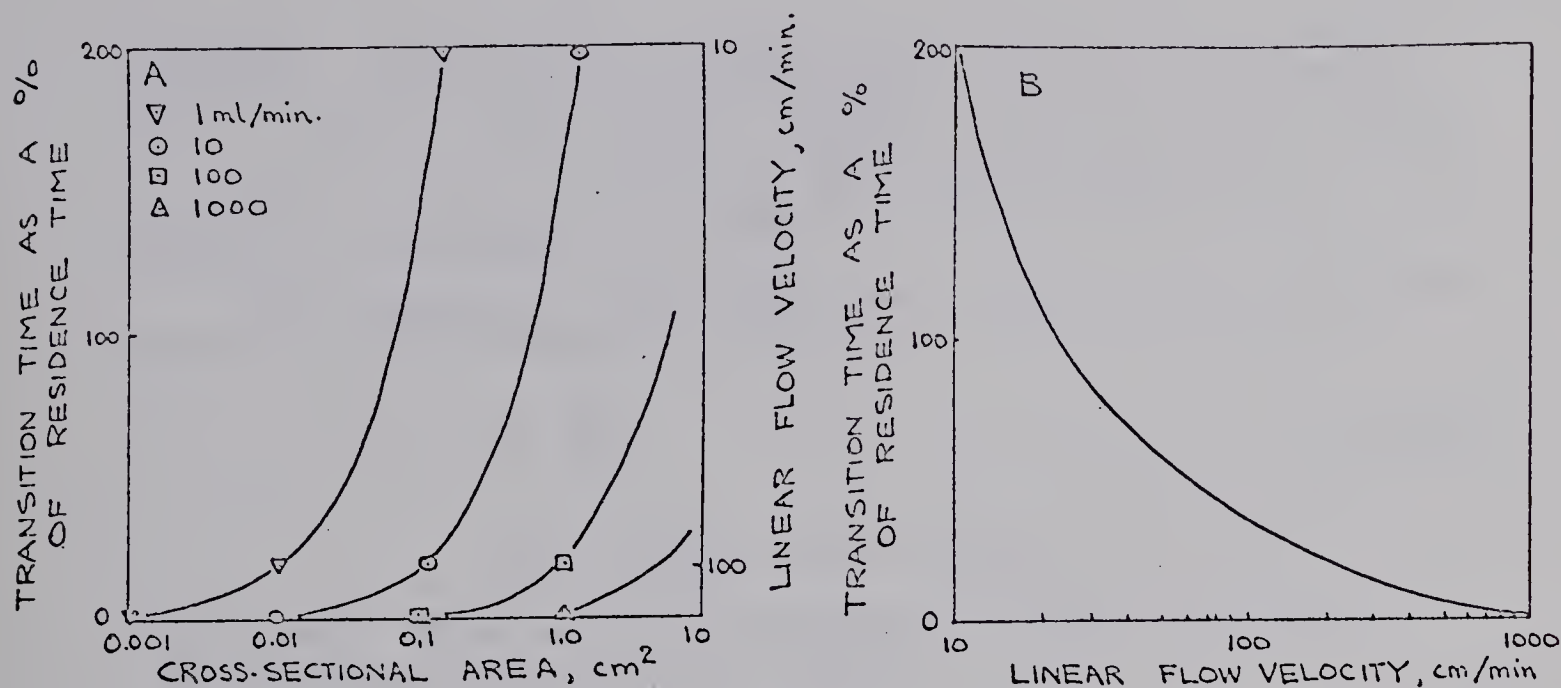


Figure 4.09 Effect of flow rate (A) and linear flow velocity (B) on the transition time expressed as a percentage of the residence time. Residence time constant at 0.05 minute. Data from Table 4.01.

The linear flow velocity may be determined by how nearly square the temperature profile is required to be, Figure 4.09. From the linear flow velocity and the volumetric flow rate the cross sectional area may be determined and hence, knowing the volume, the pyrolyzer length is established. The design geometry of the pyrolyzer is completely specified by these considerations.

There remains one additional factor to be considered, namely, the effect of thermal expansion and contraction on the transition time. The gas as it enters the hot pyrolysis tube will double its volume, in increasing its temperature from about 300 to 600°K, and will return to the original volume upon leaving the heated zone. The expansion and contraction will cause local flow non-uniformities tending to increase the length of the transition zone at the pyrolysis tube inlet and to decrease it at the outlet. The local flow



rates at these points are increasing and decreasing respectively. The net effect on transition time, the important factor, should be small and has been neglected.

Example. Suppose that adequate degradation of a sample requires a pyrolyzer residence time of 0.15 minutes at 900°K. The chromatographic system requires a flow rate of 100 ml/min and it is desired that the transition time represent at most 10 percent of the residence time. Ambient temperature is 300°K.

The volumetric flow rate and residence time requirements fix the pyrolyzer volume.

$$F_p = F \frac{T_p}{T_a} \quad (4.06)$$

$$= 100 \times \frac{900}{300} = 300 \text{ cm}^3/\text{min}.$$

The linear flow velocity required so that  $t_z \leq 0.1t_r$  is 250 cm/min from Figure 4.09 B.

$$A = \frac{F}{u} \quad (4.03)$$

$$= \frac{45 \text{ cm}^3/\text{min}}{250 \text{ cm/min}} = 0.18 \text{ cm}^2.$$

$$L = \frac{V}{A}$$

$$= \frac{45 \text{ cm}^3}{0.18 \text{ cm}^2} = 250 \text{ cm} \quad (4.0)$$

The geometry is then specified as: minimum length of 250 cm and a maximum cross-sectional area of 0.18 cm<sup>2</sup>.

#### Material of Construction

The choice of material for the construction of a tubular pyrolyzer has been widely considered. Metals and glasses have both been used and each has advantages. Metals have high thermal conductivity leading to excellent temperature uniformity. Mechanically they are easy to fabricate and are rugged and easily handled. Metals can give rise to catalytic effects (14) and change in character with use, as has been noted (64, 79) in filament types. Different metals may give different pyrolysates for the same material (14).



Glasses, particularly quartz, do not suffer from aging and have not been conclusively shown to have catalytic effects. Carbon, reported to have been formed during pyrolysis (Perry), may be removed by oxidation through the introduction of air at operating temperatures; a procedure that cannot be used with metals. Some glasses have a limited allowable temperature but quartz may be used up to its softening point of about 800°C. Although the thermal conductivity of glasses is below that of metal, an enclosing high heat capacity furnace will give a uniform temperature.

The design and dimensions of the pyrolyzer used here are given in Figure 4.10. Construction details and accessory equipment details are given in the legend of the figure.

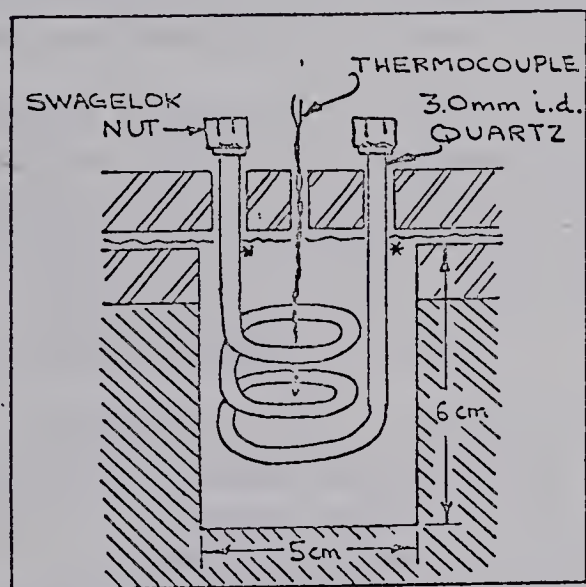


Figure 4.10 Pyrolysis tube and furnace cavity dimension.

Furnace: Canadian Laboratory Supplies Ltd. Cat. No. 37-880.  
Crucible furnace 115V, 0.37 K watt.

Pyrometer: API. 434-805R3 0-2000°F

Thermocouple: chromel - alumel, stainless steel clad.

Pyrolyzer tube: 30 mm i.d. quartz tube. Path length \* - \*  
calculated at 17.5 cm from volume measurement  
assuming uniform circular cross section.

Connections: 1/4" Swagelok, sealed with teflon tape.



#### 4.03 SYSTEMS FOR PYROLYSIS GAS CHROMATOGRAPHY

##### Desirable Conditions for Gas Phase Pyrolysis

The direct application of gas chromatography to the separation and identification of pyrolysates has previously necessitated a compromise in establishing the pyrolysis conditions. Three excerpts from Levy (67) illustrate this:

"When a pyrolysis unit is directly connected to the inlet of the gas chromatograph a number of requirements must be met for the successful gas chromatographic separation of the pyrolysis products. The pyrolysis process must therefore be carried out under the conditions prescribed by the requirements of the gas chromatograph. A number of parameters such as duration of the pyrolysis process, the flow rate through the unit, the pressure, the quantity of pyrolyzed material, the volume of the pyrolysis chamber and the nature of the carrier gas are limited within the permissible values predetermined by the requirements for optimum gas chromatographic separation."

"The maximum permissible pyrolysis duration at which the resolution is still not affected varies depending on several parameters of the gas chromatographic system such as the efficiency of the column, the total volume of the inlet system, carrier gas flow rate, etc. Pyrolysis durations can be considerably increased when temperature programming of the column is used."

"When a pyrolysis unit, either of the filament or of the reactor type, is connected to the inlet of a gas chromatograph, it becomes part of the flow system of the instrument. The pressure and the flow conditions in the inlet system of the gas chromatograph, i.e., in the pyrolysis units, are usually set to achieve optimum performance of the column. The permissible flow rates are therefore limited and will depend mainly on the diameter of the column and on the shape of the curves when one plots HETP versus linear velocity of the carrier gas. Since the flow and the pressure are mutually dependent the permissible inlet pressures (pressures in the pyrolysis unit) are also limited and depend on the flow rate selected and on the permeability of the column."

"The volume and the shape of the pyrolysis chamber can greatly affect the chromatographic process. Pyrolysis chambers of large volume will cause loss of resolution even if the duration of the pyrolysis process is short. Furthermore, the shape of the chamber should allow rapid sweeping of its contents by the carrier gas."



Levy noted that the duration of the pyrolysis can be considerably increased when temperature programming of the column is used. This advantage of PTGC as well as its usefulness in resolving mixtures of a wide range of boiling points has been pointed out by Harris and Habgood (42). A recent quantitative study of polymer degradation failed to take advantage of PTGC (66) and the scope of the work was limited by the dictates of isothermal chromatography as indicated by the following quote: "It is clearly highly desirable to carry out the degradation over a short time interval so that the resolution of the chromatographic column shall be kept as high as possible. . . ."

Two general conditions are desirable for gas phase pyrolysis. It is desirable to optimize conditions so that the products are most clearly related to the structure of the starting material. For wide utility it is necessary that the technique be such that results from different laboratories and different operators in the same laboratory be the same and constant from day to day; that is, reproducibility must be good.

The optimization of conditions necessitates equipment allowing independent control and a wide range of values of temperature, residence time, pressure, and sample concentration. Residence time and pressure are related to the geometry of the pyrolysis tube and are interrelated. Temperature may be limited by the choice of tube materials. Latitude in sample concentration and sample size will depend largely on treatment subsequent to pyrolysis.

Reproducibility will depend on the suppression or minimization of the catalytic and other variable effects, the elimination of uncontrolled secondary reactions, and accurate knowledge and reporting of such conditions as the actual temperature of pyrolysis (see Figure 4.03). The attainment of reproducible results depends primarily on the ability to control and measure the parameters noted above.



## Combined Pyrolysis and Gas Chromatography

Figure 4.11 schematically illustrates five possible methods for the combination of gas phase pyrolysis with subsequent gas chromatographic separation of the pyrolysate components.

The simplest arrangement, A, is a direct attachment of the pyrolyzer outlet to the gas chromatograph inlet. Flow rates through each component may be optimized if the gas chromatographic column requires a larger flow rate than the pyrolyzer.\* Injection time into the pyrolyzer must be short to be consistent with good chromatographic practice. The use of PTGC allows some latitude here but would require sub-ambient initial temperatures if the significant low boiling components of the pyrolysate are to be determined. It is not possible with this arrangement to independently control the pressure in the pyrolyzer as this will be a function of the combined flow rates  $F_1$  and  $F_2$ .

Essentially complete independent control of the pyrolysis parameters is possible with the arrangement shown in B. The use of a U-tube trap, described in the Appendix I, involves handling of the sample with a potential loss of sample as would be the case with aerosols. Permanent gases or other components with boiling points above the trap temperature would also be lost. Injection time into the pyrolyzer may be of any duration as it is now independent of the gas chromatographic step. Introduction into the gas chromatograph will be controlled by the efficiency of the removal of the sample by the carrier gas from the heated trap.

In arrangement C a device for cooling a precolumn or a portion of the head of the gas chromatographic column is introduced. The details of this device will be covered in Section 5.01 including a discussion of its ability to retain low boiling components. In arrangement C the head of the gas chromatographic column is maintained at a low temperature during the

---

\*The use of additive flow rates is described in Chapter 5.



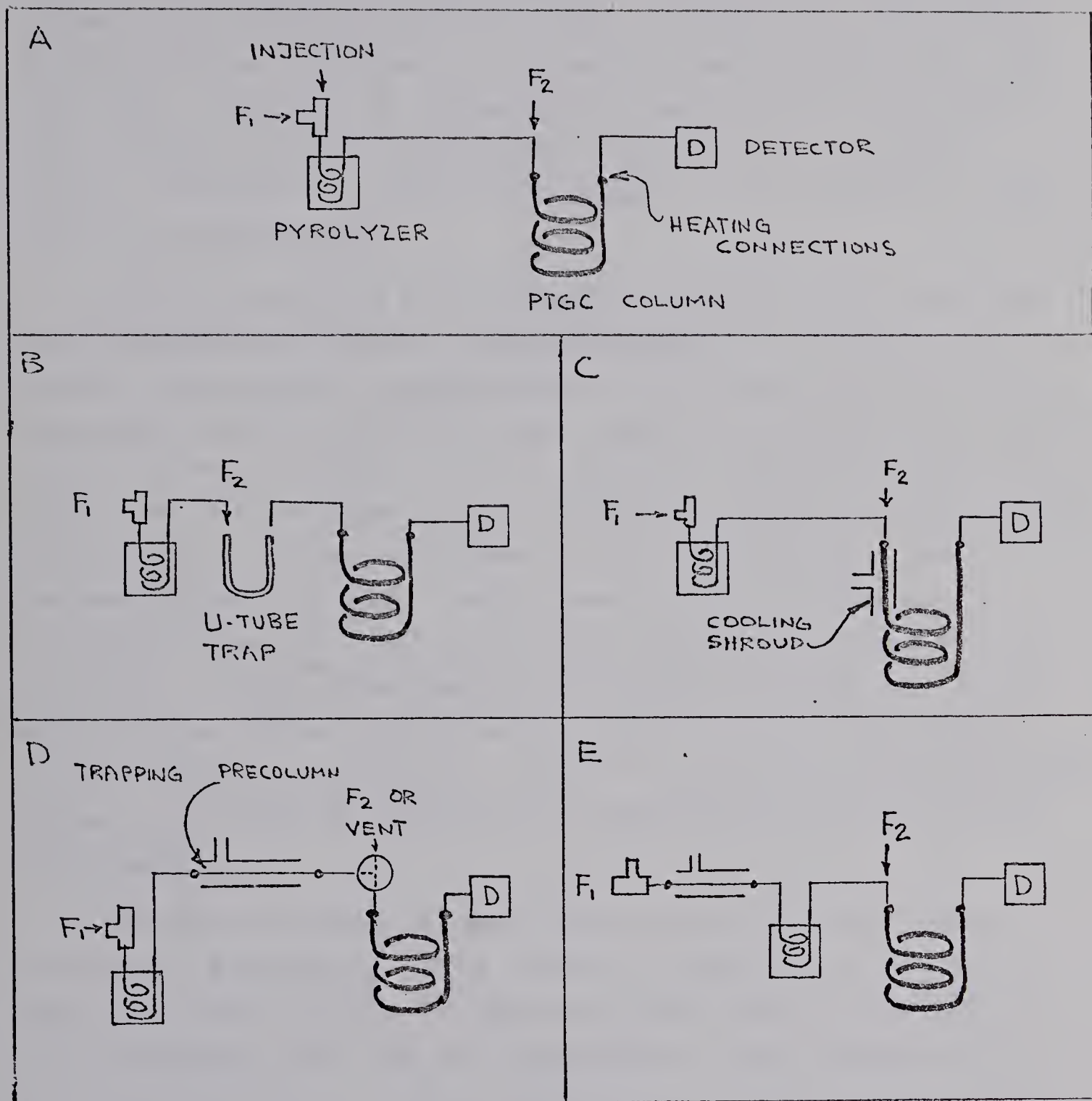


Figure 4.11 Schematic systems for independent control and optimization of pyrolysis parameters and subsequent gas chromatographic separation of pyrolysate.

Gas flow  $F_1$  optimized for pyrolysis conditions and  $F_2$  added for optimization of chromatographic column.



pyrolysis. After its completion the column is programmed. There is no handling of the sample outside the closed system thereby preventing mechanical loss. Potential difficulties arise with the presence of low boiling point substances and with the linearity of temperature program due to the lack of a uniform initial temperature distribution along the column although the latter should have little effect on analysis reproducibility.

The introduction of a separate trapping column between the pyrolyzer and the gas chromatographic column, as in D, allows still greater versatility. The column can now be programmed with less difficulty. Methane and permanent gases which are not retained in the trapping column are vented as shown and are not seen at the detector. Control of flow rates and pressure in the pyrolyser is not influenced by the gas chromatographic column. Rapid heating and removal of the pyrolysate from the trapping column duplicates rapid sample injection. This arrangement can be used to study on-column condensation effects such as the length of column required for any degree of trapping, effect of proportion of stationary phase, and trapping temperature independently of the column performance.

The final system, E, used the trapping column located before the pyrolyzer. This allows the removal of air (28 A) from the sample which, if desired in the other arrangements, can necessitate the use of a precolumn. When the material to be pyrolyzed is slowly evolved, as in the effluent gas of a prior gas chromatograph, the material can be collected and then rapidly introduced into the pyrolyzer. The production of methane and permanent gases is not a problem as they will be subjected to the same gas chromatography step as all other components of the pyrolysate. These considerations, among others, make this arrangement the choice for use in the system for the analysis of gas chromatography peaks by PGC as discussed in the final part of this thesis. The principal disadvantages of the arrangement are twofold. It does not



allow slow sample introduction into the pyrolyzer without peak spreading and cannot, therefore, be used to study such things as the concentration effect on pyrolysis. The second disadvantage, in common with the simple arrangement A, is the increase in dead space contributed by the pyrolyzer between sample introduction and detection. This is minimized by using a pyrolyzer of low volume.

#### 4.04 RESULTS AND DISCUSSION

The development of a functional model of a system using PGC as a technique for identifying gas chromatographic peaks requires some knowledge of the pyrolysis conditions adequate for the types of compounds to be examined. The pyrolysis temperature and residence time will affect the composition of the pyrolysate and the degree of pyrolysis. As a consequence these factors must be examined.

A mixture of hydrocarbons of different structural types, that is, straight- and branched-chain alkanes, alkenes and an aromatic hydrocarbon all of the same carbon number, were used to demonstrate the use of PGC in identifying gas chromatographic effluents. These compounds were, therefore, chosen for use in examining the various effects of the experimental parameters on pyrolysis.

Illustrating the effect of temperature on the extent of pyrolysis are Figures 4.12 with n-hexane and 4.13 with 2,3-dimethylbutane. Figure 4.14 shows the effect of increasing residence time on the extent of pyrolysis.

In Figures 4.12, 4.13 and 4.14 the ordinate is area percent from chromatograms using a flame ionization detector (FID). No attempt was made to reduce area percent to mole percent. This could be done with a knowledge of response factors (21), but would require identification of each peak. For direct comparison of chromatograms of the pyrolysate, i.e., pyrograms, the experimental area percent is most convenient.



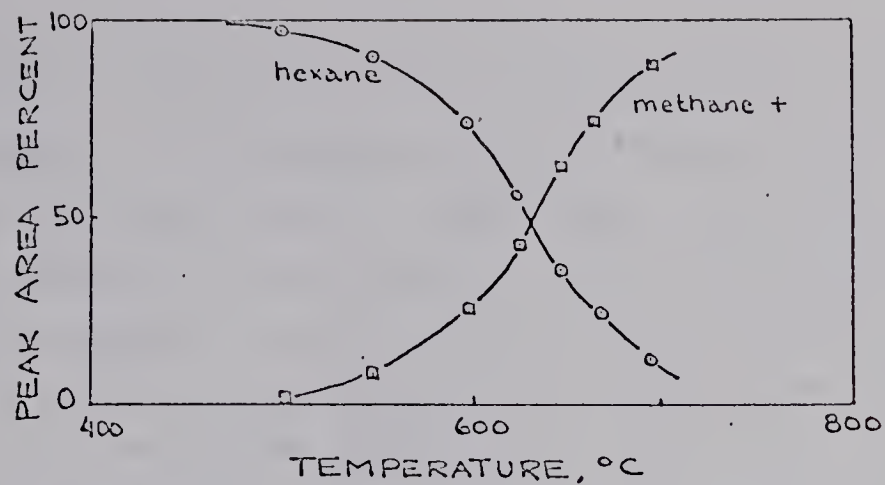


Figure 4.12 n-hexane pyrolysis as a function of temperature. Residence time constant at 7.6 seconds, F.I.D.

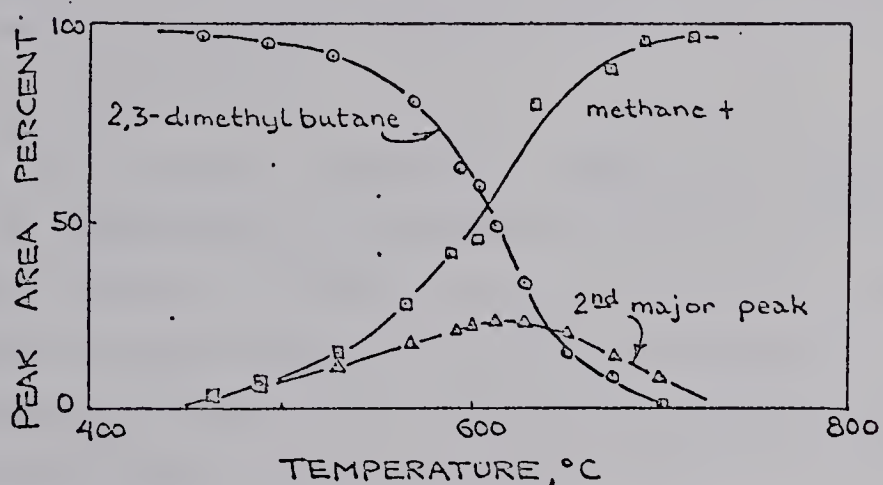


Figure 4.13 2,3-dimethylbutane pyrolysis as a function of temperature. Conditions as in Figure 4.17.

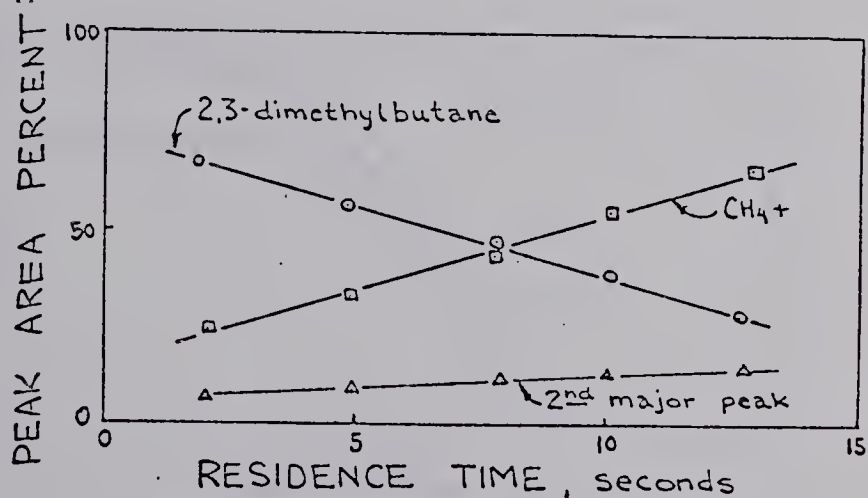


Figure 4.14 2,3-dimethylbutane pyrolysis as a function of residence time. Pyrolysis temperature = 600 °C.



It is important that too much significance not be placed on the ordinate values. For example, as in Figure 4.12 at 600°C, the area percent of the original component n-hexane, has been reduced to about 50% and methane increased to 20%. The response factors (relative sensitivities) for n-hexane and methane are 1.03 and 0.97, respectively, using the FID. The areas corrected for response become 51.5 and 19.4%. This represents a minimum change since hydrocarbons all have a response factor close to 1.0. If nonhydrocarbons are produced the necessary corrections may be much larger. Alcohols, for example, have response factors varying from 0.23 to 0.85 and acids from 0.01 to 0.65 (21).

The choice of a single pyrolyzer temperature for use with compounds of different structural types is difficult, due to the effect shown in Figure 4.15. It is not possible to choose a single temperature at which all compounds will pyrolyze to the same extent with the same residence time. A compromise temperature must be chosen and for the subsequent work in this thesis 600°C is used.

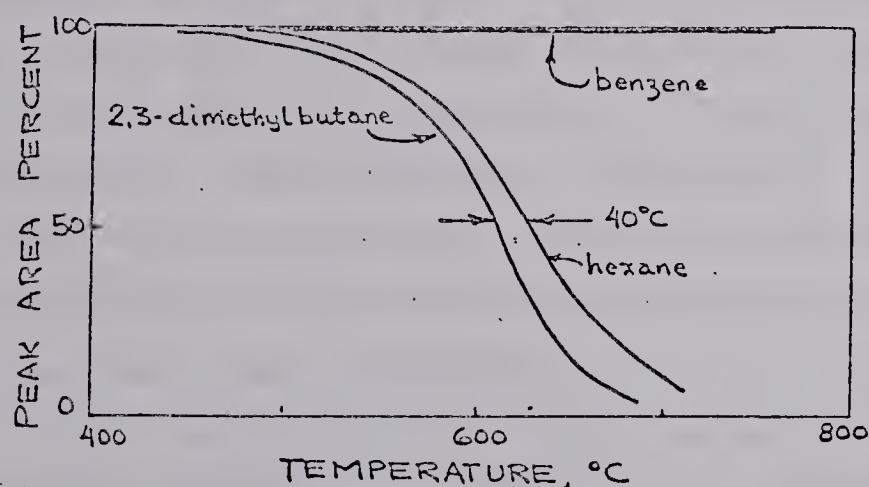


Figure 4.15 Comparison of the extent of pyrolysis as a function of temperature for 2,3-dimethylbutane, n-hexane, and benzene. Residence time = 7.6 seconds.

With the pyrolyzer temperature established, the degree of pyrolysis can be controlled by varying the residence time (Figure 4.14). This technique is suitable for individual



pyrolyses but would be operationally cumbersome in a general rapid system. Use of a variable residence time, most easily accomplished by control of flow rate, would be experimentally more convenient than altering the pyrolyzer temperature.

## DISCUSSION

The preceding sections pointed out some important considerations in the design of a gas phase pyrolyzer and illustrated some results obtained with a tubular pyrolyzer. This has not been an exhaustive treatment but was adequate to allow for the design of a pyrolyzer for gas phase pyrolysis of gas chromatographic effluents. The arguments presented for optimum design geometry should be of general applicability for tubular gas phase pyrolyzers.

The importance of accurately knowing the pyrolysis temperature has already been emphasized. There is the possibility however, that some advantages may be realized by using a known range of temperatures for pyrolysis.

The presence of some of the unpyrolyzed parent material in a pyrolysate is of less importance than having the conditions such that all compounds will pyrolyze to some degree to allow characterization or identification. Generally, once fragments have been produced by pyrolysis, they do not undergo further degradation without the use of more severe conditions (93A).

If a pyrolyzer were constructed with the temperature time profile shown in Figure 4.16, one operating condition could be used for a series of compounds of different thermal stabilities. The more thermally sensitive compounds would pyrolyze at the lower temperatures (A) with the products passing through the hotter zone relatively unmodified. Compounds more stable thermally would pass through the cooler zones of the pyrolyzer to be pyrolyzed at higher temperatures (B). Secondary reactions can make the interpretation of pyrograms more difficult but they might also simplify the



product patterns giving a better distribution for "fingerprint" identifications.

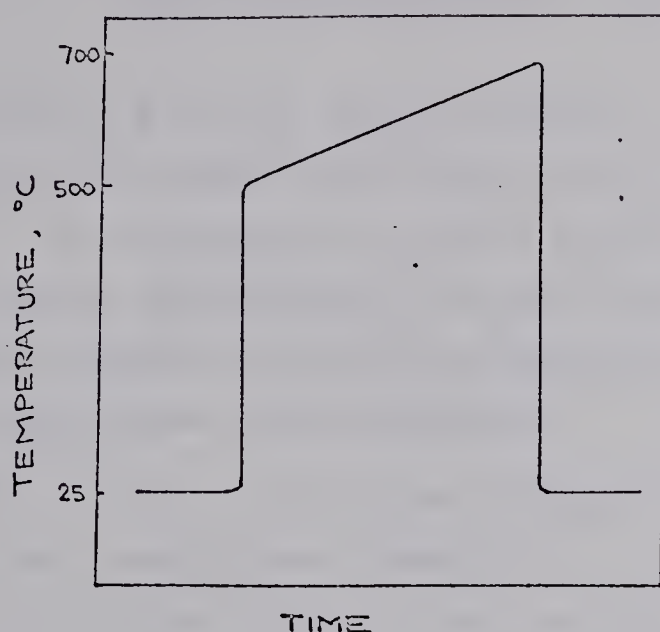


Figure 4.16 Idealized temperature profile of gradient temperature pyrolyzer.

Construction of a graded temperature pyrolyzer should present no problem. Figure 4.17 shows a possible method similar to that used by Keulemans and Perry (62) for a constant temperature pyrolyzer. Since the carrier gas undergoes a smaller temperature increase upon entering the pyrolyzer, the true profile could well be more nearly that predicted than for a "squared" temperature profile pyrolyzer.

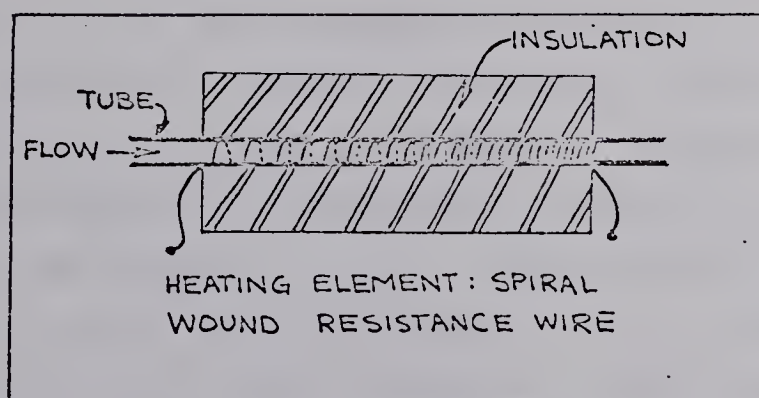


Figure 4.17 Construction of gradient temperature pyrolyzer.



## 5. SYSTEM FOR THE IDENTIFICATION OF GAS CHROMATOGRAPHIC EFFLUENTS BY PYROLYSIS GAS CHROMATOGRAPHY (PGC)

An apparatus for the identification of gas chromatographic effluents by PGC was schematically illustrated in Figure 1.03. In a general way this system is analogous to the use of a mass spectrometer as an identifying device for chromatographic peaks and follows Keuleman's (61) suggestion for a "poor man's mass spectrometer".

Levy (69) at the 11th Ottawa Symposium on Applied Spectrometry and Analytical Chemistry in 1964 delivered a paper titled "Pyrolysis Gas Chromatography (PGC) in Analogy to Mass Spectrometry". Although Levy indicated that PGC may be used for the quantitative determination of mixtures, its use will be restricted to individual compounds in this research.

Since structurally similar materials, even closely related isomers, tend to give dissimilar pyrograms, PGC may be more useful than mass spectrometry for their identification. In general, however, mass spectrometry and PGC are analogous in the elucidations of structure and for identification. Levy (69) predicted that available mass spectra could be used as a guide in structural elucidations by PGC.

A new technique for fragmenting molecules that is somewhat between pyrolysis and mass spectral fragmentation is beginning to appear in the literature. Variouslly called "high voltage electrical discharge reaction" (11), "fragmentation gas chromatography" (92), "electrical discharge pyrolysis" (91), and "arc pyrolysis" (51), the technique has been applied mostly to solid samples. This technique, indeed virtually any degradative technique, may be used in substitution for the pyrolysis phase in the system to be described here.



## 5.01 EXPERIMENTAL DESIGN

A detailed diagram of the final system arrangement is given in Figure 5.01. Full particulars of the component parts of the system which are not given in this section may be found in Appendix I.

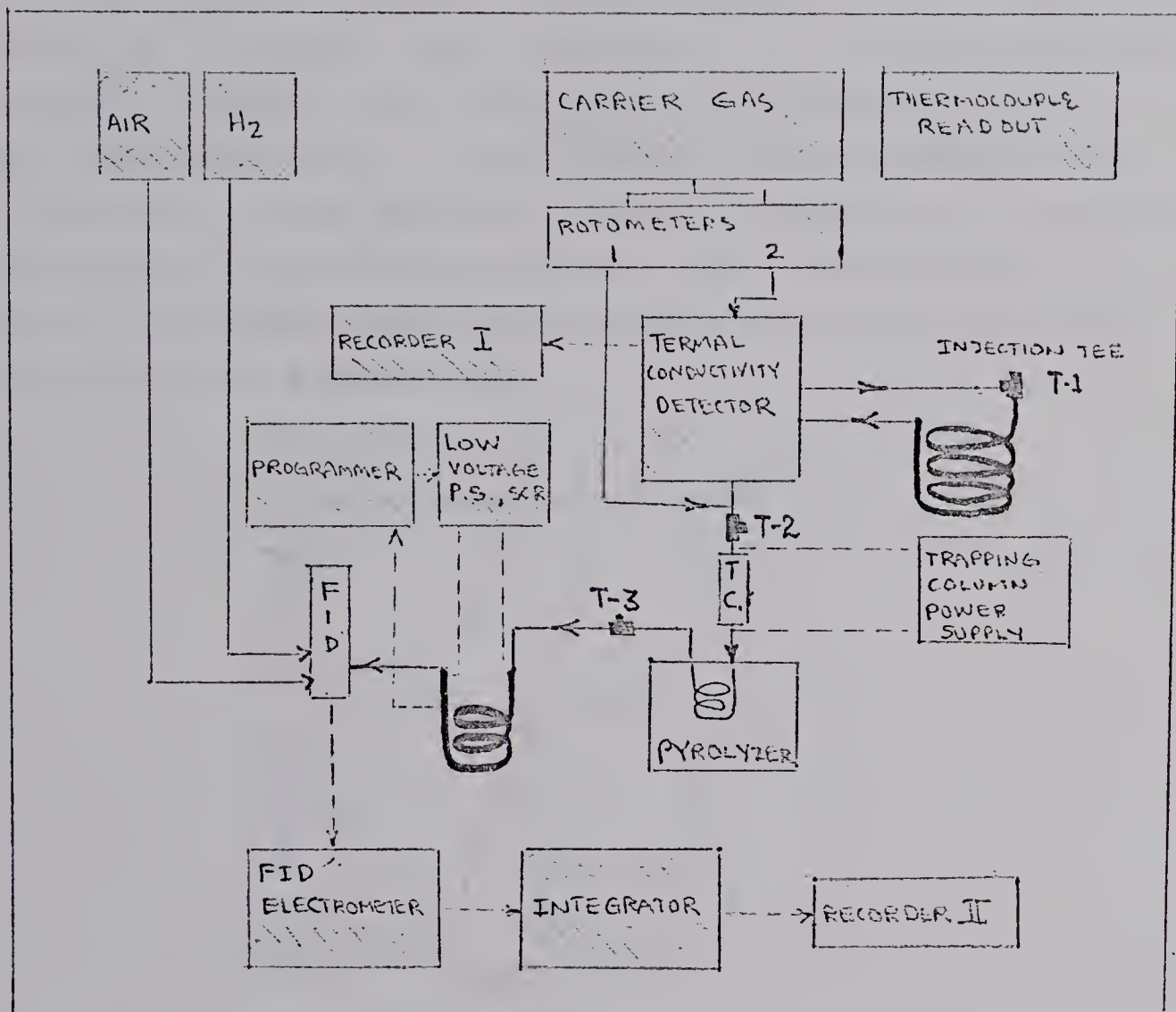


Figure 5.01 Schematic diagram of a system for the identification of gas chromatographic peaks by pyrolysis gas chromatography.

Three points of sample introduction are indicated. For use of the complete system the sample is introduced at sample injection tee, T-1. By opening T-2 and using it as a vent the initial chromatographic step alone may be studied. Direct injection into a pre-pyrolyzer or trapping column (to separate air from the sample) is accomplished using injection tee T-2. This allows PGC by passing the first column. In-



jection tee T-3 was used for an examination of the operational parameters of the second chromatographic step and was not retained in the final arrangement.

#### Additive Carrier Gas Flow Rates

As may be seen in Figure 5.02 the addition of a second gas source can be used to decrease the retention time in the system following the initial chromatographic step. This reduction in retention time, indicated by T in the figure was made without resulting in either the peak broadening or changed retention time in the initial chromatographic step. It is possible to use two gas sources to optimize flow rates in both ends of the system when the flow requirements are larger in the second part. Two points of carrier gas addition are shown in Figure 5.01.

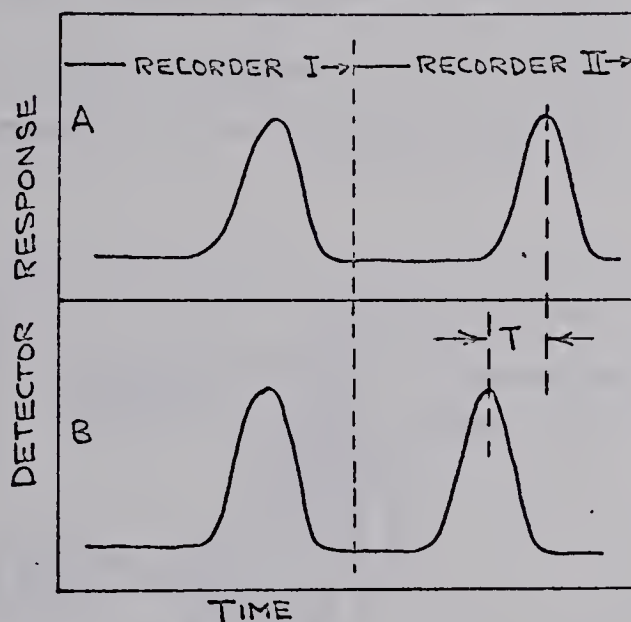


Figure 5.02 The effect of additive flow rates on retention time and peak shape. Designation recorder I and recorder II taken from Figure 5.01. Flow rate in (A) = 18 ml/min. Total flow rate in (B) =  $18 + 15 = 33$  ml/min.

#### Trapping Column

A pre-pyrolyzer or trapping column, introduced in a general way in Section 4 is shown as part of the pyrolysis system, Figure 5.01. The particular arrangement used in the final system corresponds to that shown in Figure 4.11 E with the attendant advantages discussed in conjunction with that figure.



The use of a precolumn for trapping or collecting gas phase samples has been previously reported as well as a number of other techniques to accomplish the same ends (76). Ordinary coated column packing has been used for trapping both at room temperature (4) and cryogenically (47). Trace components in air have been concentrated by cryogenic trapping (1) and molecular sieve 5A has been reported as an effective adsorbent (13) for components emerging from a gas chromatograph. These techniques have required separate trapping and handling of the device. On-column trapping procedures have also been reported (73A, 75).

Elsewhere the technique has been called "on-column trapping" (75), the trapping column called an "enrichment column" (73A) and the process studied theoretically and called "initial zone condensation" (54, 72), 33A).

The following five figures, Figure 5.04 through to 5.08, show the construction of the trapping column and the tests for its operation.

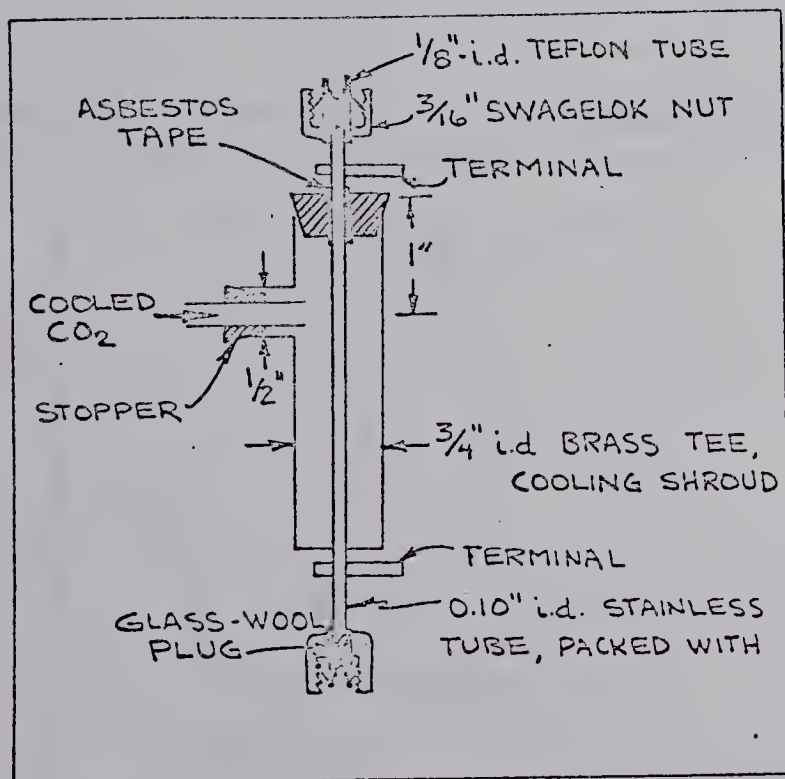


Figure 5.03 Details of the construction of the pre-pyrolyzer or trapping column. Direct electrical heating using 0 - 30 VAC, 0 - 5 amp current.



The heating and cooling characteristics for the trapping column were determined using a thermocouple positioned inside the column as shown in Figure 5.04. The characteristics are shown in Figure 5.05. For use in calculating the system capabilities the turn-around time for the trapping column, taken from this figure, is 20 seconds. The time to heat from  $-75^{\circ}\text{C}$  to  $125^{\circ}\text{C}$  is approximately 10 seconds. This then is the maximum sample introduction time. Any single component elutes during a fraction of this period so that 8 seconds would probably be a better estimate of the actual introduction time.

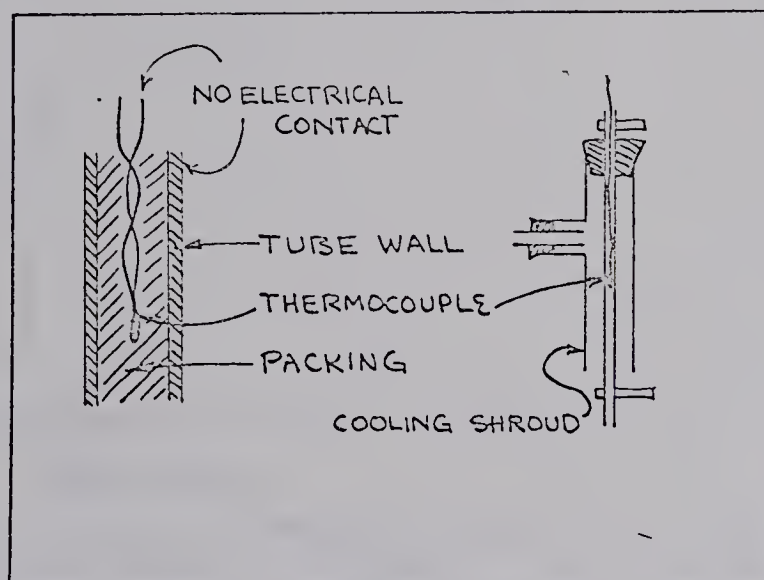


Figure 5.04 Positioning of thermocouple for the determination of the heating-cooling characteristics of the trapping column.

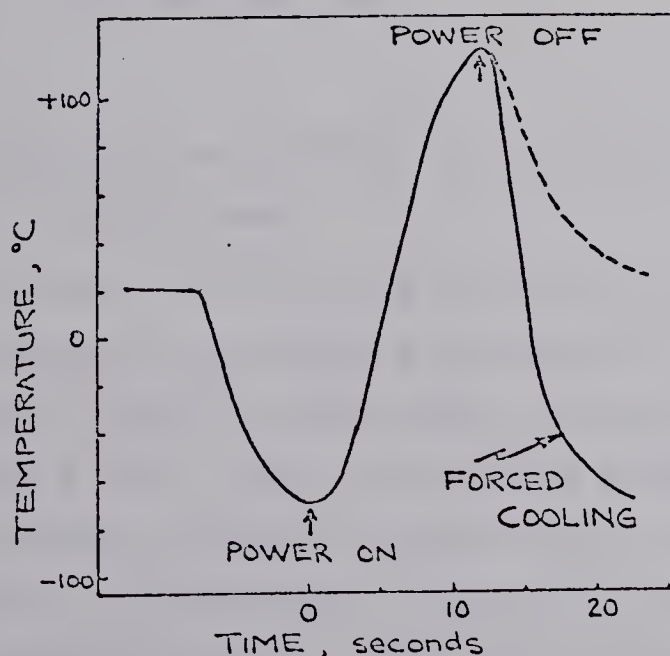


Figure 5.05 Heating-cooling characteristics for the trapping column. Electrical power at 1.9 VAC and 30 amps ON and OFF as indicated.



As an approximation to the slow elution of a compound from a gas chromatograph a plug injection system was constructed (44 A). Figure 5.06 shows a plug injection and the efficiency of the trapping column in concentration of the sample and reducing the introduction time for a subsequent operation. This plug injection approximates a peak with a base width of about 250 seconds. Rapid heating and elution

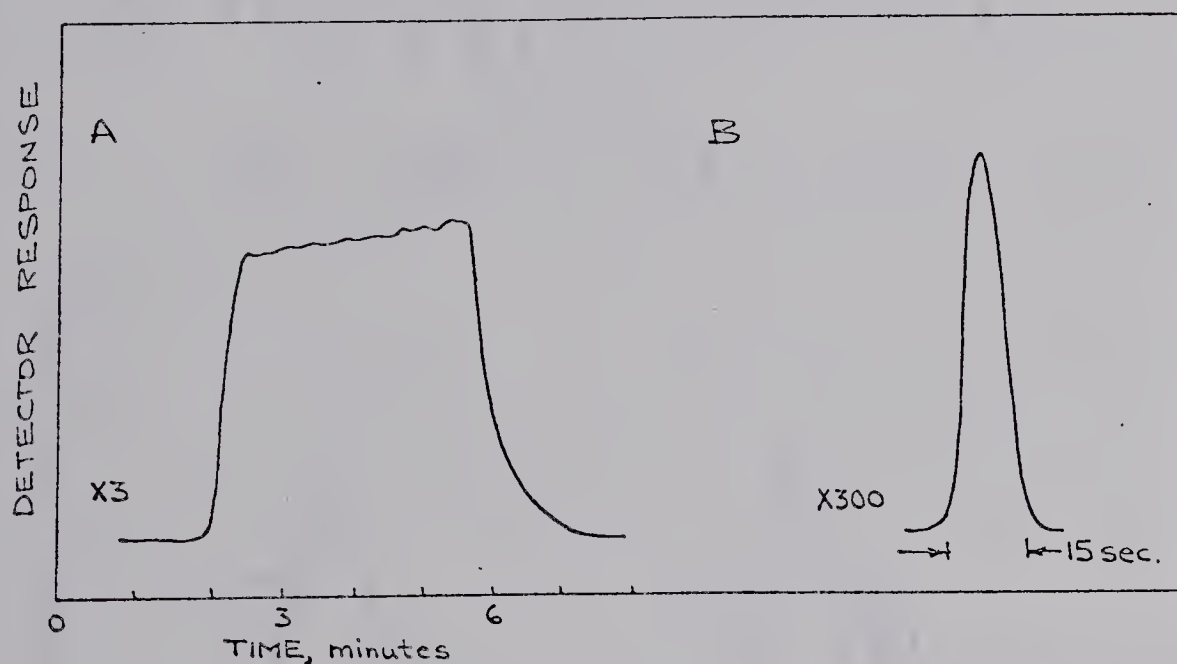


Figure 5.06 Effectiveness of trapping column. (A) Slow injection, no trapping. (B) Slow injection, trapping, subsequent elution on heating of the trapping column. Trapping column attached directly to flame ionization detector. Sample was 5 ml of helium saturated with 2,3-dimethylbutane and injected slowly using a 10 ml Hamilton gas-tight syringe and a Sage syringe pump.

from the trapping column effectively reduces the base width to 15 seconds in this case.

Materials with low boiling points, such as  $C_1$ - $C_4$  hydrocarbons, are frequent pyrolysis products. The effectiveness of the trapping column in retaining these compounds, is shown in Figure 5.07. These compounds caused no difficulty in the final system but may be important in any arrangement where trapping or condensation following pyrolysis is desired. The trapping column does not retain methane. This may be advantageous as methane is nearly always produced during pyrolysis and yields little structural information.



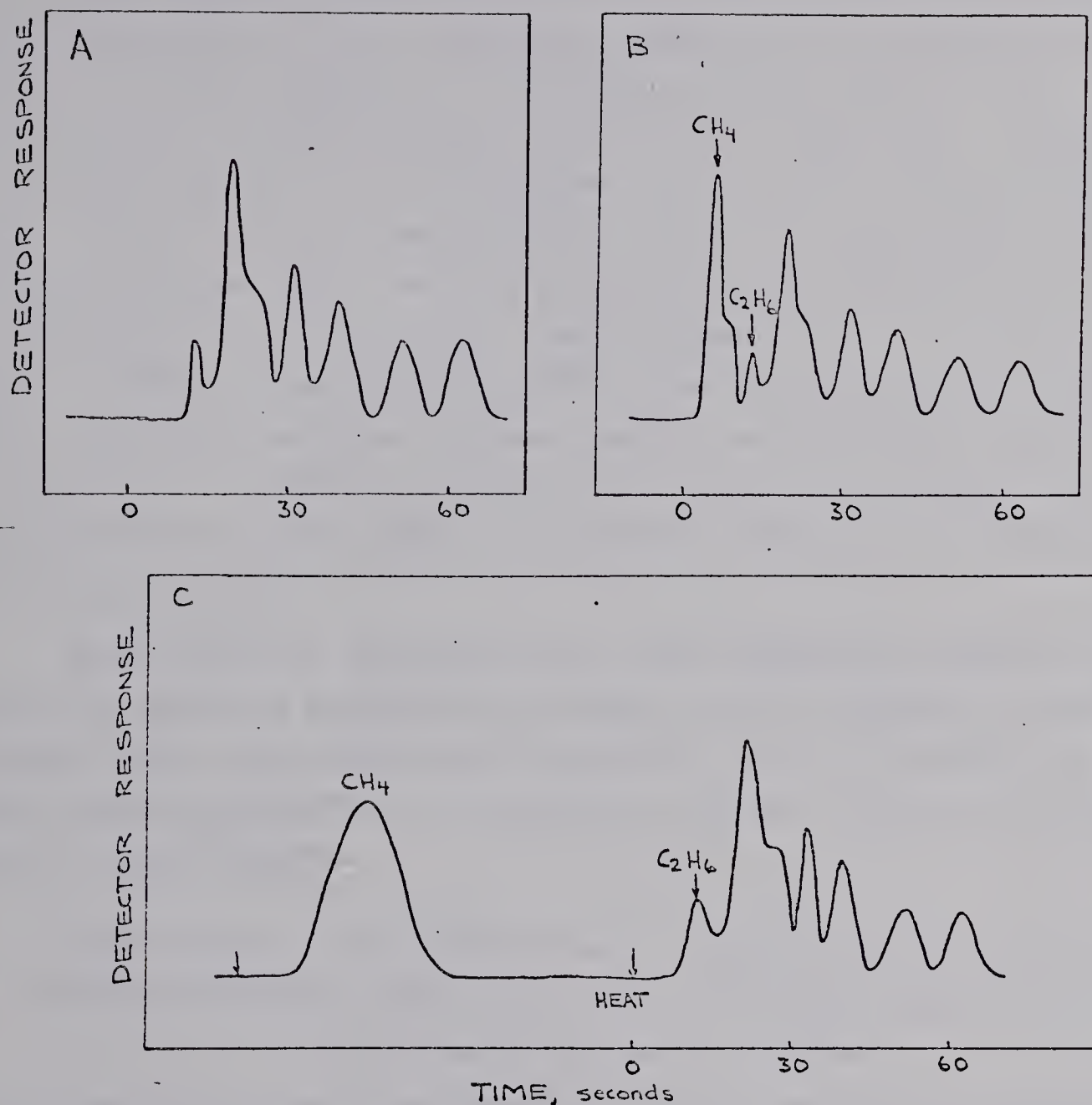


Figure 5.07 Effectiveness of trapping column in retaining a  $\text{C}_1 - \text{C}_4$  mixture of hydrocarbons. (A) and (B) illustrate separation of components and composition of the sample, no trapping. (C) illustrates trapping at about  $-170^\circ\text{C}$ . Trapping column heated as shown. A 3m, 0.10" i.d., 5% SF-96 on 60-80 mesh Chromosorb-P column was between the trapping column and the detector to give the component separation shown.



The trapping column may also be conveniently used for the examination of the processes involved in on-column trapping. If, for example, a freezing process occurs, the presence of a liquid phase should not be required. It was observed, however, that n-octane, m.p. = 56.5°C, and n-decane m.p. = 30°C, are not retained at -72°C (a temperature significantly below their melting points) in the absence of a liquid phase. On the other hand, ethane, m.p. = -172°C, b.p. = -88°C is retained at -72°C (now representing a temperature above the solutes boiling point) on 10% SF-96 coated Chromosorb. A freezing process is itself, therefore, not an explanation for the almost indefinite retention of solutes at low temperatures.

With suitable modifications this separate trapping column could be used to examine the length of the trapping condensation zone, the temperature required, and the effects of flow rates, proportion of stationary phase, and the surface area of the support.

#### Calculation of the Performance Required of the Initial Chromatographic Separation for Subsequent Application of PGC to Peak Identification

The ability of the system to handle multiple component samples depends on the resolution,  $R$ , and the difference in  $\Delta t_R$ , in the initial chromatographic separation and the turn-around time of the trapping and PGC steps. The minimum required  $R$  and  $\Delta t_R$  for the initial separation may be calculated from an analysis of the turn-around times of the subsequent sub-systems.

The cooling of a 1m column from the highest operational temperature, 225°C, to the initial temperature, 25°C, requires about 30 seconds. The cooling arrangement is shown in Figure 5.08 A. The program rate of 40°C per minute was used in the illustration of the heating and cooling characteristics of the column in part B of the figure. The linearity of the program may also be seen in the figure.



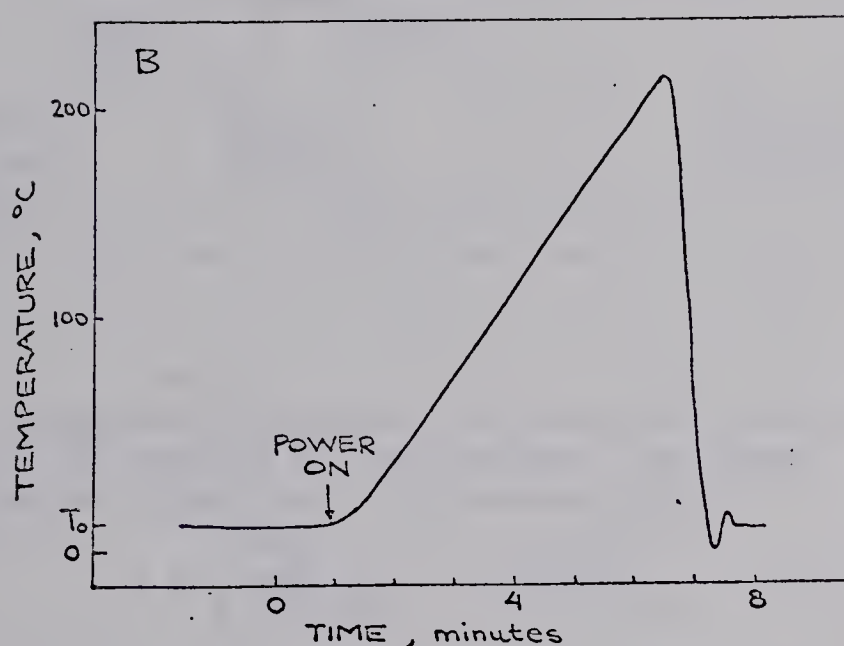
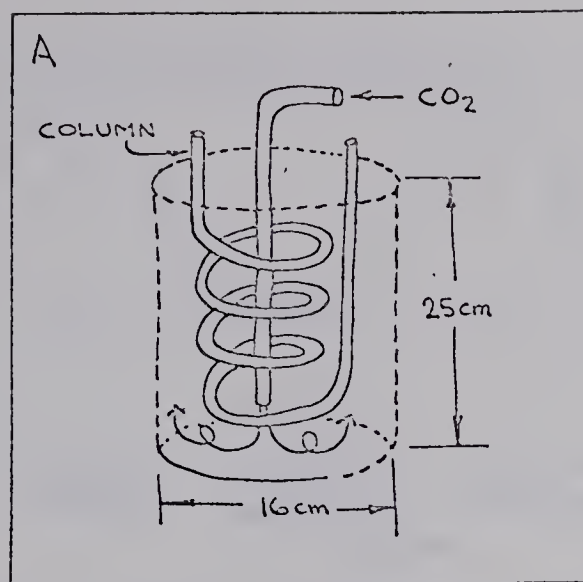


Figure 5.08 Heating-cooling characteristics for column II. (A) Shroud arrangement for containing chilled  $\text{CO}_2$  cooling blast. (B) Heating-cooling curve. Program rate was  $40^\circ\text{C}/\text{min}$ . Programmer set to re-establish  $T_0$  of  $25^\circ\text{C}$ . Direct electrical heating was used. Column dimensions were 1 m by 0.10" i.d. with gross coil diameter of 5 cm and coil length of 5 cm.

Assuming complete elution of the pyrolysate in 60 seconds and a cooling time of 30 seconds, the turn-around time for PGC step is 90 seconds. Final temperatures lower than  $225^\circ\text{C}$  give smaller cooling times decreasing this turn-around time.

The turn-around time for the trapping column is 20 seconds, as was shown in Figure 5.05.

It is now possible to calculate the performance required of the initial chromatographic step for PGC to be successfully applied in a subsequent operation. The discussion will refer to Figure 5.09.



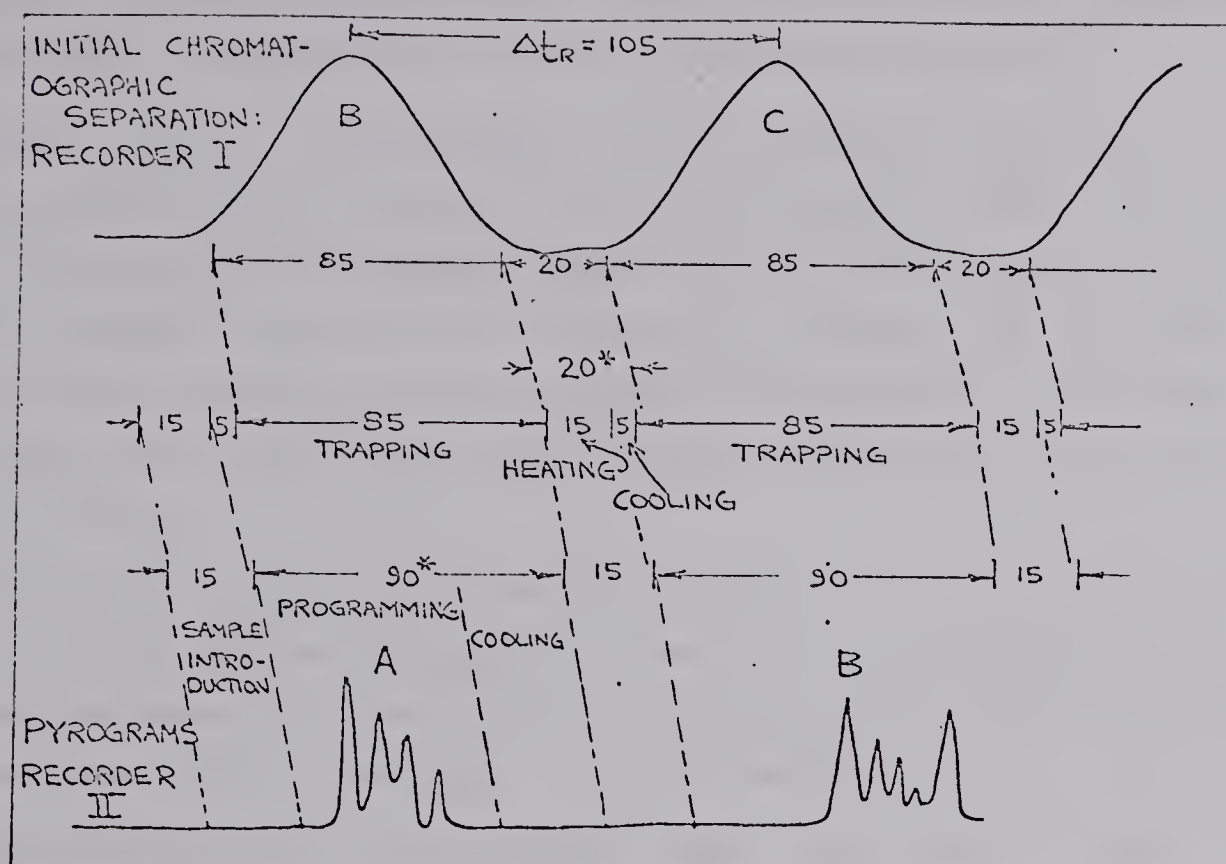


Figure 5.09 Required differences in retention times,  $\Delta t_R$ , and resolution  $R$ , required in the initial chromatographic separation for the subsequent application of pyrolysis gas chromatography.

$$R = \frac{\Delta t_R}{0.5(W_1 + W_2)} = \frac{105}{0.5(85 + 85)} = 1.24$$

Offset shown by the slope of the dashed diagonal lines represent delays in the connecting tubing or in the pyrolyzer. Experimentally this delay was kept to a minimum by short connections and except for the pyrolyzer residence time was no greater than a few seconds at any point with the flow rates used. Times marked \* are component turn-around times.

The heating of the trapping column requires 15 seconds (Figure 5.05). This corresponds to the time for introduction of the trapped sample into the pyrolyzer. At the end of this 15 second period and after a few seconds delay to allow for flow through the pyrolyzer (indicated by the offset shown by the dashed lines) the program for the second chromatographic separation is initiated. This program has a duration of 60 seconds and is followed by a maximum cooling period of 30 seconds. The time for the program and cooling combined, 90 seconds, constitute the turn-around time of the PGC step. This



90 seconds is the minimum time required between the completion of one sample introduction and the start of the next.

After sample introduction and a 5 second delay for cooling the trapping column, it again becomes effective as a trap. During the 90 second cycle of the PGC step less the first 5 seconds required for cooling, trapping of effluent of the first chromatographic column is possible. Thus the base width of a peak from the initial separation may be 85 seconds (90-5).

Trapping cannot be accomplished during the heating and cooling cycle of the trapping column, thus 20 seconds is required between the completion of the elution of the first peak and the first appearance of the second.

The difference in retention times required for the initial chromatographic separation calculated as one half of the base width of the first peak,  $1/2(85)$ , plus separation between peaks (20), plus one half the base width of the second peak  $1/2(85)$  for a total of 105 seconds.

Resolution may then be calculated as

$$R = \frac{\Delta t_R}{0.5(W_1 + W_2)} = \frac{105}{0.5(85+85)} = 1.24$$

Thus for a difference in retention times of 105 seconds a resolution of 1.24 is required.

The resolution required in the initial chromatographic step diminishes if the difference in retention times of two adjacent peaks,  $\Delta t_R$ , is greater than the 90 second minimum required by the turn-around time of the second chromatographic column.

If PGC is to be applied to any single component the minimum resolution required is 1.0 for this system. The exact requirements of resolution for increasing differences in retention times,  $\Delta t_R$ , are shown in Figure 5.10. This figure



was constructed on the basis of calculations such as shown in Figure 5.09. Reproducibility of retention times through the entire system, with or without hold-up in the trapping column, gave errors not exceeding  $\pm 3$  percent.

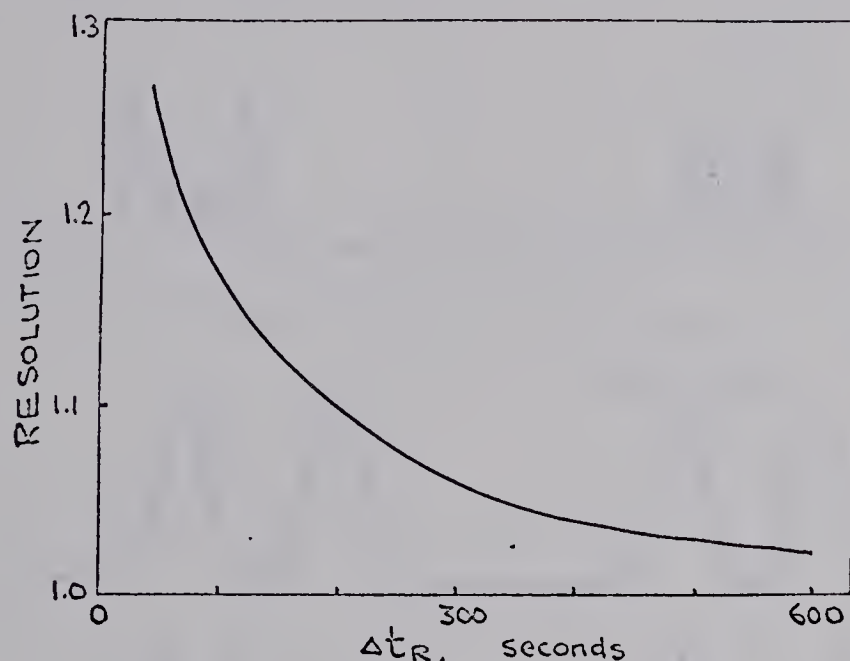


Figure 5.10 Resolution required in the initial chromatographic separation as a function of the difference in retention times,  $\Delta t_R$ , of adjacent peaks.

## 5.02 TYPICAL RESULTS

Operation of the complete system gives a quantitative analysis of the components of the original sample mixture within the limits imposed by resolution and detector response, and in addition, a pyrogram for each component. With both recorders and a digital integrator operating simultaneously, results such as shown in Figures 5.11 and 5.12 may be obtained.

In Figures 5.11 and 5.12 B the initial chromatographic separation was done isothermally. For the isothermal analysis it was desirable to use a mixture of small ranges of boiling points. For demonstrative purposes the mixture was made of six-carbon hydrocarbons of a variety of structural types. The sample mixture contained a straight chain alkane (n-hexane), a branched chain alkane (2,3-dimethylbutane), a cyclic alkene (cyclohexane) and benzene. Equal weights of each component were used in preparing the sample.



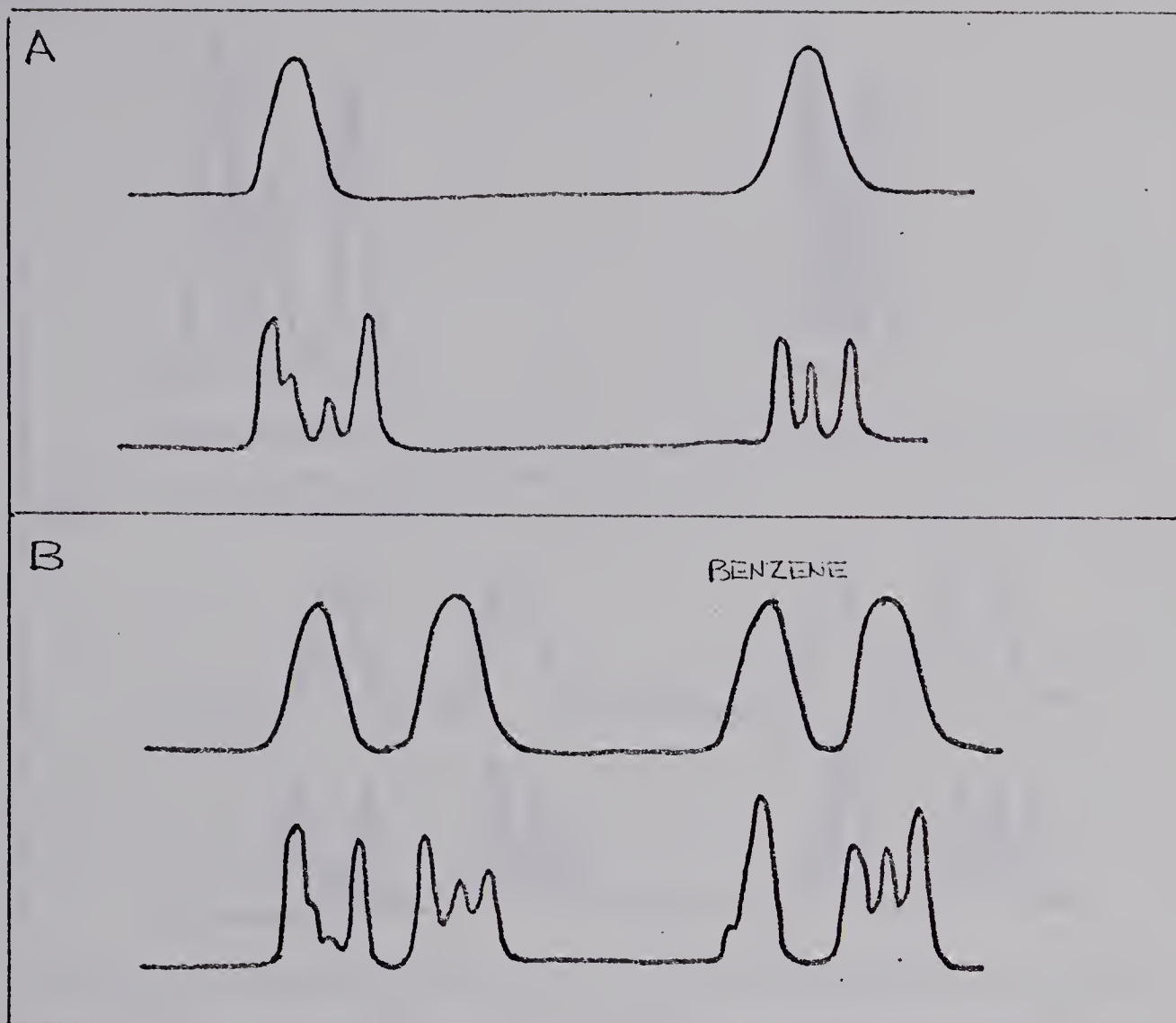


Figure 5.11 Application of pyrolysis gas chromatography to the identification of gas chromatographic peaks. Upper chromatogram in each case represents the initial chromatographic separation. The lower chromatogram in each case is the pyrogram. All separations were isothermal. The column in the initial chromatographic step was a 3 m 0.10" i.d. tube conventionally packed with 10% SF-96 coated 60-80 mesh Chromosorb-P. A sample of the mixture up to 1.0  $\mu$ l of liquid could be used with this column.

Isothermal operation of the PGC step is adequate when the original mixture is well resolved as, for example, in Figure 5.11 A and when the boiling point range of the pyrolysate is small. To use isothermal operation when the original components are less well resolved, Figure 5.11 B, necessitates a high flow rate to reduce the time required and resolution of the pyrolysate suffers.



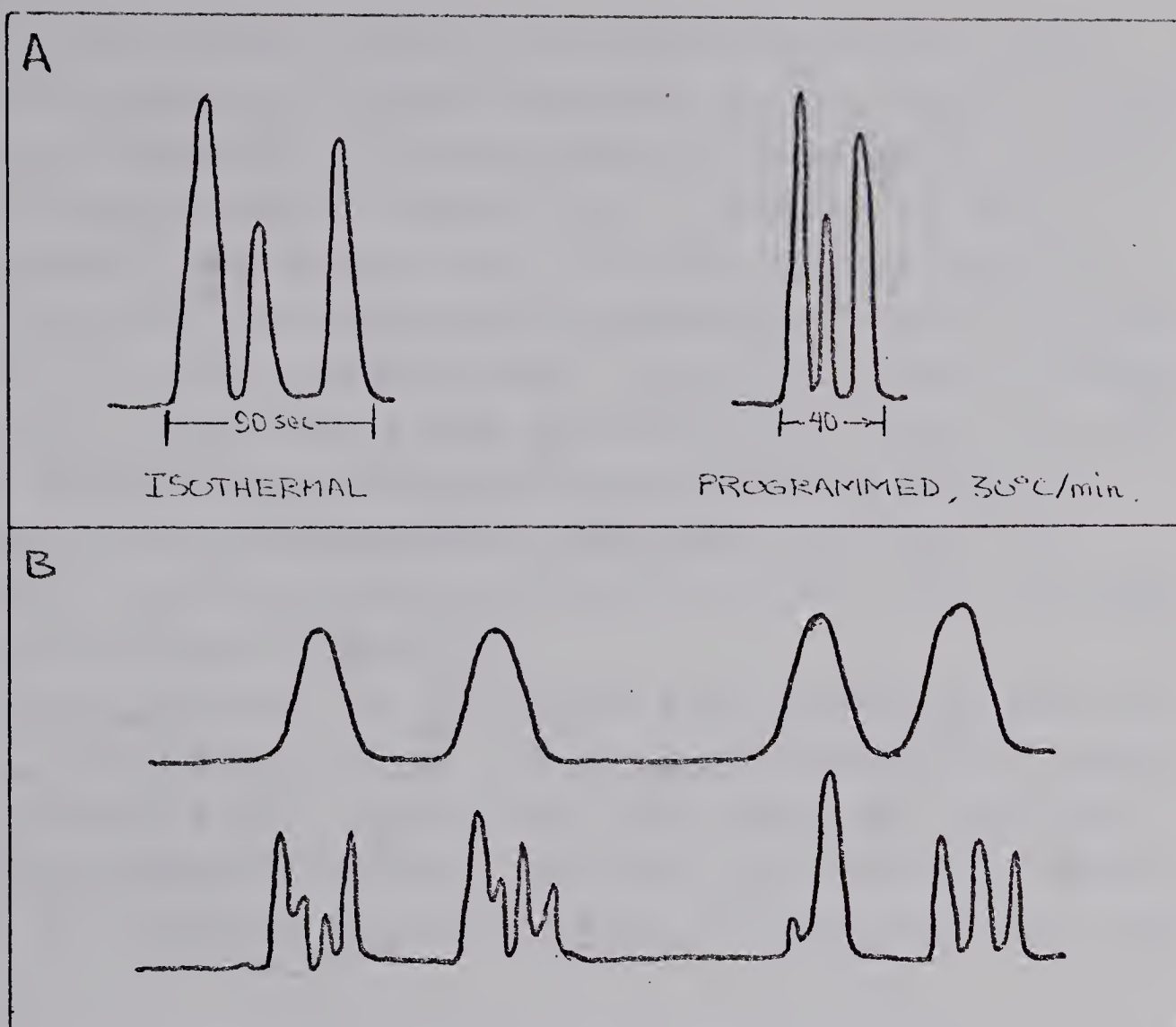


Figure 5.12 Reduction of analysis time possible with temperature programming and the consequent improvement in system performance. Pyrograms (A) for 2,3-dimethylbutane isothermal and programmed as noted. System operation in (B) parallels that shown in Figure 5.11 B but shows improved resolution in the pyrogram made possible by temperature programming.

Programming in the PGC step greatly enhances the capacity of the system. A typical reduction in analysis time without loss of resolution is shown for the pyrolysate of 2,3-dimethylbutane in Figure 5.12 A. The greater the range of boiling points of the pyrolysate the greater the benefit of PTGC in reducing analysis time.

Figure 5.12 B shows the same initial sample separation and pyrolysis as shown in Figure 5.11 B but reveals the increased resolution obtained by using PGGC in the PGC step.



If the original sample is a wide boiling point range mixture programming becomes necessary for the initial chromatographic separation. The necessity of programming in this case is illustrated in Figure 5.13. A mixture of normal hydrocarbons from pentane (b.p - 36.2°C) through dodecane (b.p = 214.5°C) was separated isothermally at 35°C and 125°C, Figure 5.13 A and B respectively. At 35°C the lower homologs were well resolved and eluted as well defined peaks but the higher homologs were retained on the column or eluted so slowly as to be undetectable. The higher homologs were eluted in a desirable manner at 125°C but the lower homologs were not adequately separated.

Programming at 6°C per minute from an initial temperature of 25°C, Figure 5.13C, allows good resolution at convenient retention times, although the peak shape for the higher homologs becomes distorted. Reduction of the initial temperature to 13°C improves the chromatogram as shown in Figure 5.14A.

A pyrogram for each hydrocarbon was produced using programming in the PGC stage, Figure 5.14 B. A new component was eluted from the initial chromatographic step on the average of every 2.6 minutes. As the higher homologs were eluted it became necessary to increase the program rate in the PGC stage due to the increasing boiling point range of the components present in each succeeding pyrolysate. As a consequence, the resolution of the C-11 and C-12 pyrolysates was poorer than that for the lower homologs.

Experimentally, only the initial chromatographic separation was linearly programmed. The column of the PGC stage was heated directly by passing an electrical current through the tube wall. The rate was determined by the voltage applied. The low voltage power supply for this heating application is shown in Appendix I.



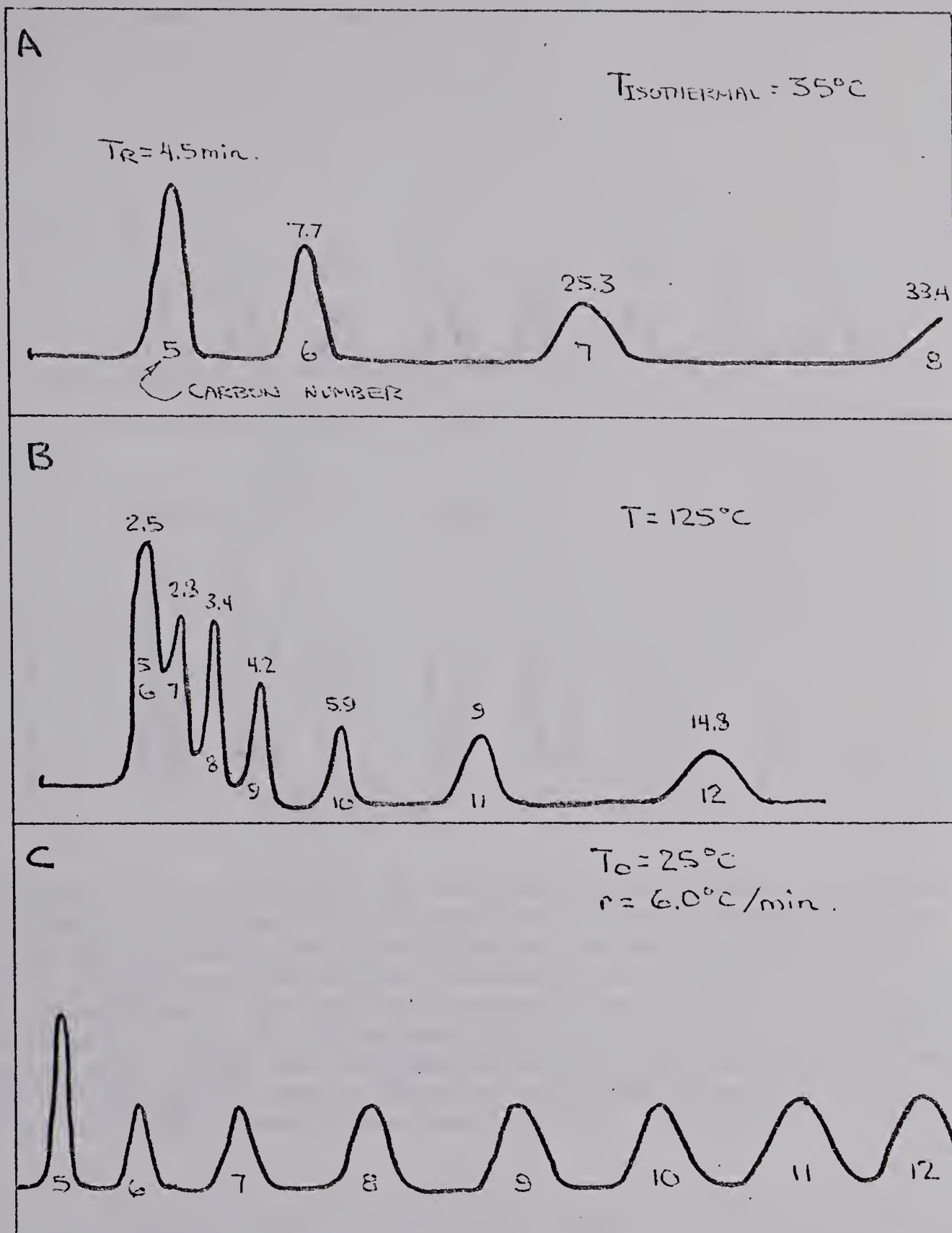


Figure 5.13 Chromatograms of  $\text{C}_5$  to  $\text{C}_{12}$  mixture of normal hydrocarbons. (A) and (B) are isothermal chromatograms at  $35^{\circ}\text{C}$  and  $125^{\circ}\text{C}$  respectively. (C) is a programmed temperature chromatogram at  $6.0^{\circ}\text{C}$  per minute with an initial temperature of  $25^{\circ}\text{C}$ . Column was  $3/16''$  i.d., 3 m packed with 5% SF-96 on 60-80 mesh Chromosorb-P. Flow rate for all runs was 20 ml/min.



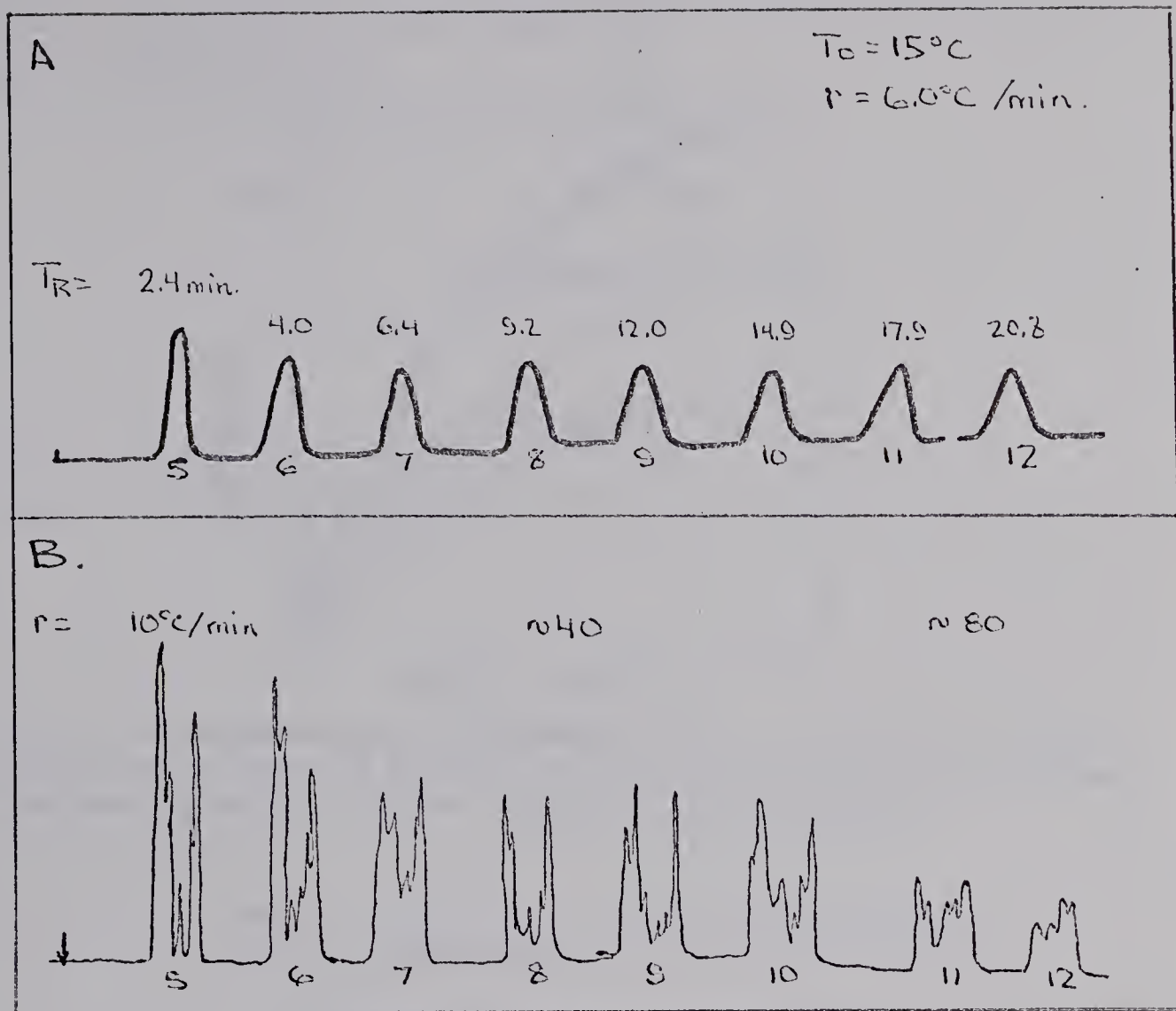


Figure 5.14 Chromatogram for  $C_5$  to  $C_{12}$  mixture of normal hydrocarbons with sequential pyrogram for each component. Figure A shows programmed temperature chromatogram with conditions optimized for resolution of mixture. Column description given in Figure 5.13. Pyrograms shown in (B) obtained using programming at approximate rates shown. Flow rate for A was 20 ml/min. and for B 32 ml/min. Pyrolysis temperature was  $620^\circ\text{C}$ . Chromatographic column used for separation of pyrolysate components was 1 m, 0.10" i.d. packed with 5% SF-96 on 60-80 mesh Chromosorb-P. Programmed at rates indicated in the figure from an initial temperature of  $15^\circ\text{C}$ .

The approximate heating rates shown in Figure 5.14 were taken from the relatively linear portion of the temperature-time curve for this particular column as shown in Figure 5.15. Direct electrical heating without the use of a controlling programmer gives a non-linear rate of temperature increase so that the values used are at best approximate ones.

To reduce the cooling time of the PGC column it was constantly immersed in a water cooled oil bath at  $15^\circ\text{C}$ .



Electrical heating of the column while in the oil bath presented no difficulties.

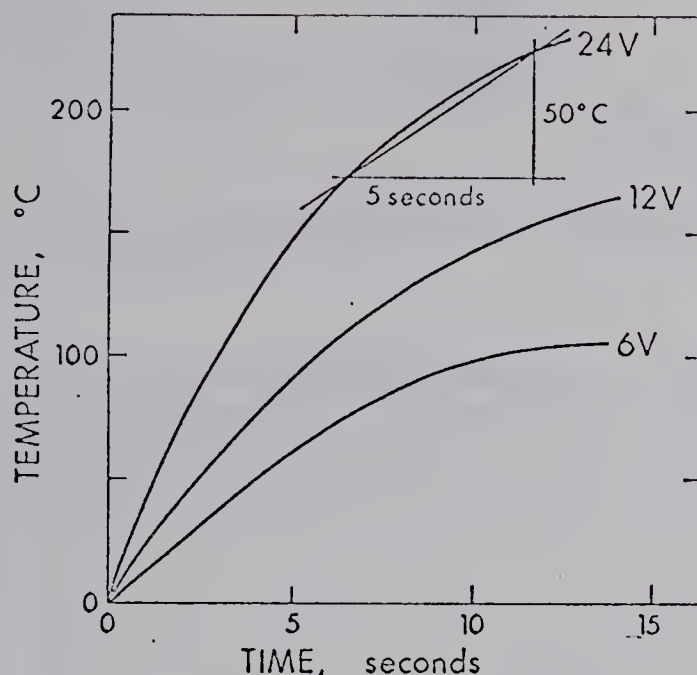


Figure 5.15 Temperature-time relationship for a 1 m 0.10" i.d. steel tube using direct electrical heating and as a function of input voltage. Column immersed in oil at 15°C to facilitate rapid cooling.

### 5.03 ALTERNATE SYSTEM ARRANGEMENTS

#### Stopped-Flow Chromatography

Several possible alternative methods could have been adopted to allow PGC to be applied to gas chromatographic effluents with less stringent experimental requirements. If it were possible to hold components in the column used for the initial chromatographic separation the PGC step could be done at a more leisurely pace.

A technique called "interrupted-elution gas chromatography" (86, 10) or "stopped-flow gas chromatography" (34) has been reported. As may be inferred from the names, the solutes are held in the column by the simple expedient of stopping the carrier gas flow. It was reported that holding times of up to 20 minutes caused "practically no spreading of retained peaks" (34). The potential usefulness of such a system made a preliminary examination desirable. The experimental design and results for this examination are shown in Figures 5.16 and 5.17.



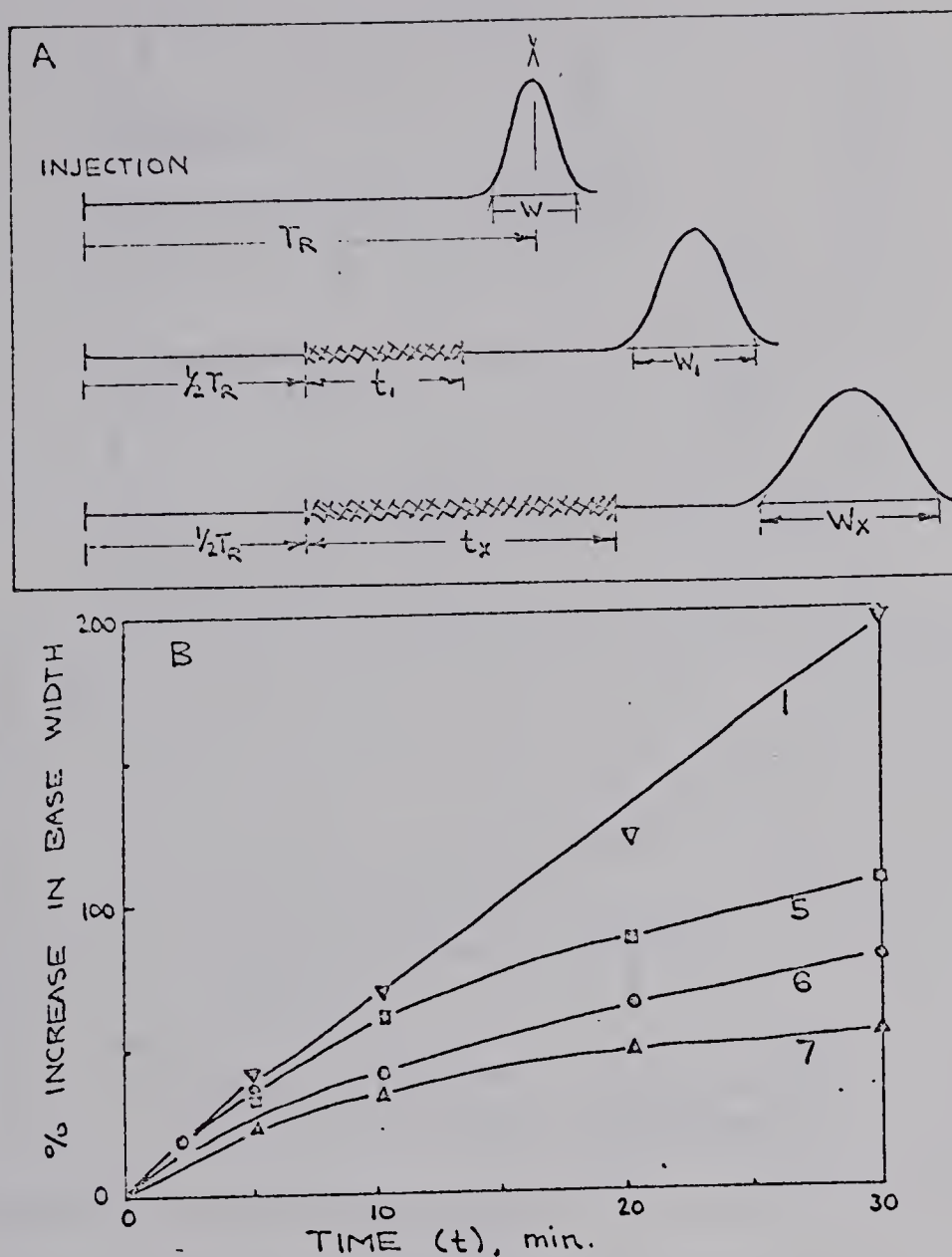


Figure 5.16 Effect of the duration of carrier flow stoppage ( $t$ ) on the peak broadening in stopped-flow chromatography. Experimental design (A) allows the duration of flow stoppage to be of varied duration ( $t$ ). Flow was stopped in each case at one-half of the retention time ( $1/2 T_R$ ). Results (B) show percent increase in base width  $\frac{W_x - W}{W} \times 100$  as a function of  $t$ .

Lines designated 1, 5 and 7 represent normal hydrocarbons of these carbon numbers with peak spreading determined on a 3 m 0.10" i.d. column. Line designated 6 represents 2,3-dimethylbutane shows peak broadening as measured on a 1 m 0.10" i.d. column. Both columns, packed with 5% SF-96 on 60-80 mesh Chromosorb-P. Sample size was 20  $\mu$ l of vapor. Temperature was 28°C.



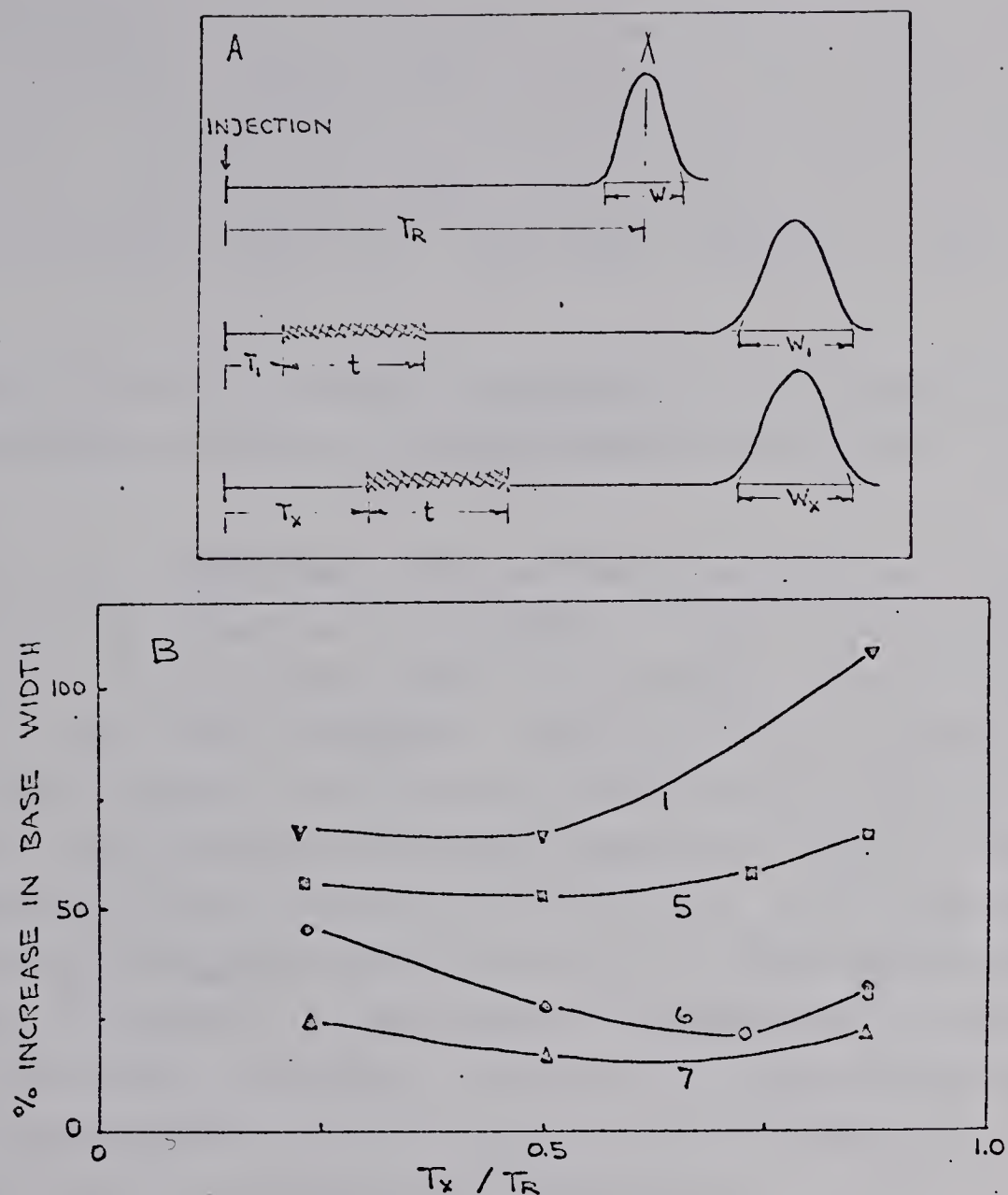


Figure 5.17 Effect of band position in column on the peak broadening in stopped-flow chromatography. The experimental design (A) allows the flow to be stopped at some time ( $T$ ) for a constant period ( $t$ ) of 10 minutes. The ratio ( $T/T_R$ ) the time where the flow was stopped ( $T$ ) to the retention time ( $T_R$ ) is used as an index of the band position in the column. The results (B) show the percentage increase in peak width as a function of the ratio ( $T/T_R$ ). Conditions and samples are as given in Figure 5.16.

Longitudinal diffusion of the solute in the gas phase is clearly recognized as a factor in peak spreading. At low flow this factor predominates to give increasingly large values of plate height. This process must continue during an interruption in carrier gas flow and is shown in Figure 5.16 B. Diffusion in the gas phase assumes that a reasonable proportion of the solute is in that phase. The degree of peak spreading in stopped flow chromatography should be, then, a function of the partition ratios of the solutes. As



seen in Figures 5.16 B and 5.17 B the solute with the lowest partition ratio, methane, did experience the greatest peak spreading. A consequence of this behavior is that for solutes at temperatures where the partition ratio is high, stopping the gas flow will contribute little to peak spreading.

The effect of the peak position in the column on the peak spreading during a flow interruption is shown in Figure 5.17 B.

For this experiment the carrier gas flow was stopped at a valve at the inlet of the column. Under these conditions the flow would continue until the pressure in the column had equalled the outlet pressure. Valving at the outlet would still have allowed the flow to continue but not until the pressure equalized at the inlet pressure. Even if the flow were simultaneously stopped by valving at both ends there would be a continuing movement of gas in the column until the pressure is uniform at some valve intermediate between the inlet and outlet pressures. This slow, exponential cessation of flow is unavoidable as is a surge at the resumption of flow and both tend to increase band spreading.

#### Selective Trapping

The statements of the capabilities of the system previously made were based on what may be unnecessarily stringent performance requirements in both the initial chromatographic separation and the subsequent PGC step.

Dhont (19) indicated that good resolution of the pyrolysis product is not necessarily required for useful information to be obtained. The identification of the components of the pyrolysates is in itself a formidable task and unnecessary, according to Kirk (64), especially when fingerprint identifications are being used.

The complete resolution demanded of the initial chromatographic step may also be unnecessary. Secondary reactions are reduced by careful pyrolyzer design and operation so that



the addition of a small amount of a second component should have little effect on the break-down pattern of the major substance. The contribution of the pyrolysis products from an impurity would then be in proportion to the degree it contaminates the major substance. If the impurity is highly pyrolyzed and the major material only slightly so, under the conditions of pyrolysis being used, good resolution may still be required. The small effect of a 10% impurity contamination on the pyrogram of 2,3 dimethylbutane is shown in Figure 5.18.

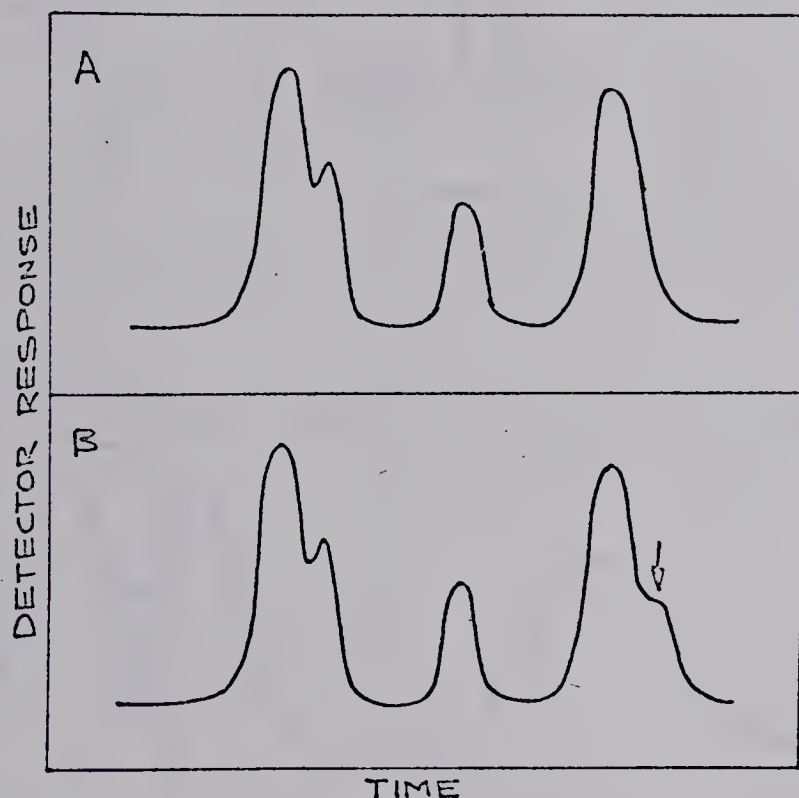


Figure 5.18 Pyrogram of 2,3-dimethylbutane (A) and a pyrogram of 2,3-dimethylbutane + 10% n-hexane impurity (B).

The use of a sensitive detector, such as the flame ionization detector as shown in use in Figure 5.01, in the PGC stage allows very small samples to be analyzed. If the initial chromatographic separation is capable of handling relatively large samples, then only a portion of each eluted material may be required for PGC to be used for identification and the remainder vented.

The minor modification of the system as shown in Figure 5.19 allows selective trapping of eluted materials from the



initial chromatographic step. As indicated in the figure, relatively pure portions of unresolved peaks could be selectively trapped although to do so would require a prior knowledge of the chromatogram. The resolution required would be reduced by introduction of this modification.

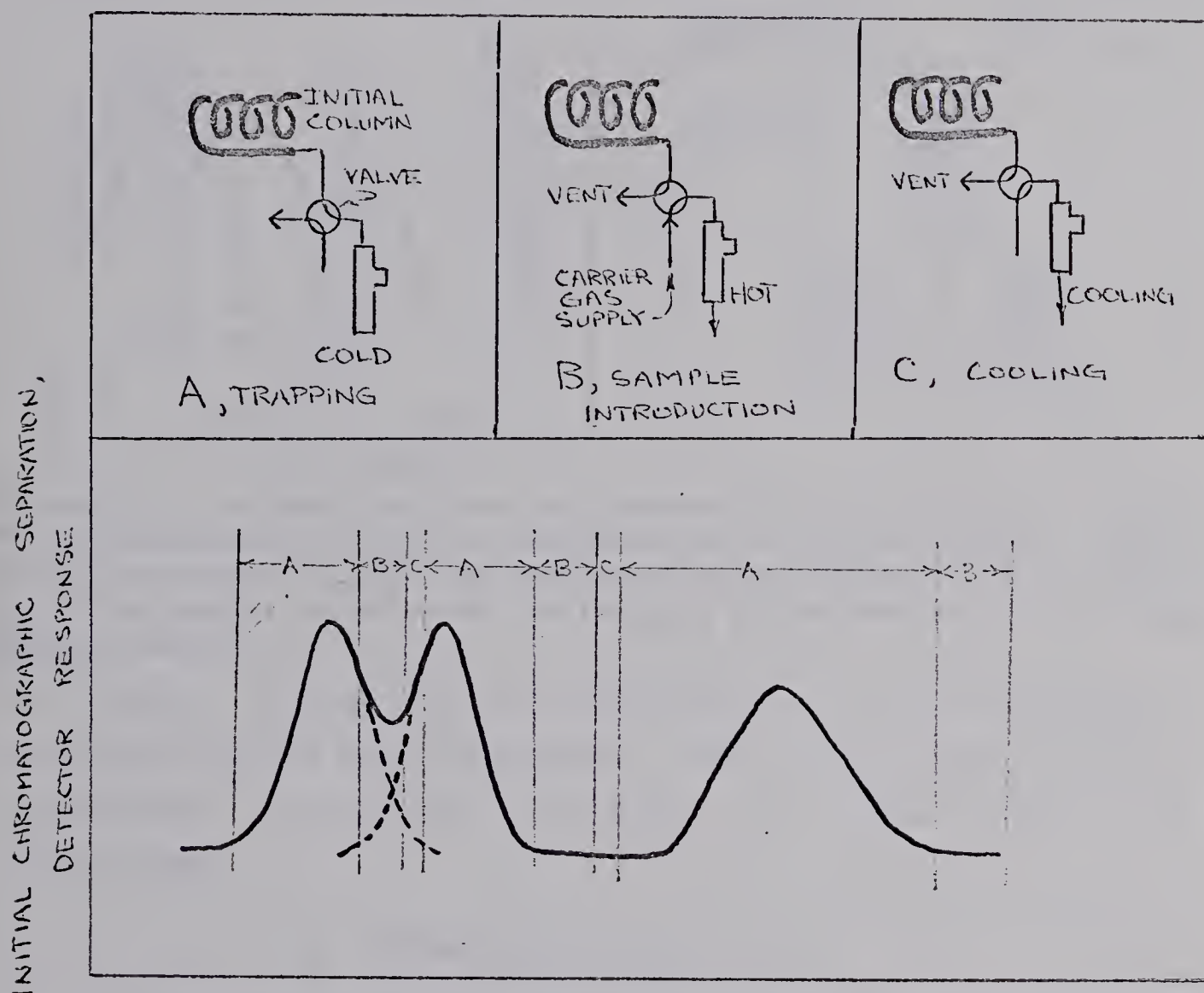


Figure 5.19 Selective trapping of effluent from initial chromatographic separation. A (shaded area) indicates that trapping is occurring. B+C requires 20 seconds, the turn-around time of the trapping column.

### Parallel Columns

The addition of a parallel column to the second chromatographic step of the system increases its overall capability as shown in the following figure, Figure 5.20.

With two cycling columns in the arrangement in Figure



520 Å, any two peaks with  $\Delta t_R > 52.5$  seconds and  $R = 1.52$  or greater, could be handled. With selective trapping the requirement for resolution at  $\Delta t_R = 52.5$  seconds is reduced to 0.875.

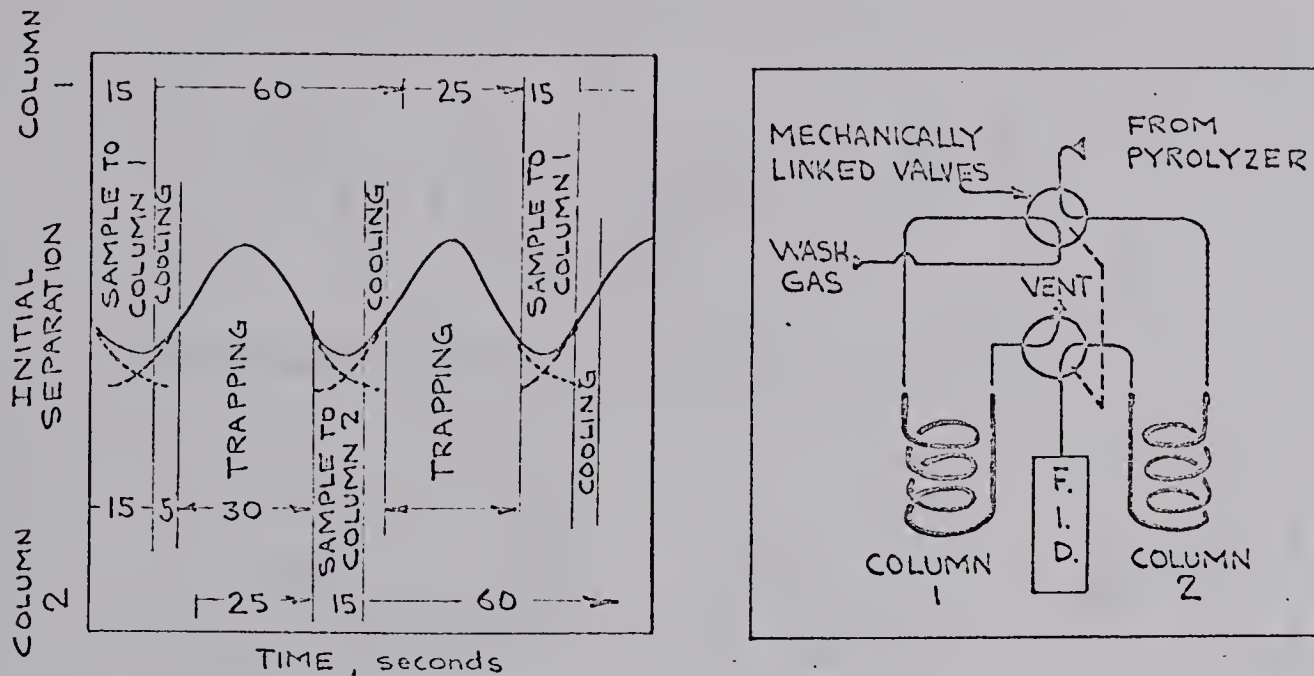


Figure 5.20 Schematic of time requirements for system with two columns in the second chromatographic step employing selective trapping, Figure 5.19. Numbers represent time; 60 for program duration, 25 for cooling column to  $T_o$ , 15 for sample introduction via trapping column heating, 5 for cooling trapping column.

Such a system would be more mechanically complex but not appreciably more expensive. The heating power supply, programmer and detector, the major cost items, would be in common use.

## Subambient Programming

If better resolution of the pyrolysate components were required, the system would have to be modified. As shown in Figure 5.08, good resolution of a mixture of  $C_1$ - $C_4$  hydrocarbons was obtained using a 3 meter 0.10" i.d. column. The programming and subsequent cooling of a column of this length increases the turn-around time for the PGC step.

Cryogenic programming and subambient PTGC have been successfully employed in the analysis of  $C_1$ - $C_4$  hydrocarbons. As an alternative to the use of longer columns a reduction of the initial temperatures was examined to see if resolution could be enhanced without increasing turn-around time.



Figure 5.21 shows the effect of program rate and initial temperature on the resolution of the pyrolysates of 2,3-dimethylbutane. An isothermal determination is included for comparison.

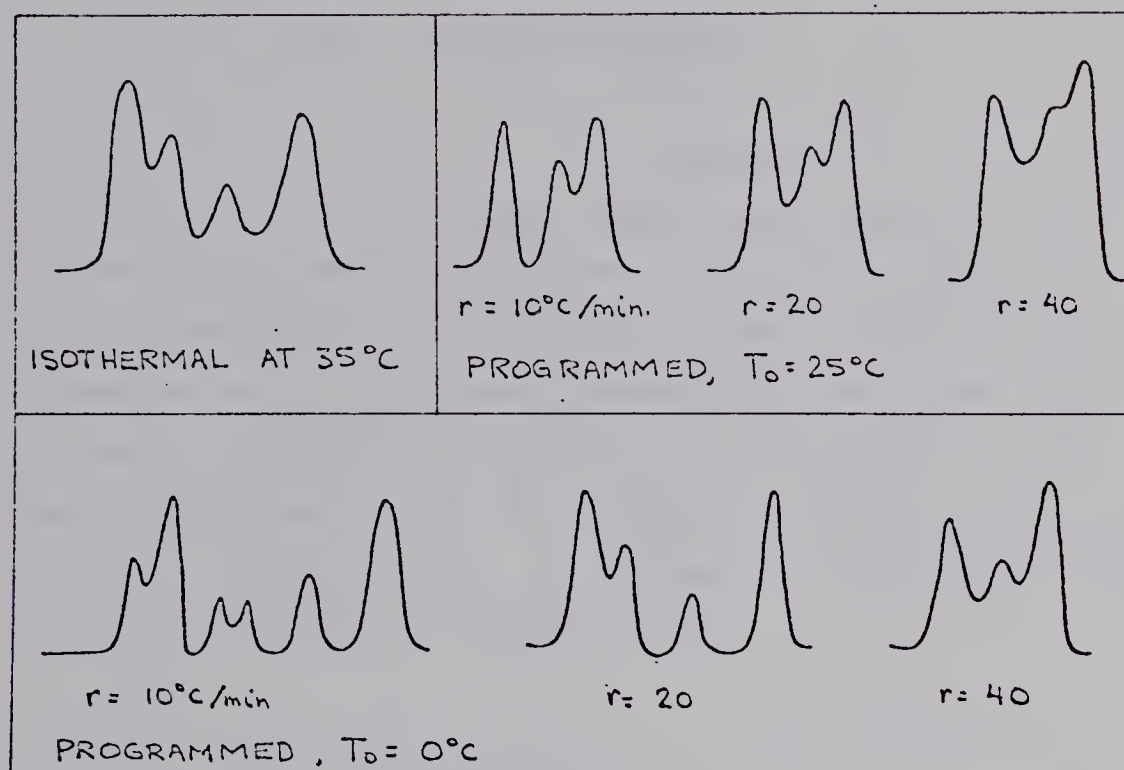


Figure 5.21 Isothermal and programmed temperature pyrograms for 2,3-dimethylbutane. Column was 1 m long and 0.10" i.d. packed with 5% SF-96 on 60-80 mesh Chromosorb-P. Pyrolyzer was at  $600^\circ\text{C}$ . Flow rate was constant for all determinations at 20 ml/min.

Reduction of the initial temperature enhances resolution, the improvement in which is particularly noticeable in conjunction with a program rate of  $10^\circ\text{C}$  per minute. The complete chromatogram of 2,3-dimethylbutane pyrolysate is produced in less than 40 seconds when programmed at  $10^\circ\text{C}$  per minute from an initial temperature of  $0^\circ\text{C}$ . Resolution under these conditions was good. Although it probably would not be needed, an increased sample volume capacity is also obtained when the initial temperature is reduced.

Any reduction in the requirements imposed by any part of the system on any other allows greater flexibility of operation. The system for the identification of gas chromatographic peaks by PGC is like all chromatographic operations,



that is, the details of operation and design are the result of compromise. A balance must be obtained between ease of operation and system flexibility; time required and resolution.

#### 5.04 FINAL COMMENTS

The identification of all the components in the pyrolysisate may be a difficult task. Good resolution is required and identifications based solely on retention temperatures, is not wholly adequate, particularly when the pyrolysisate is made up of components which are themselves complex. The problem has been resolved by Merritt and Robertson (72), who applied mass spectrometry to the identification of the individual pyrolysisate components. A schematic diagram of their analysis system is shown in Figure 5.23.

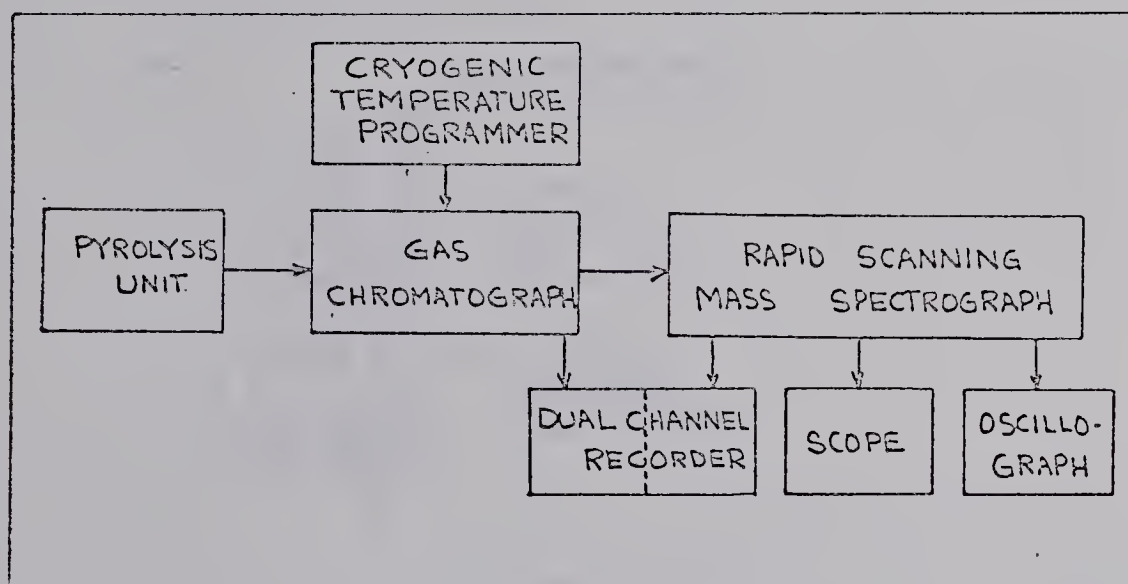


Figure 5.22 Schematic diagram of the analysis system of Merritt and Robertson (72).

One of the principal objectives of the development of the application of PGC to the identification of the components in a gas chromatographic was a simplification of the system. Although the system of Merritt and Robertson produces much information, it is clearly less than a simplification of technique.



The system for the use of PGC in identifying gas chromatographic peaks is best suited for "fingerprint technique". This technique places far less difficult requirements on the component subsystem and consequently becomes easy to use and relatively inexpensive. The problem of identifying the pyrolysis components is avoided when a "fingerprint technique" is employed.

As previously mentioned other degradative techniques may be substituted for pyrolysis in the general system. A "photolyzer" as shown in Figure 5.23 may replace the pyrolyzer in the general system. When this system was used no attempt was made to enhance photolysis by optimizing conditions and results are given only to indicate the ease with which an alternative degradative technique may be substituted for the pyrolyzer in the system.

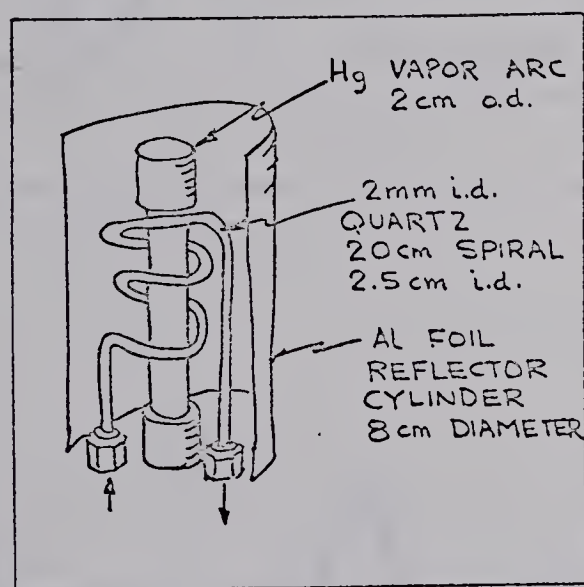


Figure 5.23 Apparatus for gas phase photolysis. The UV source was a Hanovia Chemical and Manufacturing Co., 500 watt medium pressure Hg arc. #676A.

A mass spectrogram and a pyrogram are given for comparison to the chromatogram of the photolytic degradation products of 2,3-dimethylbutane in Figure 5.24. The similarities are partially due to the manner of presentation but nevertheless the techniques do yield related types of information and all should be useful for compound identification.



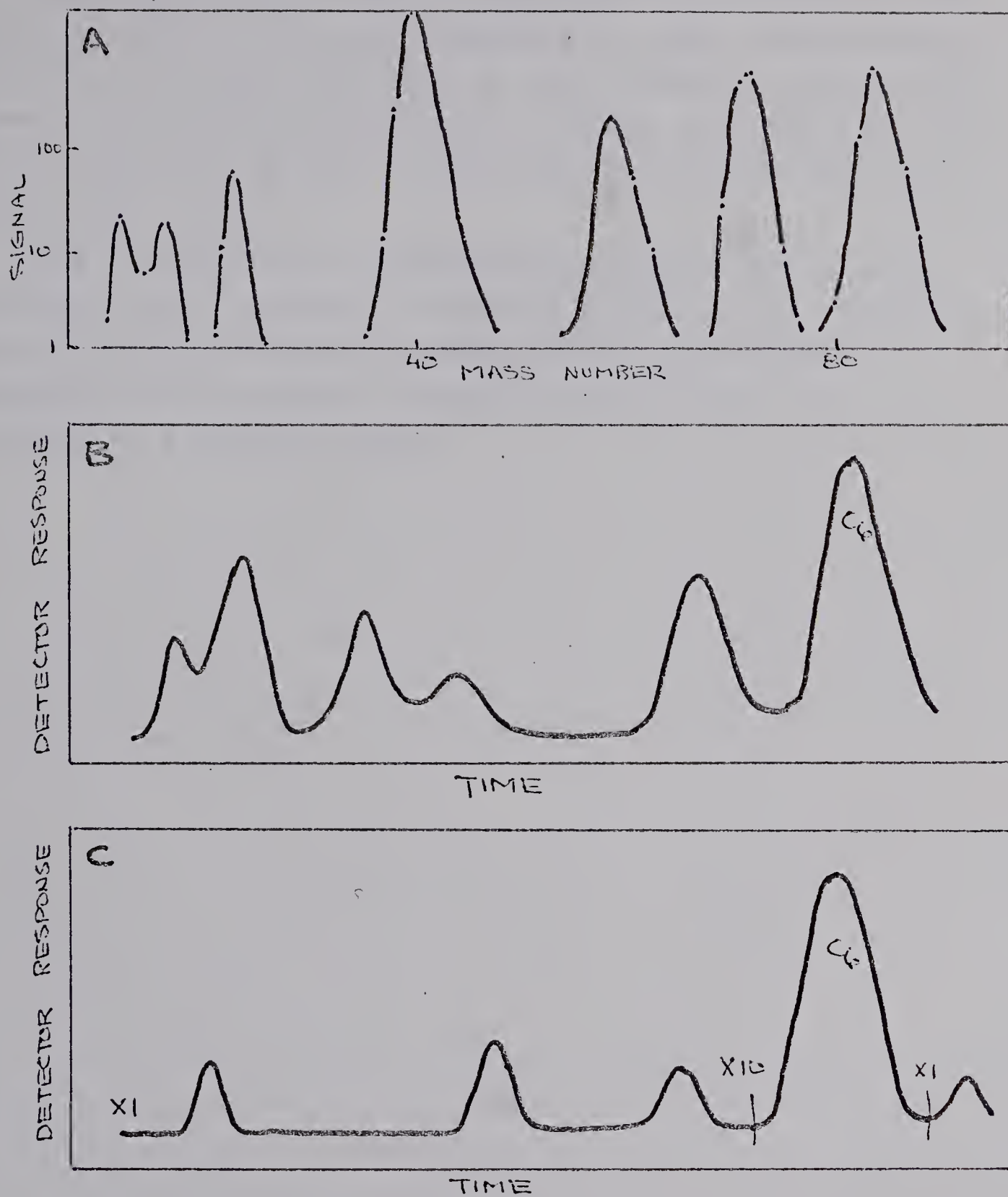


Figure 5.24 Mass spectrogram (A), Pyrogram (B), and chromatogram of the photolytic degradation products (C) of 2,3-dimethylbutane.



The usefulness of PGC in obtaining information of the type necessary to identify compounds has been established by practice and illustrated here by the different types of pyrograms for 6-carbon hydrocarbons, as shown in Figures 5.11 and 5.12 and for the series of normal hydrocarbons from C-5 to C-12, Figure 5.14.

The feasibility of sequentially applying PGC to gas chromatographic effluents have been demonstrated. Requirements of each part of the system may be independently assessed with the overall capability determined and tailored to a specific need.



## 6. SUMMARY

A low-pressure-drop column packing in the form of two concentric helicies of small diameter wire was found to have a pressure drop of less than 1 mm Hg for a 3 m column with flow rates up to 150 ml per minute. Examination of the characteristics of this column with hydrocarbon samples and SF-96 as a stationary phase revealed plate heights as low as 0.3 cm. Column conditions giving this plate height were such that resolution was not favorable. In the examination of packing openness and proportion of stationary phase it was clearly illustrated that under certain conditions changes in the column may result in the simultaneous increase of both plate height and resolution.

An apparatus is described which was capable of heating a gas chromatographic column at up to 600°C per minute and linearly programming the temperature at rates up to 400°C per minute.

Program rates from 0.4 to 400°C per minute were used with values of the ratio of program rate to flow rate at the initial temperature per gram of stationary phase,  $r/\bar{F}_{T_0}$ , from 0.002 to 20 for studies of retention temperature, resolution, and intrinsic resolution.

The difference between the retention temperature predicted from isothermal data and that obtained experimentally increased abruptly at a  $r/\bar{F}_{T_0}$  ratio of about 2. Correction of the flow rate for changes which occur during programming eliminated this difference within reasonable experimental error.

For a given program rate both resolution and intrinsic resolution passed through a maximum when examined as a function of the  $R/\bar{F}_{T_0}$  ratio. The maxima in resolution or intrinsic resolution correlate with the optimum flow rate.

Gross examination of intrinsic resolution as a function of the  $r/\bar{F}_{T_0}$  ratio for two columns of significantly differ-



ent dead spaces per gram of stationary phase revealed a roughly constant intrinsic resolution up to a  $r/\bar{F}_{T_0}$  ratio of 0.3 after which it decreased as  $r/\bar{F}_{T_0}$  increased.

The importance of having a "square" temperature profile in a gas phase pyrolyzer was established on the basis of the need of a precise determination of temperature and residence time. To obtain such a profile high linear flow velocities were shown to be favored. The design geometry of a tubular pyrolyzer may be calculated for any desired profile from the considerations presented. Generally long tubes of small inside diameter are favored.

The pyrolysis of hydrocarbons in the gas phase illustrated the effects of pyrolyzer temperature and residence time. With a fixed residence time the extent of degradation of a compound increased with increasing pyrolysis temperature and an increasing proportion of the more simple products were produced. With a fixed pyrolysis temperature increased degradation was achieved by increasing the residence time. No single combination of temperature and residence time gave equal degrees of degradation for hydrocarbons of different structural types. This illustrated the necessity for compromise in pyrolyzer design.

A system is described for the application of pyrolysis gas chromatography (PGC) to the identification gas chromatographic effluents. This system incorporated a short trapping column capable of retaining all hydrocarbons above methane in molecular weight and reducing the base width from, typically, 250 to 15 seconds. Placement of the trapping column ahead of the pyrolyzer eliminated any problems that would have been associated with the trapping of the low molecular weight materials in the pyrolysate.

Mixtures of hydrocarbons were separated in an initial chromatographic step with PGC applied to the individual components. For widely separated materials isothermal PGC was adequate. Programming the chromatographic separation of the



pyrolysate allowed a reduction in the time required without loss in resolution. For a mixture of normal hydrocarbons,  $C_5$  to  $C_{12}$ , programming was also necessary for the initial chromatographic separation.

The requirements of resolution in the initial chromatographic separation were calculated on the basis of turnaround times for the components of the system. The system described was capable of handling a component eluted every 100 seconds if the resolution was 1.2 or greater. Less rigorous requirements could be made possible by the incorporation of alternate system arrangements such as stopped-flow chromatography. Stopped-flow chromatography was briefly investigated and it was found that the extent of peak broadening resulting from the flow interruption was directly related to the extent that the solute was present in the gas phase in the column.

The system developed can be used with a number of other degradative techniques. For example, a photolyzer was used replacing the pyrolyzer. The chromatograms of the photolytic degradation products that resulted were comparable to the pyrograms which had been obtained.



# BIBLIOGRAPHY

1. Adams, J. D., Conkle, J. P., Mabson, E., Watson, J. T., Wolf, P. H., Welch, B. E., *Aerospace Med.* 37, 555 (1966).
2. Altenau, A., Kramer, R. E., McAdoo, D. J., *J. Gas Chromatog.* 4, 96 (1966).
3. Ambrose, D., Ambrose, B. A., *Gas Chromatography*, George Newnes Ltd., London, 1961. pp. 7-10.
4. Amy, J. W., Chait, E. M., McLafferty, F. W., *Anal. Chem.* 37, 1265 (1965).
5. Andrew, T. D., Phillips, S. G., Semlyen, J. A., *J. Gas Chromatog.* 1, 27 (1963).
6. Armstrong, N. W., Stauffer, G. L., Runner, M. E., Pittsburgh Conf. on Anal. Chem. and Appl. Spectrog., Feb. 21-25, 1966. Abstract of Papers, No 115, p. 81.
7. Barbour, W. M., *J. Gas Chromatog.* 3, 228 (1965).
8. Beroza, M., Coad, R. A., *J. Gas Chromatog.* 4, 199 (1966).
9. Boheman, J., Purnell, J. H., *Gas Chromatography 1958*, Besty, D. H., ed., Academic Press, New York, 1958, p. 6.
10. Borfitz, H., *Anal. Chem.* 33, 1632 (1961).
11. Borka, L., Privett, O. S., *J. Am. Oil Chemists Soc.* 42, 1070 (1965).
12. Bowen, S. W., Marks, M. L., U. S. Pat. No. 3, 097, 517 issued July 16, 1963.
13. Cartwright, M., Heywood, A., *Analyst* 91, 337 (1966).
14. Cramers, C. A. M. G., Keulemans, A. I. M., *J. Gas Chromatog* 5, 58 (1967).
- 14A Coates, J. V., et al, eds., *Gas Chromatography*, Academic Press, New York, 1958, p. 316.
15. Cox, B. C., Ellis, B., *Anal. Chem.* 36, 90 (1964).
- 15A Dal Nogare, S., Juvet, R. S., *Gas-Liquid Chromatography*, Interscience Publishers, New York, 1962.
16. Desty, D. H., ed., *Gas Chromatography 1958*, Academic Press, New York, 1958, p. xi.



17. Desty, D. H., ed., Vapor Phase Chromatography, Academic Press, New York, 1957, p. xiii.
- 17A Desty, D. H., Goldup, A., Swanton, W. T., Gas Chromatography, Brenner, N., et al, eds., Academic Press, New York, 1962. pp. 105-135.
18. Duer-Siftar, D., Bistricki, T., Tandi, T., J. Chromatog. 24, 404 (1966).
19. Dhont, J. H., Analyst 89, 71 (1964).
20. Dhont, J. H., Nature 200, 882 (1963).
21. Dietz, W. A., J. Gas Chromatog. 5, 68 (1967).
22. Duffield, J. J., Rogers, L. B., Anal. Chem. 32, 340 (1960).
23. Ellerington, T., Gas Chromatography, Desty, D. H., ed., Butterworths, London, 1958, p. 198.
24. Ibid. p. xi.
25. Ettre, L. S., Open Tubular Columns in Gas Chromatography, Plenum Press, New York, 1965.
26. Ettre, L. S., Cieplinski, E. W., Averill, W., J. Gas Chromatog. 1, No. 2, 7 (1963).
- 26A Fredrick, D. H., Miranda, B. T., Cooke, W. D., Anal. Chem. 34, 1521 (1961).
27. Fryer, J. F., M. Sc. Thesis, University of Alberta, Edmonton, Alberta, 1960.
28. Fryer, J. F., Habgood, H. W., Harris, W. E., Anal. Chem. 33, 1515 (1961).
- 28A Fusy, J., Niclaus, M., et al , Bull. Soc. Chem. France 1966, 3783 (1966).
29. Gatrell, R. L., Mao, T. J., Anal. Chem. 37, 1294 (1965).
30. Gellerman, J. L., Schlenk, H., Anal. Chem. 38, 72 (1966).
31. Giddings, J. C., J. Chromatog. 13, 301 (1964).
32. Giddings, J. C., Gas Chromatography, Brenner, N., Callen, J. E., Wiess, M. B., eds., Academic Press, New York, 1962, p. 57.
33. Giddings, J. C., Dynamics of Chromatography Part I, Marcel Dekker Inc., New York, 1965, p. 25.



- 33A Giddings, J. C., Anal. Chem. 34, 722 (1962).
- 33B Glueckauf, E., Trans. Faraday Soc. 51, 34 (1955).
34. Grisby, R. D., Boyer, E. W., The Vapor Pressure 37, No. 3 (1966).
35. Groten, B., Anal. Chem. 36, 1206 (1964).
- 35A Guiochon, G., Anal. Chem. 38, 1020 (1966).
36. Habgood, H. W., Harris, W. E., Anal. Chem. 32, 450 (1966).
37. Habgood, H. W., Harris, W. E., Anal. Chem. 34, 882 (1962).
- 37A Halasz, I., Schreyer, G., Z. anal Chem. 181, 367 (1961).
38. Harris, W. E., Habgood, H. W., J. Gas Chromatog. 4, 144, 168, 217 (1966).
39. Harris, W. E., Habgood, H. W., Talanta II, 115 (1964).
40. Harris, W. E., Habgood, H. W., Programmed Temperature Gas Chromatography, John Wiley and Sons, Inc. New York, 1966.
- 40A Ibid. p. 121.
41. Ibid. p. 171.
42. Ibid. p. 273.
43. Ibid. p. 76.
44. Ibid, Chapters 3 and 4.
- 44A Hollingshead, L. W., Habgood, H. W., Harris, W. E., Can. J. Chem. 43, 1560 (1965).
45. Hollis, O. L., Anal. Chem. 33, 352 (1961).
46. Horlick, G., Harris, W. E., Habgood, H. W., Anal. Chem. 38, 7 (1966).
47. Howlett, M. D. D., Welti, D., Analyst 91, 291 (1966).
48. Janak, J., Nature 185, 684 (1960).
49. James, A. T., Martin, A. J.P., Biochem. J. 50, 679 (1952).
51. Johns, T., Morris, R. A., Develop. in Appl. Spectroscopy 4, 361 (1965).



52. Johnson, H. W., Strass, F. H., Anal. Chem. 30, 1586 (1960).
- 52A Jones, W. L., Kieselbach, R., Anal. Chem. 30, 1590 (1958).
53. Jones, C. E. R., Reynolds, G. E. J., J. Gas Chromatog. 5, 25 (1967).
54. Juvet, R. S., Tanner, R. L., Tsao, J. C. Y., J. Gas Chromatog. 5, 15 (1967).
55. Kaiser, R., Gas Phase Chromatography, Scott, P. H., trans., Butterworths, London, 1963, p. 24.
56. Ibid., p. 39.
57. Karger, B. L., J. Gas Chromatog. 5, 161 (1967).
58. Karger, B. L., Cooke, W. D., Advances in Chromatography, Vol. I., Giddings, J. C., Keller, R. A., eds., Marcel Dekker Inc., New York, 1965, p. 309
- 58B Karger, B. L., Cooke, W. D., Anal. Chem. 36, 991 (1964).
59. Keller, R. A., Stewart, G. H., Anal. Chem. 34, 1834 (1962).
60. Keulemans, A. I. M., Gas Chromatography, 2nd Ed., Reinhold Publishing Corporation, New York, 1959, p. 124 and 194.
61. Keulemans, A. I. M., Gas Chromatography: A Symposium, Academic Press, New York, 1958.
62. Keulemans, A. I. M., Perry, S. G., Gas Chromatography, van Swaay, M., ed., Butterworths, London, 1962, p. 356.
64. Kirk, P. L., J. Gas Chromatog. 5, 11 (1967).
65. Kwantes, A., Rijnders, G. W. A., Gas Chromatography 1958, Desty, D. H., ed., Academic Press, New York, 1958, p. 125.
66. Lehrle, R. S., Robb, J. C., J. Gas Chromatog. 5, 89 (1967).
67. Levy, R. L., Chromatographic Reviews 8, 48 (1967).
68. Levy, R. L., First International Symposium on Pyrolysis and Reaction Gas Chromatography, Ecole Polytechnique, Paris, Sept. 15-16, 1966.



69. Levy, R. L., Eleventh Ottawa Symposium on Applied Spectroscopy and Anal. Chem., Sept. 9-11, 1964. Abstr. of Papers, p. 23. (See Chem. in Canada 16, 24 (1964)).
70. M & B Laboratory Bulletin VI, 26 (1965).
71. Martin, A. J. P., Synge, R. L. M., Biochem. J. 35, 1358 (1941).
72. Merritt, C., Robertson, D. H., J. Gas Chromatog. 5, 96 (1967).
73. McEwen, D. J., Anal. Chem. 35, 1636 (1963).
- 73A McKay, D. A. M., Lang, D. A., Berdick, M., Drug Cosmetic Ind. 86, 46 (1960).
74. Mon, T. R., Forrey, R. R., Teranishi, R., J. Gas Chromatog. 4, 176 (1966).
75. Morgan, M. E., Day, E. A., J. Dairy Sci. 48, 1382 (1965).
76. Neiswender, D. D., J. Gas Chromatog. 4, 426 (1966).
77. Oro, J., Ham, J., Zlatkis, A., Anal. Chem. 39, 27 (1967).
78. Palframan, J. F., Walker, E. A., Analyst 92, 71 (1967).
79. Perry, S. G., J. Gas Chromatog. 2, 54 (1964).
80. Perry, J. A., J. Gas Chromatog. 4, 194 (1966).
81. Pocaro, P. J., J. Gas Chromatog 1, No. 6, 17 (1963).
82. Pure and Applied Chemistry 8, 553 (1964).
- 82A Purnell, J. H., J. Chem. Soc. 1960, 1268 (1960).
- 82B Purnell, J. H., Nature 184, 2009 (1959).
83. Randell, E. A., Strutz, H. C., Anal. Chem. 31, 1890 (1959).
84. Rushneck, D. R., Dehler, J. L., Lab Management 4, 26(1966).
85. Said, A. S., J. Gas Chromatog. 1, No. 6, 20 (1963).
- 85A. Said, A. S., Sternberg, J. C., Beckman Instruments, Fullerton, California. In preparation.



86. Scott, R. P. W., Fowlis, I. A., Welty, D., Wilkins, T., 6th International Symp. on G. C. and Assoc. Techniques, Inst. Petro., Rome, Italy, Sept. 20-23, 1966. Preprints of Papers, No. 20.
87. Sideman, S., Gilladi, J., Gas Chromatography, Brenner, N., ed., Academic Press, New York, 1962.
88. Simon, W., Giacobbo, H., Angew. Chem. internat. Ed. 4, 938 (1965).
89. Sonntag, F., Brenstoff-Chem. 47, 263 (1966).
90. Sorenson, I., Soltoft, P., Acta Chem. Scand. 10, 1673 (1956).
91. Sternberg, J. C., Little, R. L., Anal. Chem. 38, 321 (1966).
92. Sternberg, J. C., Krull, I. H., Friedel, G. D., Anal. Chem. 38, 1639 (1966).
93. Supina, W. R., Henley, R. S., Kruppa, R. F., J. Am. Oil Chemists Soc. 43, 202A (1966).
- 93A Sutton, R. Private communication.
94. Szépe, S., J. Gas Chromatog. 5, 180 (1967).
95. Teranishi, R., Private communication to W. E. Harris.
96. Teranishi, R., Flath, R. A., Mon, T. R., J. Gas Chromatog. 4, 77 (1966).
97. Teranishi, R., Mon, T. R., Anal. Chem. 36, 1490 (1964).
98. Urone, P., Parcher, J. F., J. Gas Chromatog. 3, 35 (1965).
99. Van Deemter, J. J., Zuiderweg, F. J., Klinkenberg, A., Chem. Eng. Sci. 5, 271 (1956).
100. Watson, J. T., Bieman, K., Anal. Chem. 37, 844 (1965).
101. Weurman, C., Chem. Weekbl. 59, 489 (1963).



## APPENDIX I

Included in Appendix I are descriptions of equipment, sources of chemicals used, details of the construction on modification of equipment, equipment test results, and calibration curves. This compilation is for reference and is given as a separate section to prevent a dilution of the text material.

### Equipment and Chemicals

#### Detectors:

##### 1) Thermal conductivity (TC)

Gow-Mac Model TR-II-B, Gow-Mac Instrument Co., Madison, New Jersey, thermal conductivity cell was used in conjunction with the matching Regulated DC Power supply 9999-C. The detector block was maintained at 250°F by an internal thermostat. The filament current was normally set at 120 ma except when sensitivity requirements dictated higher values.

##### 2) Flame Ionization Detector (FID)

Instrument & Research, Inc., Walnut Creek, California, Flame Ionization Detector Kit was used. An air pump and filter and hydrogen flow restrictor supplied with the kit were used. Cylinder hydrogen was used, its flow determined by the flow restrictor at 25 psi supplied pressure. The flame head was remote from the electrometer to allow direct attachment to the column outlet. Sensitivity was also large enough that independent heating (thermostating) of the flame head was not required.



## Programmer

A number of commercially available programmers were considered. An Aerograph\* Model 329 was chosen on the basis of its mode of operation which does not limit obtainable rates due to mechanical arrangements. This programmer also uses true proportioning circuiting incorporating a silicon controlled rectifier (SCR) for power control. The unit was rated to be capable of handling a 1500 watt resistive load. It was not capable of handling the high inductive load presented by the low voltage power supply to be used for direct electrical heating necessitating its modification. This modification consists of adding a parallel set of controlling and indicating thermocouples and an output for a control signal for a high current capacity bank of SCR's. All modifications to the programmer are shown in Figure A 1.01.

The use of a variable low-voltage high current capacity power supply, Figure A 1.02 allows the accommodation of column tubes of a variety of resistances.

Thin wall stainless steel tubing, typically 0.10" i.d., 0.25" o.d., in lengths of 1 to 3 meters, was used. The columns were prepared in the form of coils of about 8 cm diameter with turns about 1 cm apart. These columns were shielded from stray air currents by enclosing them in an asbestos paper cylinder of about 15 cm diameter. The temperature of the tube wall was determined by using an iron constantin thermocouple with a Sargent SR recorder. The temperature-time curves for various input voltages for a 1 meter unpacked tube are shown in Figure A 1.03. Both packed and unpacked columns have been used successfully. The use of columns of small diameter limits the difficulty arising from thermal gradients through the cross-section of the column.

---

\*Wilkins Instrument and Research, Inc.,  
P. O. Box 313,  
Walnut Creek, California.







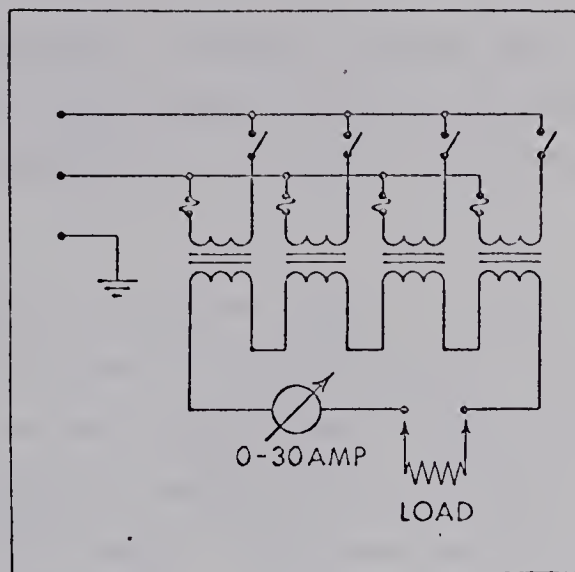


Figure A 1.02 Low voltage power supply for use with direct electrical column heating.

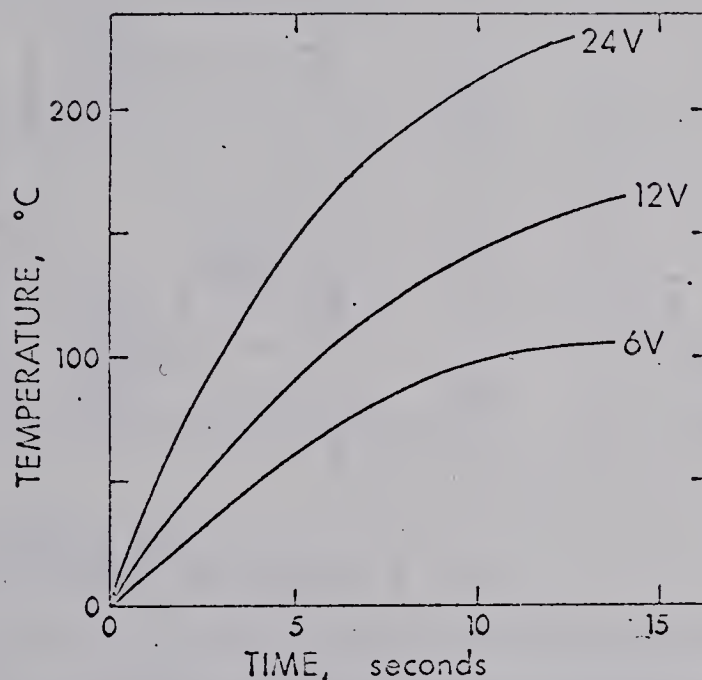


Figure A 1.03 Temperature-time relationship for direct electrical heating of a 1 meter 0.10" i.d. thin wall stainless steel tube as a function of the input voltage.

As can be seen in Figure A 1.03 the heating rate at about 200°C is 600°C per minute at the maximum voltage. This corresponds to a current of 30 amperes. As previously indicated a heating rate of 600°C per minute allows linear programming at 400°C per minute. Above 200°C a higher current capacity power supply would be required to give the heating rate necessary for linear programming at 400°C per minute.



Transformers used were 6V, 30 amp output with the primary line fused for 5 amps and individually switched so that the output voltage was variable in 6 volt increments from 6 to 24 VAC.

A wiring schematic for the high current capacity (30 amp) SCR bank developed for use in conjunction with the modified programmer and the low voltage power supply is given in Figure A 1.04. The small signal required to control the SCR bank, in the order of a few milliamps, represents the only load the programmer need accommodate.

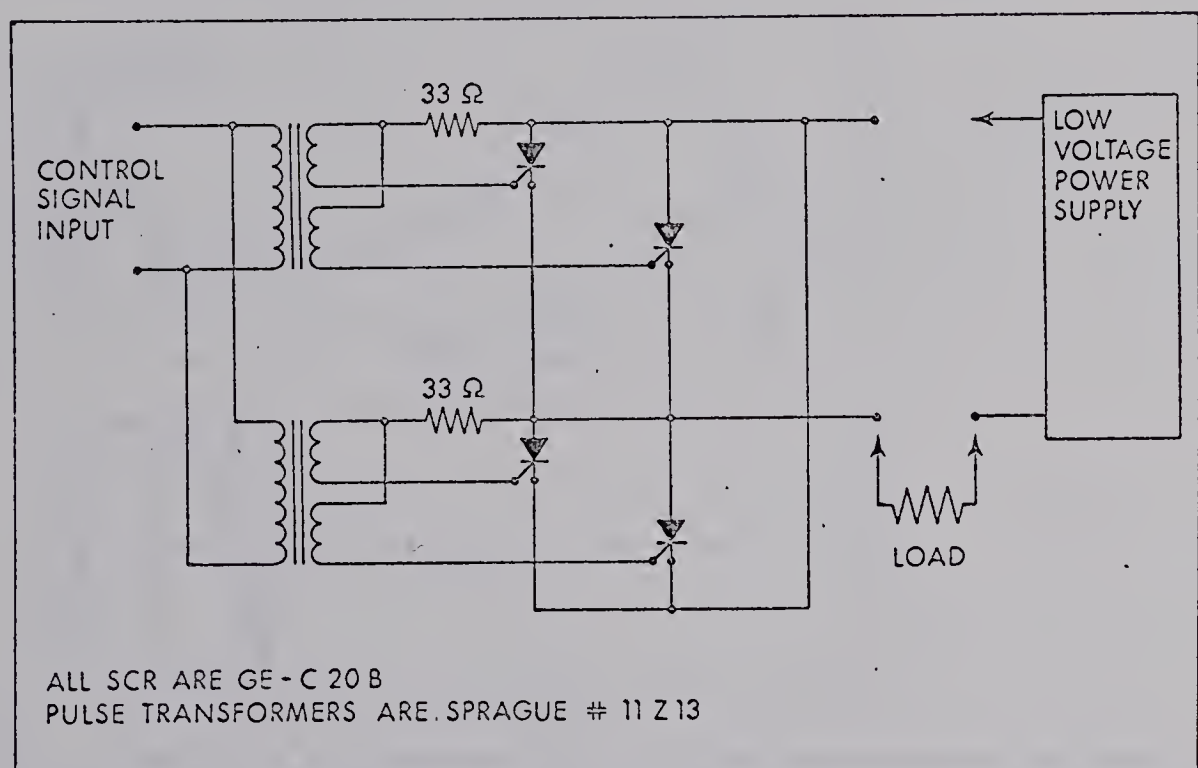


Figure A 1.04 Schematic diagram of high current capacity (30 amp) silicon controlled rectifier bank.

The two thermocouples required by the programmer must not be in electrical contact. The indicating thermocouple was electrically insulated from the column by one layer of Teflon pipe-thread-sealing tape and the controlling thermocouple was placed in direct contact with the metal column. During programming, even at the highest rate, there was no observable difference in temperature (i.e., less than about 5 degrees) between the insulated thermocouple and a third reference thermocouple attached directly to the metal column. One would expect no difference except for the thermal lag between the insulated thermocouple and the other in direct contact.



The linearity of the temperature program was experimentally checked by recording a thermocouple temperature during the program. The linearity was excellent as revealed in a detailed examination of the original recorder trace shown in reduced size in Figure A 1.05 (A). The uniformity of temperature along the column was also examined. This was accomplished by monitoring during a temperature program between two thermocouples connected in electrical opposition and placed at various positions along the column. This is shown in Figure A 1.05 (B) for a program rate of 400°C per minute. Temperature differences were less than 0.5°C.

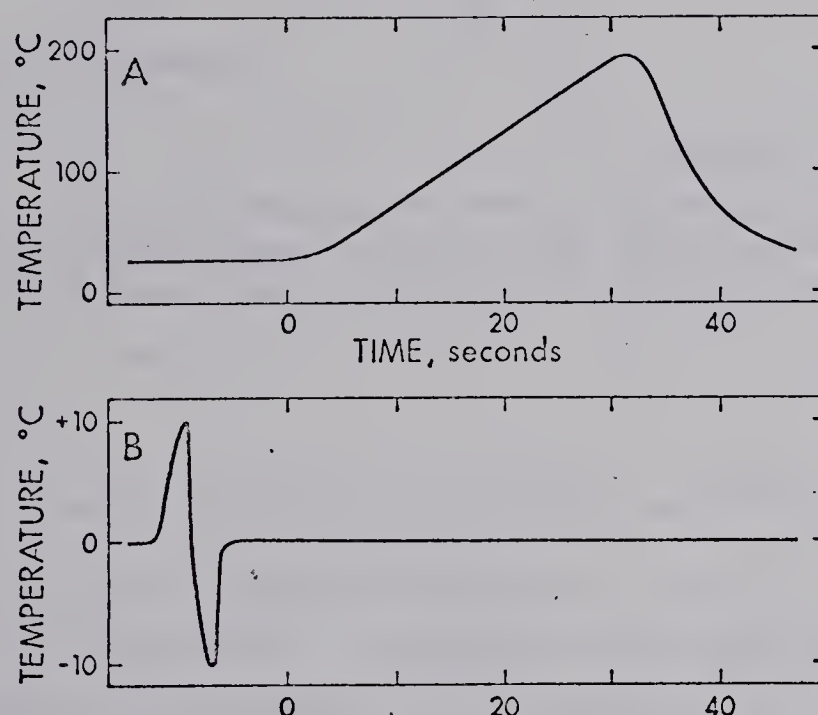


Figure A 1.05 Linearity of program rate (A) and temperature uniformity (B) during temperature programming at 400°C per minute using direct electrical heating. Temperatures recorded from thermocouples directly attached to column. Program initiation at time zero.

#### Modification for Rate Selection

The Aerograph Model 326 programmer provides switch selection of program rates from 2 to 40°C per minute in nine steps. An auxiliary switch position and input jack are also provided for accommodation of other rates. These rates are determined by the resistance provided at the jack. A continuously variable resistance provides a complete choice of program rates. The device shown in Figure A 1.06 A incorporates



both a continuously variable resistance of a switch selectable auxiliary fixed resistance position. The program rate as a function of the resistance is shown in Figure A 1.06 B.

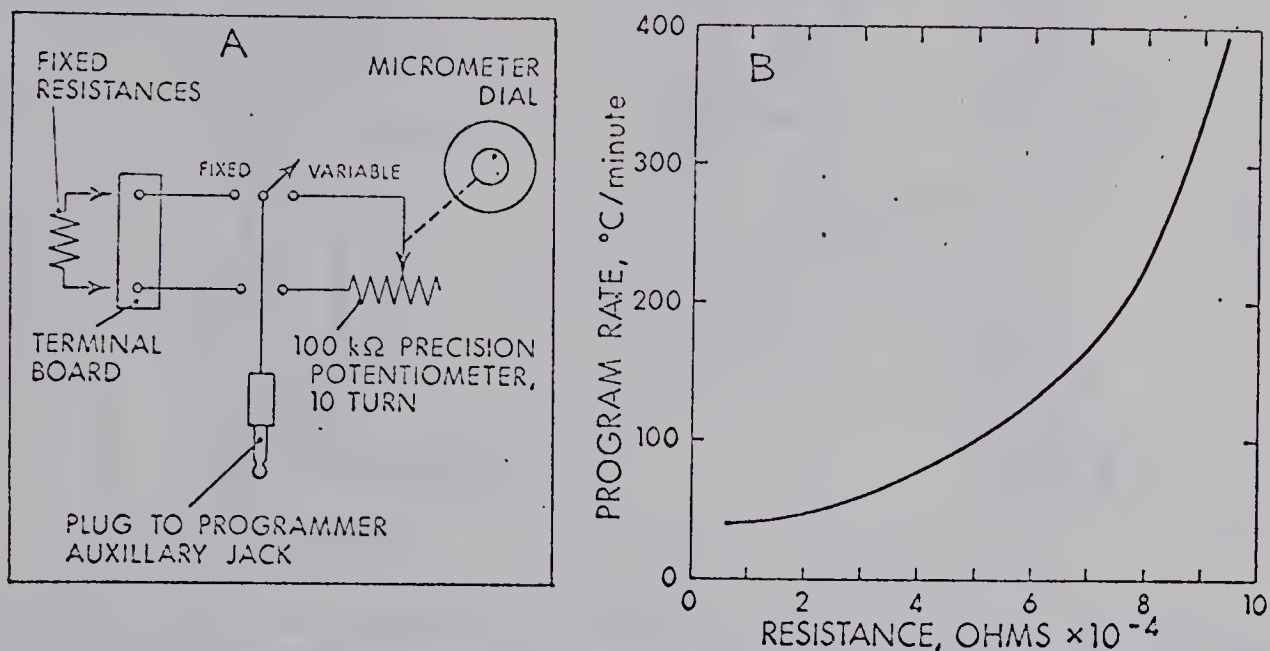


Figure A 1.06 Rate determining resistance system (A) and program rate as a function of the controlling resistance (B) for the Aerograph Model 326 Linear Temperature Programmer using direct electrical column heating.

#### Remote Program Initiation and Event Marking

As the program rate increases the total program (or analysis) time decreases. Assuming a constant error in time associated with initiation of the program the error becomes an increasing percent of the total program time at the high program rates and must be reduced to a minimum. The error in establishing the program initiation time was reduced to a minimum by the installation of an externally actuated switching relay in the programmer. Mounted on the injection tee at the head of the chromatographic column were two micro switches, Figure A 1.07. As a sample was injected into the column a rod parallel to the syringe plunger closed the switches activating the relay to initiate the program and giving an even mark on the recorder. The installation of the switching relay is shown in detail in Figure A 1.08. Thus the operation of injecting the sample also started the program and gave an indication that the program was initiated.



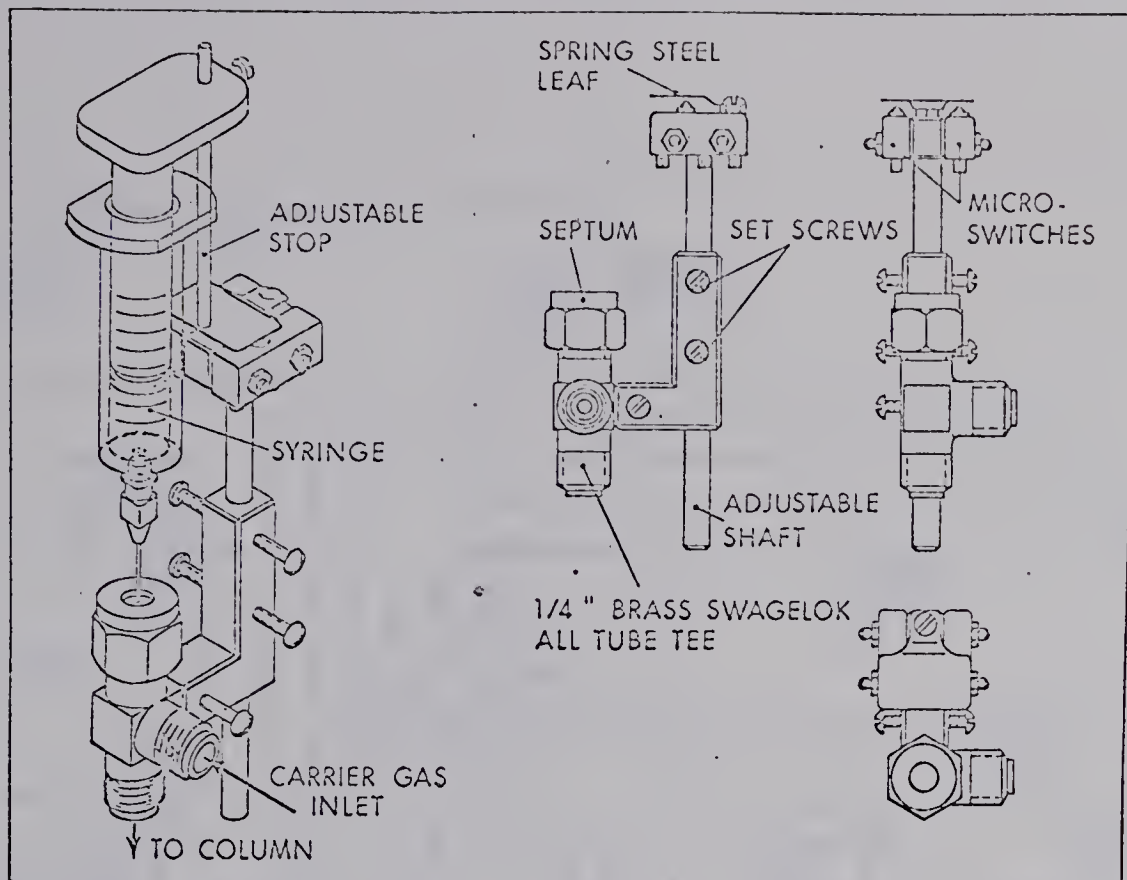


Figure A 1.07 External switch arrangement on injection tee for program initiation and event marking. Switches are Microswitch # 11 SM 1, Micro Switch, Freeport, Illinois.

#### Fast Re-equilibration at the Initial Temperature

The return of a heated column to a lower temperature, such as may be required for initial temperature of the next chromatographic determination, can limit its utility. Low heat capacity favors a high rate of temperature decrease which can be further enhanced by introduction of a cooling medium.

The use of direct electrical heating of the column and careful control of the heating rate allows a novel cooling procedure to be used. Immersion of the column in an oil bath at some temperature lower than the initial temperature of the program allows cooling rates comparable to the heating rates. The Aerograph Model 326 programmer provides for control of the initial as well as the final temperature of the program. Immersion of a column in light oil at 10°C provides cooling from 225°C to 25°C in about 25 seconds when the oil is vigorously stirred. This is net cooling rate in excess of 400° per minute. The lower "ambient" temperature of the column



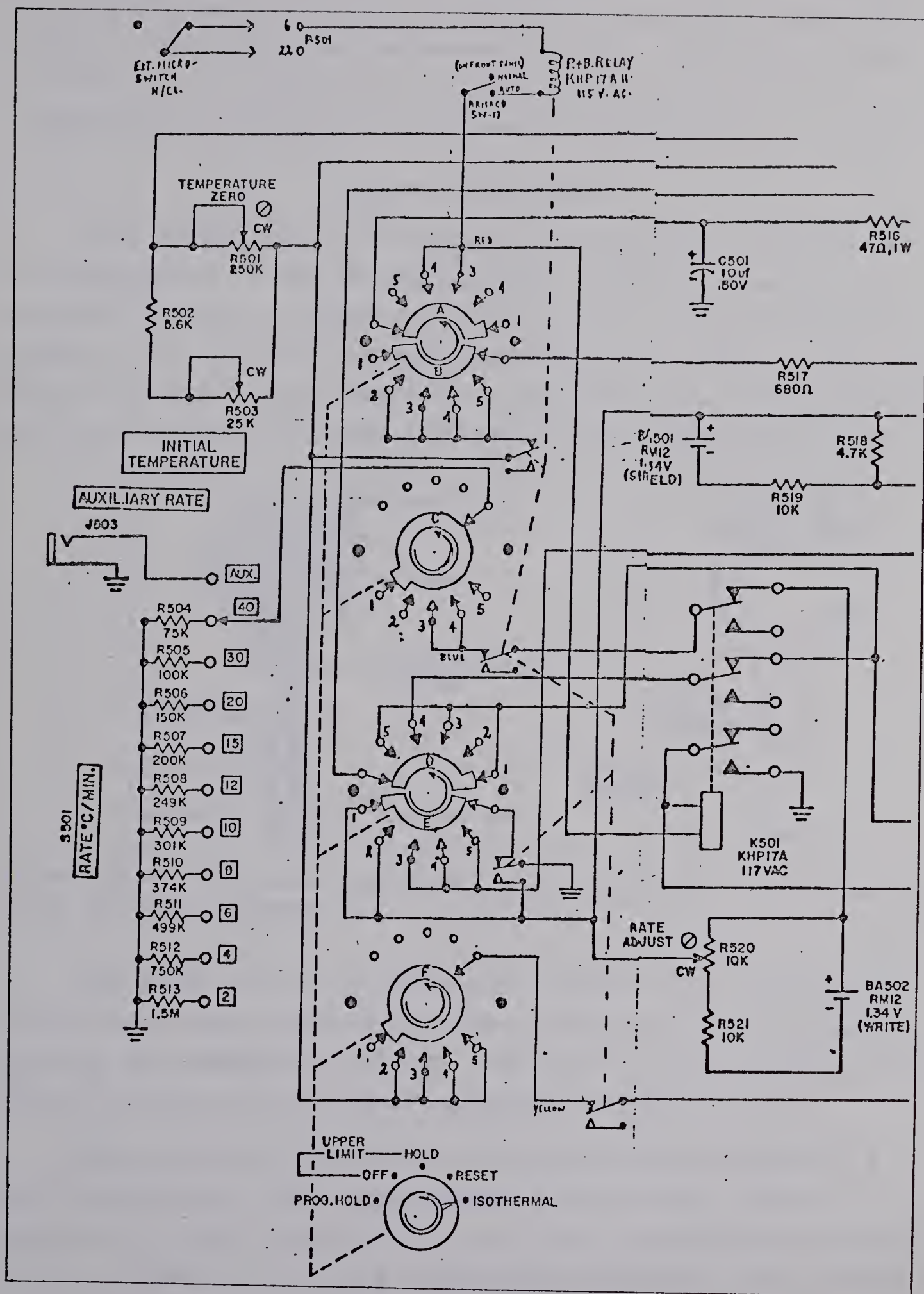


Figure A 1.08 Schematic of Aerograph Linear Temperature Programmer Model 326 with modifications for external program initiation.



did not affect the achievable program rate or the linearity of the program if the oil is quiescent during the heating phase. This technique overcomes the slow exponential return of the column temperature to the initial temperature is approximately equal to the ambient temperature.

### Column Connections

The column was electrically and thermally insulated from the remainder of the chromatographic system by the use of plastic inserts as shown in Figure A 1.09. Polyethylene was found to be suitable for temperatures below 230°C. Teflon was also used but did not maintain a gas tight seal presumably due to its plastic flow under pressure at the temperature used.

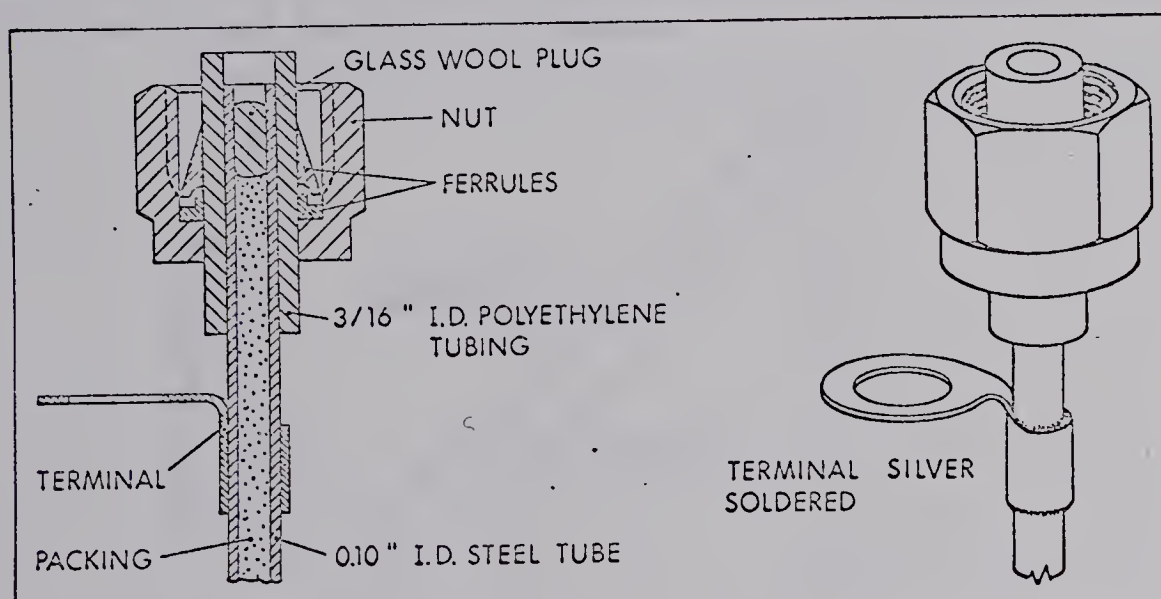


Figure A 1.09 Gas tight electrically insulating connections for use with direct electrical heating.

The flame ionization detector proved to be sensitive to induced voltages necessitating the grounding of the detector housing and connecting tubing. The type of noise produced by induced electrical currents is shown in Figure A 1.10.

The internal pyrometer for the programmer indicated a lower temperature than that measured using other thermocouples or, when immersed in an oil bath, a calibrated thermometer. Figure A 1.11 is a calibration chart for the initial temperature control of the programmer and, since both the internal pyrometer and calibrated thermometer temperatures are shown, can be used as a correction curve.



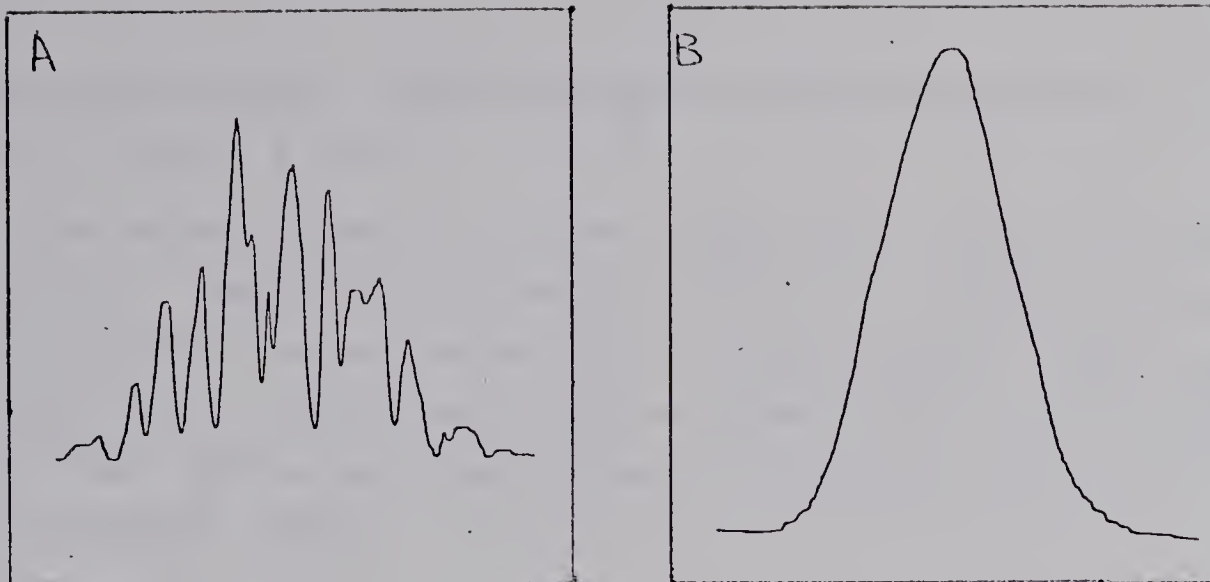


Figure A 1.10 Noise in F.I.D. detection using direct electrical heating. Shown with the detector housing ungrounded (A) and grounded (B). Both runs isothermal at 100°C maintained by direct electrical heating. The sample was 5.0  $\mu$ l of CH<sub>4</sub> at maximum electrometer sensitivity and a recorder alteration of 10X. The Chart speed was 1.0" per minute.

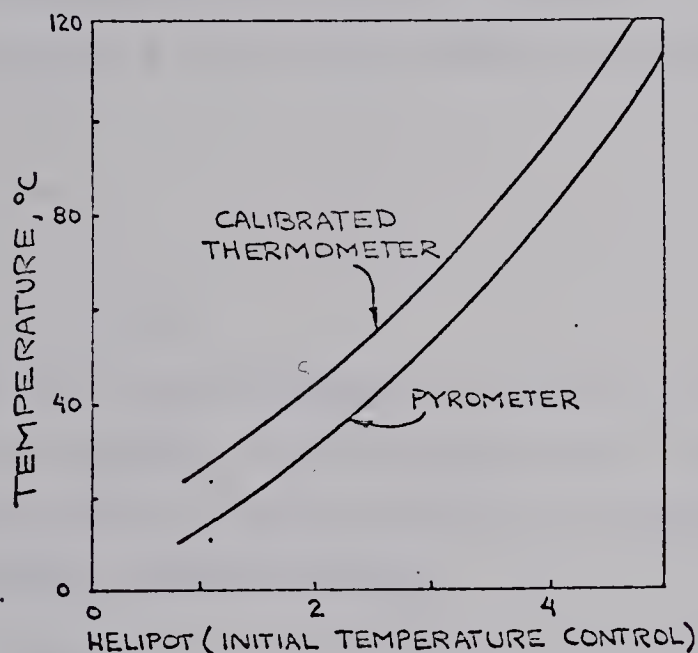


Figure A 1.11 Calibration for initial temperature control and internal pyrometer correction for Aerograph Linear Temperature Programmer Model 326.

## Recorder

The basic recorder used was the Sargent Model SR, S-72180-20, E. H. Sargent and Co., Chicago, Illinois, equipped with an event marker S-72186-05. This event marker could be remotely triggered to indicate sample injection or



program initiation or both using the switching device shown in Figure A 1.07.

This recorder had a 1.0 mv range with a built in stepped attenuator. Three chart speeds of 0.2, 1.0, and 5.0 inches per minute were switch selectable. When greater chart speeds were required a second model SR recorder with a 12 inch per minute chart drive was used. These recorders have a 1.0 second response time.

#### Integrator

The digital integrator used was a Wilken Instrument & Research, Inc., Aerograph Model 471-42 manufactured by the Infotronics Corporation, Houston, Texas. It was equipped with remote starting which was done in parallel with recorder II in Figure 5.02.

#### Chemicals

##### Hydrocarbons, liquids.

Phillips Petroleum Company, Special Products Division, Bartlesville, Oklahoma was the source of liquid hydrocarbons. All were Pure Grade listed as 99 Mol % minimum and used without additional purification.

##### Hydrocarbon, gases.

Phillips Standard Hydrocarbon mixture 40 was used to approximate lower hydrocarbon pyrolysate. Analysis for Lot 16 was as follows:



Component	Weight Percent	Mol Percent
Ethane	2.78	4.70
Propane	14.89	17.16
Propylene	16.07	19.40
Isobutane	19.53	17.08
Isobutylene	15.18	13.75
n-Butane	6.84	5.08
Butadiene-1,3	0.02	0.02
Butene-1	9.85	8.92
trans Butene-2	11.81	10.69
cis Butene-2	0.69	0.62
Isopentane	1.14	0.80
n-Pentane	Tr	Tr
trans-Pentene-2	0.27	0.43
cis-pentene-2	0.33	0.24
2-Methylbutene-2	Tr	Tr
Ethylene	0.01	0.02

#### Thermocouple readout

API Instruments Co., Chesterland, Ohio, indicating pyrometer Model    was mounted with six switch selectable thermocouples. All temperatures not requiring continuous recording were determined with this arrangement. Where oil baths were used a calibrated thermometer was also employed.

#### Syringe pump.

Slow sample injection was achieved using a Sage Model 234 syringe pump, Sage Instrument, Inc., White Plains, New York, with a variety of Hamilton gas tight syringes.

#### Sample Storage

Samples of pure liquid hydrocarbons or mixtures were stored in inverted 25 ml Erlenmeyer flasks stoppered with serum stoppers and sealed with mercury. Samples of either liquid or vapor



were removed by syringe through the stopper minimizing loss and change of composition. All mixtures made and reported on a weight scale.

#### Stationary phase.

Chromatographic stationary phases were obtained from F & M Scientific Corporation, Avondale, Pa. Those used were Silicone Fluid-Methyl SF-96. (LP 110), silicon oil DC-200 (LP126), and Silicone rubber GE-SE30 (LP-118).

#### Solid Supports.

The solid supports used were Chromosorb P., acid washed, and Chromosorb W. HMDS treated 45/60 mesh manufactured by Johns-Manville Products Corp., Celite Division and supplied through Chromatographic Specialties, Brockville, Ontario.

#### Column Tubing.

The tube used for the preparation of the columns was of 0.125 inch O.D., 0.10 inch I.D. stainless steel. The supplier was Superior Tube Co., Norristown, Pa., U. S. A.



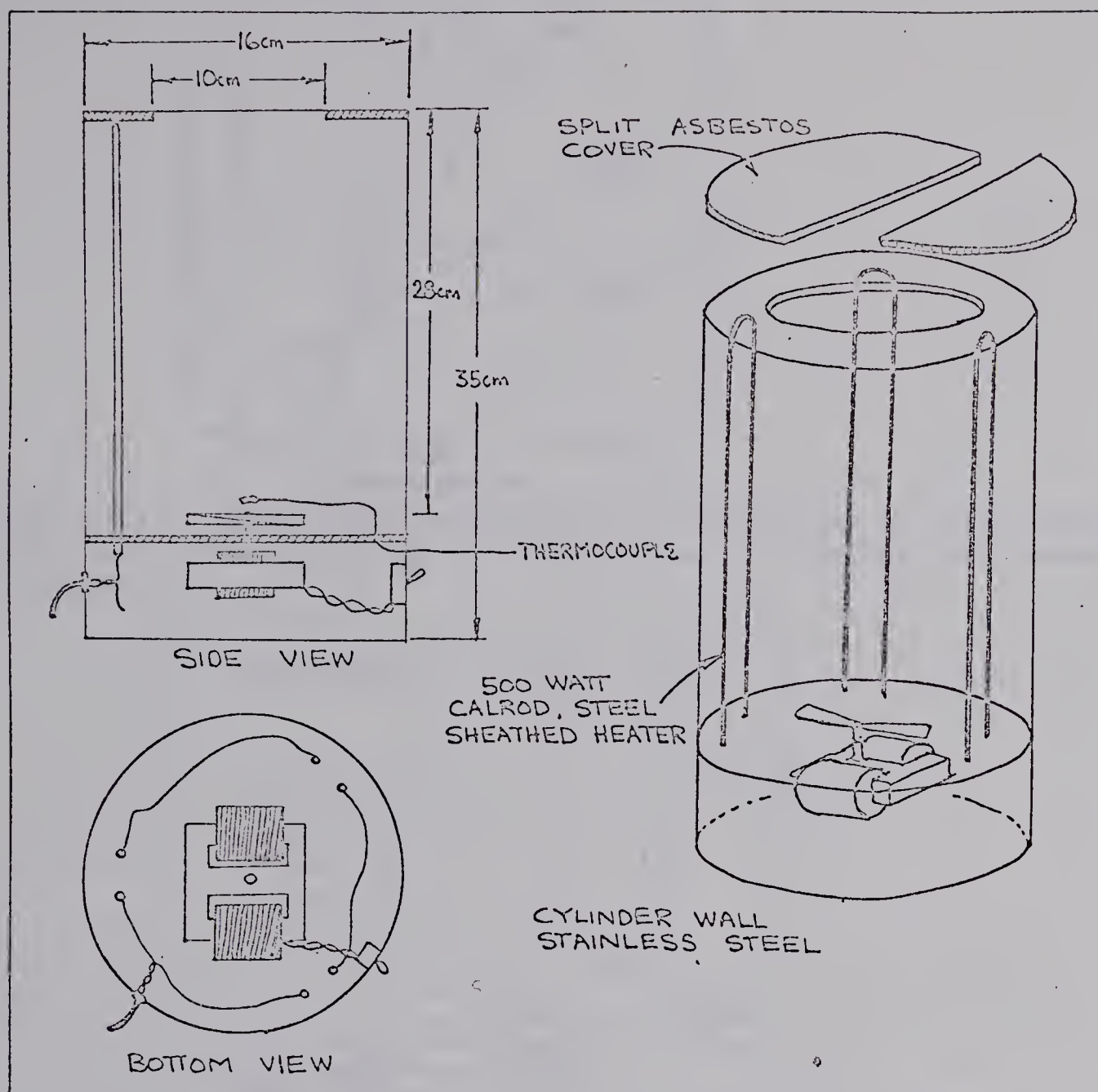


Figure A 1.12 Air bath for coiled columns. Used for isothermal determinations above 150°C and programmable at rates up to about 40°C per minute. Calrod heaters available from Central Scientific Company, Chicago, Illinois, Catalog No. 16S63-1.

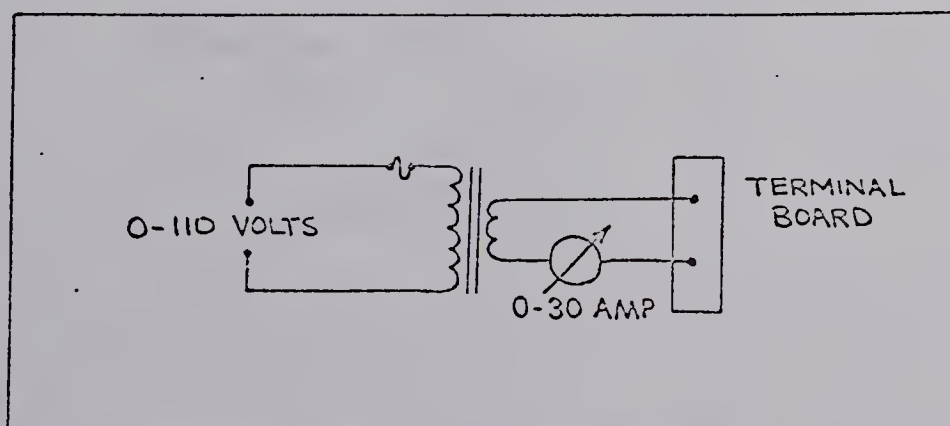


Figure A 1.14 Power supply 0-30 VAC, 0-S amp, for rapid heating of trapping column.



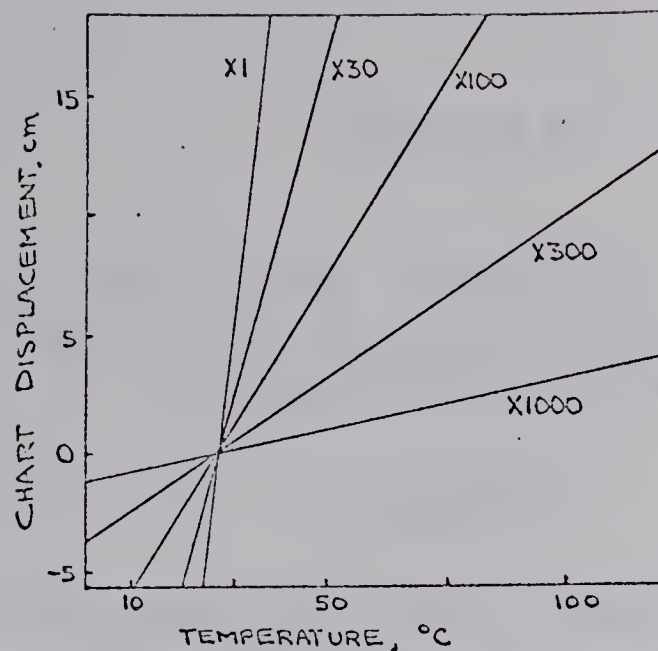


Figure A 1.13 Calibration for Sargent SR recorder for 10 iron-constantin thermocouple. Temperature vs chart displacement with recorder attenuation as a parameter.

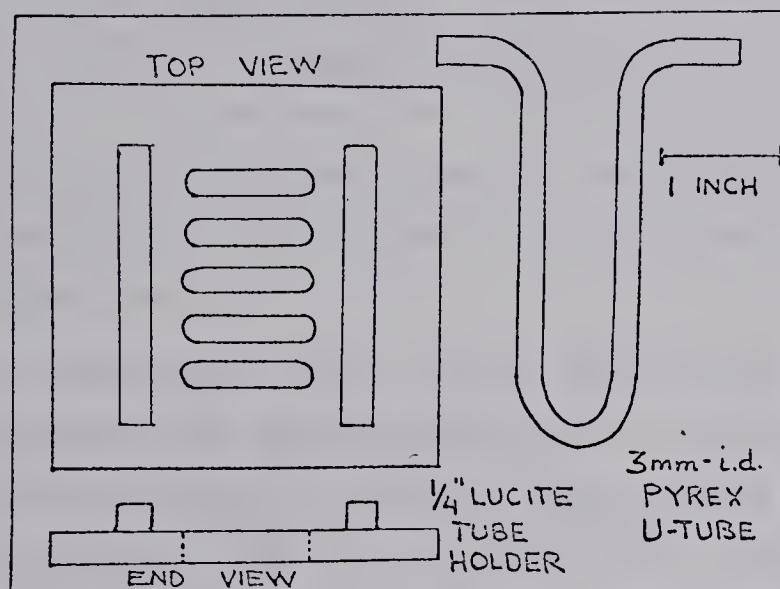


Figure A 1.15 Trapping U-tubes for gas chromatographic effluents.

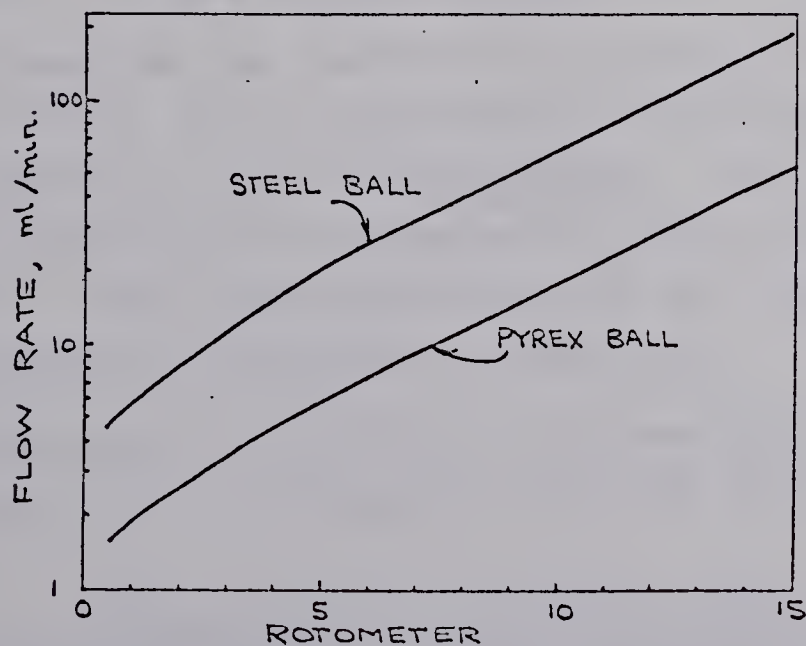


Figure A 1.16 Rotometer calibration for helium. Upper line of each pair for steel ball, lower for pyrex. Solid lines for 1 m conventional column, broken line for 1 m open tubular column. Calibrated with 10 or 50 ml soap-film flowmeter corrected to 20°C Rotometer was a Matheson model 642 B with a no. 600 tube.



## APPENDIX II

### A REVIEW OF PLATE HEIGHT, RESOLUTION AND OTHER INDICES FOR THE CHARACTERIZATION OF THE EFFECTIVENESS OF A GAS CHROMATOGRAPHIC COLUMN

#### Historical

Martin and Synge (71) first suggested the possibility of using a gaseous mobile phase in chromatographic separations. In their paper they described a theory of chromatography in which plate height was an integral part. In this work plate height, or height equivalent to one theoretical plate (HETP), was defined as "the thickness of a layer such that the solution issuing from it is in equilibrium with the mean concentration of solute in the non-mobile phase throughout the layer."

James and Martin (49) first described the use of a fully developed gas chromatographic technique and also employed the concept of plate height using it as an index of column efficiency. This was the first suggestion that the terms column efficiency and plate height could be used interchangeably in gas chromatography.

A committee on nomenclature sponsored by the Hydrocarbon Research Group of the Institute of Petroleum, London, 1956, (17) introduced the term resolution. They recommended "That column resolution be expressed in terms of theoretical plate numbers". This unfortunate use of the term resolution was acknowledged as incorrect in 1958 (52).

Resolution as currently used was first suggested by Ellerington (23) although he referred to it as a separation number

". . . definition of a number I have chosen to call a separation number by means of which one can see at once whether two peaks are completely separated or not.



$$\frac{T_2 - T_1}{\frac{1}{2}(t_1 + t_2)} "$$

A Committee on Nomenclature Recommendations (16) published in the same volume as Ellerington the following:

"The committee considered ways in which resolution might be defined, and suggest as an obvious way of expressing column resolution the formula

$$\frac{2\Delta y}{y_a + y_b}$$

where  $\Delta y$  is the distance between the peak maxima, and  $y_a$  and  $y_b$  are the intercepts cut on the base line by the tangents to the two peaks (determined where necessary by making two separate runs)."

The terms column performance, theoretical plate number, and peak resolution were used in the "Recommendations on Nomenclature and Presentation of Data in Gas Chromatography: of the International Union of Pure and Applied Chemistry (IUPAC) published in 1964 (82).

"Column Performance - An expression of column performance in terms of theoretical plate number  $n$  can be calculated by the equation

$$n = 16 \times \left( \frac{\text{retention volume}}{\text{peak width}} \right)^2$$

The theoretical plate number may vary with the compound as well as the column. Therefore the compound used should be specified. The units for retention and peak width used in (the) equation must be consistent so that their ratio  $n$  is dimensionless."

"Peak Resolution - If two compounds are well enough separated to permit a satisfactory estimation of the peak width, and the peaks are approximately Gaussian, as shown in (the) figure, the resolution may be expressed by

$$\text{Resolution} = 2 \times \frac{\text{difference between retention volumes}}{\text{sum of peak widths}}$$



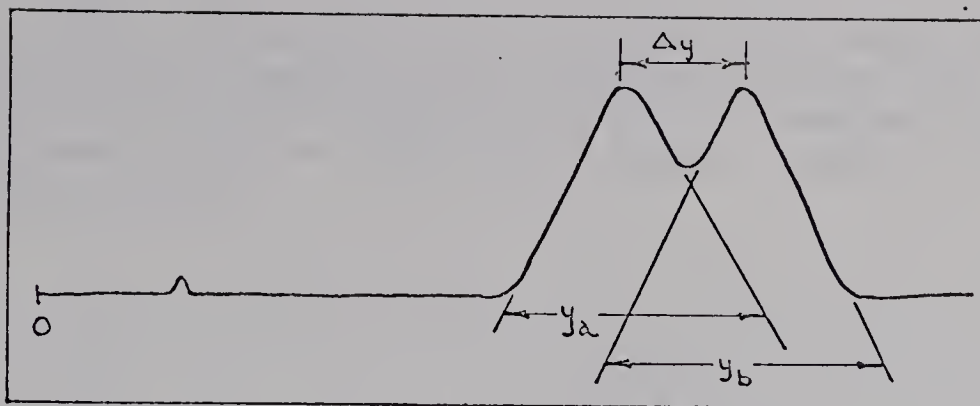


Figure A 2.01 Idealized chromatogram from IUPAC recommendations (82).

The figure, shown here as reproduced directly from the publication, is incorrect. The peak widths should be the distances on the extrapolated base line between the tangent intercepts on either side of the peaks. In the IUPAC figure the base widths were not shown on the base line but as some indeterminate distance below it. The 1964 recommendation on nomenclature of the IUPAC does not include the term column efficiency but incorporates column performance for essentially the same index.

Column performance also appears in the English translation of the works of Kaiser (55) but is related to column efficiency as used by James and Martin rather than the IUPAC usage of performance.

"The column performance is defined as the number of theoretical plates in 1 m of the column.

$$n' = \frac{n_{\text{total}}}{L}$$

$n_{\text{total}}$  = number of theoretical plates in the column

$L$  = length of the column in m . . . " (55)

Resolution also appears in the translation of Kaiser's book to a different evaluation of peak separation.

"The resolution of a pair of substances is best defined as the extent to which the peaks of two substances overlap.



This definition has an advantage over the one used in the English and American literature, in that here the maximum resolution is 1.0 and can only be achieved with an infinitely great number of theoretical plates."

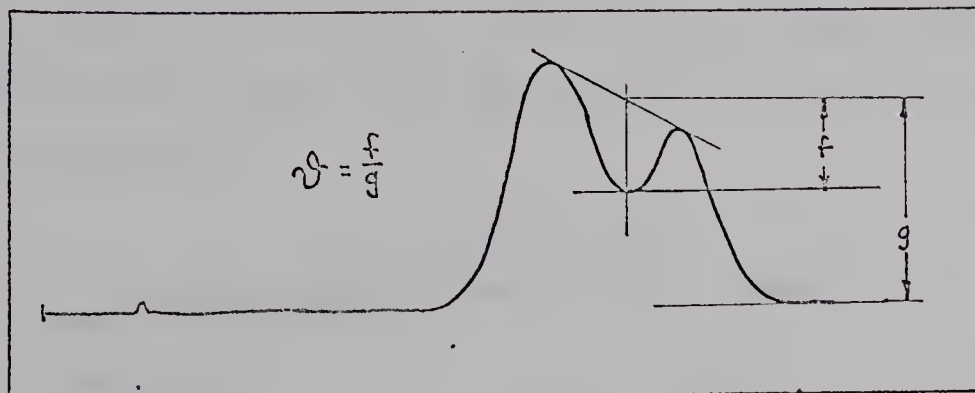


Figure A 2.02 Idealized chromatogram illustrating resolution as defined by Kaiser (55).

Dal Nogare and Juvet (15A) adopted the expression of Golay (14A) for resolution in their 1962 book Gas-Liquid Chromatography.

$$R = \frac{4(x_2 - x_1)}{y_2}$$

where  $x$  is the retention time and  $y$  the peak base width. This definition has not been widely adopted.

#### Relative Peak Separation and Peak Sharpness

Jones and Kieselbach (52A) proposed new units for simplifying the recording and interpretation of experimental data and quantitatively characterizing the degree of resolution.

The degree to which two chromatographic peaks are separated was to be defined by the relative peak separation,  $S_{12}$ . The relative peak separation, which is essentially independent of column length, was defined as the ratio of the difference in the two elution times,  $t_2 - t_1$ , to the elution time of the first peak,  $t_1$ :

$$S_{12} = \frac{t_2 - t_1}{t_1} \quad (A2.01)$$



Characterization of a single peak could be accomplished by comparison to the air peak:

$$S_{ax} = \frac{t_x - t_a}{t_a} \quad (\text{A2.02})$$

A compilation of values of  $S_{ax}$  for various compounds on a column packing would allow the calculation of relative separation of any pair:

$$S_{12} = \frac{S_{a2} - S_{a1}}{S_{a1} + 1} \quad (\text{A2.03})$$

Since  $S_{12}$  is independent of the column length,  $L$ , the ratio of elution times remains constant as the column length is increased. This is shown in Figure A2.03 where the column length has been doubled.

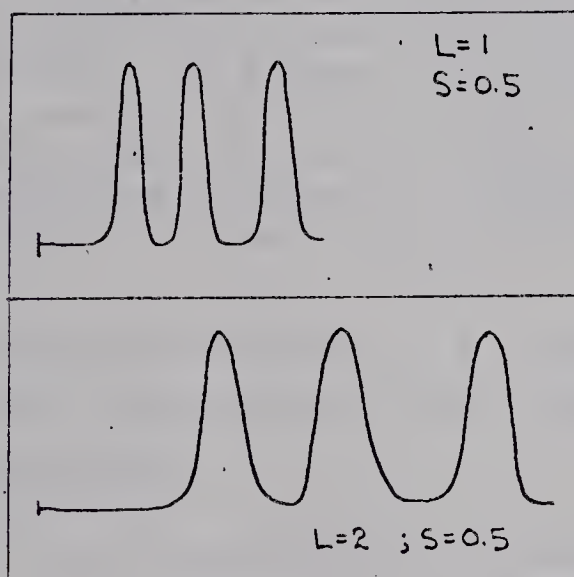


Figure A 2.03 Effect of column on relative peak separation, hypothetical chromatograms. After Jones and Kieselbach (52A).

As shown in Figure A2.03 an increase in column length, while not affecting the relative peak separation, improves the peak resolution by increasing the relative peak sharpness. Relative peak sharpness,  $Q$ , was defined by Jones and Kieselbach as the ratio of elution time,  $t_1$ , to the time base width,



W, of the peak:

$$Q = \frac{t_x}{W} \quad (\text{A2.04})$$

The number of theoretical plates,  $n$ , is related to the relative peak sharpness,  $Q$ , as in the following expression:

$$n = 16 Q^2 \quad (\text{A2.05})$$

Jones and Kieselbach pointed out three distinct advantages of using the relative peak sharpness as an index of column "efficiency".

"First, the degree of resolution between two chromatographic peaks is linearly proportional to  $Q$ , while proportional to the square root of  $n$ . Thus it is easier to apply and to create a clear mental picture of quantitative significance of  $Q$  than  $n$ . Second, the value of  $Q$  is more easily and directly measured than that of  $n$ . Third, the number of theoretical plates is a theoretical concept relating to an idealized mode of column operation, while  $Q$  is a direct measure of the quantity of practical interest, irrespective of any theoretical mode of column operation."

Figure A2.04 shows the effect of a change in relative peak sharpness on the resolution of two peaks of constant relative peak separation.

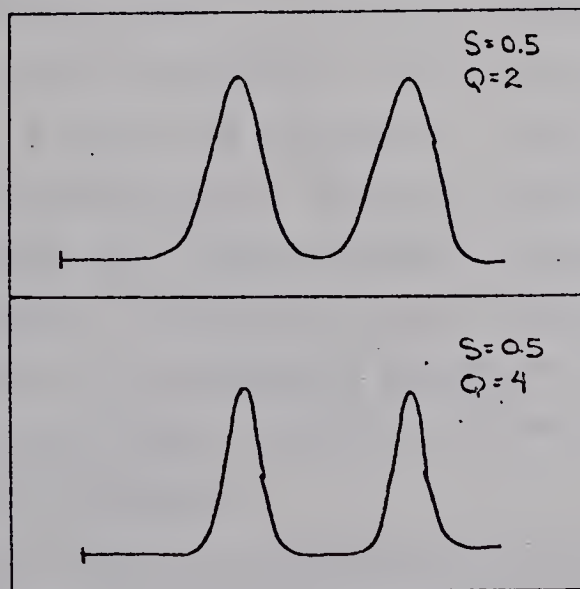


Figure A 2.04 Effect of relative peak sharpness of resolution.



Resolution, in the system of Jones and Kieselbach, was defined as the product of the relative peak separation,  $S_{12}$ , and the relative peak sharpness:

$$R = QS_{12} \quad (A2.06)$$

From which peak the value of  $Q$  was to be obtained was not specified and presumably it could be either  $Q_1$ ,  $Q_2$ , or  $Q_{av}$ . The conventional expression for resolution is

$$R = \frac{2(t_2 - t_1)}{W_1 + W_2} \quad (A2.07)$$

Resolution as defined by Equations (A2.06) and (A2.07) is the same if  $Q$  and  $S$  are more explicitly defined as

$$Q = \frac{t_1 + t_2}{W_1 + W_2} \quad \text{or} \quad \left(\frac{t}{W}\right) \text{ average}$$

$$S = \frac{t_2 - t_1}{0.5(t_2 - t_1)} = \frac{t_2 - t_1}{t_{\text{average}}}$$

### Plate Height and Resolution

The use of the theoretical plate height as an experimental measure of column efficiency was discussed by Giddings (33A) in answer to the increasing criticism of its use. Since plate height is but one parameter characterizing only one aspect of the column-solute system Giddings did not maintain that plate height was the ultimate measure of column effectiveness. Further, since the equilibrium stages required by plate theory give a "misleading picture of column processes" Giddings abandoned the parent model but retained plate height as a characterizing parameter.

"We may regard  $H$  as an experimental parameter which measures peak spreading per unit length".

$$H = L/n \text{ (in units of length)}. \quad (A2.08)$$



That this (H) is a measure of peak spread per unit length is not obvious.

From the conventional definition of resolution, Equation 6.07, Giddings developed the equation

$$R = \frac{n}{16} \cdot \frac{\Delta\rho}{\rho} \quad (\text{A2.09})$$

where  $\rho$  is the ratio of the velocity of the peak component to the velocity of air and where  $\Delta\rho/\rho$  is called the relative velocity difference. Giddings then equated  $\sqrt{n}/16$  to the resolution per unit of relative velocity difference.

Relative velocity difference is fully equivalent to the isothermal intrinsic resolution developed by Fryer, Habgood, and Harris (28)

$$R = \frac{(\sqrt{n})_{av}}{4} \cdot \frac{\Delta V}{V_{av}} \quad (\text{A2.10})$$

where  $\Delta V/V_{av}$  is the isothermal intrinsic resolution.

In the development of resolution it was necessary to have the number of theoretical plates appear as a square root. If relative peak sharpness,  $Q$ , had been used rather than plate number Equations (A2.09) and (A2.10) would have been simplified to

$$R = Q \cdot \frac{\Delta\rho}{\rho} \quad (\text{A2.11})$$

and

$$R = Q \frac{\Delta V}{V_{av}} \quad (\text{A2.12})$$

Fryer, Habgood, and Harris (28) developed a similar expression for intrinsic resolution for use in programmed temperature gas chromatography (PTGC).

$$R = \frac{\sqrt{n}}{4} R_i \quad (\text{A2.13})$$



$R_i$  is intrinsic resolution and is given by the equation

$$R_i = \frac{F}{r} \frac{\Delta T_r}{\left(\dot{V}_{T_R}\right)_{av}} \quad (\text{A2.14})$$

with terms as explained in Section 3.01. Once again plate height appears as a square root, Equation (A2.13), because the peak spreading factor was defined in terms of theoretical plate numbers. Relative peak sharpness,  $Q$ , could have been employed to advantage and would have resulted in the simpler expression

$$R = QR_i \quad (\text{A2.15})$$

Graphical presentation of the term relative peak sharpness,  $Q$ , relative peak separation,  $S$ , plate height,  $H$ , and resolution,  $R$ , for a hypothetical system are given in Figure A2.05.

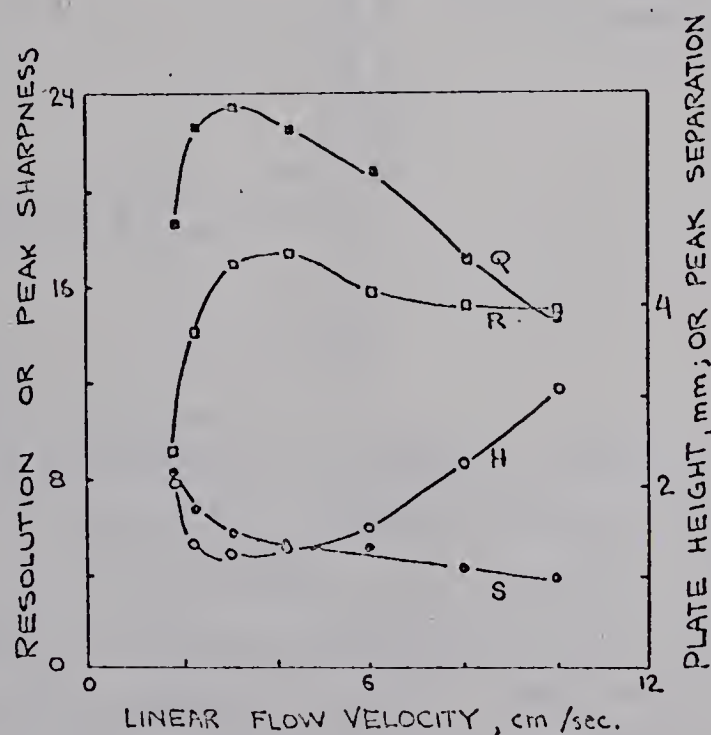


Figure A 2.05 Relative peak sharpness,  $Q$ , relative peak separation,  $S$ , plate height;  $H$ , and resolution,  $R$ , as functions of the carrier gas flow rate.  $Q$ ,  $S$ ,  $H$ , and  $R$  are defined by Equations (A2.04), (A2.01), (A2.08), and (A2.07).



Much of the theoretical work in gas chromatography has centered on the Van Deemter equation (99), the relationship expressed in this equation are often presented graphically as a plot of plate height vs carrier gas flow velocity or flow rate. Equivalent type of curve may be obtained by using the reciprocal of the peak sharpness,  $Q$ . This reciprocal of  $Q$  might be called simply the peak spread ( $Z$ ).

$$Z = 1/Q = W/V \quad (A2.16)$$

If the spread,  $Z$ , per unit length,  $L$ , is plotted against the flow rate a curve of the Van Deemter type is obtained, Figure A2.06.

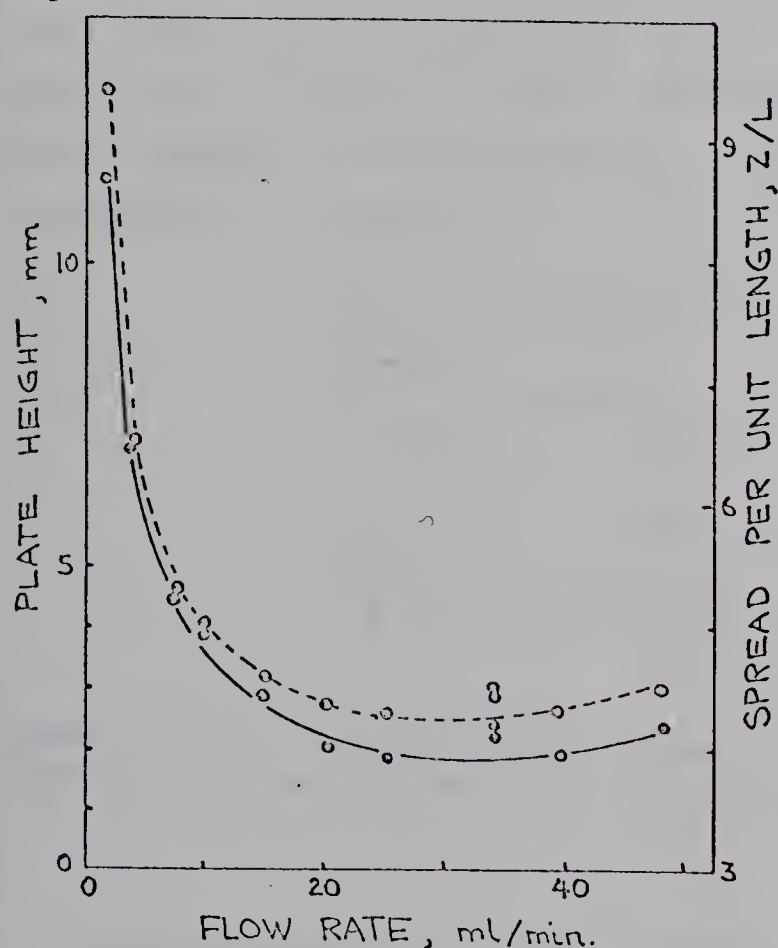


Figure A2.06 Spread per unit length (solid line) and plate height (dashed line) as functions of the carrier gas flow rate.

Some of the hesitancy to abandon plate height has resulted from the lack of a suitable equivalent index. The plot of spread per unit length,  $Z/L$ , against the flow rate, Figure A2.06, gives a curve amenable to the same mathematical analysis as the Van Deemter curve. The use of spread per unit length avoids the use of a parent theoretical model, is a measure of the chromatographic behavior of concern, and is simply calculated. The calculation of resolution as the product of  $Q$  and  $S$  simplifies the assignment of the relative importance of band spreading and separation. The use of  $H$  and



n can obscure the relative importance of these factors due primarily to the necessity of using the square root of n. Inspection of Figure A2.05 reveals immediately the direct interdependence of Q, S, and R. The use of Q and S should be encouraged.

The increase in the ratio  $V_{ds}/V$  for columns of increasing dead space per unit of stationary phase, capillary columns, causes a decrease in  $\Delta T_R / \left\{ V_{T_R} \right\}_{av}$  in PTGC. Hence intrinsic resolution, which is equal to  $(F/r) \left( \Delta T_R / V_{T_R} \right)_{av}$ , is less for capillary columns than for conventional columns. This is shown in Figure A2.07 for a conventional column of 5 ml dead space volume per gram of stationary phase and a capillary column of 500 ml per gram. Thus it is clear that plate height is not adequate as the sole index of the effectiveness of a column.

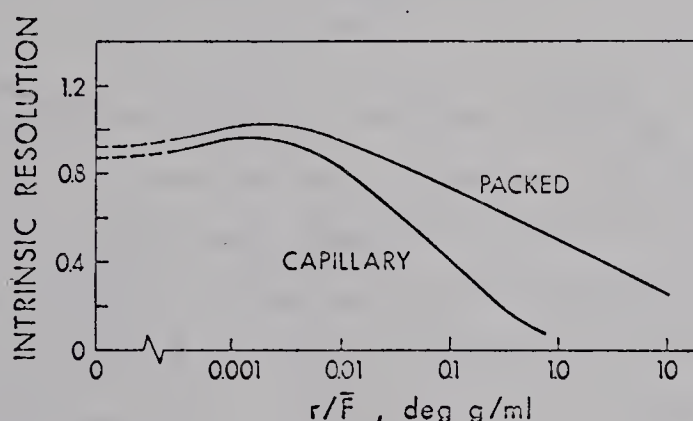


Figure A 2.07 Intrinsic resolution as a function of the ratio  $r/F$  for a conventional and a capillary column. From Habgood and Harris (37).

#### Inadequacies of Plate Height (or Number of Theoretical Plates) as the Sole Index of the Effectiveness of a Column

Glueckauf (33B) developed an expression designed to allow the calculation of the number of theoretical plates required to achieve any required degree of separation (in terms of fractional band impurity) as a function of a separation factor. The separation factor,  $\alpha$ , was the ratio of the retention volumes of the two components,  $V_{R_2}/V_{R_1}$ . Said(85)



examined the Glueckauf treatment and published a correction to the mathematical development.

The assumption implicit in the Glueckauf treatment is that adequate resolution may be obtained even with the differences in retention volumes approaching zero if a sufficiently large number of theoretical plates are available.

#### A Problem Arising From the Use of Plate Height With Capillary Columns

The formula for the calculation of the number of theoretical plates

$$n = 16 \left( \frac{V}{W} \right)^2 \quad (\text{A2.17})$$

may be rewritten

$$n = 16 \frac{V' + V_{ds}}{W}^2 \quad (\text{A2.18})$$

where  $V'$  is the net retention volume and  $V_{ds}$  is the dead space volume. In conventional columns the ratio  $V_{ds}/V'$  is usually orders of magnitude smaller than in capillary columns. The large plate numbers obtained with capillary columns may be, in part, attributed to the contribution of the dead space. Purnell (82B) pointed out that the large dead space contribution to plate numbers does not assist in achieving separations. Desty (17A) and Purnell (82A) suggested that the net retention volume,  $V'$ , be used to calculate the number of effective plates

$$n = 16 \left( \frac{V'}{W} \right)^2 \quad (\text{A2.19})$$

Halasz and Schreyer (37A) and Ettre (25) also discuss plate numbers with particular regard to capillary columns.

An examination of the effect of the proportion of stationary phase on plate height (or the number of theoretical plates) and resolution reveals that plate height cannot by itself be used as an index of the resolving power of a



column. Both plate height and resolution are functions of the proportion of stationary phase: Figure A2.08 illustrates how these factors vary with the proportion of stationary phase.

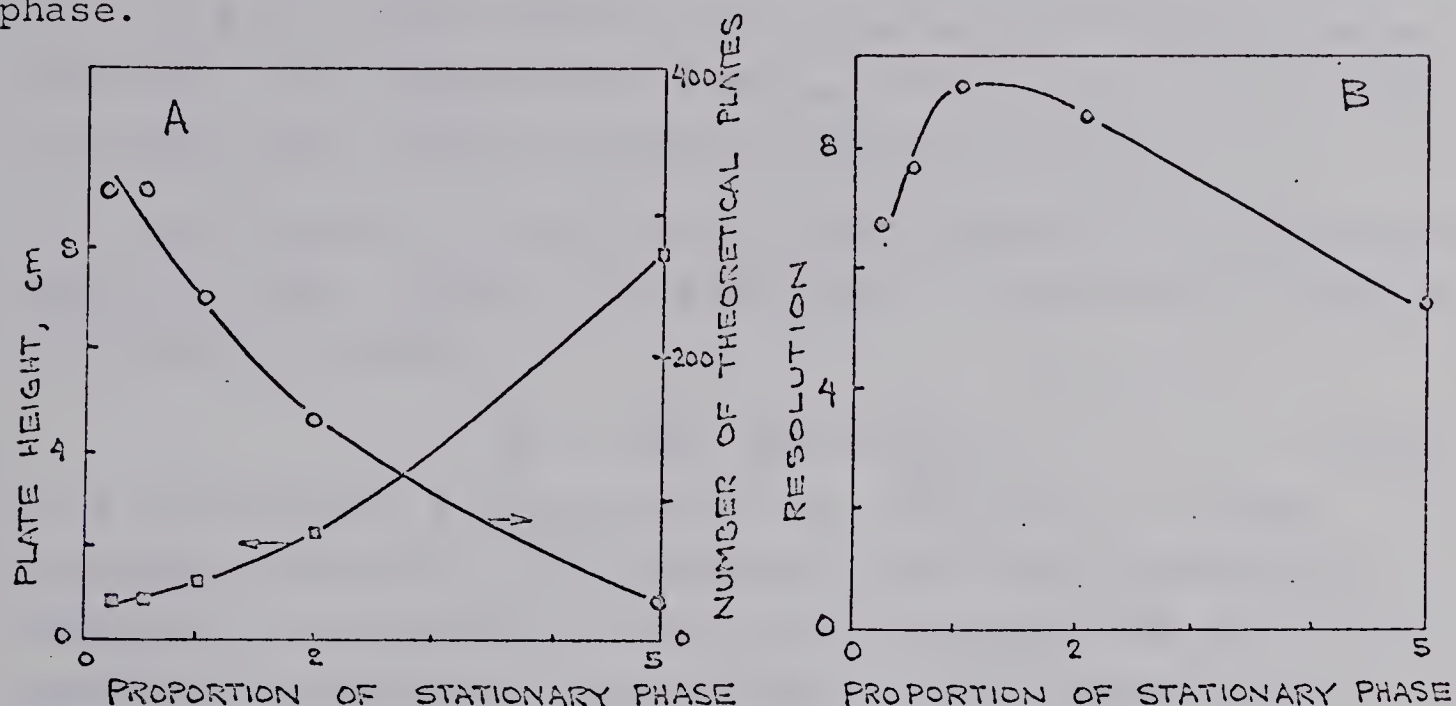


Figure A 2.08 The variation in plate height and the number of theoretical plates (A) and resolution (B) with the proportion of stationary phase. Determined using a 1 m low-pressure-drop packed column as described in Section 2.01, SF-96 as a liquid phase and n-pentane of n-heptane as samples.

Although the number of theoretical plates continues to increase as the proportion of stationary phase decrease as shown in Figure A2.08 resolution passes through a maximum and then decreases with the proportion of stationary phase. At low proportions of stationary phase the intrinsic resolution (or relative velocity difference) approaches zero and therefore resolution must also approach zero.

#### Time as a Variable in Obtaining Performance Indices For Comparing Columns

Frederick, Miranda, and Cooke (26A) in discussing the difficulty of intercomparing columns states "It is insufficient and misleading to compare two different columns by operating both under conditions of equal temperature, partial size of solid support, liquid loading, and carrier gas velocity." They further stated "It is impossible to compare the ultimate, relative efficiencies of two columns if the



elution times are markedly different". Prefaced by these statements these authors introduced the concept of time normalization.

In time normalization they adjusted the temperature so that the last component of a mixture will elute at the same time with each column or column parameter change.

Examination of the Purnell (82A) equation for resolution, Equation 6.22, reveals the importance of considering time as a critical variable.

$$R = \frac{\sqrt{n}}{4} \left( \frac{\alpha-1}{\alpha} \right) \left( \frac{k_2}{k_2+1} \right) \quad (\text{A2.20})$$

In this equation  $k$  is the partition ratio and  $\alpha$  is the relative volatility. In isothermal work with fixed chromatographic parameters  $\alpha$  and  $k$  are constants and as a consequence resolution is proportional to the square root of the number of theoretical plates. With time normalization both  $\alpha$  and  $k$  influence resolution as, for example, in the use of a shorter column where (even though the  $n$  is decreased) the temperature can be lowered to such an extent that the increase in  $\alpha$  and  $k$  will result in better resolution. As a consequence predictions from isothermal data relating changes in column parameters to resolution are not necessarily valid.

The concept of time normalization has been further developed and applied by Karger and Cooke (58, 58A, 58B) and applied to minimum time analysis by Guiochon (35A).

### Summary

The concept of theoretical plate number or plate height has been recognized as misleading if used in an attempt to understand fundamental processes in gas chromatography (33A). Relative peak sharpness is a more direct index of column effectiveness and its use results in simpler mathematical expressions for resolution. Characterization of a column



requires indices for both the factor describing peak spreading and for component separation. Time should be considered an important variable when indices of column effectiveness are being evaluated.

Adoption of new indices of column effectiveness such as relative peak separation,  $S$ , relative peak sharpness,  $Q$ , and peak spread per unit of column length,  $Z/L$ , would have distinct advantages and is recommended.



### APPENDIX III

The following references were obtained by surveying the abstracts issued between September 1, 1966 and March 31, 1967 by the Gas Chromatography Abstracting Service, Preston Technical Abstract Co., Evanston, Illinois. All papers have some reference to pyrolysis used in conjunction with gas chromatography.

1. Anon., Pyrolysis and Reaction Gas Chromatography Symposium, Ecole Polytechnique, Paris, Sept., 1966.
2. Anon., Lab Practice 15, 1017 (1966).
3. Berry, J. W., Advances in Chromatography, Vol. 2, Giddings, J. C., Keller, R. A., eds., Marcel Dekker, Inc. New York, 1966. pp. 271-291.
4. van Binst, G., Dewaersegger, L., Martin, R. H., J. Chromatog. 25, 15 (1966).
5. Burke, M. F., Dissertation Abstracts 26, No. 11:6337 (1966).
6. Curry, A. S., Belgian Assoc. of Chromatographic Symposium III (1964). pp. 19-60.
7. Deur-Siftar, D., Bistricki, T., Tandi, T., J. Chromatog. 24, 404 (1966).
8. Downing, D. T., Anal. Chem. 39, 218 (1967).
9. Drrienovskiy, P., Coll. Czech. Chem. Commun. 31, 2278 (1966).
10. Durdovich, V., Chem. Zvesti 20, 611 (1966).
11. Elsworth, R. K., Perkin, H. J., Anal. Biochem. 17, 521 (1966).
12. Fontan, C. R., Dissertation Abstracts 26, No. 12: 6998 (1966).
13. Gatrell, R. L., Mao, T. J., Anal. Chem. 37, 1294 (1965).



14. Gellerman, J. L., Schlenk, H., Anal. Chem. 38, 72 (1966).
15. Hasse, H., Melliand Textilber. 47, 434 (1966).
16. Jones, C. E. R., Reynolds, G. E. J., J. Gas Chromatog. 5, 25 (1967).
17. Keulemans, A. I. M., Walraven, J. J., Belgian Assoc. of Chromatographie Symposium III (1964), pp. 11-22.
18. Kirk, P. L., J. Gas Chromatog. 5, 11 (1967).
19. Kotani, R., Bull. Chem. Soc. Japan 39, 1767 (1966).
20. Krasnov, E. P., et al, Vysokomolekul. Soedin. 8, 380 (1966).
21. Markovec, L., Landa, S., Coll. Czech. Chem. Commun. 31, 3758 (1966).
22. Oro, J., Han, J., Zlatkis, A., Anal. Chem. 39, 27 (1967).
23. Romagnoli, R. J., Bailey, J. P., Anal. Chem. 38, 1928 (1966).
24. Sonntag, F., Brenstoff-Chem. 47, 263 (1966).
25. Stack, M. V., J. Gas Chromatog. 5, 22 (1967).
26. Sternberg, J. C., Krull, I. H., Friedel, G. D., Anal. Chem. 38, 1639 (1966).
27. Tyden, I., Talanta 13, 1353 (1966).
28. Uno, T., Miyajima, K., Nakagawa, T., Bunseki Kagaku 15, 584 (1966).









**B29878**